TECHNISCHE UNIVERSITÄT MÜNCHEN

Lehrstuhl für Mikrobielle Ökologie

Regulation of the biosynthesis of the food-borne *Bacillus cereus* toxin cereulide

Elrike Frenzel

Vollständiger Abdruck der von der Fakultät Wissenschaftszentrum Weihenstephan für Ernährung, Landnutzung und Umwelt der Technischen Universität München zur Erlangung des akademischen Grades eines

Doktors der Naturwissenschaften

genehmigten Dissertation.

Vorsitzender: Univ.-Prof. Dr. R. F. Vogel

Prüfer der Dissertation:

1. Univ.-Prof. Dr. S. Scherer
2. Univ.-Prof. Dr. M. Ehling-Schulz
(Veterinärmedizinische Universität Wien / Österreich)
3. Univ.-Prof. Dr. W. Liebl

Die Dissertation wurde am 09.06.2011 bei der Technischen Universität München eingereicht und durch die Fakultät Wissenschaftszentrum Weihenstephan für Ernährung, Landnutzung und Umwelt am 22.08.2011 angenommen.

Contents

Publications

Parts of this thesis have been published in peer-reviewed journals.

Dommel, M.#, **Frenzel, E.#**, Strasser, B., Blöchinger, C., Scherer, S., Ehling-Schulz, M. (2010). Identification of the main promoter directing cereulide biosynthesis in emetic *Bacillus cereus* and its application for real-time monitoring of *ces* gene expression in foods. Appl. Environ. Microbiol. 76: 1232-1240. (# authors contributed equally).

Frenzel, E., Letzel, T., Scherer, S., Ehling-Schulz, M. (2011). Inhibition of cereulide toxin synthesis by emetic *Bacillus cereus* via long-chain polyphosphates. Appl. Environ. Microbiol. 77: 1475-1482.

Frenzel, E., Doll, V., Pauthner, M., Scherer, S., Ehling-Schulz, M. (2011). CodY modulates expression of key virulence determinants of *Bacillus cereus.* J. Bacteriol., submitted 06/2011.

Frenzel, E., Grunert, T., Lücking, G., Ehling-Schulz, M. (2011). Plasmid-chromosome crosstalk in emetic *Bacillus cereus*. In preparation.

Frenzel, E., Scherer, S., Saalmüller, A., and Ehling-Schulz, M. (2011). Cereulide biosynthesis is a bistable phenomenon in *B. cereus* F4810/72. In preparation.

Messelhäußer, U., **Frenzel, E.,** Ehling-Schulz, M. (2011). Emetic *B. cereus* are more volatile than thought: Recent food-borne outbreaks and prevalence studies in Germany. In preparation.

Doll, V., **Frenzel, E**., Schmid, R. M., Ehling-Schulz, M., and Vogelmann, R. (2011). Role of *Bacillus cereus* protein sphingomyelinase for early epithelial cell death *in vitro* and *in vivo*. In preparation.

Other publications:

Frenzel, E., Schmidt, S., Niederweis, M., Steinhauer, K. (2011). Importance of porins for biocide efficacy against *Mycobacterium smegmatis*. Appl. Environ. Microbiol., 77: 3068-3073.

Summary

Emetic *Bacillus cereus* is increasingly recognized as the etiological agent of usually mild, but occasionally lethal food-borne illnesses, which are provoked by intoxication with the peptide toxin cereulide. Cereulide is a heat-stable, cyclic depsipeptide assembled by a nonribosomal peptide synthetase (NRPS). The encoding *ces* operon genes are located on the megaplasmid pCER270, resembling the virulence plasmid pXO1 of *B. anthracis*. For an improvement of food safety and consumer protection concepts, detailed information on the prevalence of emetic *B. cereus* and cereulide in different types of food, targeted prevention strategies for toxin synthesis, and knowledge on extrinsic factors and the underlying intrinsic mechanisms that control the Ces NRPS synthesis are mandatory.

By applying a combination of a most probable number (MPN) routine diagnostic method with recently developed PCR- and cell culture-based detection assays, a survey on dairy-based German retail products revealed contamination rates of 8-14% with emetic *B. cereus* and 3-10% with cereulide, indicating that especially food ingredients bear a risk of cross-contamination to the end products and that both, toxin and pathogen incidence, is obviously higher that hitherto anticipated.

Since the current methods for cereulide detection are not suitable for large-scale screening purposes, a luciferase-based emetic reporter strain was used to establish a novel biomonitoring system for a rapid risk assessment of toxin production in foods. The *ces* promoter activity was strongly influenced by the food matrix and correlated well with the amount of extracted cereulide, thus enabling the establishment of three risk categories for foods with respect to their toxin synthesis promoting potential.

The application of long-chain polyphosphates, widely used food additives, inhibited cereulide synthesis for the first time in a targeted manner. HPLC/ESI-TOF-MS-based toxin quantification in two polyP-treated model foods showed that cereulide amounts were reduced by 70 to 100%, although *B. cereus* growth was not completely inhibited. qPCR monitoring revealed that polyP exposure significantly reduced the transcription of *ces* operon genes. These data indicate a differential effect on toxin synthesis independent of growth inhibition, and point towards a sensible intracellular polyP/P_i ratio, whose state of equilibrium seems to be crucial to allow cereulide synthesis.

A combination of a *Bacillus subtilis* database-founded *in silico* footprinting analysis with the subsequent identification of homologous transcription factors in the emetic reference strain *B. cereus* F4810/72 by a Best Reciprocal Hit analysis, allowed the examination of the *in vitro* affinity of transcription factors towards the *ces* promoter region by protein/DNA binding studies (EMSAs). The global regulators CodY, DegU, ComK, and PerR specifically interacted with the *ces* promoter, indicating that cereulide synthesis is fine-tuned by a complex network of chromosomally-encoded regulatory proteins.

Deletion of *codY* confirmed its central role as a key regulator of pathogenicity. By means of HEp-2 assays, qPCR, overexpression studies, EMSAs, and several detection methods for *B. cereus* virulence factors, CodY was found to be a direct repressor of cereulide synthesis and an indirect activator of virulence-associated proteins, including the medically important enterotoxins, which were since now regarded to be under major control of the quorum sensing regulator PlcR.

The cross-talk between the *ces* gene cluster and chromosomally encoded elements was further analyzed by *lux*-reporter studies and proteome analyses. The *ces* promoter response in the genetical background of a pCER270 plasmid-cured F4810/72 derivative, and a strain devoid of the *ces* operon demonstrated that toxin synthesis-activating factors are encoded on the virulence plasmid and in the *ces* gene cluster itself. A 2-D DIGE approach revealed that the plasmid encodes regulators that control surface layer expression in an analogous way to *B. anthracis*, and that the presence of pCER270 tempers the expression of PlcR regulated virulence genes, presumably by the plasmid-located interfering constituents of a Rap-Phr quorum sensing system. The upregulation of detoxifying and core metabolic enzymes upon *ces* cluster removal stressed the tight connection between the cereulide synthesis and the primary metabolism.

Finally, a *gfp*-reporter was fused *in situ* to the *ces* promoter area on pCER270, and analysis of its activity on a single cell level demonstrated for the first time that cereulide synthesis is a bistable phenomenon with only a small subpopulation of the cells exhibiting toxin synthesis.

This study provides important data for the elevation of food safety with regards to emetic *B. cereus* and draws a thorough picture on the complexity of the regulation of *ces* NRPS gene expression in emetic *B. cereus*, thereby pointing out missing information and possible clues to solve the puzzle of toxin synthesis regulation in these emerging pathogens.

Zusammenfassung

Emetische *Bacillus cereus* gewinnen zunehmend an Bedeutung als Auslöser von Lebensmittel-assoziierten Erkrankungen, die durch eine Intoxikation mit dem Peptidtoxin Cereulid hervorgerufen werden. Die Synthese des hitzestabilen, zyklischen Depsipeptids wird durch eine nichtribosomale Peptidsynthetase (NRPS), der Cereulid-Synthetase, katalysiert. Die biosynthetischen *ces*-Operon Gene sind auf einem Megaplasmid kodiert, welches Ähnlichkeit zu dem Virulenzplasmid pXO1 von *Bacillus anthracis* aufweist. Um Lebensmittelsicherheits- und Verbraucherschutzkonzepte zu verbessern, sind Kenntnisse über die Inzidenz von Cereulid und emetischen *B. cereus* in verschiedenen Lebensmitteltypen, sowie gezielte Strategien zur Hemmung der Toxinsynthese und die Erforschung von extrinsischen und intrinsischen Faktoren, welche die Toxinsynthese beeinflussen, zwingend erforderlich.

Die Untersuchung von milchbasierten Lebensmitteln und deren Ingredienzien mittels einer Kombination aus routinediagnostischen Methoden (MPN) und PCR- sowie Zellkultur-basierter Toxin-Nachweistechniken ergab, dass 8-14% der Produkte mit emetischen *B. cereus* und 3-10% der Produkte mit Cereulid belastet waren. Diese Ergebnisse deuten darauf hin, dass Ingredienzen eine Eintragsursache für die Pathogene und das Toxin in die Endprodukte darstellen können, und dass das Intoxikationsrikiso offensichtlich höher ist, als bislang angenommen.

Die gegenwärtig verfügbaren Methoden zur Cereulid- Quantifizierung sind nicht für großflächig angelegte Untersuchungen geeignet. Daher wurde ein Luciferase (*lux*)-basierter *B. cereus*-Reporterstamm zur Etablierung eines neuartigen Biomonitoring-Systems genutzt, welches die Expression der Cereulidsynthetase-Gene im Lebensmittel visualisiert. Die Signalintensität hing stark von der Art der beimpften Lebensmittelmatrix ab und korrelierte mit der Menge an synthetisiertem Cereulid, so dass eine Risiko-Kategorisierung von Lebensmitteln hinsichtlich des Potentials zur Cereulidbildung vorgenommen werden konnte.

Die Toxinsynthese wurde durch den Einsatz von Lebensmittelzusatzstoffen, langkettigen Polyphosphaten (PolyP), erstmals gezielt gehemmt. Eine HPLC/ESI-TOF-MS-basierte Cereulid-Quantifizierung zeigte, dass die Konzentration in Modelllebensmitteln um 70 bis 100% reduziert werden konnten, obwohl das Wachstum des emetischen Typstammes nicht vollständig inhibiert war. Eine qPCR-basierte Analyse ergab, dass subletale PolyP-Konzentrationen die Transkription der *ces* Gene signifikant erniedrigten. Somit weist die Cereulidsynthese im Vergleich zum zellulären Wachstum höchstwahrscheinlich einen engeren Phosphat-Toleranzbereich auf und wird durch das intrazelluläre PolyP/P_i-Gleichgewicht beeinflusst.

Durch eine Kombination aus *in silico* Footprinting-Analysen in einer *Bacillus subtilis*-spezifischen Datenbank und Identifizierung von homologen Transkriptionsfaktoren in *B. cereus* F4810/72 durch eine Best Reciprocal Hit Analyse konnten gezielte *in vitro* Protein-DNA Bindestudien durchgeführt werden. Die globalen Regulatoren CodY, DegU, ComK und PerR

interagierten spezifisch mit dem *ces* Promotor, was darauf hindeutet, dass die Cereulidsynthese durch ein äußerst komplexes Netzwerk an chromosomal-kodierten Regulatoren gesteuert wird.

Deletion des pleiotropen Regulators CodY bestätigte seine zentrale Rolle als Pathogenitäts-regulator. Protein-DNA Bindestudien, qPCR, Überexpressionsstudien, und Nachweismethoden für weitere Virulenz-Determinanten zeigten, dass CodY als direkter Repressor der Cereulidsynthese fungiert und darüber hinaus einen indirekten Aktivator für sekretierte Virulenzfaktoren wie die Enterotoxine darstellt, von denen bislang angenommen wurde, dass ihre Expression durch den Quorum sensing-Regulator PlcR gesteuert wird.

Die Kommunikation zwischen dem pCER270-kodierten Cereulid-synthetase-Gencluster und chromosomal kodierten Elementen wurde weiterhin durch *lux*-Reporter-Studien und 2-D DIGE Experimente untersucht. Die *ces* Promotoraktivität im genetischen Hintergrund einer pCER270-plasmidfreien Stammvariante und in einer *ces* Cluster-Inaktivierungsmutante ergaben, dass das Plasmid autoregulatorischen Einfluss auf die Cereulidsynthese ausübt und aktivierende Faktoren kodiert. Differentielle Proteomstudien zeigten, dass auf pCER270 Regulatoren kodiert sind, welche die Expression von Surface-Layer-Proteinen in analoger Weise zu *B. anthracis* steuern, und dass die Gegenwart des Plasmids die Expression von PlcR-regulierten Virulenzfaktoren negativ beeinflusst, was vermutlich auf ein plasmidständiges Rap/Phr-Quorum sensing-System zurückzuführen ist. Die Inaktivierung des *ces* Genclusters verursachte eine verstärkte Expression von metabolischen und detoxifizierenden Enzymen, was darauf hindeutet, dass Primärstoffwechsel und Toxinsynthese eng miteinander verknüpft sind.

Mittels eines Reporterstammes, in dem *gfp* Gene transkriptionell mit dem *ces* Promotorbereich auf dem pCER270-Plasmid fusioniert wurden, konnte durch Einzelzell-Analysen erstmals gezeigt werden, dass die Cereulidsynthese in *B. cereus* F4810/72 ein bistabiles Phänomen darstellt, und nur in einer Subpopulation der Zellen induziert wird.

Diese Studie liefert wichtige Daten, die zukünftig zur Verbesserung der Lebensmittelsicherheit in Bezug auf das Intoxikationsrisiko durch Cereulid genutzt werden können. Darüber hinaus verdeutlichen die Ergebnisse dieser Studie die Komplexität des regulatorische Netzwerks, welches die Expression der *ces* NRPS Gene in emetischen *B. cereus* steuert. Abschließend werden bestehende Wissenslücken und mögliche Lösungswege aufgezeigt, die zu einem verbesserten Verständnis der Toxinsynthese-Regulation in diesem interessanten Pathogen beitragen können.

Abbreviation and Symbol Index

2-D ..... Two dimensional
AA ..... Amino acid
APS ..... Ammonium persulfate
ATCC ..... American Type Culture Collection
BCAA ..... Branched chain amino acid
BeT ..... Symmetrical best hit
BHI ..... Brain Heart Infusion
BRH ..... Best Reciprocal Hit
BSA ..... Bovine serum albumin
CFU ..... Colony Forming Unit
DBTBS ..... Database of transcriptional regulation in *Bacillus subtilis*
DIGE ..... Differential gel electrophoresis
DTT ..... (*2S,3S*)-1,4-Bis-sulfanylbutane-2,3-diol (dithioreithol)
EDTA ..... 2,2',2",2"'-(Ethane-1,2-diyldinitrilo)tetraacetic acid
EMSA ..... Electrophoretic mobility shift assay
FDR ..... False-discovery rate
GFP ..... Green fluorescent protein
GTP ..... Guanosine-5'-triphosphate
His_6 ..... Hexahistidine-tag
HPLC ..... High performance liquid chromatography
ICCD ..... Intensified charge-coupled device
ILV ..... L-isoleucine/L-leucine/L-valine
LA ..... *Listeria* Agar
LB ..... Luria Bertani
LC ..... Liquid chromatography
lux ..... Luciferase genes
MS ..... Mass spectrometry
MYP ..... Mannitol-egg yolk-polymyxin
NRP ..... Nonribosomal peptide
NRPS ..... Nonribosomal peptide synthetase
OD ..... Optical density
PAA ..... Polyacrylamide
PAGE ..... Polyacrylamide gel electrophoresis
PBS ..... Phosphate buffered saline
PC ..... Plate Count
PC-PLC ..... Phosphatidylcholine-specific phospholipase C
PI-PLC ..... Phosphatidylinositol-specif phospholipase C
PMSF ..... Phenylmethylsulfonyl fluoride
polyP ..... Long-chain polyphosphate
QS ..... Quorum sensing
RBC ..... Red blood cell
RNAP ..... RNA polymerase
ROI ..... Region of interest
ROS ..... Reactive oxygen species
SDS ..... Sodium dodecyl sulfate
sp. ..... Species (sing.)
SPH ..... Shingomyelinase
spp. ..... Species (pl.)
TAE ..... Tris/Acetate/EDTA

TB ..... Tris/Borate
TBE ..... Tris/Borate/EDTA
TCA ..... Tricarboxylic acid cycle
TCS ..... Two component system
TEMED ..... *N*,*N*,*N*′,*N*′-tetramethyl-ethane-1,2-diamine
TF ..... Transcription factor
TOF ..... Time Of Flight
v/v ..... Volume per volume
VE ..... Valinomycin equivalents
w/w ..... Weight per volume
WT ..... Wild type

Δ ..... Gene knockout *via* allelic replacement

1 Introduction and Research Objectives

1.1 *Bacillus cereus* and its closest relatives

Within the genus *Bacillus*, the *Bacillus cereus* group comprises six genetically highly related species: *B. cereus*, *B. anthracis*, *B. thuringiensis*, *B. weihenstephanensis*, *B. mycoides*, and *B. pseudomycoides* (Gordon *et al.* 1973; Priest and Alexander 1988; Lechner *et al.* 1998; Nakamura 1998). These low-GC, gram-positive, facultative anaerobic species are capable of forming endospores, and both, their chromosomal gene content and their gene synteny is well conserved (Helgason *et al.* 2000; Rasko *et al.* 2005). Especially *B. cereus*, *B. anthracis*, and *B. thuringiensis* strains are close relatives that share more than 99% identity in their 16S rDNA sequences and tend to intermix within the three main phylogenetic clades of the *B. cereus* group. This led to a questioning of the species definition despite of the varying pathogenic potential of these strains (Ash *et al.* 1991; Helgason *et al.* 2000; Didelot *et al.* 2009; Kolsto *et al.* 2009; Ehling-Schulz *et al.* 2011). The few distinguishing phenotypic traits such as cold-adaptation, specialized morphology, and virulence factor synthesis are therefore traditionally used to delineate a species within this group. Notably, most of these discriminating features are encoded by genes that are located on mobile genetic elements: plasmids.

B. anthracis is the well known etiological agent of the fatal mammalian disease anthrax, and has gained a prominent role as category A-type bioterrorism weapon (Jernigan *et al.* 2002). The genes encoding the main virulence determinants (the anthrax toxins, the poly-γ-D-glutamate capsule, and the anthrax toxin regulator AtxA) are located on the two virulence plasmids pXO1 and pXO2, respectively (Mock and Fouet 2001). Similarly, the *B. thuringiensis*-characteristic *cry* genes for δ-endotoxin synthesis are encoded on plasmids. The δ-endotoxins are insecticidal crystal proteins, which are used since a century as biopesticides to control insect pests in crop cultivation (Aronson and Shai 2001; Berry *et al.* 2002; Lemaux 2008).

B. cereus is recognized as a food spoilage organism, but also as an opportunistic pathogen that provokes two types of food-borne, gastrointestinal diseases (diarrhea and emesis), as well as extraintestinal infections, such as periodontitis or septicemia, that occasionally arise from nosocomial origin (recently reviewed by Stenfors Arnesen 2008 and (Bottone 2010). Most of the virulence factors, including the diarrhea-causing enterotoxins, are chromosomally encoded, whereas the genetic determinants of the emetic syndrome are located on pXO1-like megaplasmids (Ehling-Schulz *et al.* 2006). These virulence-plasmid harboring *B. cereus* strains (termed emetic *B. cereus*) form a clonal lineage, which is, in contrast to non-emetic *B. cereus* strains, phylogenetically very closely related to *B. anthracis* (Ehling-Schulz *et al.* 2005; Guinebretiere *et al.* 2008; Ehling-Schulz *et al.* 2011). The species *B. mycoides* and *B. pseudomycoides* display a characteristic rhizoidal colony morphotype on solid growth media (Nakamura 1998; Di Franco *et al.* 2002). *B. weihenstephanensis* is a psychrotolerant food spoiling organism, which can be distinguished from the other species by the ability to grow

below 7°C, and by specific signature sequences in the cold shock protein A (*cspA*) gene (Lechner *et al.* 1998).

Noticeably, *B. cereus* group members are capable of exchanging their plasmids by conjugational transfer even in complex matrices such as foodstuff (Van der Auwera *et al.* 2007). Therefore, it is not surprising that anthrax-like disease causing *B. cereus* strains that carry pXO1- and pXO2-like plasmids have already been isolated (Hoffmaster *et al.* 2004; Klee *et al.* 2006). These "cross-breed" or "borderline" strains may have emerged via horizontal transfer of the extra-chromosomal elements.

1.2 Pathogenicity of *B. cereus*

Bacillus cereus is ubiquitous in the environment and a common saprophytic inhabitant of the soil, which can contain up to 10^5 spores per gram (Guinebretiere and Nguyen-The 2003; Vilain *et al.* 2006). Transmission readily occurs to foods, and especially foodstuff of plant origin (e.g. vegetables, fruits, rice and spices), but also foods bearing a risk to be cross-contaminated from the soil (e.g. raw milk, eggs, and meat) can serve as a source of isolation (Kramer and Gilbert 1989; Te Giffel *et al.* 1997; Schoeni and Wong 2005). *B. cereus* is a well-known biodegradative food spoilage organism that accounts for substantial economic losses in the dairy industry (Becker 2005; Schoder *et al.* 2007). The spoilage and decrease of the shelf life of pasteurized milk-derived products is mainly caused by the activity of exoenzymes, such as phospholipases and proteases, which can induce off-flavor and coagulation (Christiansson *et al.* 1989). The spores of *B. cereus* are inherently resistant towards a variety of conservation processes (e.g. heating, pasteurization, and dehydration), and towards chemical disinfection and preservation procedures (Novak *et al.* 2005; Carlin *et al.* 2006; Stenfors Arnesen *et al.* 2008; Abee *et al.* 2011). This poses a special risk to mass catering facilities and to industrial food processing lines, where ineffective sanitation processes can lead to biofilm formation and re-contamination of the foodstuffs (Andersson *et al.* 1995; Ehling-Schulz *et al.* 2011).

B. cereus is classified as a Hazard group 2 organism, since it induces two distinct food-borne gastrointestinal diseases and triggers local and systemic infections, such as periodontitis, endophthalmitis, meningitis, or septicaemia (Drobniewski 1993; Stenfors Arnesen *et al.* 2008; Bottone 2010). Extraintestinal infections, which are rare but often lethal for immunocompromised or premature individuals, are frequently connected to traumatic injuries, indwelling catheters, and to nosocomial transmission. These disease patterns are thought to arise from the unspecific activity of an array of tissue-destructive and cytolytic exoenzymes, such as cereolysin O (Clo), collagenase, shingomyelinase (SPH), phosphatidylinositol-specific (PI-PLC) and phosphatidylcholine-specific (PC-PLC) phospholipases, and several proteases (Drobniewski 1993; Beecher *et al.* 2000; Beecher and Wong 2000; Kotiranta *et al.* 2000; Miyoshi and Shinoda 2000; Chung *et al.* 2006). Likewise, the combined activity of hemolysin II, neutral metalloproteases, and immune inhibitor metalloproteases (InhA family) is discussed

to counteract host immune responses (Kastrup *et al.* 2008; Cadot *et al.* 2010; Guillemet *et al.* 2010).

Contrarily, food poisonings resulting in the diarrheal or the emetic syndrome are attributed to specific agents: the heat-labile pore-forming enterotoxins Nhe (nonhaemolytic enterotoxin), CytK (cytotoxin K), and Hbl (haemolysin BL) that act on intestinal epithelial cells (Beecher and Macmillan 1991; Lund and Granum 1996; Lund *et al.* 2000), and cereulide, a heat-stable, lipophilic peptide toxin (Ehling-Schulz *et al.* 2004). The diarrheal syndrome is a classical toxicoinfection, which is elicited by the consumption of 10^5 to 10^7 vegetative *B. cereus* cells or spores with the food. These are thought to germinate and multiply in the small intestine, and to locally produce the enterotoxins, which leads to abdominal cramps and diarrhea within 6 to 12 hours (Stenfors Arnesen *et al.* 2008). Though usually self-limiting, cases of fatal enteritis have been reported (Fagerlund *et al.* 2007). In contrast, the emetic syndrome is provoked by an intoxication with cereulide, which is preformed during vegetative growth of *B. cereus* in foods and leads to nausea, heavy vomiting and abdominal cramps when ingested at concentrations around 10 µg per kilogram of body weight (Shinagawa *et al.* 1995; Jääskeläinen *et al.* 2003). The symptoms are presumably induced by the interaction of cereulide with duodenal 5-HT_3 serotonin receptors leading to the stimulation of the afferent vagus nerve (Agata *et al.* 1995). The intoxication is characterized by a short incubation time of around 0.5 to 6 hours after food consumption, but usually declines after 24 hours. Besides these less acute symptoms, a number of studies indicate a high toxicity potential concerning immuno-modulatory, neuro- and hepatotoxic modes of actions (Mikkola *et al.* 1999; Paananen *et al.* 2002; Andersson *et al.* 2007). Several of the latter phenomena are based on the potassium ionophoric properties of cereulide, which leads to a depolarization and uncoupling of ATP synthesis in mitochondria (Kawamura-Sato *et al.* 2005; Andersson *et al.* 2007). This effect is also used to detect and quantify cereulide in cell line-based bioassays. Due to their lower toxic capacity, children and immunosuppressed individuals are especially vulnerable and cases of fatal liver failure or encephalopathy have been reported (Mahler *et al.* 1997; Dierick *et al.* 2005; Posfay-Barbe *et al.* 2008; Shiota *et al.* 2010). In heavy intoxications cereulide was found to enter the blood stream, and concentrations of 4 ng/ml blood serum were detected (Shiota *et al.* 2010). Emetic intoxications can further mimic Reye's syndrome (Ichikawa *et al.* 2009), to which no defined causative agent had been associated so far.

Cereulide (Fig. 1) is a cyclic dodecadepsipeptide composed of alternating α-amino and α-hydroxy acid monomers (D-*O*-Leu--D-Ala--L-*O*-Val--L-Val)$_3$ that is structurally related to the ionophoric macrolide antibiotic valinomycin (Agata *et al.* 1994). Due to the alternating amino and ester bonds and its cyclic structure, cereulide is extremely stable and withstands a broad pH range (2-11), heat (150°C), and enzymatic cleavage. Therefore, the toxin is neither inactivated by thermal processing during food manufacturing or reheating of prepared foods, nor by low pH conditions in the stomach or by digestive enzymes in the intestine (Melling *et al.* 1976; Granum and Lund 1997; Agata *et al.* 2002; Rajkovic *et al.* 2008). Furthermore, cereulide is too small (1.2 kDa) to be restrained by sterile filtration processes in the food production line. Consequently, several studies focused on antimicrobial compounds to suppress *B. cereus*

growth in food, including bacteriocins, terpenoid substances, organic acids, and others (see e.g. (Russell and Gould 2003; Galvez *et al.* 2007; Morente *et al.* 2010; Ter Beek and Brul 2010). However, targeted strategies to prevent toxin formation in the food production chain and in foods are still missing.

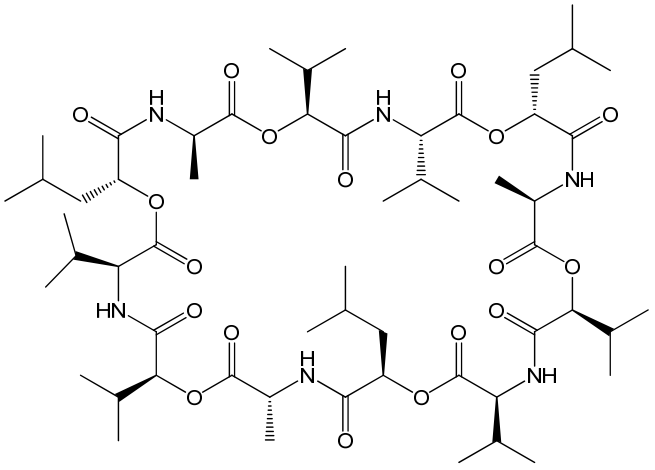

Figure 1: Chemical structure of cereulide, the cyclic peptide toxin produced by the emetic lineage of *B. cereus* strains. The tetradepsipeptide unit (D-*O*-Leu--D-Ala--L-*O*-Val--L-Val) is repeated three times.

In most countries, *B. cereus* food-borne poisonings are probably underestimated for a number of reasons: Incubation time and symptoms of the emetic syndrome resemble those caused by *Staphylococcus aureus* foodborne intoxications (Ehling-Schulz *et al.* 2004). However, in several cases *S. aureus* is not detected in the specimen (Fricker *et al.* 2007). Furthermore, *B. cereus* testing is not driven routinely in public health facilities, since reporting of isolated cases is not mandatory. Moreover, specific molecular detection and identification methods for emetic strains have only recently been developed (Ehling-Schulz *et al.* 2004; Ehling-Schulz *et al.* 2006; Fricker *et al.* 2007) and are not standardized for routine diagnostics in public health facilities yet. However, there is an enhanced awareness of the *B. cereus* problematic in public health and food authorities, and the incidences of food-borne outbreaks caused by *Bacillus* toxins are more frequently recorded throughout the last years (Anonymous 2009). For instance, the European Food Safety Authority (EFSA) reported on 45 verified food-borne outbreaks caused by *B. cereus* toxins in Europe in 2008, including 1,132 cases and 41 hospitalizations; thereby exceeding the numbers of proven intoxications caused by *Clostridium* spp. and *S. aureus* (Anonymous 2010). Large-scale emetic outbreaks are further characterized by high incidence rates with up to 100% concerned individuals (Shinagawa *et al.* 1985; Essen *et al.* 2000; Fricker *et al.* 2007). Cereulide intoxications are commonly, but not exclusively, linked to farinaceous and starchy foods, such as rice and pasta dishes that were prepared in large quantities (e.g. in mass caterings or restaurants) and had not been refrigerated properly (Kramer and Gilbert 1989). In other outbreaks, milk and ricotta cheese were the contaminated source (Ehling-Schulz *et al.* 2011). It is generally accepted that cereulide synthesis is influenced by the type of implicated food and that the presence and growth of emetic strains does not necessarily lead to detectable toxin levels (Agata *et al.* 2002; Rajkovic *et al.* 2006; Dommel *et al.* 2010). However, the factors influencing cereulide production in foodstuff are widely unknown.

1.3 Regulation of virulence factor expression in *B. cereus*

1.3.1 Transition and stationary phase virulence factors

The majority of currently known *B. cereus* virulence-associated factors is controlled by the transcriptional regulator PlcR (Phospholipase C Regulator), which is active during the transition state. PlcR and its signaling peptide PapR constitute a quorum sensing system that belongs to the RNPP family of quorum sensing proteins of gram-positive bacteria (named after the receptor proteins Rap, Npr, PlcR, and PrgX) (Declerck *et al.* 2007). Although *B. cereus* strains encode Rap and Npr regulators, their contribution to pathogenicity has received little attention, whereas the PlcR regulon has been thoroughly characterized for non-emetic *B. cereus* and *B. thuringiensis* (Gohar *et al.* 2008; Pomerantsev *et al.* 2009). After secretion, the inactive PapR propeptide is processed by an extracellular neutral protease (NrpB). The active heptapeptide is then reimported by an oligopeptide permease system (Opp) and bound by the PlcR regulator, which in turn activates its own transcription as well as the synthesis of around 40 secreted and cell-wall associated proteins whose genes are preceded by a PlcR binding motif. Among them are the enterotoxins Nhe and Hbl, hemolysins like CytK and cereolysin O, but also several proteases, such as the immune inhibitor metalloprotease 2 (InhA2), and the lipolytic enzymes sphingomyelinase and PC- and PI-dependent phospholipases (Gohar *et al.* 2008). Activity of PlcR is thus controlled in a cell-density-dependent manner, but also by the master regulator of sporulation, Spo0A, which represses *plcR* transcription and hence, virulence factor secretion under nutrient limiting conditions in the stationary phase (Lereclus *et al.* 2000). Interestingly, this major virulence determination system is inactive in *B. anthracis*, since the PlcR protein is C-terminally truncated due to a nonsense mutation. This leads to the absence of lecithinase and hemolytic activities, which are typical for non-emetic *B. cereus,* and to a comparably smaller secretome (Gohar *et al.* 2005). The observation that overexpression of PapR-PlcR resulted in severe sporulation defects in *B. anthracis*, led to the hypothesis of an incompatibility of the PlcR-PapR regulon and the virulence factor regulon of the pXO1-plasmid-born regulator AtxA (Mignot *et al.* 2001). This might have caused the inactivation of PlcR; however, this hypothesis is controversially discussed since then.

Moreover, there is mounting evidence that additional regulatory mechanisms influence or replace the PlcR-attributed regulation of pathogenicity. For instance, anthrolysin O, a homolog of cereolysin O, was recently found to be expressed independently from PlcR in *B. anthracis* (Ross and Koehler 2006). Likewise, synthesis of the emetic toxin cereulide is regulated PlcR-independent (Ch. 1.3.2). In non-emetic *B. cereus*, enterotoxin synthesis is dependent on the metabolic and the redox cell status: Nhe expression is controlled in a complex fashion by the carbon catabolite-control protein A (CcpA), the key metabolic enzyme lactate dehydrogenase A (LdhA), the redox-sensing two-component system ResDE, and the regulator of anaerobic and fermentative growth, Fnr (Duport *et al.* 2006; Zigha *et al.* 2007; van der Voort *et al.* 2008; Laouami *et al.* 2011). In light of this complexity, one might anticipate that the regulation of

virulence gene expression in emetic *B. cereus* is further complicated by the presence of pXO1-like virulence plasmids.

1.3.2 Cereulide and its biosynthetic genes

Cereulide is synthesized enzymatically by a nonribosomal peptide synthetase (NRPS) (Ehling-Schulz *et al.* 2005). NRPSs are large multienzyme complexes that catalyze the ribosome-independent synthesis of a broad diversity of peptide products, which often display antibiotic, antitumor, or immunosuppressor features (Caboche *et al.* 2010). NRPS products are usually short and made up of 2 to 50 monomers that contain a high proportion of nonproteogenic amino acids (Caboche *et al.* 2008). NRPSs complexes are organized in repetitive modules that selectively incorporate one amino acid, α-hydroxy acid, or carboxylic acid monomer in the peptide product (Marahiel *et al.* 1997). Usually, the order of the modules is colinear to the order of the monomers in the assembled depsipeptide (von Döhren *et al.* 1997). The modules harbor specialized enzymatic units called domains (reviewed by (Finking and Marahiel 2004; Strieker *et al.* 2010). The core of each module is made up of an adenylation domain (A) for the activation of the monomer, an adjacent peptidyl carrier protein domain (PCP), which is activated by 4′-phosphopantheteinyl and binds the amino acyladenylate, and a condensation domain (C), which catalyzes the amide or ester bond formation and the chain elongation. The thioesterase domain (TE) terminates the synthesis by hydrolytic cleavage, and in some cases by oligomerization and cyclization of the mature peptide.

The plasmid-located cereulide biosynthetic genes are organized in a 24-kb cluster (Fig. 2) (Ehling-Schulz *et al.* 2006). The 5′ end encodes a putative hydrolase/acyltransferase (CesH), whose function is, with respect to cereulide synthesis, unclear. *cesH* and the adjacent *cesP* gene are separated by a 990-bp noncoding region. CesP is a 4′-phosphopanthetheinyl transferase (PPTase), which are typically associated with their cognate NRPS enzymes. PPTases posttranscriptionally activate the NRPS modules by converting the inactive apo-carrier proteins to the active holo-forms by catalyzing the transfer of a coenzyme A-derived 4′-phospho-pantheteine moiety to a serine residue of the PCP domains (Lambalot *et al.* 1996). The following *cesT* gene codes for a putative type II thioesterase, which possibly removes misprimed monomers and reactivates the catalytic NRPS domains (Schwarzer *et al.* 2002). CesA and CesB constitute the core NRPS modules that tether, activate and incorporate the four cereulide monomers into the cyclic peptide (compare Fig. 1). The CesA2 and CesB2 submodules install D-alanine and L-valine, respectively, whereas CesA1 and CesB1 bind precursors of branched-chain amino acids, namely α-ketoisocaproic acid and α-ketoisovaleric acid. Due to a unique insertion of ketoacyl reductase domains in the A domains, which is only found in the assembly lines of cereulide and the structurally related cyclopeptide valinomycin, the achiral α-ketoacids are reduced *in situ* to the chiral D- or L-α-hydroxyacid-moieties (Magarvey *et al.* 2006). Precursor condensation results in the assembly of the basic tetradepsipeptide unit D-*O*-Leu–D-Ala–L-*O*-Val–L-Val, which is repeated three times within the mature toxin (Fig. 1). The terminal *cesCD* genes encode a putative integral membrane

transport protein with high homology to the drug resistance and immunity (DRI) subfamily of ABC transporters, however, their function is not completely elucidated yet (Lücking 2009). However, targeted inactivation of *cesCD* resulted in a cereulide-deficient phenotype, although the *ces* NRPS genes were transcribed. This might point towards a role in connecting cereulide export with its biosynthesis (Lücking 2009).

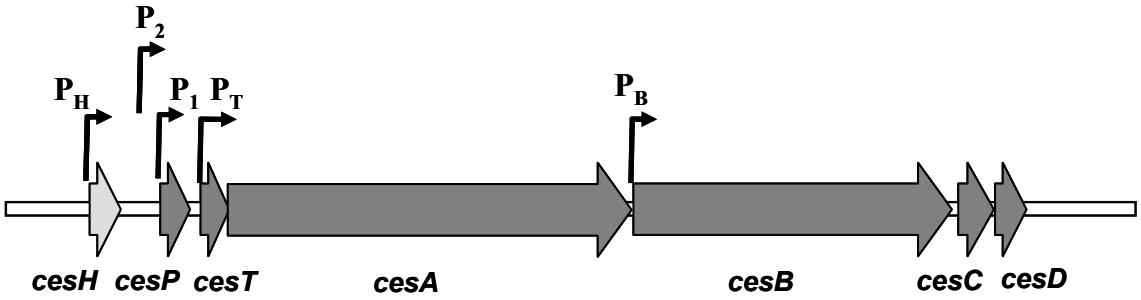

Figure 2: Genetic organization of the cereulide biosynthetic gene cluster of emetic *B. cereus* (Dommel *et al.* 2010). The *ces* operon encodes a 4´-phosphopantetheinyl transferase (*cesP*), a thioesterase (*cesT*), two cereulide synthetase NRPS modules (*cesA* and *cesB*), and an ABC transporter (*cesCD*). Bent arrows indicate the position of the main (P_1), accessory (P_2), and intracistronic (P_T and P_B) promoter regions, respectively. The adjacently situated *cesH* gene encodes a hydrolase/acyltransferase of unknown function, which is transcribed from its own promoter (P_H).

The structural *cesPTABCD* genes are co-transcribed from the main *cesP1* promoter as a single 23-kb polycistronic transcript, whereas *cesH* is transcribed from its own promoter (P_H, Fig. 2) (Dommel *et al.* 2010). Besides P_1, a second promoter region (P_2) that includes putative -35 and -10 σ^A-recognition sites and a transcription start site, is located 256 bp upstream of the *cesP* translation start. However, promoter deletion studies indicated that the isolated P_2 region is inactive; therefore, the regulatory input of this promoter is unclear. The *ces* cluster further contains two intracistronic promoters: P_T and P_B that showed weak activity under standard cultivation conditions. These might ensure an appropriate expression of the distal genes (Dommel *et al.* 2010).

Transcription of the *ces* operon is strict temporally regulated and occurs during the exponential phase of growth (Dommel *et al.* 2011). After a rapid onset, transcription ceases towards undetectable mRNA levels in the early stationary phase, pointing towards a tight and/or complex regulation on the transcriptional level. During the lag phase and the early exponential phase, expression is controlled by the AbrB-Spo0A circuit: the transition state regulator AbrB acts as a direct transcriptional repressor until the early σ^A-dependent expression of the master regulator of sporulation (Spo0A) relieves the AbrB-mediated effect by inhibiting AbrB synthesis (Fig. 3) (Lücking *et al.* 2009). The later sporulation process *per se* is not essential for cereulide synthesis, since inactivation of σ^H, the alternative sigma factor that drives late *spo0A* transcription and sporulation, had a slight, but no significant influence on toxin production. The slight effect is presumably based on a regulatory relay that connects σ^H, AbrB, and Spo0A, whereas a distinct correlation seems unlikely, because the *ces* promoter region lacks a typical

σ^H-RNAP consensus sequences (Lücking 2009). In contrast to its role in enterotoxin secretion, the quorum sensing system PapR-PlcR does not participate in cereulide synthesis (Lücking *et al.* 2009), suggesting that PlcR-mediated virulence factor production and cereulide synthesis are controlled by completely different, independent networks.

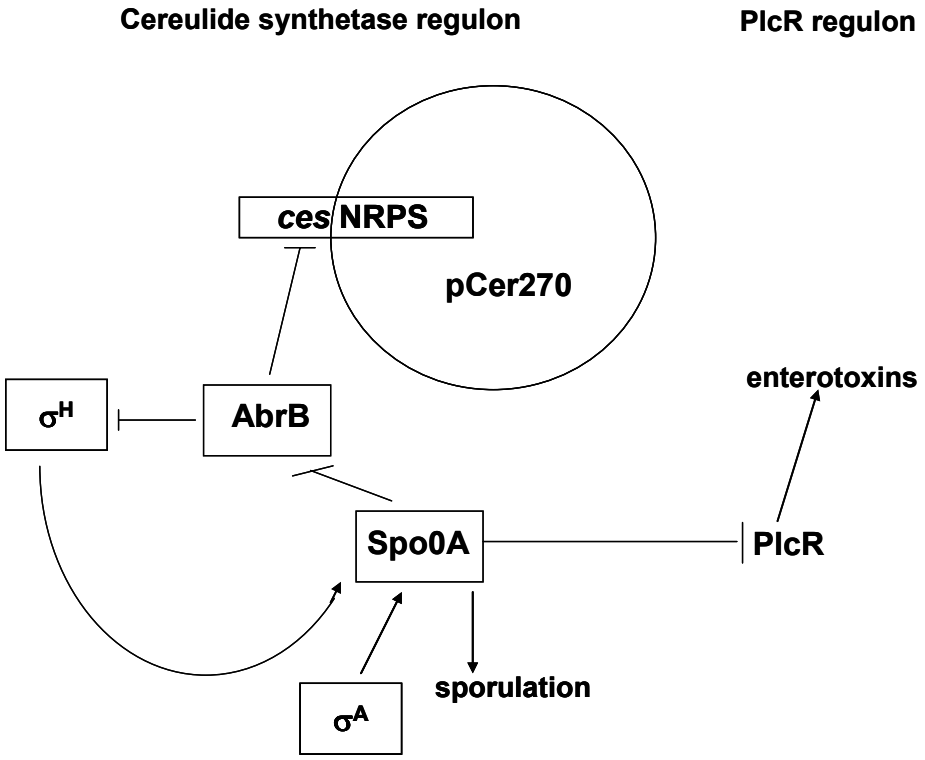

Figure 3: Current model of the regulation of the pCER270-plasmid-borne cereulide synthetase (*ces*) gene expression and expression of PlcR regulon genes in the emetic *B. cereus* reference strain F4810/72. The figure was modified after (Lücking 2009).

Without exhibiting influential nucleotide polymorphisms in the *ces* promoter region or in the structural NRPS genes, the toxigenic potential of emetic *B. cereus* strains varies up to 1,000-fold (Häggblom *et al.* 2002; Apetroaie *et al.* 2005; Ehling-Schulz *et al.* 2005; Carlin *et al.* 2006). An initial study on the low cereulide producer IH41385 revealed that, although *ces* gene transcription follows the same kinetics as in the emetic reference strain F4810/72, *ces* mRNA levels were substantially lower, which points towards a major regulatory effect on the transcriptional level (Dommel *et al.* 2011). However, neither activators responsible for the exponential onset of *ces* operon expression nor repressors that might cause the sudden shut down of transcription have been identified so far. This complicates the elucidation of intrinsic factors contributing to the different toxicity potentials of emetic strains, whose identification would be a critical point for rapid risk assessments in *B. cereus* food safety surveys.

1.4 Research objectives

Emetic *B. cereus* is increasingly recognized as the etiological agent of usually mild, but occasionally lethal food-borne intoxications provoked by the heat-stable depsipeptide cereulide. An improvement of food safety and consumer protection concepts was hampered by the lack of knowledge on the incidence of cereulide and emetic strains in different types of food, by the lack of fast and specific detection methods for cereulide in complex matrices, and by the lack of inhibition strategies targeting at the toxin synthesis process.

The application-oriented objectives of this thesis were to (i) assess the occurrence of emetic strains and cereulide in dairy-based foods and their ingredients (Chapter 1), (ii) evaluate the *in situ* performance of a luciferase-based emetic reporter strain to reflect toxin synthesis levels depending on the extrinsic stimuli of complex food matrices and to establish a basic risk categorization system for foods (Chapter 2), (iii) develop a targeted inhibition strategy for cereulide production in model food systems (Chapter 3).

Cereulide synthesis varies up to 1,000-fold between different emetic strains. A risk assessment with respect to differing toxigenic potentials of emetic strains was further aggravated by the gap of knowledge regarding the regulation of cereulide synthesis. To gain insight into the intrinsic factors and regulatory mechanisms governing the biosynthesis of cereulide, central objectives of this thesis were to (iv) identify transcription factors that directly act on *ces* gene expression in the emetic model strain F4810/72 (Chapter 4), (v) characterize the *in vivo* function of one transcription factor with respect to *B. cereus* pathogenicity (Chapter 5), (vi) analyze the embedding of the *ces* cluster-encoding pCER270 megaplasmid in the global metabolism of F4810/72 (Chapter 6), and (vii) monitor *ces* gene expression on a single cell level (Chapter 7).

2 Materials and Methods

2.1 Bacterial strains and plasmids

All strains used in this study are listet in Table 1. *E. coli* TOP10 and INV110 were used for general cloning purposes. *E. coli* BL21(DE3) served as a host for heterologous protein expression, since it displays a reduced protease activity due to the lack of *ompT* and *lon* proteases. Strains ColD and E3 were used for the isolation of colicins necessary for selective *B. cereus* isolation in heterogramic conjugation experiments. Genomic DNA of *B. subtilis* subsp. *subtilis* strain NCIB3610 was used to amplify promoter regions or protein encoding genes for gel mobility shift experiments. *B. cereus* F4810/72 was originally isolated from a rice dish involved in an emetic food poisoning case in the United Kindom (Turnbull *et al.* 1979). F4810/72 is the first completely sequenced emetic strain, and is therefore regarded as the emetic reference strain, which served as the model organism to study cereulide synthesis regulation in the present study. Further, two environmental strains (CEI and EROI) were included in this study: one strain was isolated from clinical specimen and the other strain originated from a food poisoning outbreak.

All plasmids used and constructed in this study are listed in Table 2. pCR2.1-TOPO (Invitrogen) served as general cloning vector. pAT113 is a suicide vector carrying the transfer origin of IncP plasmid RK2 in order to allow conjugational transfer to gram-positive bacteria by *E. coli* strains with IncP plasmids, such as *E. coli* pRK24 (Trieu-Cuot *et al.* 1991). Due to the presence of the attachment site of Tn*1545* on the plasmid backbone, pAT113 does not replicate in *B. cereus* but integrates by recombination (Trieu-Cuot *et al.* 1991). pWH1520 was originally constructed for xylose-inducible large-scale protein overexpression in *Bacillus megaterium* (Rygus and Hillen 1991; Rygus *et al.* 1991) and was used to construct a *B. cereus* strain overexpressing the transcriptional regulator CodY. pMDX[P_1/*lux*], a pXen1 derivative (Francis *et al.* 2000), is a luciferase-based reporter plasmid, which contains a 238-bp fragment of the *ces* operon main promoter region (P_1) transcriptionally fused to the *luxABCDE* genes (Dommel *et al.* 2010). pET28b(+) (Novagen) was used for heterologous expression of *Bacillus* proteins in *E. coli*, because it allows both, cloning of C-terminally, and N-terminally His_6-tagged proteins.

Table 1: Bacterial strains used in this study[a]

Strain	Relevant genotype or characteristics	Reference/ source
E. coli		
TOP10	General cloning host	Invitrogen
INV110	Methylase-deficient cloning host	Invitrogen
BL21(DE3)	Expression of recombinant proteins; *E. coli B* F^- *omp*T *hsd*$S_B(r_B^-m_B^-)$ *gal dcm* (DE3)	Novagen
DH10B	Non-entomopathogenic strain used for insect infection assays	(Durfee *et al.* 2008)
JM83/pRK24	Donor strain for conjugation; *ara* Δ(*lac-proAB*) *strA* φ80*lac*ZΔM15; Tra^+, Mob^+, Amp^r, Tc^r	(Trieu-Cuot *et al.* 1991)
ColD	Colicin D producing strain for heterogramic conjugation	Institut Pasteur
E3	Colicin E3 producing strain for heterogramic conjugation	Institut Pasteur
B. subtilis		
subsp. *subtilis* NCIB3610	*B. subtilis* type strain NCIB3610; BGSC 3A1; ATCC 6051; prototrophic wild type strain; surfactin-producer	(Srivatsan *et al.* 2008; Zeigler *et al.* 2008)
B. cereus		
F4810/72	Emetic reference strain, wild type; isolated from a foodborne outbreak in 1972; also termed AH187	UK (PHLS); (Turnbull *et al.* 1979)
F48(pCER270-)	pCER270-cured derivative of F4810/72 (cereulide non-producer)	(Lücking 2009)
F48ΔcesP/polar	*cesP* deletion mutant of F4810/72; polar effect of spectinomycin cassette leads to inactivation of the whole *ces* cluster (cereulide non-producer); Spc^r	(Lücking 2009)
F48ΔplcR	*plcR* deletion mutant of F4810/72; Δ*plcR*::*spc*; Spc^r	(Lücking *et al.* 2009)
F48ΔcodY	*codY* deletion mutant of F4810/72; Δ*codY*::*spc*; Spc^r	This study
F48pWHCodY	F4810/72 harboring pWHCodY for *codY* overexpression; Tc^r	This study
F4810/72[P_1/*lux*]	F4810/72 harboring the harboring the P_1-*lux*-reporter plasmid pMDX[P_1/*lux*]; Cm^r	(Dommel *et al.* 2010)
F4810/72[pXen1]	F4810/72 harboring the promoterless *lux*-reporter plasmid pXen1; Cm^r	(Dommel *et al.* 2010)
F48(pCER270-)[P_1/*lux*]	F48(pCER270-) harboring the P_1-*lux*-reporter plasmid pMDX[P_1/*lux*]; Cm^r	This study
F48ΔcesP/polar[P_1/*lux*]	F48ΔcesP/polar harboring the P_1-*lux*-reporter plasmid pMDX[P_1/*lux*]; Cm^r	This study
CEI[P_1/*lux*]	Emetic clinical strain isolated from a catheter harboring the P_1-*lux*-reporter plasmid pMDX[P_1/*lux*]; Cm^r	This study
EROI[P_1/*lux*]	Emetic outbreak-strain isolated from a rice dish harboring the P_1-*lux*-reporter plasmid pMDX[P_1/*lux*]; Cm^r	This study
F48icesGFP	F4810/72 carrying a P_{cesP}-*gfp*-*spc* fusion integrated at the native *cesP* promoter region on pCER270	This study

[a] The annotations Str^r, Spc^r, Cm^r, Amp^r and Tc^r indicate resistance of the according strain to the antibiotics streptomycin, spectinomycin, chloramphenicol, ampicillin, and tetracyclin, respectively. Tra^+, self transferable; Mob^+, mobilizable.

Table 2: Vectors and recombinant plasmids used in this study[a]

Plasmid	Relevant genotype or characteristics	Reference or source
pCR 2.1-TOPO	Cloning vector; Amp^r, Kan^r	Invitrogen
TOPO/spc	pCR 2.1 TOPO with spectinomycin resistance cassette from pUC1318; Spc^r	(Lücking *et al.* 2009)
TOPOΔcodY/spc	TOPO-derivative containing up- and downstream regions of *codY* flanking a Spc^r cassette; Amp^r, Kan^r; Spc^r	This study
TOPO/P_{cesP}/GFP-spc/cesP	TOPO-derivative containing a *ces* promoter-GFP fusion and the *cesP* ORF flanking a Spc^r cassette for integration on the pCER270 plasmid; Kan^r, Amp^r, Spc^r	This study
pAT113	Conjugative suicide vector; *oriR* pACYC184, *oriT* RK2; Tra^-, Mob^+, *att*Tn*1545*, MCS pUC19; Kan^r, Erm^r	(Trieu-Cuot *et al.* 1991)
pAT113ΔcodY/spc	pAT113-derivative containing up- and downstream regions of *codY* flanking a Spc^r cassette for homologous recombination; Kan^r, Erm^r, Spc^r	This study
pAT113[GFPint]	pAT113-derivative containing a *ces* promoter-GFP fusion and the *cesP* ORF flanking a Spc^r cassette for integration on the pCER270 plasmid; Kan^r, Erm^r, Spc^r	This study
pWH1520	*Bacillus* spp. expression vector; xylose-inducible, ColE1 *ori*, pBC16 *ori*; Amp^r, Tc^r	(Rygus and Hillen 1991)
pWHCodY	Promoter-less *codY* in pWH1520; Amp^r, Tc^r	This study
pMDX[P_1/*lux*]	Luciferase reporter construct; transcriptional fusion of main *ces* promoter to *luxABCDE* genes; pXen1-derivative; Amp^r, Cm^r	(Dommel *et al.* 2010)
pET28b(+)	IPTG-inducible *E. coli* expression vector for N- or C-terminal His_6-tag fusion proteins; T7*lac* promoter; Kan^r	Novagen
pET28-*codY*	Promoter-less *codY* with N-terminal His_6-tag in pET28b;Kan^r	This study
pET28-*abrB*	Promoter-less *abrB* with C-terminal His_6-tag in pET28b; Kan^r	(Lücking *et al.* 2009)
pET28-*comK*	Promoter-less *comK* with C-terminal His_6-tag in pET28b; Kan^r	This study
pET28-*perR*	Promoter-less *perR* with C-terminal His_6-tag in pET28b; Kan^r	This study
pET28-*ccpA*	Promoter-less *ccpA* with C-terminal His_6-tag in pET28b; Kan^r	This study
pET28-*degU*	Promoter-less *degU* with C-terminal His_6-tag in pET28b;Kan^r	This study
pET28-*sinR*	Promoter-less *sinR* with C-terminal His_6-tag in pET28b; Kan^r	This study

[a] Derivatives contain the same origins of replication and selection markers as the parental plasmids. ColE1 ori, origin of replication for *E. coli*; pBC16 ori, origin of replication for *Bacillus* spp.; Kan^r, kanamycin resistance; Amp^r, ampicillin resistance; Tc^r, tetracyclin resistance; Erm^r, erythromycin resistance; Spc^r, spectinomycin resistance; Tra^-, non-self-transferable; Mob^+, mobilizable.

2.2 Media and growth conditions

Media components were obtained from Merck, Oxoid, and Sigma-Aldrich. Media were prepared with dH_2O, adjusted to pH 7.2 and autoclaved for 17 min at 121°C. When required, media were solidified by addition of 15 gram agar per liter. Modified MOD medium (Glatz and Goepfert 1976; Rosenfeld *et al.* 2005) was prepared with ddH_2O and autoclaved for 10 min at 110°C. Stock solutions of C-sources and trace elements were prepared with ddH_2O, filter sterilized (0.22µm pore size), and added to the cooled MOD medium.

LB:	10 g/l peptone from casein 5 g/l yeast extract 10 g/l NaCl
TSB:	15 g/l tryptone 5 g/l soy peptone 5 g/l NaCl
SOC:	20 g/l tryptone 5 g/l yeast extract 10 mM NaCl 2.5 mM KCl 10 mM $MgCl_2$ 10 mM $MgSO_4$ 20 mM D-glucose
MOD:	8 ml/l 1000x trace elements 6 g/l $(NH_4)_2SO_4$ 1 g/l K_2HPO_4 0.04 g/l $MgSO_4$ x $7H_2O$ 10 ml/l 2 M C-source 2 g/l L-glutamic acid 0.39 g/l L-glycine 0.91 g/l L-valine 0.91 g/l L-threonine 0.4 g/l L-methionine 0.36 g/l L-histidine 0.46 g/l L-arginine 0.91 g/l L-aspartic acid 0.04 g/l L-cysteine 0.46 g/l L-arginine 0.7 g/l L-isoleucine 1.37 g/l L-leucine 0.28 g/l L-phenylalanine 1.18 g/l L-lysine 0.66 g/l L-serine 0.042 g/l L-tyrosine

PC:	5 g/l peptone from casein 2.5 g/l yeast extract 1 g/l D-glucose
MYP:	10 g/l casein peptone 10 g/l D-mannitol 1 g/l meat extract 10 g/l sodium chloride 0.013 mg/l polymyxin B 0.025 g/l phenol red 50 ml/l egg-yolk emulsion
Trace elements: (1000x) (MOD)	675 mg/l $FeCl_2$ x 6 H_2O 50 mg/l $MnCl_2$ x 4 H_2O 30 mg/l Na_2MoO_4 x $2H_2O$ 275 mg/l $CaCl_2$ 85 mg/l $ZnCl_2$ 30 mg/l $CoCl_2$ x 6 H_2O 40 mg/l $CuSO_4$ 24 mg/l $NaSeO_4$
TSPB:	17 g/l casein peptone 3 g/l soy peptone 5 g/l NaCl 2.5 g/l D-glucos 2.5 g/l K_2HPO_4 10 ml/l polymyxin B supplement (50,000 IU)
BHIG:	37 g/l BHI broth 10 g/l D-glucose

E. coli strains were routinely grown on lysogeny broth (LB) agar or in LB medium at 150 rpm and 37°C. Super Optimal Catabolite repression (SOC) medium was used in *E. coli* transformation procedures. *B. cereus* F4810/72 (WT) was grown on plate count (PC) agar at 30°C, whereas gene deletion mutants were cultured on LB. Unless stated otherwise, *B. cereus* strains were routinely precultured (16 h, 30°C, 150 rpm) in LB medium. Main cultures (100 ml LB) were inoculated with 10^3 CFU ml^{-1} and vigorously shaken in baffled flasks with 150 rpm at 30°C. Growth was monitored by measuring the optical density at 600nm (OD_{600}). Following antibiotics were added when appropriate: ampicillin (120 µg ml^{-1}) or kanamycin (50 µg ml^{-1}) for *E. coli*; tetracyclin (10 µg ml^{-1}), spectinomycin (100 µg ml^{-1}), erythromycin (3 µg ml^{-1}), chloramphenicol (5 µg ml^{-1}), or combinations thereof, for *B. cereus* strains.

Tryptic soy broth (TSB) was used as *B. cereus* growth medium in erythrocyte hemolysis assays (Ch. 2.9.4), since preliminary experiments revealed that supernatants of LB grown cultures did not exhibit hemolytic activity. Brain Heart Infusion Glucose (BHIG) medium was used to stimulate production of enterotoxins by *B. cereus* (Ch. 2.9.2). MOD medium was used to assess

the influence of several C- and N- sources on cereulide production under chemically defined conditions (Ch. 3.5.1). The enrichment medium trypticase soy-polymyxin broth (TSPB) and mannitol-egg yolk-polymyxin (MYP) agar, a selective *B. cereus* group medium (Mossel *et al.* 1967), were used for isolation and detection of presumptive *B. cereus* strains from foods (Ch. 2.4.1). Typically, *B. cereus* in unable to ferment mannitol and forms pink colored colonies with rough and dry morphology, that are surrounded by a zone of precipitation. This so called lecithinase reaction is based on the egg-yolk hydrolyzing activity of phosphatidylcholine-specific phospholipase C (PC-PLC) and phosphatidylinositol-specific phospholipase C (PI-PLC). MYP and the *Bacillus cereus* group plating medium (BCM; ready-to-use plates; Biosynth AG) were further used for phenotypical characterization of *B. cereus* gene deletion mutants (Ch. 3.5.1). For this purpose, 5 µl of LB-grown overnight cultures were dropped on the plate surface and incubated at 30°C for 24 h. On BCM agar, production of phosphatidylinositol-specific phospholipase C (PI-PLC) leads to cleavage of the chromogenic substrate 5´-Bromo-4-chloro-3-indoxyl myo-inositol-1-phosphate which results in blue-turquoise colony appearance.

2.3 Chemicals

Chemicals and cell culture equipment were obtained from AppliChem, Baker, Biochrom, Carl Roth GmbH, Merck, Riedel-deHaen, Serva, and Sigma-Aldrich. For preparation of the defined MOD medium, chemicals with the highest purification grade available were used. Valinomycin, a depsipeptide antibiotic produced by *Streptomyces* spp., was from Sigma (≥ 98% TLC). The stock solution was prepared with 96% ethanol. Decoyinine, a nucleoside analog antibiotic produced by *Streptomyces* sp. S2113, was from Enzo life sciences (≥ 95% TLC). The stock solution was prepared with 1 M KOH solution. Other buffers and solutions were generally prepared with dH_2O or ddH_2O, respectively and autoclaved for 17 minutes at 121°C. Heat-labile substances were dissolved in ddH_2O and filtered through a sterile filter of 0.22 µm pore size. If necessary, the pH was adjusted.

For food additive experiments (Ch. 3.3), three different mixtures of food-grade, long-chain sodium polyphosphate salts (glassy, SPG) were obtained from BK Giulini GmbH (Ladenburg, Germany; Table 3). Stock solutions of 10% (w/v) were prepared with ddH_2O. The pH was adjusted to 6.8 with 3 M NaOH in order to exclude the influence of pH effects in the experiments. According to their solubilities, solutions of polyP 2 and 3 were filter sterilized, while polyP 1 solution was autoclaved (121°C, 10 min). Heat treatment has no effect on the functionality of polyPs (Loessner *et al.* 1997). Solutions were prepared freshly prior to each experiment.

Table 3: Properties of food-grade, long-chain sodium polyphosphates (polyPs) used[a]

PolyP blend	Mean P_2O_5 content (%) ± SD	Mean pH (1% solution) ± SD	Food additive declaration[b]
polyP 1	69.0 ± 1.0	6.0 ± 0.5	E 452[a], E 339[b]
polyP 2	68.0 ± 1.0	7.0 ± 0.5	E 452, E 339
polyP 3	68.5 ± 1.0	3.7 ± 0.3	E 452

[a] The mixtures were obtained from BK Giulini GmbH (Ladenburg, Germany).
[b] E 452, sodium polyphosphate; E 399, sodium orthophosphate

2.4 Food microbiology techniques

2.4.1 MPN method for enumeration of presumptive *B. cereus*

Presumptive *B. cereus* were enumerated with a 3-tube-3-dilution most-probable-number (MPN) method according to the international standard EN ISO 21871:2006 (“Microbiology of food and animal feeding stuffs - Horizontal method for the determination of low numbers of presumptive *Bacillus cereus* - Most probable number technique and detection method”). Retail foods and food ingredients obtained from industrial partners were prepared for the MPN test according to the standard guidelines EN ISO 8261:2001 (“Milk and milk products - Preparation of test samples and dilutions for microbiological examination”) and EN ISO 6887: Parts 1-5 (“Microbiology of food and animal feeding stuffs - Preparation of test samples, initial suspension and decimal dilutions for microbiological examination”). In brief, suspensions, emulsions or solutions of solid specimen were prepared by homogenizing 10 gram in 90 ml of quarter-strength Ringer's solution as specified for the product group. Usually, solid foods were homogenized for 5 min with a Stomacher while liquid foods remained undiluted. Of the food slurries, 10 ml were added to 10 ml double concentrated TSPB and 1 ml or 0.1 ml, respectively, were added to 10 ml of single concentrated TSPB. These inoculations were performed in triplicate, resulting in 9 test tubes for each sample. After incubation for 24 h at 30°C, growth was confirmed by streaking 10 µl (one loopful) of each test tube on one third of a MYP agar plate. After 24 and 48 hours of incubation, the MPN was calculated based on the number of tubes/agar tests confirmed positive for presence of *B. cereus* colonies. The MPN of *B. cereus* cells per gram of sample (statistical significance of $p<0.05$) was determined according to the standard prEN ISO 7218:2005 “Microbiology of food and animal feeding stuffs - General requirements and guidance for microbiological examinations” (German version). Both, colonies with characteristic *B. cereus* appearance and “atypical”, but pink colored colonies were isolated on MYP and PC agar for further differentiation by standard or multiplex PCR targeting the *ces* genes (Ch. 2.6.3).

Ringer's solution: 2.25 g/l $NaCl_2$
0.105 g/l KCl
0.12 g/l $CaCl_2$
0.05 g/l $NaHCO_3$
pH 7.0 ± 0.2 at 20°C

2.4.2 Detection of emetic *B. cereus* by standard and multiplex PCR

To detect cereulide producing *B. cereus*, genomic DNA or cell lysates were prepared from overnight cultures of the respective colonies and used as amplification template. A standard Thermo-Start-Taq PCR reaction (Ch. 2.6.3) was carried out with the primer pairs CesF1/CesR2 or 800F2/800R2 targeting different sites of the *cesB* gene (Table 4). For toxin gene profiling according to (Ehling-Schulz *et al.* 2006), primer pairs were used in a Thermo-Start-Taq PCR setup in the following concentrations: CesF1/CesR2 0.2 µM, CKF2/CKR5 0.4 µM, HD2F/HA4R 1 µM, and NA2F/NB1R 0.3 µM. The annealing temperature was set to 50°C and elongation was performed for 1 min.

Table 4: Oligonucleotides used for *ces* gene detection and toxin gene profiling of *B. cereus* strains

Primer	Sequence (5´- 3´)[a]	Target gene	Amplicon size (bp)	Reference[b]
800F2	GACAAGAGAAATTTCTACGAGCAAGTACAAT	*cesB*	635	(1)
800R2	GCAGCCTTCCAATTACTCCTTCTGCCCACAGT	*cesB*		(1)
CesF1	GGTGACACATTATCATATAAGGTG	*cesB*	1271	(2)
CesR2	GTAAGCGAACCTGTCTGTAACAACA	*cesB*		(2)
CKF2	ACAGATATCGGICAAAATGC	*cytK1*	421	(3)
CKR5	CAAGTIACTTGACCIGTTGC	*cytK1*		(3)
HD2F	GTAAATTAIGATGAICAATTTC	*hbl*	1091	(3)
HA4R	AGAATAGGCATTCATAGATT	*hbl*		(3)
NA2F	AAGCIGCTCTTCGIATTC	*nhe*	766	(3)
NB1R	ITIGTTGAAATAAGCTGTGG	*nhe*		(3)

[a] Sequence polymorphisms were covered by substituting strain specific bases by inosine (I).
[b] (1) (Ehling-Schulz *et al.* 2004); (2) (Ehling-Schulz *et al.* 2005); (3) (Ehling-Schulz *et al.* 2006).

2.4.3 Enrichment of *B. cereus* in food samples

Enrichment of *B. cereus* in food samples and food ingredients (Ch. 3.1) was performed according to the standard methods recommended by FDA (Food and Drug Administration), ISO (International Organization for Standardization), and LFGB (Lebensmittel-, Bedarfsgegenstände- und Futtermittelgesetzbuch). Therefor, 10 g of the food sample was added to 90 ml BHIG broth and homogenized with a Stomacher. Prior and after incubation at 30°C for 24 hours (static conditions), 500-µl aliquots were removed for subsequent TaqMan real-time analysis (Ch. 2.4.4). A second homogenized sample was equally prepared, but artificially inoculated with 10^3 CFU ml^{-1} *B. cereus* F4810/72 in order to monitor the efficiency of DNA extraction

from the matrix. The removed aliquots were centrifuged (13,000 rpm, 3 min) and stored at minus 20°C until use.

2.4.4 DNA extraction from food and TaqMan real-time PCR

DNA was isolated from spiked and unspiked, as well as enriched and non-enriched food samples with the NucleoSpin Food Kit (Macherey-Nagel) according to the manufacturer's instructions. The isolated DNA was further used in a TaqMan-based real-time PCR developed for specific detection of the *cesA* gene of the cereulide synthetase operon (Fricker *et al.* 2007). In brief, 25 µl-RT-PCR reactions contained 5 µl of isolated DNA, 0.5 µM of the primer pair ces_TaqMan_for/ces_TaqMan_rev targeting the *cesA* gene, and 0.5 µM of the primer pair IPC_for/IPC_rev targeting pUC19 plasmid (Fermentas) as internal amplification control in onefold Brilliant Multiplex QPCR Mater Mix (Stratagene). Additionally, pUC19 was provided in ca. 170 copies and the *cesA* and IAC probes (ces_TaqMan_probe [FAM/TAMRA] and IAC_probe [HEX/TAMRA]) were added to a final concentration of 0.2 µM. Reactions were run in a Smart Cycler (Cepheid) with the following cycling program: initial denaturation at 95°C for 10 min, followed by 40 cycles of 95°C for 15 sec, and 55°C for 60 sec, conducted with a thermal ramp of 2.5°C per second. A negative control reaction containing 5 µl of ddH_2O served to exclude the presence of contaminating DNA.

2.4.5 Artificial inoculation and growth of *B. cereus* in foods

Various foods were obtained from local consumer markets and prepared according to the manufacturers´ instructions if necessary. Prior to experiments, putative intrinsic *B. cereus* contamination was tested by plating on selective MYP agar. PolyP-free organic oat milk and a polyP-free dairy-based infant food formula obtained from German retail served as model food matrices in toxin inhibition experiments (Ch. 3.3). In these cases, polyP stock solutions were added aseptically to the food in desired concentrations and batches were homogenized with a stomacher. Under sterile conditions, 30-g portions of the foods were filled in Petri dishes and were spot inoculated with four 25-µl drops of *B. cereus* wild type or reporter strain overnight cultures, respectively. This resulted in an approximate cell titer of 10^3 CFU per gram. One series was instantly used to determine the initial cell count (see below), while the remaining plates were sealed to prevent moisture evaporation and were incubated for 24 h at 24°C to simulate food spoilage. Immediately after inoculation as well as after incubation (24 h, 24°C), enumeration of viable cell counts was carried out for both strains. Therefor, whole portions of food (30 g) were comminuted with 270 ml of a 0.025 % Tween 80 solution (pH 7.0) using a Stomacher. The homogenates were serially 10-fold diluted in LB broth and 100 µl were spread in double on LB (wild type) or LB plates supplemented with 5 µg ml^{-1} chloramphenicol (reporter strain) for conventional plate counting. Colonies with characteristic appearance were counted after 16-20 h incubation at 30°C. The increase in viable cell counts per gram of food within 24 h [N_i, expressed as $\log_{10}$ CFU g^{-1}] was determined as follows: $N_i = N_{24}-N_0$ (where N_{24} is the $\log_{10}$ CFU g^{-1} after 24 h and N_0 is the $\log_{10}$ CFU g^{-1} directly after inoculation).

Food samples prepared in parallel were used to determine cereulide production by *B. cereus* F4810/72 after 24 h (see Ch. 2.4.7 and Ch. 2.9.1). Samples spiked with the luminescent reporter strain were used to monitor cereulide synthetase promoter activity (Ch. 2.4.8).

2.4.6 Extraction of foods for cereulide quantification

For cereulide quantification by HPLC-MS and HEp-2 assays, untreated foods or model foods artificially spiked with *B. cereus* F4810/72 wild type (see Ch. 2.4.5) were used. Each food sample (30 g) was extracted with 20 ml of 96% ethanol by shaking on a rocking table (24 h, 23°C). The extracts were centrifuged twice (8,500*g*, 20 min, 23°C) to remove extraction residuals and food debris. To estimate the toxin recovery rate, control samples were spiked with the commercially available, structurally related depsipeptide valinomycin to a final concentration of 25 µg g^{-1}. These samples were left for one hour at RT, and were then extracted as described above. To exclude an interfering toxic background effect of the food extracts on the HEp-2 cells in the cytotoxicity bioassay (Ch. 2.9.1) and to exclude that foods inherently contained cereulide, extracts of unspiked control food samples were additionally included. Prior to analytical measurements (Ch. 2.4.7) supernatants were membrane filtrated (0.2 µm; PTFE membrane, Phenomenex).

2.4.7 Cereulide quantification (HPLC/ESI-TOF-MS)

Analysis of cereulide amounts in model food extracts (Ch. 3.3) was performed with high-performance liquid chromatography (HPLC)/electrospray ionization-time of flight mass spectrometry (ESI-TOF-MS). Therefore, an Agilent rapid resolution HPLC system (series 1200) connected to a time-of-flight mass spectrometer (G1969A; 6210 TOF LC/MS) running in the positive electrospray ionization mode was used. Chromatographic separation was performed on a Prontosil 120-3-C18 column kept at 50°C (100 mm x 2 mm i.d., 3 µm; Bischoff Chromatography) by 20 µl sample injection and MeOH/H_2O as mobile phase (flow rate 200 µl min^{-1}). Prior to starting a chromatographic run, the composition of the mobile phase was kept at 100% solution A. Separation was developed by increasing solvent B to 30% within 1 min followed by a linear gradient of solvent B from 30% to 100% within 8 min. The effective mobile phase was held for 16 min, with an increased flow rate (250 µl min^{-1}) in the last 4 min. After each run, the composition was reset to 100% solution A. HP-0921 and purine (ES-TOF Reference Mass Solutions; Agilent) in solution B were used as mass correcting standards being continuously mixed in the post-column flow (100 µl min^{-1}). ESI interface parameters were as follows: 350°C drying gas temperature, 7 L min^{-1} drying gas flow and 45 psig nebulizer gas pressure. For mass spectrometric detection (positive ion polarity mode) capillary and `fragmentor´ voltage were set to 5000 V and 250 V, respectively. Each sample was measured at least in triplicate. Data were acquired and processed with the Mass Hunter Workstation software (B.01.02, Agilent). Valinomycin served as a surrogate calibration standard for cereulide quantification. Standard dilutions were analyzed at least once in each sample sequence. To quantify cereulide and valinomycin abundance, integrated extracted ion current (EIC) chromatograms with ion ranges

(m/z) of 1,170.5 to 1,193.5 for cereulide and of 1,128.5 to 1,151.0 for valinomycin targeting the NH_4^+ and K^+ adducts, respectively, were used (compare Pitchayawasin *et al.* 2003). Calibration curves extrapolated from integrated peak areas were plotted to calculate cereulide amounts *via* linear regression.

Solvent A:	MeOH/H_2O 10:90 (v/v) 10 mM ammonium acetate pH 7.4	Solvent B:	MeOH/H_2O 90:10 (v/v) 10 mM ammonium acetate pH 7.4

2.4.8 Reporter gene analysis of *ces* promoter activity in model foods

For visualization and quantification of the *ces*P1-promoter driven luciferase activity, *B. cereus* F4810/72[P_1/*lux*] was grown on agar plates or in foods as described above (Ch. 2.4.5). Images were captured after 24 h with a photon-counting ICCD camera (Hamamatsu Photonics, model 2400-32) and bioluminescence intensity (acquired for 2 sec with a binning factor of 1) was superimposed on grey-scale images as false color renderings. Quantification of the total photon counts via region of interest (ROI) analysis was performed according to instructions of the Living Image 2.10 software (Caliper Life Sciences) and the implemented IGOR Pro 4.01 software tool (WaveMetrics). The circle ROI tool was used to manually define the entire Petri dish area as the ROI (dimensions were kept constant throughout all experiments), and the bioluminescence intensity was recorded as the total photon counts for all pixels inside the ROI (total counts). An empty area in the image was included as average background ROI to correct for auto-fluorescence of the samples and was used for background correction of the signals.

2.5 Computational techniques / *in silico* analyses

Raw data analysis and graph generation, as well as curve fitting, non-linear regression, and statistical analyses (Student's t-test) were performed with SigmaPlot 09 (Systat Software). For processing DNA and protein sequence data, and to design oligonucleotide primers for standard PCR and qPCR, Vector NTI™ suite 8 (Invitrogen) was used. Nucleotide sequences of *B. cereus* and *B. subtilis* strains were obtained from the Entrez Genome database of the National Center for Biotechnology Information (NCBI) (http://www.ncbi.nlm.nih.gov). DNA or protein homology search was performed on the NCBI Basic Local Alignment Search Tool (BLAST) server (Altschul *et al.* 1997). Identification of orthologous transcription factors was performed according to the Best Reciprocal Hit (BRH) method (Altschul *et al.* 1997) using a reciprocal BLASTP search approach (Altschul *et al.* 1990; Remm *et al.* 2001). The bidirectional matching protein pairs (or symmetrical best hits: BeTs) were finally considered as orthologs when the degree of AA similarity was ≥ than 50% (Chothia and Lesk 1986; Sander and Schneider 1991) and the randomly defined, conservative significance threshold (Expectation value or E-value) of $E= 1 \times 10^{-10}$ was not exceeded. Information on gene regulation and functions of proteins in *B. subtilis* were obtained from the SubtiWiki database (http://www.subtiwiki.uni-goetingen.de/wiki/index.php/Main_Page) (Lammers *et al.* 2010). Signal peptide prediction was

carried out on the SignalIP 3.0 server, accessible at http://www.cbs.dtu.dk/services/SignalP/ (Bendtsen *et al.* 2004). Protein structures were obtained from the RSBC PDB protein databank (http://www.rsbc.org) and protein structure visualization was performed with the PyMOL software (available at http://www.pymol.org/). *In silico* prediction of CodY binding sites in the *B. cereus* F4810/72 genome was performed with the xBASE 2.0 genome database accessible at http://xbase.bham.ac.uk (Chaudhuri *et al.* 2008). The proposed CodY consensus binding motif AATTTTCWGAAAATT (den Hengst *et al.* 2005; Belitsky and Sonenshein 2008) was used to query putative CodY boxes in a region restricted from +400 to -100 nucleotides relative to the translational start site of the genes. Settings were allowed to include sequences with up to three mismatches from the consensus box. *In silico* footprinting on the *ces* operon promoter region was carried out on the Database of Transcriptional Regulation in *Bacillus subtilis* (DBTBS) server accessible under http://dbtbs.hgc.jp (Sierro *et al.* 2008).

2.6 Nucleic acid techniques

2.6.1 Isolation of plasmid DNA from *E. coli*

Depending on the DNA amount needed, plasmid DNA was purified from exponential growth phase cultures of *E. coli* strains using the GenElute Plasmid Miniprep Kit (Sigma) or the Pure-Link HiPure Plasmid Midiprep Kit (Invitrogen) following the manufacturers´ manuals.

2.6.2 Isolation of genomic DNA from *Bacillus* spp.

Genomic DNA of *B. cereus* F4810/72, *B. cereus* food isolates, and *B. subtilis* subsp. *subtilis* str. 168 was isolated from overnight cultures with the Gentra Puregene Yeast/Bacteria Kit (Qiagen). Prior to purification according to the manufacturer´s protocol, cells were disrupted with 0.1 mm zirconia/silica-beads (Carl Roth GmbH) in a RiboLyser homogenizer (Hybaid) to increase DNA yields.

2.6.3 Standard PCR

Oligonucleotide primers used in this work are listed in the Tables 5, 6, and 7. In general, 10 to 60 ng plasmid DNA or 50 to 400 ng chromosomal DNA were used as template. For cloning purposes, high fidelity DNA amplification was carried out with either *Pfu* DNA Polymerase (Promega) or Herculase II Fusion DNA Polymerase (Agilent/Stratagene). Colony PCR with the GoTaq Flexi DNA Polymerase (Promega) was used for plasmid or insert detection after transformation or conjugation of bacteria. For this purpose, cell material was dissolved in 100 µl of ddH_2O, boiled for 5 min, centrifuged (2 min, 13,000 rpm), and 1 to 2 µl of the supernatant were used as reaction template. For toxin gene profiling of *B. cereus* strains hot-start PCR with the Thermo-Start *Taq* DNA Polymerase (Thermo Scientific) was performed, in order to reduce non-specific amplification in the multiplex reactions. Annealing temperatures were 46 to 70°C

depending on the PCR type and the melt temperature of the oligonucleotides used, respectively. $MgCl_2$ solution (25 mM) and dNTPs (20 mM) were purchased from Thermo Scientific.

Pfu PCR (50 µl volume)			Cycling program		
40.5 µl	ddH_2O		Initial denaturation	94°C	2 min
5 µl	*Pfu* 10x buffer		Denaturation	94°C	30 sec
50 pmol	3'-oligonucleotide	30x	Annealing	Tm-5°C	30 sec
50 pmol	5'-oligonucleotide		Extension	72°C	2min/kb
0.4 mM	each dNTP		Final extension	72°C	8 min
1.5 U	*Pfu* polymerase				

Herculase PCR (50 µl volume)			Cycling program		
32 µl	ddH_2O		Initial denaturation	95°C	4 min
10 µl	Herculase 5 x buffer		Denaturation	95°C	25 sec
20 pmol	3'-oligonucleotide	30x	Annealing	Tm-5°C	30 sec
20 pmol	5'-oligonucleotide		Extension	72°C	30sec/kb
0.4 mM	each dNTP		Final extension	72°C	8 min
1.5 U	Herculase II Fusion polymerase				

Go TaqFlexi PCR (25 µl volume)			Cycling program		
16 µl	ddH_2O		Initial denaturation	95°C	2 min
5 µl	GoTaq 5 x buffer		Denaturation	95°C	35 sec
25 pmol	3'-oligonucleotide	25x	Annealing	Tm-7°C	30 sec
25 pmol	5'-oligonucleotide		Extension	72°C	1.5min/kb
0.4 mM	each dNTP		Final extension	72°C	5 min
1.5 mM	$MgCl_2$				
1.2 U	GoTaq Flexi polymerase				

Thermo-Start Taq PCR (50 µl volume)			Cycling program		
36.85 µl	ddH_2O		Initial denaturation	95°C	15 min
5 µl	10 x buffer		Denaturation	95°C	30 sec
50 pmol	3'-oligonucleotide	30x	Annealing	Tm-5°C	30 sec
50 pmol	5'-oligonucleotide		Extension	72°C	1min/kb
1.5 mM	each dNTP		Final extension	72°C	4 min
1.5 mM	$MgCl_2$				
1.0 U	Thermo-Start Taq polymerase				

2.6.4 DNA agarose gel electrophoresis

DNA samples (3 to 30 µl) were premixed with 6x loading dye solution (Fermentas). Buffer for DNA agarose gel electrophoresis was 1x TAE (Sambrook *et al.* 1989). Gels were run in horizontal gel chambers with a constant voltage of up to 10 V/cm gel lengths for 20 to 60 minutes depending on the loaded fragment size. Gels were stained with ethidium bromide (0.5 µg ml^{-1}) and photographed under UV light. GeneRuler 100 bp DNA ladder or GeneRuler DNA Ladder Mix (Fermentas) was used to determine the size and amount of DNA fragments.

Agarose gel:	0.8-2% (w/v) agarose	TAE:	2 M Tris
(0.8-2%)	in 1x TAE	(50x)	1 M acetic acid
			0.05 M Na_2EDTA
			pH 8.3 (acetic acid)

2.6.5 Enzymatic modification of DNA

All molecular cloning procedures were carried out using standard techniques (Ausubel *et al.* 1987; Sambrook and Russell 2001). In general, 1 µg of plasmid DNA or 200 ng of PCR products were digested (37°C for 1-4 h) with 1 to 5 U of restriction enzymes (Fermentas) using the appropriate buffer system (Fermentas). If blunt or single cut, linearized plasmids were dephosphorylated with 1 to 2 U of Shrimp Alkaline Phosphatase for 30 min at 37°C (Fermentas) to avoid religation. Ligation of vector and insert DNA (in total 0.15 to 1 µg) was carried out in molar rations of 1:1, 1:3, and 3:1, using T4 DNA ligase at 22°C or 15°C for 1 to 12 hours, according to the manufacturer's recommendation (Fermentas, Promega, or Roche).

2.6.6 Purification and concentration of DNA fragments

Restricted plasmid DNA and probes for gel mobility shift assays were purified from agarose gels with the E.Z.N.A Gel Extraction Kit (OMEGA Bio-Tek). PCR amplification products and restricted PCR products were purified with the E.Z.N.A Cycle Pure Kit (OMEGA Bio-Tek).

2.6.7 Isolation of total RNA from *B. cereus*

For RNA isolation, aliquots of 1 to 2 ml were removed from *B. cereus* cultures at intended growth phases, harvested (10,000*g*, 4°C, 2 min), frozen in liquid nitrogen, and stored at -80°C. Pellets were thawed on ice, resuspended in 900 µl TRIzol reagent (Invitrogen) and homogenized with a RiboLyser (Hybaid) using 0.1 mm zirconia/silica beads (Carl Roth GmbH). Chloroform (200 µl) was added for phase separation, and the RNA-containing aqueous phase was collected after centrifugation (12,000*g*, 4°C, 15 min). RNA was precipitated with 500 µl of 100% isopropanol (12,000*g*, 4°C, 10 min), and washed once with 1000 µl of 75% ethanol. 5 µg of RNA were subsequently treated with 10 U RQ1 DNase I (Promega) to degrade contaminating DNA. Again, proteins were separated by treatment with 100 µl chloroform (15,000*g*, 4°C, 15 min). After sodium acetate/ethanol precipitation (1/10 volume of 3M NaOAc pH 5.2 in 96% EtOH), RNA was washed twice with 70% ethanol, dried at room temperature, and resuspended in DEPC-treated ddH_2O. RNA purity and quantity were determined by monitoring the ratio of UV absorbance at 260/280 nm and by agarose gel electrophoresis. Efficacy of DNA removal was confirmed using RNA as PCR template along with 16S primers (Table 5.4).

2.6.8 Reverse transcription (RT-PCR)

For quantification of relative *ces* gene expression (Ch. 3.3.2), cDNA was synthesized using M-MLV Reverse Transcriptase (RNase H Minus, Promega) and gene specific reverse primers (Table 5) targeting the reference *rrn* gene (16S rDNA) and *cesA*, respectively. First, primer annealing was carried out by heating a mixture of 100 ng of total RNA, 2 pmol of reverse primer, and 1 mM of each dNTP in a 8-min-temperature ramp (75°C-70°C-65°C-60°C-55°C-

50°C-45°C-42°C), which was hold at 42°C. Then, cDNA synthesis was initiated by adding 100 U reverse transcriptase, 20 U RNase OUT, and 10 mM DTT (all Invitrogen). The reaction was incubated for 1 hour at 42°C.

For quantification of multiple virulence factor mRNA levels in the same RNA preparations (Ch. 3.5.2), cDNA synthesis was carried out with random hexamer primers in order to reduce the intersample variations that might occur due to slightly different RT conditions in individual reactions (Pfaffl 2001). In this case, first strand synthesis of 1 µg of total RNA was performed with the qScript cDNA Supermix following the manufacturer´s protocol (Quanta Biosciences). First strand synthesis was checked by conventional PCR using gene specific forward and reverse primers with 1 µl of cDNA reaction mixture as template.

2.6.9 Quantitative real-time PCR (qPCR)

Quantitative real-time PCR (qPCR) was performed in 25-µl singleplex reactions containing 1 µl of cDNA (equivalent to 10 ng total RNA), 2 pmol of gene specific primers (Table 5), and one fold SYBR Green I Mastermix (ABgene). Reactions were run in a Smart Cycler II (Cepheid) with following cycling conditions: initial polymerase activation (95°C, 15 min), 40 amplification cycles (95°C for 30 sec; annealing temperature Tm (Table 5) for 30sec; 72°C for 45 sec), and final melting curve generation of the amplicons with a ramp of 0.2°C/sec (Tm to 95°C). The melting temperature of the amplicons was analyzed for each reaction to ensure specificity of amplification and suitable C_t values (cycle at which fluorescence of the reaction reaches the threshold level) were recorded.

To monitor gene expression in a given sample compared to an external reference condition (calibrator sample), relative gene expression ratios (RE) were calculated with the REST (Relative Expression Software Tool) method according to Pfaffl (Pfaffl 2001; Pfaffl *et al.* 2002). For reasons of comprehensibility, the developed mathematical model is given in Equation 1.

$$\mathrm{RE} = \frac{(E_{\mathrm{target}})^{\Delta \mathrm{Ct}_{\mathrm{target}}\,(\mathrm{calibrator\text{-}sample})}}{(E_{\mathrm{reference}})^{\Delta \mathrm{Ct}_{\mathrm{reference}}\,(\mathrm{calibrator\text{-}sample})}}$$

Equation 1: Mathematical model underlying the REST software tool (Pfaffl *et al.* 2002) used for determination of relative gene expression in qPCR experiments. *RE*, relative quantification of target gene in comparison to a reference gene; *E*, primer-specific PCR efficiency; *target,* gene of interest; *reference,* housekeeping gene; *calibrator,* external reference condition (i.e., control); *sample,* condition of interest; Δ*Ct,* difference in Ct values between calibrator and sample.

The 16S rDNA (*rrn*) gene was used as reference gene throughout all experiments. C_t values of the untreated *B. cereus* F4810/72 control culture harvested at an OD_{600} of 1 were used as external reference condition in polyP experiments (Ch. 3.3.2). To assess *cesA* expression kinetics (Ch. 3.5.1), C_t values of samples harvested from *B. cereus* F4810/72 cultures at an

OD_{600} of 0.2 were set as calibrator. For quantitation of virulence factor expression in the *codY* strain (Ch. 3.5.2), C_t values of wild type samples harvested at the same optical density as the mutant samples served as calibrator. Primer-specific PCR efficiency (*E*) was routinely determined by a decimal cDNA calibration-dilution curve analysis with following slope calculation according to $E=10^{[-1/slope]}$ (Pfaffl 2001). Only primer pairs with a high linearity (correlation coefficient r > 0.990), and with an amplification efficiency of *E* = 1.60 to 2.10 were used for qPCR experiments.

Table 5: Oligonucleotides developed for qPCR

Primer	Sequence (5´- 3´)	Target gene / NCBI locus tag[a,b]	Tm[c] (°C)	Reference[d]
16SA1	GGAGGAAGGTGGGGATGACG	*rrn*	63.0	(1)
16SA2	ATGGTGTGACGGGCGGTGTG	*rrn*		(1)
cesA_for	GATTACGTTCGATTATTTGAAG	*cesA* BcAH187_pCER270_0023	53.0	(2)
cesA_rev	CGTAGTGGCAATTTCGCAT	*cesA* BcAH187_pCER270_0023		(2)
cesB_for	TTAGATGGTATTCTTCACTTGGC	*cesB* BcAH187_pCER270_0022	57.0	(2)
cesB_rev	TTGATACAAATCGCATTCTTATAACC	*cesB* BcAH187_pCER270_0022		(2)
QcodY_for	GCATTTACGATTACCGAACGAG	*codY*; BCAH187_A3875	57.8	This study
QcodY_rev	AAATTGAAGAAGAAGCACGTAGC	*codY*; BCAH187_A3875		This study
QnheA_for	AGCGGCTCTTCGTATTCA	*nheA*; BCAH187_A1995	53.0	This study
QnheA_rev	GCCTCTGCTTCAGTTTGT	*nheA*; BCAH187_A1995		This study
Qclo_for	TCTTGCAGGTAACGTATGTG	*clo*; BCAH187_A3327	55.0	This study
Qclo_rev	GGCTGGAGCAGTAGATGATTT	*clo*; BCAH187_A3327		This study
QinhA1_for	TCTCTACGTATTTTTCGACAGC	*inhA1*; BCAH187_A1437[e]	56.4	This study
QinhA1_rev	AATCCACTACACCAAGGAAAC	*inhA1*; BCAH187_A1437[e]		This study
QinhA2_for	CACCAGCATGGAGTGTAA	*inhA2*; BCAH187_A0800[f]	54.0	This study
QinhA2_rev	AACGCCTTGTAATCCAGAA	*inhA2*; BCAH187_A0800[f]		This study
QinhA3_for	CGCATCAGCACCATAATCT	*inhA3;* BCAH187_A3035[g]	55.0	This study
QinhA3_rev	ATCTGGCGGAAGCTACAC	*inhA3;* BCAH187_A3035[g]		This study
Qnpr599_for	TCTGGAACGGATCACAAAT	*npr599*; BCAH187_A0727	54.0	This study
Qnpr599_rev	TCGTGACCAATAACATCAATAC	*npr599*; BCAH187_A0727		This study
Qsph_for	GACGAGTACGTCCTATTTGGTG	*sph*; BCAH187_A0805	58.3	This study
Qsph_rev	CAAATGACGGGTTCGCATGGTC	*sph*; BCAH187_A0805		This study
QplC_for	AGTGACGGATGGAAATGGAT	*plC*; BCAH187_A0804	53.9	This study
QplC_rev	CTGAATGTATCCAGCAGTAAC	*plC*; BCAH187_A0804		This study
spo_F_RT	AGCGTTTGGACAAGAAGATG	*spo0A*; BCAH187_A4301	56.0	(3)
spo_R_RT	TATGAGCAGGCACACCAAT	*spo0A*; BCAH187_A4301		(3)
abrB_for	TCGTGTAGTAATTCCGATTGA	*abrB*; BCAH187_A0046	54.0	(3)
abrB_rev	TGAAGCTCGTTTAAGATTTGC	*abrB*; BCAH187_A0046		(3)
QplcR_for	TCTCTGCCTCATCATACTCC	*plcR*; BCAH187_A5529	54.0	This study
QplcR_rev	AAGGCGATTGAAATATCTTGC	*plcR*; BCAH187_A5529		This study
QilvE_for	TCGCCTAGTTGTATCGAGAGG	*ilvE1*; BCAH187_A1555	59.8	This study
QilvE_rev	ACTCCAGCCAATTTCGCTTCG	*ilvE1*; BCAH187_A1555		This study

[a] Accession number of the pCER270 (also designated pBCE or pAH187_270) plasmid sequence: GenBank [DQ889676] (Rasko *et al.* 2007).
[b] Accession number of the *B. cereus* AH187 genome sequence: GenBank [CP001177], RefSeq [NC_011658].
[c] Tm, annealing temperature.
[d] (1) (Martineau *et al.* 1996); (2) (Dommel *et al.* 2011); (3) (Lücking 2009).
[e] Immune inhibitor A metalloprotease InhA1; 93% AA identity to *Bcer* ATCC14579 InhA1 [locus tag: BC1284].
[f] Immune inhibitor A metalloprotease; 96% AA identity to *Bcer* ATCC14579 InhA2 [locus tag: BC0666].
[g] Immune inhibitor A; 95% AA identity to *Bcer* ATCC14579 InhA3 [locus tag: BC2984].

2.7 Transformation and mutagenesis of bacteria

2.7.1 Transformation of *E. coli*

Preparation of chemically competent *E. coli* cells was performed according to a standard protocol using $MgCl_2$ and $CaCl_2$ solutions (Sambrook and Russell 2001). For transformation, 100-µl aliquots of competent cells were thawed on ice and mixed with ligation reactions (20 to 800 ng total DNA) or plasmids (10 to 100 ng DNA). After 15 to 30 min incubation on ice, cells were heat-shocked for 60 seconds at 42°C, and again placed on ice for 2 min. For regeneration, 900 µl SOC broth was added followed by an outgrowth at 37°C for 45 min to 90 min. Cells were spread on appropriate selective media and incubated at 37°C.

2.7.2 Transformation of *B. cereus*

Prior to electroporation in *B. cereus*, plasmids were transferred in non-methylating *E. coli* INV110 to enhance transformation efficiency. Additionally, INV110-isolated plasmid samples were desalted by drop dialysis on a cellulose filter disc (V-type, 0.025µm, Millipore) floating on ddH_2O for 20 min. For preparation of electrocompetent *B. cereus* cells, a pre-culture was diluted 1:100 in fresh LB medium supplemented with 2% (w/v) glycine and incubated until an OD_{600} of 0.5 to 0.6 was reached. Washing of the culture was achieved by repeated centrifugation (3,500*g*, 4°C, 10 min) and gentle resuspension in ice-cold glycerol solutions ($1/5^{th}$ of culture volume): first in 2.5%, then in 5%, and in 10%. Finally, cells were resuspended in $1/100^{th}$ volume of 10% glycerol and aliquots of 100 µl were frozen in liquid N_2 and stored at -80°C.
For electroporation, cells were thawed on ice, carefully mixed with 0.5 to 2 µg plasmid DNA and incubated on ice for 1 to 2 min. Mixtures were then transferred to pre-cooled electroporation cuvettes with 0.4 cm gap width and pulsed (U = 2.0 kV, R = 200 Ω, C = 25 µF). Cells were supplied with 1 ml pre-warmed LB broth and outgrown for 2 hours at 30°C. Cells were spread on selective LB medium plates and incubated for at least 1 day at 30°C.

2.7.3 Allelic gene replacement by heterogramic conjugation

To achieve gene disruption in *B. cereus* group strains, transfer of suicide vectors such as pAT-constructs by heterogramic conjugation has proved to be a successful strategy. To construct a pAT-plasmid derived suicidal vector, upstream and downstream flanking regions of the gene to be inactivated (GOI) were amplified by PCR thereby introducing restriction sites compatible to the TOPO/spc vector. Both PCR products were cut, sequenced (TOPO2.1_for and TOPO2.1_rev), and cloned on either side of a spectinomycin (*spc*) resistance cassette in the TOPO/spc vector. This construct was further subcloned in the MCS of the conjugative suicide vector pAT113 either by direct excision or by PCR amplification. The resulting construct was sequenced with pAT113_for and pAT113_rev to ensure correct orientation. The plasmid was introduced in *E. coli* JM83/pRK24, a strain that carries the self-transferable IncP plasmid

pRK24, which is capable of plasmid mobilization (Thomas and Smith 1987). *E. coli* JM83/pRK24/pAT113ΔXY/spc was used as the donor strain in a heterogramic conjugation and mating procedure as described previously (Pezard *et al.* 1991; Trieu-Cuot *et al.* 1991). Therefore, *B. cereus* F4810/72 and the conjugal strain were grown in LB medium to an optical density of 0.5. 50 ml of *E. coli* culture were harvested (7,500 rpm, 22°C, 5 min) and carefully washed once with 10 ml LB medium. For mating, 5 ml of the *B. cereus* culture were added, the pellet was carefully resuspended and the strain mixture was harvested (7,500 rpm, 22°C, 5 min). After addition of 1 ml LB medium, the cell mixture was dropped on two 0.45-µm HA filter disks (Millipore) placed on a LB agar plate without antibiotics and incubated bottom-down for 12 to 18 h at 37°C. For transconjugant selection, bacteria were removed from the filter disks and resuspended in a solution containing colicin D and colicin E. Colicin solutions were obtained by cholorform extraction of mitomycin C-induced cells of *E. coli* ColD or *E. coli* E3 respectively. To select for gene deletion mutants, the bacterial solutions were spread in 300-µl aliquots on LB plates containing 100 µg ml^{-1} spectinomycin and 100 mg ml^{-1} polymyxin. After incubation at 30°C for 1 day, transconjugants were screened for allelic exchanges due to double crossover recombination events. Positive candidates were spectinomycin resistant, but sensitive to erythromycin. Moreover, loss of the pAT113 plasmid backbone, correct localization of the insertion and presence of the *spc* cassette was confirmed by PCR and sequencing.

2.7.4 Construction of *E. coli* protein expression strains

For recombinant protein expression, DNA fragments encoding *ccpA*, *codY*, *comK*, *perR*, and *sinR* were amplified from genomic DNA of *B. cereus* F4810/72 using the oligonucleotide primer pairs listed in Table 6. The *degU* gene was amplified from genomic DNA of *B. subtilis* 3610. To achieve C-terminal His_6-tag-fusions constructs, gene stop codons were replaced by a *Xho*I restriction site and start codons were integrated in the *Nco*I restriction site. N-terminal protein-His_6-tag-fusions were obtained by restriction with *Nde*I and *Xho*I. The gene start codon was integrated in the *Nde*I site and the *Xho*I site was placed downstream of the stop codon to avoid read-through. Fragments were ligated into the equally cut expression vector pET28b(+). Constructs were verified by double stranded sequencing using the primers pET28_for and pET28_rev.

Table 6: Oligonucleotides developed for cloning and mutational purposes

Oligonucleotide and purpose	Sequence (5´-3´)[a]
Construction of *codY* null mutant	
CodY1Kpn_for	CC**GGTACC**ATTTTAGATGTAAGAAGTTT
CodY1Spe_rev	GG**ACTAGT**AAATTCTTACATGAACTTGC
CodY2Xho_for	G**CTCGAG**GTTTTTGCTAATAATTCCAT
CodY2Xba_rev	G**TCTAGA**TCGCATTGTGAAAGAAGAAA
CodY_for	CGAAGATGTGCTCGATTGCTTC
CodY_rev	CGTTATTACAGAGCGCAGCAGG
CodYfl1_for	CACGTAAGAAGTCAATTGCCTTC
CodYfl2_rev	AAGAATTGTAGAATCGTAAGGGA
SPCF2	GGAAGTTCAATAGTTGGAGTATATC
SPCR2	CTTAACGAGTGCTTTCACCTTTG
pAT113_for	ATGACCATGATTACGCCAAGC
pAT113_rev	AGATCCGCGCGAGCTGTA
TOPO2.1_for	CTGGCCGTCGTTTTAC
TOPO2.1_rev	GTCATAGCTGTTTCCTG
Overexpression of *codY* in *B. cereus*	
CodY-R2_pWH1520	CGC**ACTAGT**ATGGAATTATTAGCAAAAAC
CodY-Pro_R	GG**GCATGC**TTAGTTTGTTTTCAATTTAG
pWH1520_for	GTTCACTTAAATCAAAGGGG
pWH1520_rev	GTCGGATCAATTCATCGATA
TetR_for	CGATGAAGATGGATTTTCTATTATTGC
TetR_rev	CGATTTAGAAATCCCTTTGAGAATGT
Construction of reporter strains	
iGFP_1Kpn	GAG**GGTACC**GAGTTATGAATGAAAATTCT
iGFP_1Xba	GGG**TCTAGA**TGAAAAATCCCTCTTTTAAA
iGFP_RSpe	GTG**ACTAGT**GGATTTGTCCTACTCAAGCT
iGFP_2EcoRV	GCG**GATATC**ATGAAACACATAGAGCATAA
iGFP_2Xho	ACA**CTCGAG**CACTAATTTATAGACTGCCA
iGFP_2Sal	GAA**GTCGAC**CACTAATTTATAGACTGCCA
iGFP_for	GATGAAATTCATAGCTAGGGGGGATT
iGFP_rev	GCATCTCCATCATCCCCCCATTATGTAA
pXen1MCS_for	GATTAAGTTGGGTAACGCCA
pXen1MCS_rev	TGTAAGCAAAAAGTTTCCAA
Overexpression of His_6-tag proteins in *E. coli*	
CodYEXNde_for	GCG**CATATG**GAATTATTAGCAAAAACA
CodYEXXho_rev	GGG**CTCGAG**GAGAAGAGTTTTATAAATTA
CcpAEXNco_for	CTG**CCATGG**AGATGAACGTAACAATAT
CcpAEXXho_rev	AGA**CTCGAG**CTTCGTTGAATCTCTAAA
ComKNco_for2	ACG**CCATGG**ATATGGAAAGTAAAGTAGAA
ComKXho_rev2	TGT**CTCGAG**CACATCCTCTTCTCTAAC
PerR2Nco_for	GAT**CCATGG**CGGTGGTCAAAGAAGAAT
PerR2Xho_rev	TTA**CTCGAG**CGCCTTATGACACTCTGG
ResDEXNco_for	CGC**CCATGG**TGAACCGTTGTGGTAAAA
ResDEXXho_rev	CTG**CTCGAG**GTCGTTCACAACCTCAAA
SinREXNco_for	ACG**CCATGG**ATATGATTGGAGAACGTATA
SinREXXho_rev	GTC**CTCGAG**TTTTTGATCTTGCTTCCATTTT
DegUEXNco_for [b]	GTC**CCATGG**TTGTGACTAAAGTAAACA
DegUEXXho_rev [b]	TAT**CTCGAG**TCTCATTTCTACCCAG
pET28_for	TTAATACGACTCACTATAGGGG
pET28_rev	GCTAGTTATTGCTCAGCGG

[a] Restriction sites are in boldface.
[b] Expression of *B. subtilis* subsp. *subtilis* NCIB3610 DegU protein.

2.7.5 Construction of a *B. cereus codY* deletion mutant

To construct a *B. cereus* F4810/72 *codY* null mutant, flanking regions of the *codY* gene were amplified with the primer pairs CodY1Kpn_for/CodY1Spe_rev (5´ region) and CodY2Xho_for/CodY2Xba_rev (3´ region). Obtained fragments were digested with *Kpn*I/*Spe*I or with *Xho*I/*Xba*I, respectively, and successively cloned into the spectinomycin cassette containing TOPO-derivative to produce TOPOΔcodY/spc. The gene exchanging construct was then introduced into pAT113 by *Kpn*I and *Xba*I restriction, giving rise to the suicidal vector pAT113ΔcodY/spc, which was further introduced into *E. coli* JM83/pRK24 for heterogramic conjugation. After mating, gene disruption by double crossover events was identified as described above (Ch. 2.7.3). PCR and context sequencing with the primer pairs SPCF2/SPCR2 and CodYfl1_for/CodYfl2_rev confirmed the appropriate genetic locus of the spectinomycin cassette and total gene inactivation was confirmed by qPCR (QcodY_for/QcodY_rev) and immunoblotting (Ch. 2.8.7) with a rabbit polyclonal anti-CodY antibody (Joseph *et al.* 2005) kindly provided by A.L. Sonenshein, Tufts University, USA.

2.7.6 Construction of a *B. cereus codY* overexpression strain

The *codY* ORF lacking its own promoter was amplified using CodY-Pro_R and CodY-R2_pWH1520. The fragment was introduced in the *Spe*I and *Sph*I restriction sites of pWH1520 to obtain pWHCodY, in which *codY* expression is under transcriptional control of a xylose-inducible promoter (Rygus and Hillen 1991). The plasmid was passaged through the non-methylating *E. coli* strain INV110 and further introduced in *B. cereus* F4810/72 by electroporation. Maintenance was verified by PCR specifically targeting the pWH1520 vector (primer: pWH1520-for/pWH1520-rev and TerR_for/TetR_rev). The expression of *codY* in complementation and overexpression strains was confirmed by qPCR and quantified by Western Blot analysis (Ch. 2.8.7). To induce and monitor overexpression, a 10% (w/v) D-xylose stock solution was added to final concentrations of 0.01%, 0.05% and 0.1% (v/v), respectively.

2.7.7 Construction of *ces*-luciferase reporter strains

To determine the *ces* promoter activity in different genetic backgrounds, the reporter plasmid pMDX[P_1/*lux*] was electroporated in a clinical emetic isolate (CEI), in a strain isolated from a rice dish of a recent food-borne outbreak (EROI), the megaplasmid-cured *B. cereus* F48(pCER270-) and the *ces* cluster inactivation strain F48ΔcesP/polar, resulting in the strains CEI[P_1/*lux*], EFOI[P_1/*lux*], F48(pCER270-)[P_1/*lux*], and F48ΔcesP/polar[P_1/*lux*]. The reporter plasmid pMDX[P_1/*lux*] carries a fusion of the *luxABCDE* genes to the main promoter region (P_1) of the *cesPTABCD* operon (Dommel *et al.* 2010). For quantification of the promoter activity, strains were cultured in LB medium and aliquots of 200 µl were added to the wells of a 96-well microtiter plate with flat clear bottom (White/µClear plates, Greiner Bio-one). Bioluminescence was measured at 490 nm with a Wallac 1420 Victor^3 multilabel plate reader

(Perkin Elmer) and was recorded as Relative Luminescence Units (RLU). RLUs were further normalized to the optical density of the cell suspension, measured at 600 nm.

2.7.8 Construction of a *ces*-GFP reporter strain

In order to monitor *ces* transcription at its native locus, heterogramic conjugation was used to integrate a transcriptional fusion of the *ces* promoter region with a coupled green fluorescent protein (GFP)-spectinomycin cassette on the pCER270 megaplasmid. The cloning strategy is depicted in Figure 4. At first, a region was amplified from genomic DNA of F4810/72 that included parts of the *cesH* gene and the complete non-coding region between *cesH* and *cesP*, directly ending 3´ at the start codon of *cesP* (primer: iGFP_1Kpn and iGFP_1Xba). This region was designed to be the recombination region 1 (rr1). Rr1 was cloned into the compatible restriction sites (*Kpn*I and *Xba*I) of the vector pAD123 (Dunn and Handelsman 1999), thereby fusing the *ces* promoter region to *gfpmut3a*, an optimized, red-shiftet GFP variant (Cormack *et al.* 1996). The promoter-GFP fusion was amplified from pAD123/ces-GPF using the primer pair iGFP_1Kpn and iGFP_RSpe, resulting in a 2-kb fragment that was digested with *Kpn*I and *Spe*I, and further ligated into the equally cut TOPO/spc vector, resulting in the cesProm/GFP-TOPO/spc plasmid. In this step, the promoter-GFP fusion was linked to a spectinomycin cassette, needed as selectable marker for heterogramic conjugation. Next, the primers iGFP_Xho and iGFP_2Xho were used to amplify the recombination region 2 (rr2) from genomic DNA of F4810/72, starting with the start codon of *cesP* and comprising a 1.3 kb downstream fragment. This amplicon was cut with *Xho*I, and cloned in the cesProm/GFP-TOPO/spc construct. This resulted in a *gfp-spc* fusion, which was framed with the *ces* promoter (upstream) and the *cesP* gene (downstream), giving rise to the TOPO-derivative P_{cesP}/GFP-spc/cesP. The whole cassette was amplified from the TOPO backbone with iGFP_1Kpn and iGFP_2Sal, cut with *Kpn*I and *Sal*I, and introduced into the suicide vector pAT113 by using compatible ends (Fig. 4). The resulting construct pAT113[GFPint] was finally transformed in *E. coli* JM83/pRK24 for heterogramic conjugation (see above). Transconjugant colonies selected on LB spc100/polymyxin100 were screened with an IVIS imaging system (Caliper Life Sciences) for GFP fluorescence. One brightly fluorescing colony was further analyzed by PCR (primer: iGFP_for and iGFP_rev) and sequencing, in order to verify the presence of the *gfp-spc* cassette fusion and to verify the correct insertion on the pCER270 plasmid by double homologous recombination. The strain was designated *B. cereus* F48icesGFP.

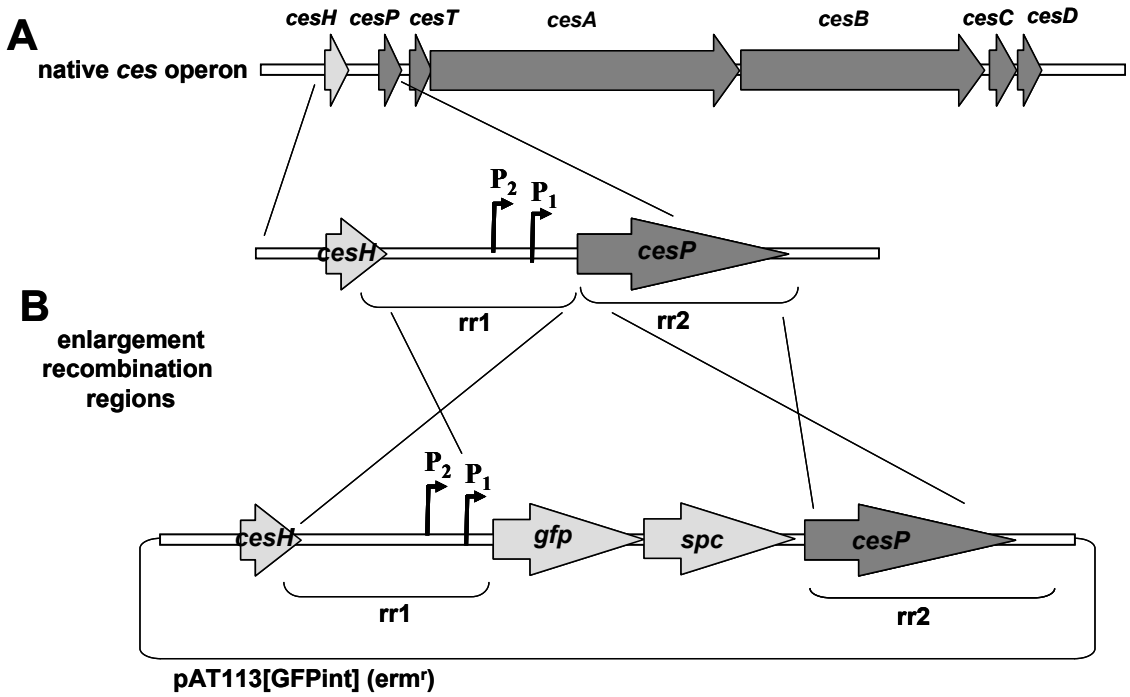

Figure 4: Strategy for construction of the suicide plasmid pAT113[GFPint] for integration of a P_{cesP}-*gfp*-*spc* fusion in the native *cesP* locus on the megaplasmid pCER270 in *B. cereus* F4810/72. (A) Structure of the native *ces* operon on pCER270 in *B. cereus* F4810/72 that is polycistronically transcribed from the P_1-main promoter upstream of *cesP* (B) (Dommel *et al.* 2010). For homologous recombination, recombination region 1 (rr1) comprising the *cesP* promoter region and parts of the *cesH* gene was amplified from genomic DNA and fused to a *gfpmut3a* and a spectinomycin cassette derived from pAD123 and TOPO/spc vectors, respectively. Further, recombination region 2 (rr2) comprising the entire *cesP* gene and a short downstream sequence, was fused downstream of the *spc* cassette. The complete assembly was cloned into the conjugative suicide vector pAT113 and was used for heterogramic conjugation. For details of construction and strain mating see the describing text (Ch. 2.7.8). erm^r: erythromycin resistance.

To analyze GFP expression in single cells of the reporter strain, fluorescence microscopy was carried out with a fluorescence microscope (Olympus BX51) equipped with an Olympus U-MWB2 filter cube (BP470-490 nm excitation filter and BA 515 nm barrier filter). Fluorescence images and phase-contrast images were captured, processed and overlaid with an F-view camera and the CellF software (Olympus).

2.8 Protein biochemistry techniques

2.8.1 Protein quantification

The protein quantification method was chosen in accordance with intended use of proteins and protein preparation. Protein quantifications were performed according to the manufacturer's instructions using BSA as reference standard.

For determination of protein amounts in culture supernatants (Ch. 2.9.3), and in protein fractions for Western blot analysis Roti-Quant solution (Carl Roth GmbH) was used, which is a Coomassie Dye-based method (Bradford assay). Samples were measured in 96-well microtiter plate scale. Due to the increased glycerol concentration in dialyzed protein fractions for gel mobility shift assays, determination of protein concentration was carried out with the Roti-Quant universal Kit (Carl Roth GmbH). The Biuret-based reaction is coupled to a colorimetric enhancer reaction and is claimed to be less sensitive towards interfering substances such as glycerol, detergents or imidazole than Bradford-based protein assays. Determination of protein concentration in samples for 2-D electrophoresis was carried out with the 2-D Quant Kit (GE Healthcare). As the proteins are precipitated in this assay, presence of chaotropes, detergents and ampholytes in the sample preparation buffer (Ch. 2.8.3) does not interfere with the copper-based colorimetric reaction.

2.8.2 Preparation of cytosolic protein fractions for Western blot analysis

B. cereus F4810/72, F48ΔcodY, F48pWHCodY, and *B. cereus* pWH1520 were grown in LB medium. CodY overexpression was induced with various amounts of D-xylose. Cells were collected (6,000*g*, 10 min, 22°C) in the mid-logarithmic growth phase (OD_{600}=7) and washed twice in buffer A to inhibit unspecific protease activity. The pellets were frozen in liquid nitrogen and stored overnight at -80°C. Then, pellets were thawed on ice, resuspended in 3 ml buffer B and disrupted by two passages through a French Pressure cell press (140 mPa). The soluble, cytosolic protein fraction was separated by repeated centrifugation of the lysates at 15,700 rpm for 20 min at 4°C. After quantification of the total protein concentration (Ch. 2.8.1), aliquots of the supernatant were stored at -80°C.

Buffer A:	50 mM Tris-HCl pH 7.5 50 mM KCl 1 mM DTT 0.5 mM PMSF pH 7.5	Buffer B:	50 mM Tris-HCl pH 7.5 2 mM EDTA pH 7.5 1 mM Pefabloc pH 7.5

2.8.3 Pre-fractioning of cytosolic and secreted proteomes for 2-D DIGE

For preparation of sub-proteomes for two-dimensional difference gel electrophoresis *B. cereus* F4810/72, F48(pCER270-), and F48ΔcesP/polar were grown in LB medium to an optical density of 8, corresponding to the mid-exponential growth phase. Cells were collected by centrifugation with 6,000 rpm for 10 min at 22°C. For preparation of the extracellular protein fraction ("secretome"), the supernatant was rapidly filtered through 0.22 µm pore-size filter and placed on ice. Proteins were precipitated overnight at 4°C by adding ice-cold trichloroacetic acid (TCA) solution to a final concentration of 10% (v/v). The precipitate was centrifuged (12,000 rpm, 1 h, 4°C) and the protein pellet was washed 6 times with 2 ml 100% acetone. After discarding the supernatant, the pellet was dried at 30°C and finally resuspended in DIGE

lysis/labeling buffer. The harvested culture cell pellets were washed two times in buffer C (6,000 rpm, 10 min, 22°C) and shock frozen in liquid nitrogen. For French Pressure cell disruption, pellets were thawed in 3 ml DIGE lysis/labeling buffer, and pressed at 140 mPa. The soluble protein fraction of these whole cell lysates was prepared by repeated centrifugation (15,700 rpm, 20 min, 4°C). Before storing the samples at -80°C, the total protein concentration of all fractions was determined.

Buffer C:	50 mM Tris-HCl pH 7.5 1 mM EDTA 1 mM Pefabloc pH 7.5	DIGE lysis/ labeling buffer:	7 M urea 2 M thiourea 4% (w/v) CHAPS 30 mM Tris 4 mM Pefabloc SC pH 8.5 (at 4°C)
TCA solution:	500 g TCA 227 ml ddH_2O		

2.8.4 Recombinant protein expression and purification

In order to perform gel mobility shift assays, proteins encoded in pET28b(+)-derivatives were isolated from *E. coli* BL21(DE3) as soluble, His-tag fusion proteins as follows. LB-grown overnight cultures were diluted 1:100 and incubated at 37°C, 150 rpm. Protein expression was induced by adding 1 mM IPTG to exponentially growing cells (OD_{600} 0.6 to 0.8). After incubation for 3 h, cells were harvested (6,000*g*, 4°C, 10 min), and washed twice with buffer A to block unspecific protease activities. Cell pellets were shock frozen in liquid nitrogen and stored at -80°C until use. For purification, cells were resuspended in a 1/30 volume of native lysis buffer containing 25 U/ml Benzonase endonuclease (Merck) to avoid contamination of gel mobility assay reactions with unspecific nucleic acids, and 1 mM Pefabloc SC (Merck) as broad-spectrum protease inhibitor, respectively. Cells were disrupted with a French press (140 mPA) and cellular debris was removed in two 20-min centrifugation steps at 15,700 rpm at 4°C. Soluble His-tag proteins were purified from the crude extracts by gravity flow using affinity columns with nickel-charged resins (Ni-NTA Fast Start Kit or Ni-NTA Superflow Columns; both Qiagen). Column-priming and -loading was carried out with native lysis buffer according to the manufacturer's protocol. Contaminating proteins were removed with 6 to 8 column volumes of washing buffer. Target proteins were eluted in a one step reaction with elution buffer and four 0.5 ml fractions were collected separately. Elution fractions were dialyzed with a 10-fold volume of BS buffer using polyethersulfone ultrafiltration columns with a 5-kDa or 10-kDa cut-off, respectively (Vivaspin 500 concentrators, Sartorius Stedim). Purified PerR-His_6 protein was dialyzed against TEDG buffer instead of BS buffer. Proteins were checked for purity by SDS-PAGE (Ch. 2.8.6) and concentrations were determined with the Roti-Quant Universal protein assay kit (Carl Roth GmbH), using bovine serum albumine (Bio-Rad) as standard. The fraction containing ≥ 98% of the pure target protein was subsequently used for gel mobility shift experiments (Ch. 2.8.5).

Buffer A:	50 mM Tris-HCl pH 7.5 50 mM KCl 1 mM DTT 0.5 mM PMSF pH 7.6	Native lysis buffer:	50 mM NaH_2PO_4 300 mM NaCl 10 mM imidazole pH 8.0
Washing buffer:	50 mM NaH_2PO_4 300 mM NaCl 20 mM imidazole pH 8.0	Elution buffer:	50 mM NaH_2PO_4 300 mM NaCl 250 mM imidazole pH 8.0
BS buffer:	50 mM Tris-HCl pH 7.5 50 mM KCl 10 mM $MgCl_2$ 0.5 mM Na_2EDTA pH 8.0 10 % (v/v) glycerol	TEDG buffer:	50 mM Tris-HCl pH 8.0 0.5 mM Na_2EDTA pH 8.0 2 mM DTT 10 % (v/v) glycerol

2.8.5 Gel mobility shift assay

Affinity of His-tagged transcription factors (Ch. 3.4.2) to promoter regions of interest (Table 7) was analyzed with non-radioactive native PAGE in gel mobility shift assays (for a recent Nature Protocol, see (Hellman and Fried 2007). Binding reactions (i.e. binding and running buffer composition, PAA-gel concentration, effector molecule concentration, and pre-incubation conditions) were optimized with a promoter region known to be controlled by the respective transcription factor. Binding buffers for individual proteins (see below) were adapted from previously published gel retardation experiments (Hamoen *et al.* 1998; Shivers and Sonenshein 2005; Traore *et al.* 2006; Susanna *et al.* 2007). Aliquots of binding buffers were stored at -20°C, and were not re-used after thawing once.

Purification and retaining of an active PerR-His_6 protein state was difficult for the following reasons: PerR is an H_2O_2 sensing dimer, which contains two metal ions per monomer with one being a zinc ion that is assigned a structural role and locks the dimerization domain (Herbig and Helmann 2001). The second metal binding site coordinates a regulatory metal ion (Mn^{2+} or Fe^{2+}) required for DNA binding (Traore *et al.* 2006; Jacquamet *et al.* 2009). While both PerR-Zn-Mn and PerR-Zn-Fe are able to bind to DNA, only PerR-Zn-Fe can be induced by H_2O_2 to dissociate from DNA. A metal-catalysed histidine oxidation by bound Fe^{2+} leads to oxygen incorporation into the protein, and further to the loss of DNA binding ability due to profound structural rearrangements (Traore *et al.* 2006; Traore *et al.* 2009) (Fig. 5).

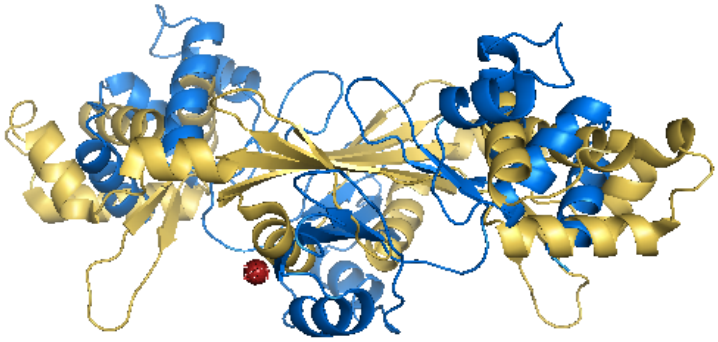

Figure 5: Molecular model of the reorganization of DNA binding domains in *B. subtilis* PerR due to histidine-oxidation by hydrogen peroxide. The structures were modeled based on PDB entries 2FE3 and 2RGV retrieved from the RCSB protein database. The superposition was generated with PyMOL (DeLano Scientific LLC). The yellow ribbon structure indicates the oxidized PerR dimer (PerR-Zn-ox) incapable of DNA binding. The blue ribbon structure depicts the active protein form (PerR-Zn-Mn). The red dot indicates a Zn^{2+} ion essential for physiological function of the regulator. The model was created in relation to a figure published by (Duarte and Latour 2010).

Under most growth conditions the PerR protein contains the Fe^{2+} ion and is highly sensitive towards oxidation during the purification procedure (Lee and Helmann 2006). Therefore, purification of PerR-His_6 was carried out under high EDTA concentrations, which are thought to reduce protein oxidation by removal of loosely associated ions (Lee and Helmann 2006). To obtain a protein state capable of DNA binding in the gel mobility shift assays, PerR was subsequently incubated with an excess of $MnCl_2$ and EDTA was omitted from the binding and running buffers.

In 20-µl binding buffer reactions, increasing amounts of protein were mixed with 50 or 100 ng of the respective promoter fragment and with an equimolar amount of randomly chosen *B. cereus* DNA fragment, serving as competing nucleic acid. To exclude unspecific binding, proteins were incubated in separate reactions with unspecific DNA fragments and/or with promoter fragments devoid of transcription factor binding sites. Reactions were left at 20°C for 25 min, premixed with 4 µl DNA loading dye (Promega) and loaded on non-denaturing gels. Concentrations of native PAA gels were 4% for CcpA, 6% for ComK and DegU, and 10% for CodY, PerR, and SinR proteins, respectively. CodY-EMSAs were performed in the presence of 10 mM L-isoleucine and 2 mM GTP in the EMSA binding buffer I, and in the presence of 10 mM ILV in 1x TBE running buffer, since ILV and GTP are synergistically acting co-repressor molecules of *B. subtilis* CodY (Ratnayake-Lecamwasam *et al.* 2001; Shivers and Sonenshein 2004; Handke *et al.* 2008).

TBE buffer was also used for SinR, ComK, DegU, and CcpA experiments. PerR-His_6 aliquots were pre-incubated with 0.75 mM $MnCl_2$ solution (30 min, 22°C) and EMSAs were performed in 1x TB running buffer. To phosphorylate DegU-His_6, 2 µg of the protein were incubated in a buffer containing 25 mM acetyl phosphate and 50 mM Tris-HCl pH 7.4 for 30 min at 37°C.

In general, buffers were cooled to 4°C, gels were pre-run for 10 to 40 min at 120 V, and a constant voltage from 120 to 190 V was applied for the main runs that were performed at 15°C. DNA was detected post-electrophoretically by ethidium bromide staining and UV irradiation.

Native PAA gel: (10%)	7.5 ml acrylamide (40%) 1.62 ml bisacrylamide (2%) 4 ml 5x gel running buffer 7.68 ml ddH_2O 0.2 ml 10% (w/v) APS 0.02 ml TEMED
EMSA binding buffer I (10x): (CodY/SinR)	50 mM Tris-HCl pH 8.0 750 mM KCl 2.5 mM Na_2EDTA pH 8.0 0.5% (v/v) Triton X-100 62.5% (v/v) glycerol 1 mM DTT
CcpA binding buffer (5x):	50 mM Tris-HCl pH 7.5 250 mM KCl 5 mM Na_2EDTA pH 7.5 0.25% (v/v) Nonidet P-40 50% (v/v) glycerol 5 mM DTT
ComK binding buffer (5x):	100 mM Tris-HCl pH 7.5 500 mM KCl 25 mM $MgCl_2$ 43.5% (v/v) glycerol 2.5 mM DTT
PerR binding (10x):	0.5 M Tris-HCl pH 7.5 1.5 M NaCl 0.5% (v/v) Triton X-100 50% (v/v) glycerol 1 mM DTT
DegU binding buffer (5x):	100 mM Tris-HCl pH 8.0 500 mM KCl 25 mM $MgCl_2$ 0.2% (v/v) NP-40 50% (v/v) glycerol 0.25 mg/ml BSA
TBE buffer: (5x)	450 mM Tris 450 mM boric acid 10 mM EDTA pH 8.3 (NaOH)
TB buffer: (5x)	450 mM Tris 450 mM boric acid pH 8.3 (NaOH)

Table 7: Oligonucleotides developed for generation of gel mobility shift assay probes

Primer	Sequence (5´- 3´)	Target promoter region (gene)[a,b]	size (bp)	Reference[c]
cesP_F_EMSA1	CTACAAGAAAACCTGTAAAAATTAG	*cesP*, 3´end (short)	368	(1)
PPP1_rev2	TTTATGCTCTATGTGTTTCATTG			(1)
cesPIII_for	GCTCTTTAGTTCCTTCATGACTT	*cesP*, 5´end	488	This study
cesPIII_rev	GAAGCACACGTTGAAGAAGC			This study
cesPI_for	CTTCTTCAACGTGTGCTTCTA	*cesP*, 3´end (long)	523	This study
cesPI_rev	GTGTTTCATTGAAAAATCCCTC			This study
cesB_EMSA_F	TCAATGAAAACGTAGACGGTGTTG	*cesB*	362	This study
cesB_EMSA_R	ACCTTTGCTACTTGTCGTTCAATC			This study
EMSAunsp7_for	ATGGTGGCGGAGTAAGTGGTTGGA	control fragment	301	This study
EMSAunsp7_rev	AAAGGAATCGGTTTAACCAACGCACTG			This study
EMSAunsp8_for	GAACATTATTTTTGCGAGAACGAG	control fragment	201	This study
EMSAunsp8_rev	TATTGGCGTTCTTGTTCTGTGAA			This study
inhA1_EMSA_F	ATGTAATTCCTCCCTAATTATCGGTC	*inhA1*	349	This study
inhA1_EMSA_R	TTGTTCATCCCTTATTTCCTCCCCTA			This study
inhA2_EMSA_F	GTCACAGTGTTCACGTAACTGACG	*inhA2*	332	This study
inhA2_EMSA_R	CCTCCAGTTTTCTGGTCAGACTCT			This study
inhA3_EMSA_F	TATTTCCTCCCTAGTGTCTGCAA	*inhA3*	250	This study
inhA3_EMSA_R	GCCAATTCCTTAGCTACTACTTAG			This study
Nhe_EMSA_F	CAGTCTAGTTTACTCATTCGTGCG	*nheA*	576	This study
Nhe_EMSA_R	CGATTCACACACGAACCATCTCTC			This study
PCplc_EMSA_F	GAAAAAAAGAGTAAAGCATGTGGATG	*plC*	252	This study
PCplc_EMSA_R	GCATTAGTTTAGATAAGCCTTAATAAT			This study

Table 7- *continued*

clo_EMSA_F	GAGTGCATAGACTAACTAATACACA	*clo*	378	This study
clo_EMSA_R	TTCAAGAAGAGTGGTAGCATCATCA			This study
plcR_EMSA_F	CTGCGTGCATACTTACTCACCAT	*plcR*	262	This study
plcR_EMSA_R	GGTGTGAATAACTTCTGCTACTGC			This study
npr599_EMSA_F	GCAGGAACATTTGTAGTTATGGC	*npr599*	372	This study
npr599_EMSA_R	TTTAGAATCCGCAAATGCAGAGC			This study
spo0A_EMSA_F	CCATATCCTCTTGAGCAGCTACA	*spo0A*	324	This study
spo0A_EMSA_R	GCTCCGCAAGAGGTGTTTTTTGT			This study
abrB_EMSA_F	CCCTATGGACATATGATACCAATC	*abrB*	324	This study
abrB_EMSA_R	ACCAATCGGACTTTTACGAGCAAT			This study
PepsAF2	GTCGTTATTTCGTTCATTATAAGGAATT	*epsA*; BSU34370[d]	225	(2)
PepsAR2	TCATGTATTCATAGCCTTCAGCCTT			(2)
comK3_EMSA_F	TTCACGATCACAATGCTGCTATTT	*comK*	355	This study
comK3_EMSA_R	ACTTTCCATATTCCACTATCTCCTT			This study
ilvBBS_F	CCGGTTCTCTGTGGAAAACTTTAT	*ilvB*; BSU28310[d]	475	This study
ilvBBS_R	ATTAATGTATGCCGAGGGAACAAG			This study
comKBsu_EM_F	CCAATGCCTTTTTTATAGTATATG	*comK*; BSU10420[d]	297	This study
comKBsu_EM_R	CTGTTTTCTGACTCATATTATGG			This study
srfA_EMSA_F	GTACACATAGTCATGTAAAGATT	*srfAA*; BSU03480[d]	242	This study
srfA_EMSA_R	TTATCTTTCTACCGTTCAGTTTAA			This study

[a] Accession number of pCER270 (also designated pBCE or pAH187_270) plasmid sequence: GenBank [DQ889676] (Rasko *et al.* 2007).
[b] Accession number of *B. cereus* AH187 genome sequence: GenBank [CP001177], RefSeq [NC_011658].
[c] (1) (Lücking *et al.* 2009); (2) (Kearns *et al.* 2005).
[d] BSU: primer were designed on basis of the reference genome of *Bacillus subtilis* subsp. *subtilis* 168 [GenBank AL009126] (Kunst *et al.* 1997; Barbe *et al.* 2009) and EMSA probes were amplified from genomic DNA of the closely related strain *Bacillus subtilis* subsp. *subtilis* NCIB3610 (Srivatsan *et al.* 2008; Zeigler *et al.* 2008).

2.8.6 Denaturing protein separation (SDS-PAGE)

Standard SDS-polyacrylamide gel electrophoresis (Laemmli 1970) was performed with 8% to 15% 0.75 mm-resolving gels, depending of the size of the target protein. An exemplary protocol for casting of two 15%-minigels is given below. Prior to gel loading, suitable amounts of samples were mixed with an equal volume of Laemmli sample buffer (BioRad) and boiled for 5 to 10 min. PageRuler Prestained Protein Ladder (Fermentas) was used as protein size standard. Electrophoresis was performed in vertical chambers at low constant voltage of 50 to 100 V during stacking, and was raised up to 120 to 180 V until the dye front ran off the gel bottom. Gels were fixed and stained in Coomassie staining solution for 15 to 120 min and destained for 1 to 12 hours in destaining solution and dH_2O additionally using paper wicks to absorb excessive dye. Occasionally, gels were stained for 90 min with Oriole Fluorescent Gel Stain (BioRad), a dye that fluoresces when bound to protein, and visualized by UV irradiation.

Resolving gel:	7.5 ml acrylamide (37.5:1)	Stacking gel:	0.83 ml acrylamide (37.5:1)
(15%)	3.75 ml 1.5 M Tris-HCl pH 8.8	(5%)	0.63ml 0.5M Tris-HCl pH6.8
	3.45 ml ddH_2O		3.4 ml ddH_2O
	0.15 ml 10% (w/v) SDS		0.05 ml 10% (w/v) SDS
	0.15 ml 10% (w/v) APS		0.05 ml 10% (w/v) APS
	0.01 ml TEMED		0.01 ml TEMED

2x Laemmli sample buffer:	950 µl Laemmli buffer (BioRad) 50 µl ß-mercaptoethanol	SDS running buffer (10x):	0.25 M Tris 1.92 M glycine 1 % (w/v) SDS pH 8.3
Coomassie staining solution:	0.25% (v/v) Coomassie Blue R-250 45% (v/v) isopropanol 9% (v/v) acetic acid 45.75 % (v/v) ddH_2O	Coomassie destaining solution:	40% (v/v) ethanol 10% (v/v) acetic acid 50% (v/v) ddH_2O

2.8.7 Western blot

For specific detection of CodY, 30 µg of PAGE-separated proteins were transferred onto PVDF membranes (Hybond-P, Amersham Biosciences) using a semi-dry-blotting system (PHASE GmbH). The PVDF membrane was incubated in 100% methanol, equilibrated in transfer buffer and placed on buffer-soaked absorbent paper (Whatman) in the apparatus. The PAA gel was placed on the membrane and covered with absorbent paper layers. Blotting was carried out with 1.5 mA/cm^2 gel for 1 to 2 hours. For all following steps, the membrane was incubated at room temperature under continuous shaking. The membrane was incubated in blocking solution (1 hour), rinsed three times with 1x PBS and treated with the primary antibody solution (1 hour). After discharging and washing with 1x PBS, the secondary antibody solution was applied (1 hour), followed by washing with 1x PBS. Detection was carried out with the SuperSignal West Pico Chemiluminescent Substrate (Thermo Scientific). Signals were visualized and photographed by exposing an X-ray film (Lumi-Film Chemiluminescent Detection Film, Roche) to the membrane.

TBS: (1x)	50 mM Tris-HCl pH 7.4 150 mM NaCl pH 7.4	Transfer buffer: (1x)	50 mM Tris 39 mM glycine 20% (v/v) methanol 0.039 % (w/v) SDS
Blocking solution:	5% (w/v) fat free milk powder in 1x TBS	Primary antibody solution:	1:10,000 Anti-CodY-AB in blocking solution (Joseph *et al.* 2005)
Secondary antibody solution:	1:20,000 goat anti-rabbit IgG-HRP in blocking solution (Santa Cruz Biotechnology, sc-2030)		

2.8.8 Two-dimensional differential gel electrophoresis (2-D DIGE)

Dr. Tom Grunert introduced Elrike Frenzel to fluorescence two-dimensional differential gel electrophoresis (2-D DIGE) experiments and MALDI-TOF/MS(MS) and carried out the the majority of 2-D DIGE gels. Protein identification was carried out jointly by Elrike Frenzel and Dr. Tom Grunert at the Proteomic Core Facility of the University of Veterinary Medicine Vienna.

For 2-D DIGE, protein fractions were adjusted to a pH of 8.5 (50 mM NaOH) and were labeled with CyDye Fluor minimal dyes (GE Healthcare) according to the manufacturer's instructions. The experiment was designed to include four biological replicates per strain (F4810/72, F48(pCER270-), and F48ΔcesP/polar) and per condition (cytosolic protein fraction and secreted protein fraction), i.e. 12 samples of cytosolic proteins and 12 samples of extracellular proteins. The labeling scheme is given in Table 8. Per sample, 25 µg of protein were incubated with 200 pmol Cy3 or Cy5 dye for 30 min on ice and kept in the dark. The pooled internal standard was prepared by incubating 25 µg protein of a mixture of all 12 samples per condition with 200 pmol Cy2. The labeling reaction was stopped by addition of 1 µl Stop solution and samples were further prepared for isoelectric focusing (IEF) by adding one volume of DIGE 2x sample buffer. The first dimension was run on 24 cm IPG strips with a linear pH gradient of 4-7 (GE Healthcare). Prior to cup-loading of the samples, IPG strips were rehydrated in a reswelling tray with 350 µl rehydration buffer per strip for 12 to 16 h. In total, 75 µg of protein (25 µg of each, the two strain samples (Cy3/Cy5) and the internal standard mix (Cy2) were co-separated on each gel strip.

Table 8: Labeling and separation scheme for 2-D DIGE experiments[a]

No. of gel	Cy2	Cy3	Cy5
1	Equimolar mix (A1-4; B1-4; C1-4)	B2	C1
2	Equimolar mix (A1-4; B1-4; C1-4)	A1	B3
3	Equimolar mix (A1-4; B1-4; C1-4)	C3	A4
4	Equimolar mix (A1-4; B1-4; C1-4)	A3	C2
5	Equimolar mix (A1-4; B1-4; C1-4)	B4	A2
6	Equimolar mix (A1-4; B1-4; C1-4)	C4	B1

[a] Each gel was loaded with 25 µg of the Cy2 labeled internal standard comprising an equimolar protein mix obtained from four biological replicates of *B. cereus* F4810/72 (samples A1-4), F48ΔcesP/polar (samples B1-4), and F48(pCER270-) (samples C1-4) and with 25µg strain-specific protein labeled with Cy3 or Cy5. Co-separation and dual-channel analysis allowed a direct comparison of the protein patterns of two strains. The scheme was applied for cytosolic protein fractions as well as for extracellular ("secreted") protein fractions.

Simultaneous IEF of 6 strips was performed in an Ettan IPGphor 3 system (GE Healthcare) with the following conditions per step (S): S1, 150 V for 1.5 h; S2, 300 V for 1.5 h; S3, 600 V for 1 h; S4, linear gradient from 600 to 8,000 V for 0.5 h; S5, 8,000 V for 3 h; resulting in a total of ca. 30,000 Vh. Electrode paper wicks were changed at least three times. Prior to second-dimension-separation, IPG strips were equilibrated for 15 min in equilibration buffer A containing 10 mg ml^{-1} DTT and 15 min in equilibration buffer B containing 40 mg ml^{-1} iodacetamid. In the second dimension, proteins were separated on isocratic 10% SDS-PAGE gels at 13 mA/gel for 14 h in an Ettan Daltsix vertical electrophoresis unit (GE Healthcare). Fluorescence images were acquired with a Typhoon 9400 scanner (GE Healthcare) using separate laser excitation for each of the three Cy-dyes. Image processing, spot detection, inter-gel matching of spot maps and initial statistical analysis was performed with the DeCyder

software (Version 5.02, GE Healthcare). A master gel was obtained by automated matching of all spots per gel and by further fusing the six gel images of each condition. After spot detection on the master gel, the spot mask was overlaid on the individual gel scans (Cy2, Cy3, or Cy5) to compute individual spot volume ratios. Therfore, the volume of a particular sample spot was calculated in relation to the volume of the corresponding pooled Cy2 protein spot (internal standard). Changes in the spot volume were considered significant on the basis of false-discovery rate (FDR) calculations using the R-software program (http://www.r-project.org/) with a a significance p-value cutoff of 0.05. Spots were selected for identification on basis of following criteria, previously publishe by (Radwan *et al.* 2008): (i) spot/volume ratios were changed more than 1.5-fold, (ii) spot did not overlap with neighbouring spots, (iii) spot quantity was sufficient for MS analysis, and (iv) stainability of spot was sufficient for manual spot picking.

DIGE 2x sample buffer:	7 M urea 2 M thiourea 4% (w/v) CHAPS 0.5%(v/v) carrier ampholytes 3-10 2% (w/v) DTT pH 8.5 (at 4°C)	Rehydration buffer:	6 M urea 2 M thiourea 1% (w/v) CHAPS 0.4% (w/v) DTT 0.5% (v/v) carrier ampholytes 3-10
Stop solution:	10mM lysin	10% APS:	0.1 g/ml
2nd dimension gel (12.5%):	25 ml acrylamide (37.5:1) 19 ml separation buffer (pH 8.6) 30 ml ddH_2O 0.55 ml 10% (w/v) APS 0.017 ml TEMED	Separation buffer:	1.5 M Tris-HCl pH 8.6 0.4% (w/v) SDS pH 8.6
Running buffer (10x):	25 mM Tris 192 mM glycine 0.1% (w/v) SDS pH 8.3	Equilibration buffer (A/B):	50 mM Tris-HCl pH 8.8 6 M urea 30% (v/v) glycerol 2% (w/v) SDS (A) 10 mg/ml DTT (B) 40 mg/ml iodacetamid

2.8.9 Protein identification by MALDI-TOF-MS(MS)

Identification of differentially expressed proteins was carried out by Matrix-Assisted-Laser-Desorption/Ionization–Time-Of-Flight-(Tandem)Mass-Spectrometry (MALDI-TOF-MS(MS)). Acidic silver nitrate staining was used for MS-compatible detection of protein spots, as described previously (Miller and Gemeiner 1992). Spots were manually excised from the gels, pooled and destained by using 30 mM potassium ferricyanide and 100 mM sodium thiosulfate as chemical reducers (Gharahdaghi *et al.* 1999). For *in-gel* digestion, gel pieces were washed with 200 µl acetonitrile (ACN) and dried in a vacuum centrifuge. Subsequently, 12.5 ng μl^{-1} sequencing grade trypsin (Roche) in 25 mM NH_4HCO_3 solution were added for gel rehydration. After 30 min at 4°C, excess solution was replaced by 25 mM NH_4HCO_3 and the digest was

incubated at 37°C for 12 h. The supernatant was collected and peptides were eluted from the gel with a solution containing 66% ACN and 33% of 0.1% trifluoroacetic acid (TFA), placed for 60 sec in an ultrasonic bath. Elution was repeated twice. After drying the pooled peptide fractions, samples were dissolved in 0.1% transcription factorA and further desalted and concentrated using Zip-Tip$_{\mu}$-C_{18} extraction pipette tips (Millipore). Mass spectra were acquired on a MALDI-TOF instrument (Ultraflex II, Bruker Daltonics). Settings for external instrument calibration are described elsewhere (Radwan *et al.* 2008). Well characterized ions of trypsin autolysis products, keratin, blank gel artefacts and matrix clusters were removed from the mass spectra, as described previously (Radwan *et al.* 2008). If possible, the two strongest signals of the MS spectrum were subjected to further MS/MS analysis. Peptide mass fingerprinting (PMF) of the resulting m/z peak list and analyses of the MS/MS peptide sequences were performed on a MASCOT server (Matrix Science) by applying the non-redundant NCBI protein database of *B. cereus* group sub-database (taxon identification 86661; accessed from 07/2010 to 11/2010). The remaining search parameters were set as follows: mass accuracy, 100 ppm; fixed modification, carbamidomethylation; variable modifications, methionine oxidation and acetylation of the N-terminus; missed cleaves, one. For MS/MS analysis, identical parameters were applied with a product ion tolerance of 1.0 Da. The identity of a protein spot was considered significant, if the scores of database searches exceeded the algorithm's significance threshold ($p < 0.05$) for PMF and/or MS/MS data at least two times independently for the respective target protein. If proteins were not functionally assigned in *B. cereus* F4810/72, BLASTP analysis was carried out to identify homologous proteins in other *B.cereus* group strains.

2.9 Methods for virulence factor detection

2.9.1 Cereulide quantification (HEp-2 cell assay)

The HEp-2 cell based cytotoxicity assay was used to determine cereulide levels in autoclaved cell culture samples or in ethanolic extracts of spiked and unspiked food samples (Ch. 2.4.6). The stability of cereulide is not affected by thermal or organic solvent treatment (Rajkovic *et al.* 2008), while heat-labile enterotoxins should be denatured and not interfere with the assay. The cytotoxicity assay was carried out as previously described (Finlay *et al.* 1999; Lücking *et al.* 2009). A two-fold dilution series of the samples was prepared in MEM-Earle medium in 96-well microtiter plates. MEM medium contained 2% ethanol to ensure solubility of the depsipeptides. A dilution series of the structurally related ionophor valinomycin served as internal standard. HEp-2 cells were added to 7×10^4 cells per well, and plates were incubated for 48 h at 37°C in 5% CO_2 atmosphere. After removing 100 µl supernatant from each well, viability of the cells was determined by addition of 10 µl of the tetrazolium-based reagent WST-1 (Roche), which is reduced by the activity of mitochondrial dehydrogenases. Absorbance at 450/620 nm was measured in a microtiter plate reader. Cereulide titer (given as 50% inhibitory

concentration) of the test samples were calculated from the resulting dose-response curves, and were expressed as valinomycin equivalents (VE).

MEM-Earle medium: Minimum Essential Medium Eagle with Earle salts; supplemented with 2% (v/v) FCS, 1% sodium pyruvate (v/v), and 0.4% (v/v) penicillin-streptomycin.

2.9.2 Enterotoxin quantification (Vero cell assay)

For preparation of the assay samples, *B. cereus* precultures were diluted 1:100 in brain heart infusion (BHI) broth supplemented with 1 µg ml^{-1} vitamin B_{12} and grown to an optical density (OD_{600}) of 10. Harvested supernatants were filtered (0.22 µm pore-size) and mixed with 1 mmol/liter EDTA to inhibit proteolytic activity. Samples were stored at -20°C until use. Cytotoxicity of culture supernatants mediated by the pore-forming activity of the non-hemolytic enterotoxin complex (Nhe) was quantified using a cell culture assay based on a Vero cell line. Activity tests were carried out as described previously (Dietrich *et al.* 1999). In brief, samples were twofold serially diluted in MEM medium containing 1% FCS in 96-well microtiter plates and Vero cells (100 µl) were added to $1x10^4$ cells per well. Plates were incubated for 24 h at 37°C in 5% CO_2 atmosphere. After discarding of 100 µl supernatant, viability of the cells was determined by addition of 10 µl WST-1(Roche) per well, analogous to the HEp-2 cell assay (Ch. 2.9.1). Enterotoxin titer were determined as the reciprocal of the sample dilution that resulted in a cell viability inhibition of 50%.

MEM-Earle medium: Minimum Essential Medium Eagle with Earle salts; supplemented with 1% (v/v) FCS, 1% sodium pyruvate (v/v), and 0.4% (v/v) penicillin-streptomycin.

2.9.3 Phosphatidylcholine-specific phospholipase C (PC-PLC) assay and sphingomyelinase (SPH) assay

Supernatants of *B. cereus* F4810/72 and F48ΔcodY cultivated in LB broth were harvested (6,500*g*, 4 min, 4°C) at optical densities at 600 nm (OD_{600}) of 7, 14, 16 (Δ*codY*) or 18 (WT), and 22 hours after inoculation (corresponding to early-exponential, mid-exponential, transition, and late stationary growth phases, respectively). Samples were frozen immediately and stored at -20°C. Enzymatic sphingomyelinase activity was determined with the Amplex Red Sphingomyelinase Assay Kit (Invitrogen/Molecular Probes). Production of phosphatidylcholine-specific phospholipase C was quantified with the EnzChek Direct Phospholipase C Assay Kit (Invitrogen/Molecular Probes). Both assays were performed according to the recommended protocols. Supernatant samples (100 µl) were serially diluted with 1x reaction buffer in µ-clear-bottom microtiter plates (Greiner Bio-One). Reactions were developed by adding the respective substrate master mix, incubated light-protected for 60 min at 37°C (SPH assay) and for 30 min at 30°C (PC-PLC assay) at 400 rpm in a microplate thermo-shaker (DTS-2 ELMI Ltd.). Fluorescence intensity was measured with a Wallac 1420 Victor^3 multilabel plate reader (Perkin Elmer) at excitation/emission wavelengths of 530/585 nm or

490/535 nm for the SPH and PC-PLC assay, respectively. Enzyme amounts (milliunits per milliliter; mU/ml) in culture supernatants were estimated by plotting standard curves of relative fluorescence units (RFU) generated by known *B. cereus* PC-PLC and SPH concentrations that are provided as internal standard with the assay kits. Curve fitting and non-linear regression was performed with SigmaPlot 09 (Systat Software). Phospholipolytic activities were determined from three independent cultures of each strain and finally normalized to the protein concentration of the respective supernatant which was determined with a Bradford-based protein assay, resulting in mU per µg of protein.

2.9.4 Horse red blood cell (hRBC) hemolysis assay

Defibrinated horse blood (Oxoid) was washed with 0.9% sodium chloride solution (1,500 × g, 4 min, 22°C) until the supernatant remained clear. The red blood cells (RBCs) were resuspended to a 2% working solution and, if necessary, further adjusted to a density, which gave an OD_{540} value of ca. 1.2 when 100% RBC lysis (Max) was induced by addition of an equal volume of tryptic soy broth (TSB) containing 0.1% SDS. The RBC working solution was prepared fresh prior to each experiment. *B. cereus* overnight cultures were diluted 1:100 in TSB and incubated under continuous shaking at 150 rpm, 30°C. Cultures were grown to an optical density of 10 (OD_{600}), harvested (6,500*g*, 2 min, 22°C), and supernatants were filtered through 0.22-µm pore size filter for an instant use in the assay. Twofold dilution series of the supernatants prepared with TSB were incubated with an equal volume (600 µl) of RBC working solution for 15 min at 37°C. To remove unlysed erythrocytes, reactions were centrifuged (1 min, 8,000 × g), and hemoglobin release in the supernatant fluid was measured at 540 nm (OD_{540}). RBCs incubated with TSB medium served as background hemolysis controls (BHC). The hemolytic activity in each dilution-reaction, calculated as $[(Sample_{OD540}\text{-}BHC_{OD540})/(Max_{OD540}\text{-}BHC_{OD540})] \times 100$, was plotted against the dilution factor to obtain a dose-response curve. The reciprocal of the dilution causing 50% hemolysis was considered as hemolytic titer as suggested earlier (Callegan *et al.* 2002).

3 Results

3.1 Detection of emetic *B. cereus* and cereulide in foods

A polyphasic approach was used to determine the natural contamination of dairy-based foods with emetic *B. cereus* and cereulide. In particular, this study focused on the identification of potential contamination sources, such as food ingredients, that might be entrance points of *B. cereus* and the toxin in complex end-products. The workflow for the food sample analysis is depicted in Figure A1 in the Appendix.

The screening was carried out within a two-year period from 12/2007 to 10/2009 and included ready-to-eat foods obtained from local retail markets as well as foods and food ingredients obtained from industrial partners within the framework of an AiF-funded project. All samples were examined before their expiry date. Additionally, foods were analyzed that were suspected to be spoiled with *B. cereus*. The latter were food-remnants connected to a food poisoning case in a German school or were provided by different manufacturers, and included UHT milk, different cheese samples, and milk substitute products.

Enumeration of presumptive *B. cereus* was carried out with a most-probable number (MPN) procedure according to the EN ISO guideline 21871. *B. cereus*-like organisms were detected in 18 out of 36 ready-to-eat foods and in 9 out of 21 food ingredients (Table 9). However, cell counts were generally low in the majority of samples. Cell counts exceeding 100 CFU g^{-1} were exclusively found in food ingredients, including texturing agents such as milk proteins, whey milk powder or thickeners (Table 11).

Table 9: Incidence of presumptive *B. cereus* in retail foods and food ingredients as examined using the most-probable-number (MPN) method EN ISO 21871:2006 [a]

		Percentage of *B. cereus* group organisms detected within the range[b]			
	Number of samples	< 0.3 CFU g^{-1}	0.3 to 10 CFU g^{-1}	10 to 100 CFU g^{-1}	> 100 CFU g^{-1}
Retail products	36	50	19	31	0
Food ingredients	21	52	10	19	19

[a] The screening was carried out over a two-year-period (2007 to 2009) and included dairy-based foods and food ingredients obtained from German retail markets or partners from the dairy industry within the framework of an AiF-funded research project.
[b] The detection limit of the MPN method is 0.3 CFU per gram of food.

B. cereus-like colonies recovered from food were purified on PC agar for further differentiation by PCR targeting the cereulide synthetase (*ces*) genes. Since *B. cereus* strains can exhibit atypical colony morphology or weak reaction on selective MYP agar, both, colonies with characteristic appearance and atypical, but mannitol-negative colonies were investigated. In addition foods and food ingredients were tested for contamination with cereulide using a HEp-2 cell based biotoxicity assay (Table 10). In 14% of the foods and in 19% of the ingredients, the presence of emetic strains was confirmed indirectly by *ces* gene specific TaqMan real-time PCR performed on DNA isolated from the food samples (Tables 10 and 11). For instance, emetic *B. cereus* was obviously present in the whole milk powder, but was not detected by the MPN-enrichment procedure. The measurements of food extracts in the biotoxicity assay showed that 3% of the foods and 10% of the food ingredients contained the emesis causing toxin cereulide itself. Cereulide was detected in amounts ranging from 0.14 to 0.72 µg g^{-1}.

Table 10: Summary of the survey on the occurrence of presumptive *B. cereus*, emetic *B. cereus,* and cereulide in retail foods, food ingredients and foods suspected to be contaminated with *B. cereus*

Food	Number of samples	MPN-positive for presumptive *B. cereus* (MPN) (%)	Presence of emetic strains (colony PCR) (%)	Presence of *ces* genes (TaqMan PCR) (%)	Presence of cereulide (HEp-2 assay) (%)
Retail products	36	50	8	14	3
Food ingredients	21	48	14	19	10
Contaminated food	23	ND[b]	35	36	37

[a] ESL, extended shelf life.
[b] ND, not determined.

Table 11 provides an overview on the occurrence of emetic *B. cereus* and its emetic toxin cereulide for a selection of analysed foods and food ingredients. For reasons of confidentiality, a comprehensive dataset of the complete survey was not enclosed.

Table 11: Occurrence of presumptive *B. cereus*, emetic *B. cereus*, and cereulide in selected dairy-based foods and their ingredients

Food	Cell count presumptive *B. cereus* (MPN g^{-1})[a]	Presence of emetic strains (colony PCR)	Presence of *ces* genes (TaqMan PCR)	Presence of cereulide (HEp-2 assay)
Whole milk (ESL)[b]	< 0.3	-[c]	-[c]	-[c]
Camembert cheese	< 0.3	-	-	-
Sweet whey powder	240	-	-	-
Condensed milk	< 0.3	-	pos	-
Whole milk powder	93	-	pos	-
Dairy-based infant food	23	pos	pos	-
Thickening agent	480	-	-	-
Liquid whole egg	220	pos	-	pos
Strawberry preparation	3.6	pos	pos	NP[d]
Processed cheese with caraway seeds	3.6	pos	pos	NP
Herbed butter	43	pos	pos	pos

[a] Detection limit: 0.3 CFU g^{-1}.
[b] ESL, extended shelf life.
[c] No emetic strains, *ces* genes, or cereulide present in the sample.
[d] NP, detection not possible due to interfering background in the HEp-2 assay.

Analysis of food remnants implicated in a food poisoning case and ready-to-eat foods that were suspected to be contaminated with *B. cereus* showed that emetic strains were present in 35% of the samples (Table 10). Concordantly, presence of the cereulide synthetase encoding *ces* genes was confirmed by TaqMan real-time PCR and cereulide was detected with the HEp-2 assay. Thus, emetic *B. cereus* was unambiguously the causative agent of food contamination in different dairy-based foods analyzed between 2007 and 2009.

3.2 Evaluation of a P_1-*lux* reporter strain as a rapid screening tool for cereulide synthesis in foods

The execution of large-scale surveys for screening of cereulide in complex matrices is hampered by the lack of appropriate and fast toxin detection methods. Therefore, the suitability of a previously constructed cereulide synthesis reporter strain was evaluated with regards to its *in situ* applicability in foods. The strain was constructed by transcriptionally fusing a 238-bp region covering the main cereulide synthetase promoter $cesP_1$ to a *luxABCDE* cassette on the plasmid pXen1, thereby creating pMDX[P_1/*lux*] (Dommel 2008). The reporter plasmid was introduced into the emetic type strain *B. cereus* F4810/72, so that the effects of extrinsic signals acting on the promoter activity could be monitored through the emitted bioluminescence. To

exclude cryptic promoter activity, F4810/72 transformed with a promoterless luciferase construct was used as the negative control. After spot inoculating media of diverse nutrient compositions, F4810/72[P_1/*lux*] could be unambiguously detected with an ICCD camera system, whereas luminescence was not emitted by the negative control strain F4810/72 [pXen1] (Fig. 6).

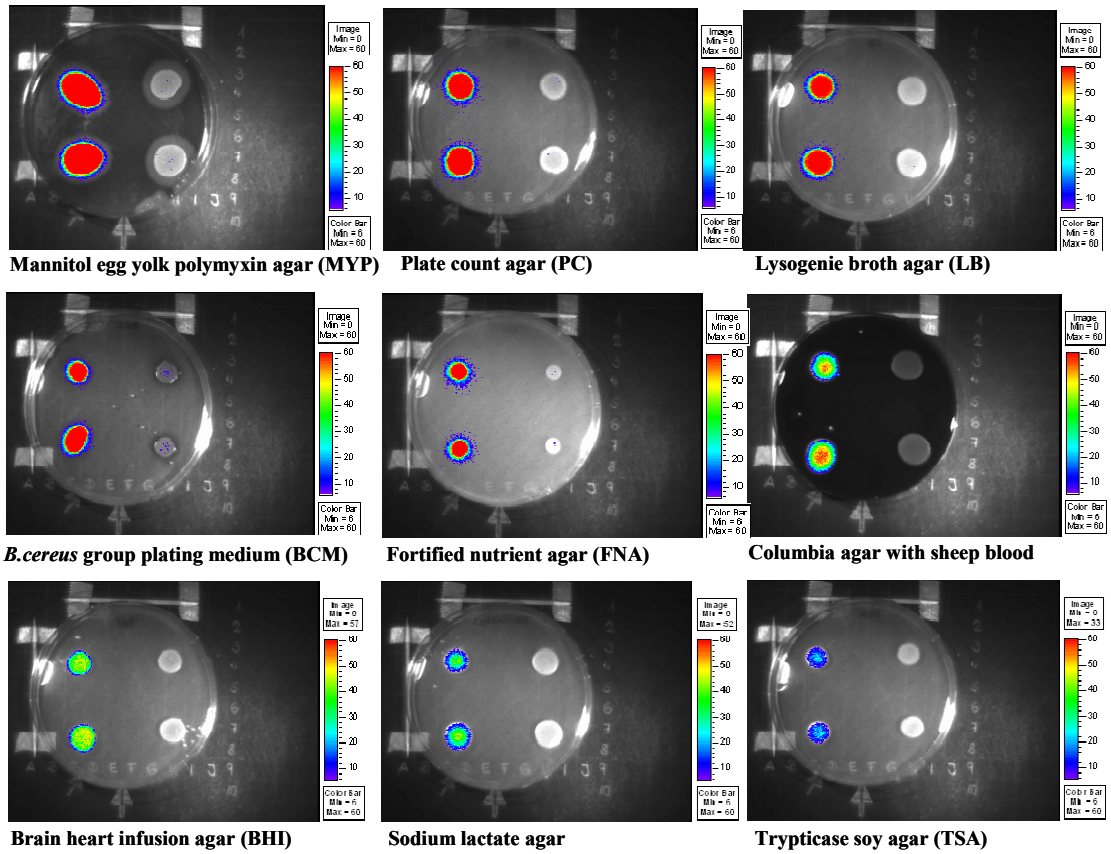

Figure 6: Monitoring of cereulide synthetase promoter activity on various growth media. The bioluminescent reporter strain *B. cereus* F4810/72[P_1/*lux*] (left hand side) and a promoter-less control strain (*B. cereus* F4810/72[pXen1], right hand side) were inoculated as 2 x 25 µl drops on various culture media. After incubation for 24 h at 24°C, the luciferase gene expression was visualized with a Hamamatsu image collector equipped with the Living image/IGOR Pro 4.01 software.

The intensity of the luminescence signals was strongly dependent on the growth substrates available, indicating that transcription of the cereulide synthetase genes was promoted by media containing carbohydrates (MYP, PC, and BCM agar), while the P_1 promoter activity was comparably lower on media such as Columbia agar, BHI, and TSA, which contain higher amounts of rich proteinaceous ingredients (e.g. sheep blood, brain heart infusion and peptones). Media which promoted P_{cesP1} activity also contained yeast or meat extracts (MYP, PC, LB, BCM, and FNA).

To establish a rapid real-time monitoring method for foods, different combinations of reporter strain inoculum sizes, incubation temperatures and incubation times were tested. An optimal combination was obtained by incubating 30-g food portions in sealed Petri dishes for 24 hours

at 24°C; the temperature reported to be optimal for cereulide synthesis (Häggblom *et al.* 2002). The foods were spiked with four 25-µl drops of the *B. cereus* reporter strain, corresponding to 10^3 CFU per gram of food. A total of 115 foods were artificially inoculated and the activity of P_{cesP1} was visualized with the ICCD camera. Representative images are shown in Figure 7.

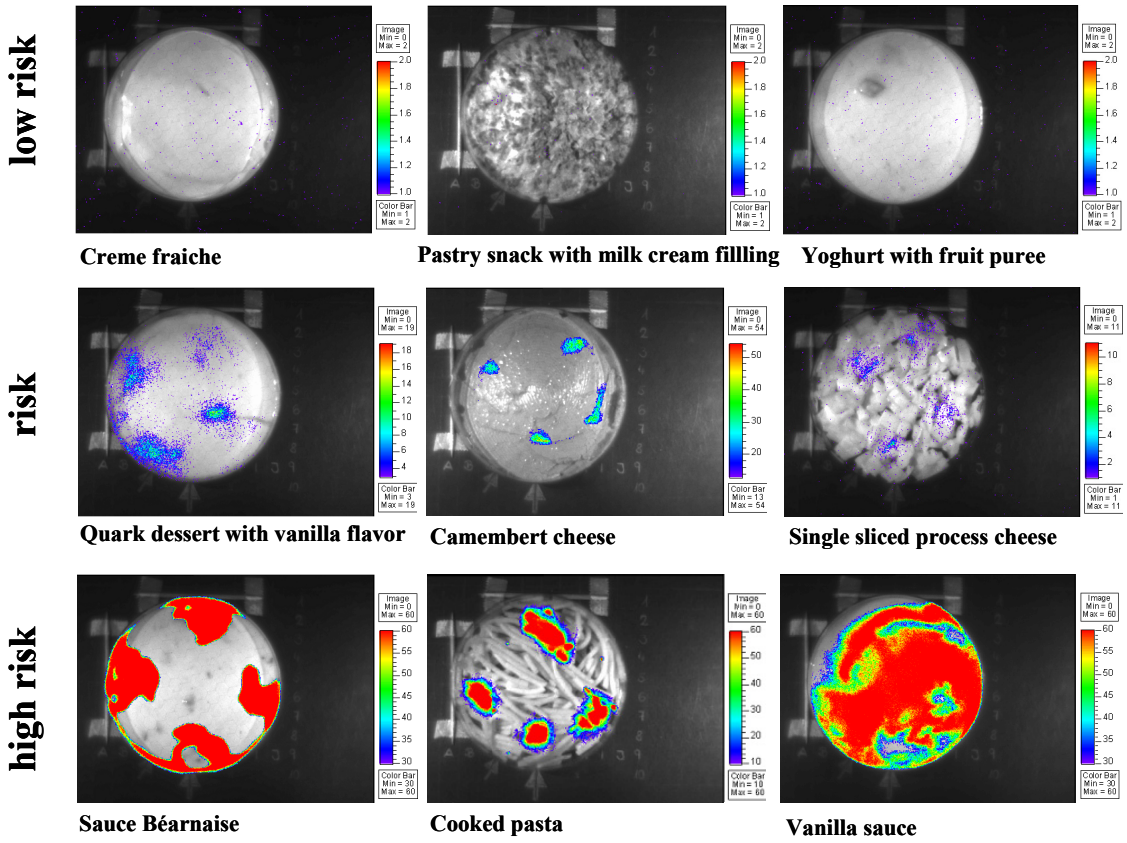

Figure 7: Real-time monitoring of cereulide synthetase promoter activity in retail food using the bioluminescent reporter strain *B. cereus* F4810/72[P_1/*lux*]. After incubation for 24 h at 24°C, the luciferase gene expression controlled by the main cereulide synthetase promoter P_1 was detected and visualized with a photon-counting ICCD camera. The signal intensities are shown as false-color renderings with a false-color scale that were superimposed on gray-scale images of the respective food sample. According to the intensity of luminescence signals, foods were designated as low risk, risk, and high risk products regarding their potential to support cereulide synthesis (compare Table 12). Representative images of a screening of over one hundred foods are shown.

To quantify the emitted bioluminescence signals, total photon counts were determined in a software-assisted region of interest (ROI) analysis. The transcription efficiency of the *ces* gene cluster was strongly influenced by the food matrix and varied by 5 orders of magnitude. According to the ROI analysis, foods were categorized into three main classes regarding their potential to support cereulide production: high risk, risk, and low risk foods (Fig. 7). Derived mean ROI values of each risk category and the corresponding determined threshold values are listed in Table 12.

Table 12: Threshold values for software-assisted categorization of food products regarding their potential to support cereulide synthesis[a]

Food category	Mean ROI sum	Minimal ROI sum	Maximal ROI sum
Low risk	5.2E+02	4.2E+01	8.3E+02
Risk	2.9E+04	1.3E+03	6.7E+04
High risk	3.8E+06	2.1E+05	9.7E+06

[a] A set of 115 foods was inoculated with a *lux*-based *B. cereus* reporter strain for monitoring cereulide synthesis. Bioluminescence imaging was carried out with an ICCD camera system. The total photon count was quantified *via* region of interest (ROI) analysis as described in Materials and Methods.

In summary, 45% of the foods were categorized as high risk foods, while the remaining 22% and 33% were categorized as risk or low risk foods, respectively. In general, products classified as insensitive were dairy-based and displayed a low pH value (e.g., cream cheese, yoghurt and unsweetened quark), had a high fat content like chocolate and nut spread or were characterized by low water availability (dried fruits, pastries). Proteinaceous food stuff combined with high fat amounts such as minced beef or milk powder-based process cheeses were categorized as sensitive (Fig. 7). Additionally, dairy products dulcified with glucose or fructose (quark desserts, cream-filled soft biscuits) fell in the sensitive class in terms of the risk of cereulide production. The group of highly sensitive products comprised farinaceous foods, as well as reconstitutable dried ingredients (e.g. rice, pasta, milk powder, and pectin-based thickeners). Moreover, foods with a high content of quickly available carbohydrates, especially fructose and sucrose, were predominantly classified as highly sensitive such as rice pudding, vanilla sauce and powdered diet supplements. Dairy-and cereal-based infant food formulas, which were additionally enriched with vitamins or trace elements, promoted exceptional high *ces* promoter activities.

To further strengthen the suitability of the *lux*-strain as an indicator organism for the risk of cereulide formation, a selection of foods was characterized regarding the coherence of cell counts, *ces* promoter activity, and cereulide levels (Table 13). The model food systems differed with respect to the nutrient composition and the initial pH. Prior to inoculation, all foods were tested negative for natural contamination with emetic *B. cereus* by using selective plating media and PCR targeting the *ces* genes (data not shown).

To assess the influence of the reporter plasmid on strain multiplication, viable cell counts for both, wild type *B. cereus* F4810/72 and the bioluminescent strain were enumerated by conventional plate counting. Almost identical cell numbers were observed for both strains after incubation for 24 h at 24°C (Table 13), showing that maintenance of the episomal construct has no major influence on *B. cereus* growth. To correlate the P_1 driven transcript synthesis, i.e. the ROI analysis, with the amount of cereulide produced by wild type *B. cereus* F4810/72, the toxin quantity was determined with the HEp2-cell based cell culture assay. To circumvent the problem of food matrix-dependent extraction efficiencies, standardized amounts of valinomycin, a commercially available depsipeptide with similar physico-chemical properties as

cereulide, were spiked into parallel food batches, and the extracts were used for calculation of the toxin recovery rate. Furthermore, measurements of unspiked food sample extracts ensured that cereulide was absent in the retail food, that the extracts had no interfering toxic effect on the HEp-2 cells (data not shown). As illustrated in Table 13, cereulide amounts matched the luminescence-defined risk categories, suggesting that the intensity of the luciferase signals broadly reflects the quantity of toxin synthesized in these matrices. Moreover, the data underline that cereulide synthesis strongly depends on the composition of the food, as cell counts were identical in the Sauce Béarnaise and in cooked rice, whereas the cereulide production varied considerably.

Table 13: Correlation of cell counts, cereulide synthetase promoter activity, and cereulide production of emetic *B. cereus* F4810/72 in different foods after 24 h at 24°C[a]

		Mean *B. cereus* cell count ± SD (log CFU g^{-1})				
Food	pH	F4810/72	F4810/72 [P_1/*lux*]	P_1 activity (total counts in ROI)[b]	Mean cereulide concn ± SD (µg g^{-1})[c]	Category[d]
Sauce Béarnaise	5.8	7.4 ± 0.1	7.3 ± 0.2	8.2E+06	8.0 ± 1.6	HR
Liver sausage	6.2	7.9 ± 0.0	7.9 ± 0.2	3.1E+05	2.4 ± 1.7	HR
Cooked rice	7.0	7.6 ± 0.1	7.5 ± 0.2	1.9E+06	1.8 ± 0.6	HR
Camembert cheese	7.9	6.7 ± 0.1	6.9 ± 0.4	6.7E+04	0.6 ± 0.4	R
Vanilla quark dessert	5.1	6.0 ± 0.0	6.0 ± 0.3	2.3E+04	1.0 ± 0.4	R
Pastry snack milk filling	5.9	6.2 ± 0.4	5.9 ± 0.3	8.3E+02	ND	LR
Crème fraiche	4.5	4.5 ± 0.1	4.3 ± 0.3	7.1E+02	ND	LR

[a] Test were performed in triplicate. ND, not detectable.
[b] Average of three independent measurements
[c] Toxin amounts were determined with the HEp-2 cell based cytoxicity assay
[c] Potential to support cereulide synthesis. HR, high-risk food; R, risk food; LR, low-risk food

B. cereus F4810/72 was originally isolated from rice involved in an emetic food poisoning case in the UK in 1972. As decades of laboratory culturing might have modified the original features of this strain, the P_1-*lux* construct was additionally introduced into two other recently obtained emetic *B. cereus*: one clinical isolate and one food isolate from a food poisoning outbreak caused by a rice dish. To evaluate the functionality of the reporter plasmid in different genetic backgrounds, strains were grown on cooked rice, and luminescence was recorded with the ICCD camera. As shown in Fig. 8, P_1 was also active in these strains and responded with similar signal intensity. Consistent with this, toxin quantifications revealed the presence of similar cereulide amounts ranging from 1.8 to 2.2 µg per gram of food.

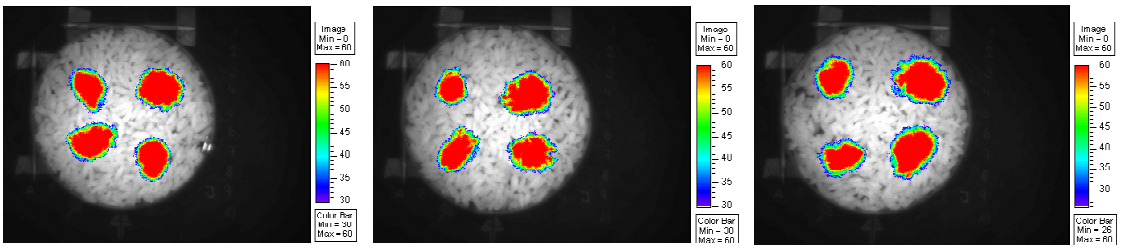

Figure 8: The P_1 cereulide synthetase promoter of *B. cereus* F4810/72 is equally active in the background of different emetic strains. Panels show the emetic reference strain F4810/72, one emetic isolate from a recent food-borne outbreak, and one clinical isolate. All isolates were transformed with the pMDX[P_1/*lux*] luciferase reporter plasmid and cultivated for 24 h at 24°C on cooked rice. Luciferase signals emitted by the reporter strains were detected with a photon-counting ICCD camera and are shown as false color renderings that were superimposed on grey-scale food images.

Taken together, this study showed that the *lux*-based emetic *B. cereus* reporter strain is a suitable tool for a rapid visualization and preliminary evaluation of cereulide toxin synthesis in complex environments such as foods. Furthermore, data imply that the level of cereulide synthesis strongly depends on extrinsic parameters such as the nutrient composition of the spoiled food.

3.3 Inhibition of cereulide synthesis by long-chain polyphosphates

The luciferase-based reporter strain was further used to examine the capability of food additives to suppress cereulide production in model foods. Long-chain polyphosphates (polyPs) and derived orthophosphoric blends were chosen, since these food additives are classified as GRAS (generally recognized as safe) and are extensively used in the dairy and meat industry owing to their functional aspects regarding emulsification andstabilization, and in second line as antimicrobial agents.

3.3.1 Influence of polyPs on cereulide synthesis in model foods

To initially assess the impact of polyPs on the activity of the *ces* promoter, a dairy-based infant formula was chosen, which supported a very high promoter activity (Ch. 3.2) and was therefore regarded to be a “high-challenge” trial product. According to the manufacturer, this product was not blended with polyP. Portions of the reconstituted infant formula were treated with 5% of three polyP formulations that differed with respect to the total phosphate content (P_2O_5), the average chain length and the orthophosphate content (Table 3 in Material and Methods).

One control and the treated food samples were artificially spiked with F4810/72[P_1/*lux*] and further analyzed by luminescence imaging according to the established protocol (Ch. 3.2). After mimicking temperature abuse of the food by incubation at 24°C for 24 hours, the *ces* operon promoter was highly active in the untreated control sample (Fig. 9). By contrast, treatment with 5% polyP 2 and polyP 3 almost completely repressed bioluminescence, whereas moderate signal intensities were observed with polyP 1.

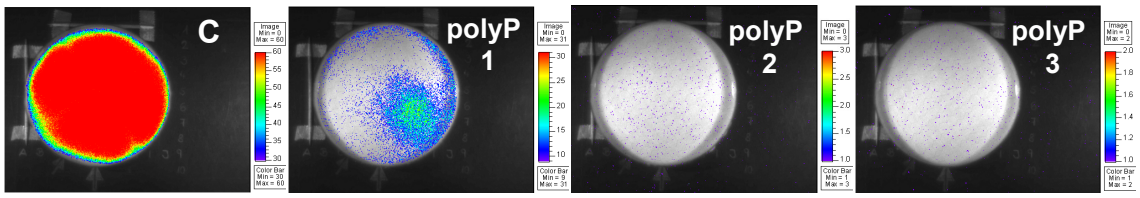

Figure 9: Long-chain polyphosphates reduce cereulide synthetase promoter activity in infant food. Reconstituted infant food was inoculated with the bioluminescent *B. cereus* reporter strain F4810/72[P_1/*lux*] and food spoilage was simulated by incubation at 24°C for 24 h. Influence of 5% polyPs on *ces* promoter activity was visualized after 24 h with a photon-counting ICCD camera (Hamamatsu Photonics, model 2400-32). C, untreated control; polyP, food-grade, long-chain polyphosphate mixtures. Representative images of four independent experiments are shown.

To decipher whether *lux* activity was reduced due to cell lysis or due to transcription inhibition and to further correlate growth and toxin production, the experiment was repeated and viable cell counts for both, *B. cereus* F4810/72 wild type and the reporter strain were determined. Additionally, samples spiked with the wild type were extracted with 96% ethanol and toxin quantification was carried out with the HEp-2 cell culture assay and with a HPLC/ESI-TOF-MS analysis.

As summarized in Table 14, the three polyP mixtures caused different effects on growth and cereulide synthesis. Enumeration of cell counts revealed that growth was not affected by 5% polyP blend 1. In comparison, polyP 3 inhibited cell growth by 1 log unit, and treatment with 5% polyP 2 led to bacteriostatic and slight bactericidal effects since only the initial cell inoculum was recovered. Control LC/MS measurements of unspiked food extracts and of samples directly extracted after inoculation with *B. cereus* showed that cereulide was absent in the retail food and cereulide was not introduced from the F4810/72 pre-cultures. Cereulide was detected predominantly in its NH_4^+ adduct form, followed by the toxicologically important, highly stable K^+ complex (data not shown). However, occurrence of the NH_4^+ adduct is a typical bias introduced by analytical procedures (Pitchayawasin *et al.* 2003). LC/MS data were in good agreement with the HEp-2 assay data, suggesting that the higher structure of the ionophor necessary to induce toxicity was not altered by polyP addition (Table 14). In correlation with the ROI analysis of the reporter strain spiked samples, high cereulide concentrations of 6 µg g^{-1} were detected without polyP addition, whereas toxin concentrations were significantly reduced by the food additives, to 31% (polyP 1), 6.0% (polyP 2), and 1.6% (polyP 3). Differences in the final cell counts could not be detected between the control and the polyP 1 samples, indicating

that the inhibition of toxin synthesis was no effect simply based on the inhibition of bacterial growth.

Table 14: Effects of polyPs on cell count, cereulide synthetase promoter activity, and cereulide production by emetic *B. cereus* in infant food after 24 h at 24°C[a]

	Mean N_i (log_{10} CFU g^{-1}) ± SD of *B. cereus* F4810/72[b]	Mean N_i (log_{10} CFU g^{-1}) ± SD of *B. cereus* F4810/72[P_1/*lux*][b]	*ces* synthetase promoter activity (total ROI count)[c]	Mean cereulide concn. (µg g^{-1} food) by LC/MS analysis	Cereulide concn. (%) by cytotoxicity assay[d]
Control	4.0 ± 0.3	3.8 ± 0.1	6.3E +07	6.4 ± 1.5	100
5% polyP 1	4.1 ± 0.2	3.9 ± 0.1	5.8E +06	2.0 ± 0.8	31
5% polyP 2	-0.1 ± 0.4	-0.2 ± 0.2	7.1E +03	0.4 ± 0.8	6.8
5% polyP 3	3.2 ± 0.2	3.0 ± 0.2	3.1E +03	0.1 ± 0.1	1.5

[a] Before incubation, food samples were inoculated with the *B. cereus* wild type or the bioluminescent reporter strain F4810/72[P_1/*lux*] resulting in 10^3 CFU g^{-1}. All experiments were performed at least in triplicate. Values are given as means with standard deviations.
[b] N_i, increase in viable cell counts per gram of food after 24 h (see Materials and Methods).
[c] Bioluminescence emitted by the emetic reporter strain quantified by a region-of-interest (ROI) analysis deduced from the whole Petri dish area (Fig. 9). Data are from an average of four independent experiments.
[d] Data are derived from three independent HEp-2 cytotoxicity assays and represent mean values. The toxin amount produced in absence of polyP was set to 100%.

Industrial oat milk, which was the subject of a *B. cereus* spoilage case analyzed in Chapter 3.1, was used as a second model food to assess the the inhibitory effects of PolyPs on cereulide synthesis. *B. cereus* F4810/72 produced 1 µg toxin per gram of food in untreated oat milk samples. This corresponds to one-sixth of the toxin amount in infant food, although final cell counts were higher in oat milk (Table 15). As observed in the infant food assay, the efficacies of the polyP blends differed with respect to growth and the inhibition of toxin synthesis (Table 15). While cell multiplication was only marginally affected in the presence of 0.1% polyPs, cereulide concentrations were reduced by 50 to 89%. In line with the infant formula experiment, polyP 3, the mixture with the highest polyP content lacking ortho-phosphate, was most efficient in reducing toxin synthesis. Nevertheless, all formulations inhibited toxin formation in a dose-dependent manner and amounts of cereulide dropped by 89% to 94% under the influence of 0.3% polyPs. Treatment with 0.5% caused a bacteriostatic (polyP 2) or slightly bacteriolytic (polyP 3) effect, whereas *B. cereus* was reduced by only 1 log unit in the presence of the mixture with the highest orthophosphate content, polyP 1. Importantly, the remaining viable cells did not produce cereulide, and toxin synthesis was completely prevented under these conditions.

Table 15: Effects of polyPs on cell count and cereulide production by emetic *B. cereus* in organic oat milk after 24 h at 24°C[a]

PolyP formulation (vol-%)	Mean N_i ($\log_{10}$ CFU g^{-1}) ± SD of *B. cereus* F4810/72[b]	Mean cereulide concn. (µg g^{-1} food) by LC/MS analysis[d]	Cereulide concn. (%) by cytotoxicity assay[d]
Control	5.3 ± 0.1	1.3 ± 0.3	100
polyP 1			
0.1%	5.3 ± 0.1	0.7 ± 0.2	51
0.2%	5.0 ± 0.0	0.4 ± 0.1	14
0.3%	4.9 ± 0.0	0.3 ± 0.1	11
0.5%	3.8 ± 0.3	ND[d]	0
polyP 2			
0.1%	5.2 ± 0.1	0.5 ± 0.1	31
0.2%	4.8 ± 0.1	0.4 ± 0.0	11
0.3%	4.3 ± 0.1	0.2 ± 0.2	8.6
0.5%	0.0 ± 0.2	ND	0
polyP 3			
0.1%	5.1 ± 0.1	0.4 ± 0.1	11
0.2%	4.8 ± 0.1	0.3 ± 0.1	8.6
0.3%	4.0 ± 0.0	0.2 ± 0.2	5.7
0.5%	-0.2 ± 0.1	ND	0

[a] Before incubation, food samples were inoculated with *B. cereus* F4810/72 resulting in 10^3 CFU g^{-1}. Data are given as means ± SD from three independent experiments.
[b] N_i, increase in viable cell counts per gram of food within 24 hours at 24°C.
[c] Data are derived from three independent HEp-2 cytotoxicity assays and represent mean values. The toxin amount produced in absence of polyP was set to 100%.
[d] ND, not detectable (detection limit ≤ 50 ng ml^{-1} cereulide).

3.3.2 Influence of polyPs on cereulide synthesis under defined conditions

To gain insight into the molecular effects of polyP exposure, the impacts of the three polyP blends on the phenotype of *B. cereus* and on *ces* gene transcription was examined under less complex conditions. *B. cereus* F4810/72 was grown in PC medium in the presence of a sublethal concentration (0.03%) of the polyP mixtures, since microscopic analysis revealed that concentrations above 0.05% caused lytic effects (data not shown). Under this condition, cell growth was impaired and commencement of logarithmical growth was delayed (Fig. 10). Under the influence of polyP 2 and 3 cell division was arrested and cell shape deformation occurred. As in the food experiments, the growth inhibition efficacy was strongly dependent on the type of polyP blend, with the mixture containing the lowest orthophosphate content (polyP 3) being the most effective. In presence of polyP 2 and polyP 3 cells were 3-to 4-fold longer compared to the untreated control culture (Fig. 10). Concordantly, exponential growth with normal division was resumed after 17 h in presence of polyP 1, whereas the onset of exponential growth was substantially delayed under polyP 2 and polyP 3 influence.

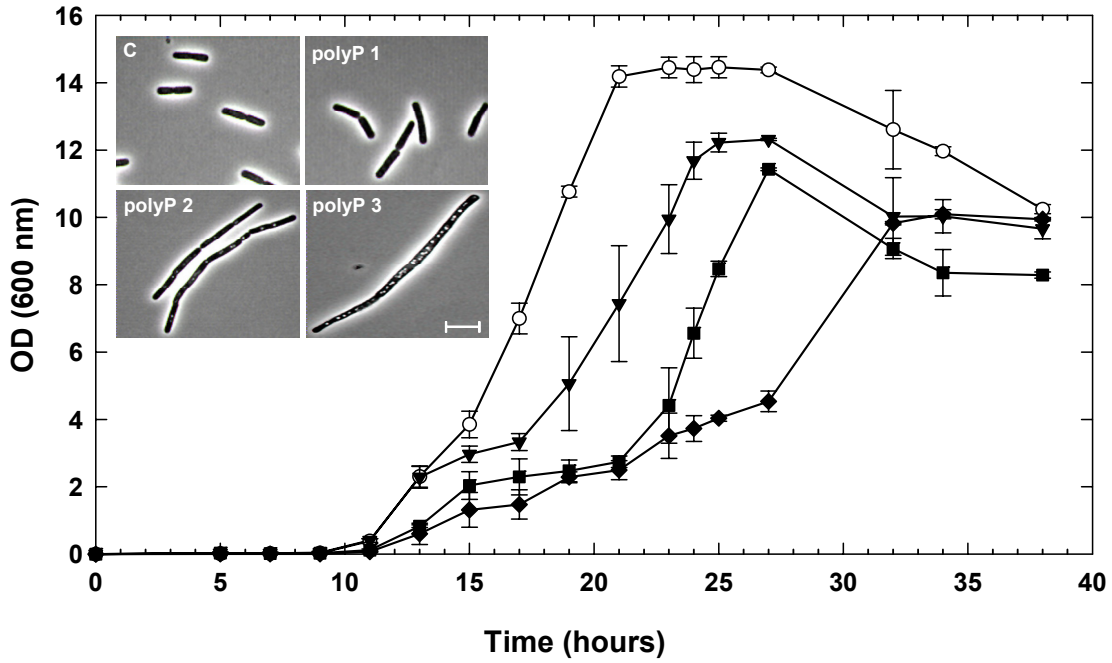

Figure 10: Effects of sublethal polyP concentration on growth and cell shape of emetic *B. cereus* in liquid culture**.** *B. cereus* F4810/72 was grown in PC medium in the absence (control, ○) and in the presence of 0.03% food-grade, long-chain polyphosphates (polyP 1, ▼; polyP 2, ■; polyP 3, ♦). Growth was monitored at an optical density of 600 nm. Standard deviations are derived from three independent measurements. Phase-contrast microscope images were taken 21 h after inoculation (C, control; polyP 1-3, elongated cells under influence of 0.03% polyphosphates; white scale bar represents 5 µm).

To examine the expression of the *ces* operon on a transcriptional level, qPCR was applied. As expected, maximal *ces* transcription was observed in the late-exponential growth phase of the control culture (17 h after inoculation, compare Fig. 10), thereafter transcription was strongly down regulated (Fig. 11). In accordance to this finding, maximum transcription was delayed under polyP influence (Fig. 11) but was detected when cells had resumed exponential growth-like stages with shorter cell lengths, suggesting that cereulide synthesis is connected with growth phases characterized by rapid cell division. Importantly, exposure to all three polyP formulations significantly reduced the *ces* transcript levels, which were 3- to 4-fold lower compared to the control.

Ces gene transcript levels were further compared with the toxin amounts. As polyPs did not alter the cytotoxicity of cereulide (Ch. 3.3.1), the HEp-2 assay was used for toxin measurements as sample preparation for the assay is readily performed by simple autoclaving of liquid culture aliquots. Without polyPs cereulide became detectable 17 h after inoculation and accumulated progressively during late logarithmical and stationary phase (Fig. 11). In contrast, cultures exposed to food additives remained non-toxic at least for 24 hours. In the stationary phase cereulide was detectable in all polyP treated cultures; however, toxin amounts were 3-fold reduced. This is in agreement with the lower transcription of the *ces* genes.

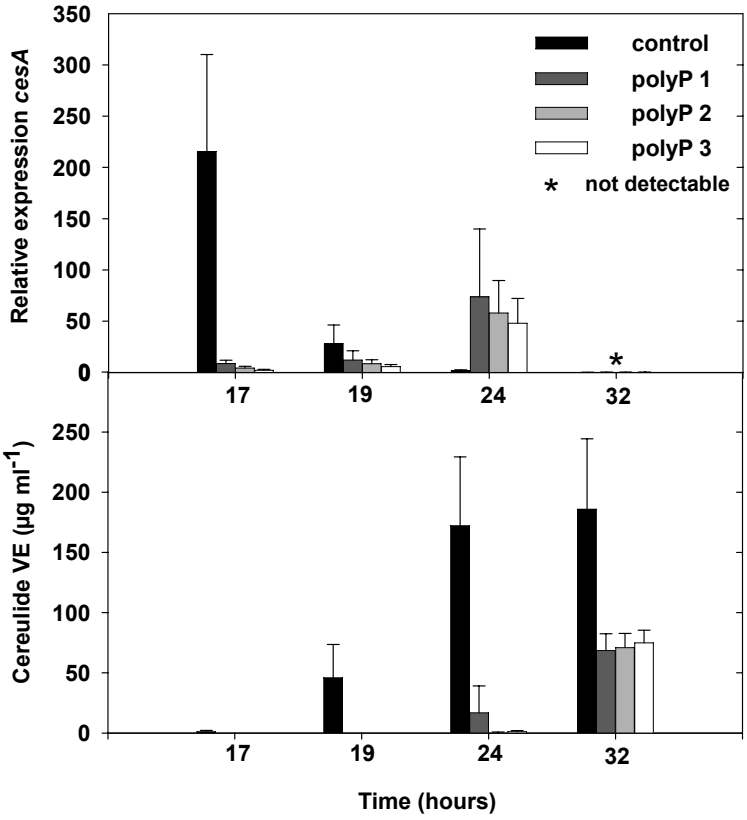

Figure 11: Influence of sublethal polyP concentration on *ces* gene transcription and cereulide synthesis in liquid culture. *B. cereus* F4810/72 was grown in PC medium in the absence (black bar) and in the presence of 0.03% of three food-grade, long-chain polyphosphate mixtures (grey and white bars, polyP1-3). Transcript levels of *cesA* were determined at indicated time points in relation to 16S rRNA transcript levels of the same RNA preparations. Error bars indicate standard deviations from three independent cultures and nine independent qPCR measurements, respective-ly. Cereulide quantity, given as valinomycin equi-valents (VE), was assessed with the HEp-2 cell cytotoxicity assay.

To finally distinguish simple inhibition of growth from inhibition of toxin synthesis, the impact of polyPs at subinhibitory concentrations with respect to vegetative cell growth was investigated. Figure 12 illustrates that addition of 0.01% polyPs had no inhibitory effect on the growth rate of *B. cereus* F4810/72 and anomalies in the cell form were not observed. However, cereulide synthesis was significantly reduced by 30 to 60% after 24 and 32 hours of cultivation, respectively. Thus, consistent with the data obtained with the food experiments, polyP exposure clearly reduced the level of *ces* promoter driven NRPS expression and inhibited cereulide production in a dose-dependent manner.

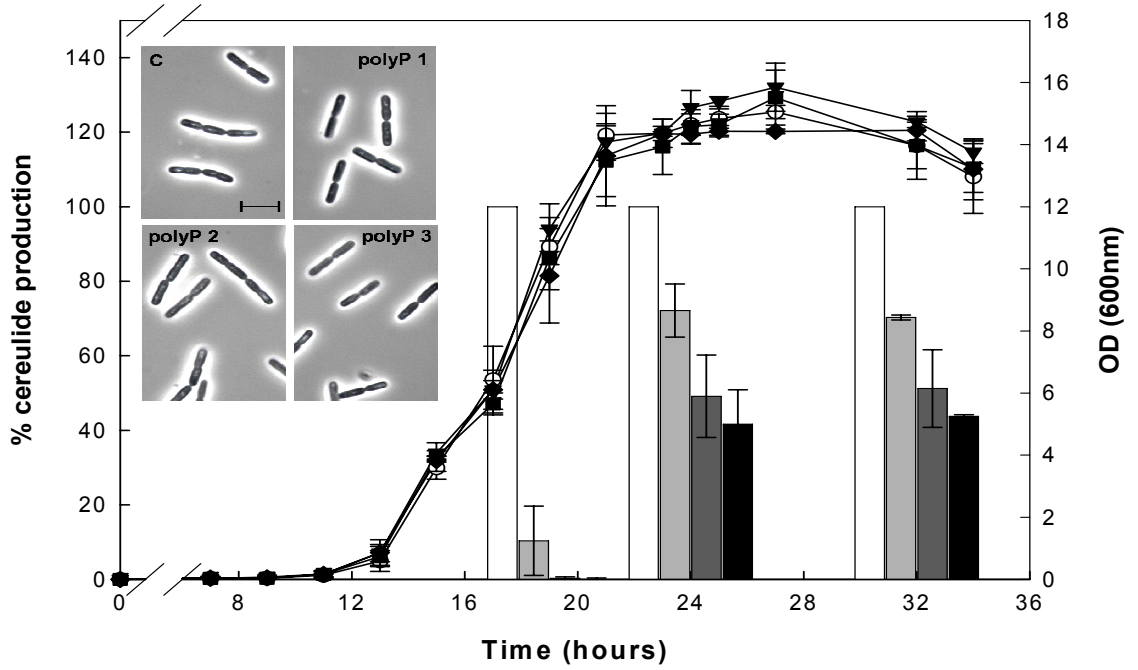

Figure 12: Growth and toxin production of emetic *B. cereus* in the presence of 0.01% polyP. *B. cereus* F4810/72 growth in PC medium in the absence (○, control culture) and in the presence of three food-grade polyphosphate blends (polyP 1, ▼; polyP 2, ■; polyP 3, ♦) was followed by measurement of optical density at 600 nm. Phase-contrast microscope images were captured 21 h after inoculation (C, control; polyP 1-3, cells treated with 0.01% polyphosphates). The black scale bar represents 5 µm. Cereulide was quantified with the HEp-2 cell based toxicity assay after 19, 24 and 32 hours, respectively. Toxin quantity was set to 100% for the untreated culture (white bars) to display reduction of toxin synthesis under the influence of polyP 1 (pale grey bars), polyP 2 (dark grey bars) and polyP 3 (black bars). Error bars correspond to standard deviations derived from three independent experiments.

3.4 Identification of transcription factors involved in regulation of *ces* NRPS expression

The previous chapter showed that extrinsic factors, such as the composition of the food matrix or food additives, can profoundly influence cereulide production. However, information on how these signals are sensed and become integrated in the regulatory network of cereulide synthesis is scarce. Nevertheless, the tightly temporal regulated transcription of the biosynthetic *ces* genes during exponential cell growth indicates that, besides AbrB, additional regulatory proteins must play a role as activators and/or repressors. With the aim of identifying transcription factors that directly bind to the main promoter region of the *ces* operon, *in silico* footprinting analyses was combined with an experimental evaluation of a selection of transcription factors by electrophoretic mobility shift assays.

3.4.1 *In silico* binding prediction and Best Reciprocal Hit analysis

Besides the experimental and computational characterization of the σ^B and the PlcR regulon, information on transcription factor regulons is missing for *B. cereus*, which would allow an *in silico* assembly of the *cis*-regulatory consensus motifs and hence, would allow a direct search for transcription factor binding motifs in the *ces* cluster promoter region. To retrieve transcription factor candidates for gel mobility experiments, *in silico* footprinting was therefore carried out using the Database of Transcriptional Regulation in *Bacillus subtilis* (DBTBS). The weight matrix search algorithm was used to predict the binding probability and recognition sites of 33 *B. subtilis* transcription factors towards the entire 990-bp non-coding region between *cesH* and the translation start of *cesP* (Fig. 2). Sigma factors were excluded from this study. For the remaining transcription factors, the prediction threshold was set to a p=5% significance level. (Detailed data of footprinting results are listed in Table A1 in the Appendix). No binding was predicted for AraR, BkdR, CcpA, ComA, CtsR, Fnr, Hpr (ScoC), IolR, Mra, PucR, RocR, Spo0A, SpoIIID, and Xre. In accordance with the previously verified role of AbrB as transcriptional repressor of the *ces* genes (Lücking *et al.* 2009), an AbrB binding site was predicted in close proximity to the presumably σ^A-dependent promoter elements of P_{cesP1}. Furthermore, putative binding sites spatially associated with the P_{cesP1}/P_{cesP2}-core regions were found for CodY, ComK, DegU, GlnR, LevR, LexA, MntR, PerR, PurR, SinR, TnrA, and Zur. The matching score, that is a measure for the potential of the predicted motif to participate in regulation, varied between 4.94 (DegU) and 9.21 (HrcA) (Table A1, Appendix). However, as the GC-content of *B. cereus* genomes is on average lower compared to *B. subtilis* genomes (around 35% versus 44%), the score value was considered to be less predictive than localization and quantity of the presumptive binding sites.

To examine whether physiologically related proteins exist in *B. cereus* F4810/72, a set of candidate transcription factors was selected on the basis of following assumptions: (i) expression or activity of the transcription factor could correlate with the time point of cereulide NRPS expression (ii) presumptive binding motifs lie in proximity to the *ces* main promoter region (iii) several binding sites are predicted, and (iv) the transcriptional regultor exhibits a broad regulon rather than a specialized function. Additionally, ComA, a major activator of surfactin NRPS expression in *B. subtilis* was included.

Prediction of orthologous proteins between the "reference" strain *B. subtilis* subsp. *subtilis* strain 168 (BSU168) and *B. cereus* F4810/72 (also termed BCAH187) was performed on the National Center for Biotechnology Information (NCBI) web site. At that time, the majority of F4810/72 RefSeq records had not passed the NCBI curation process, thus genes were in the "provisional" status or had no assigned function. Therefore, identification of genes that are most likely to share the same function in both organisms was performed by means of a Best Reciprocal Hit (BRH) BLASTP search approach (for details of stringency, see Materials and Methods; Ch. 2.5). The BRH procedure is exemplified in Figure 13. For this purpose, the protein showing the most significant primary structure similarity in *B. cereus* F4810/72 was

recorded as the first target. In some cases, however, two or more genes matched with similar or acceptable stringency and were additionally examined (Fig. 13 and Table 16). Conversely, the retrieved *B. cereus* F4810/72 sequence was used to query the homolog showing the most significant amino acid sequence similarity in the reference organism *B. subtilis* 168. The results of the BRH analysis are summarized in Table 16.

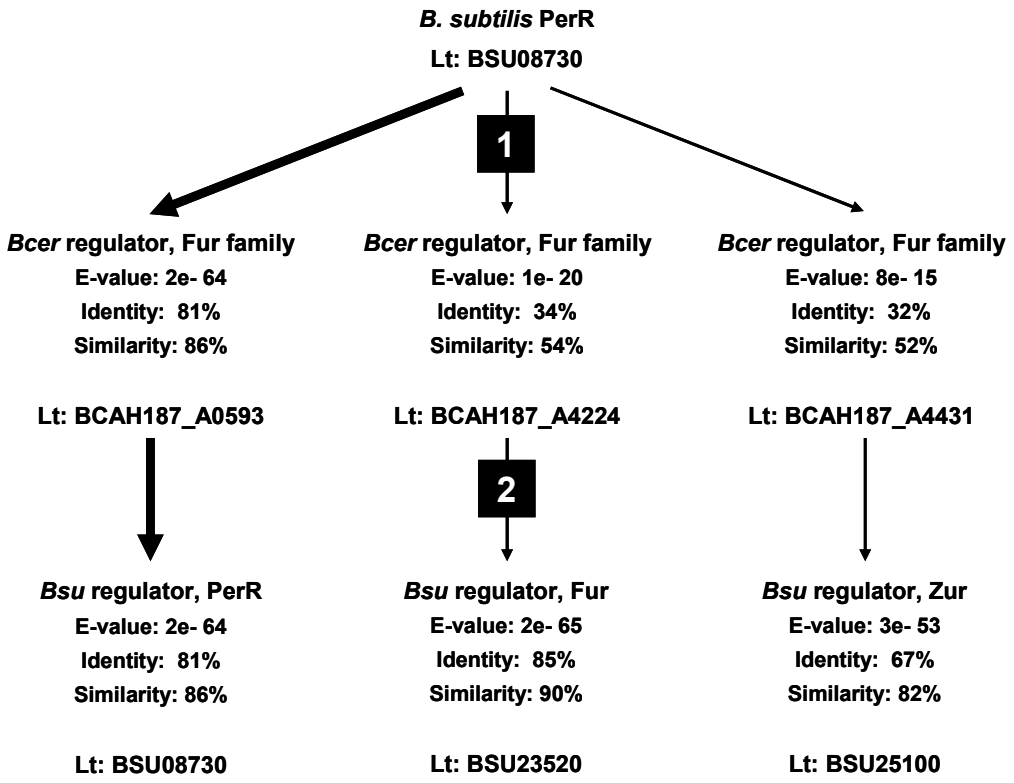

Figure 13: Example for identification of orthologous transcriptional regulators in *B. cereus* and *B. subtilis* by the BRH method. Step 1 indicates the initial BLASTP run that retrieves candidate proteins with assumed similar physiological functions as those described for the query protein of *B. subtilis*. Step 2 indicates the reciprocal BLASTP search that enhances the precision of functional assignment to uncharacterized *B. cereus* proteins. Thick arrows indicate the Best Reciprocal Hit. Lt, NCBI protein Locus tag.

Table 16: Transcription factor orthologs predicted with the Best Reciprocal Hit method: BLASTP was used to identify transcriptional regulators with putative similar functions in *B. subtilis* 168 and *B. cereus* F4810/72[a]

Transcrip-tion factor	BLASTP to F4810/72[b]	Reciprocal BLASTP to BSU168[c]
PerR (BSU08730)	**Fur family regulator** (BCAH187_A0593) E: 2e-64; I: 81%; S: 86% **Fur family regulator** (BCAH187_A4224) E: 1e-20; I: 34%; S: 54% **Fur family regulator** (BCAH187_A4431) E: 8e-15; I: 32%; S: 52%	**PerR** (BSU08730) E: 2e-64; I: 81%; S: 86% **Fur** (BSU23520) E: 2e-65; I: 85%; S: 90% **Zur** (BSU25100) E: 3e-53; I: 67%; S: 82%
CodY (BSU16170)	**CodY** (BCAH187_A3875) E: 4e-116; I: 82%; S: 93%	**CodY** (BSU16170) E: 3e-116; I: 82%; S: 93%
ComA (BSU31680)	**Response regulator** (BCAH187_A5591) E: 3e-23; I: 32%; S: 57% **Response regulator** (BCAH187_A1601) E: 5e-21; I: 32%; S: 54% **Response regulator** (BCAH187_A2375) E: 2e-16; I: 28%; S: 53% **Response regulator** (BCAH187_A1913) E: 1e-15, I: 27%; S: 53% **Response regulator** (BCAH187_A5531) E: 3e-15; I: 25%; S: 51%	**YhcZ** response regulator (BSU09330) E: 2e-56; I: 53%; S: 72% **LiaR** response regulator (BSU33080) E: 6e-78; I: 65%; S: 84% **YhcZ** response regulator (BSU09330) E: 2e-56; I: 53%; S: 74% **YfiK** response regulator (BSU08300) E: 4e-36; I: 39%; S: 62% **YvfU** response regulator (BSU34060) E: 6e-73; I: 53%; S: 74%
ComK (BSU10420)	**Putative competence transcrip. factor** (BCAH187_A1292) E: 1e-35; I: 40%; S: 62%	**ComK** (BSU10240) E: 1e-35; I: 40%; S: 62%
DegU (BSU35490)	**Response regulator** (BCAH187_A5591) E: 2e-44; I: 42%; S: 63% **Response regulator** (BCAH187_A2375) E: 9e-43; I: 40%; S: 62% **Response regulator** (BCAH187_A1601) E: 2e-41; I: 37%; S: 63% **Response regulator** (BCAH187_A1913) E: 1e-31; I: 35%; S: 56% **Response regulator** (BCAH187_A5531) E: 3e-28; I: 30%; S: 53%	**YhcZ** response regulator (BSU09330) E:2e-56; I:53%; S: 72% **YhcZ** response regulator (BSU09330) E:2e-56; I:53%; S: 74% **LiaR** response regulator (BSU33080) E:6e-78; I: 65%; S: 84% **YfiK** response regulator (BSU08300) E: 4e-36; I: 39%; S: 62% **YvfU** response regulator (BSU34060) E: 6e-73; I: 67%; S: 80%
HrcA (BSU25490)	**Heat-inducible repressor HrcA** (BCAH187_A4449) E: 5e-127; I: 64%; S: 80%	**HrcA** (BSU25490) E: 5e-127; I: 64%; S: 80%
MntR (BSU24520)	**MntR** (BCAH187_A4333) E: 1e-66; I: 86%; S: 93%	**MntR** (BSU24520) E: 1e-66; I: 86%; S: 93%
SinR (BSU24610)	**SinR** (BCAH187_A1435) E: 9e-39; I: 68%; S: 84%	**SinR** (BSU24610) E:9e-39; I: 68%; S: 84%
TnrA (BSU13310)	**GlnR** (BCAH187_A3755) E:2e-11; I: 44%; S: 63%	**GlnR** (BSU17450) E:6e-41; I: 63%; S: 78%

[a] BLAST sequences were selected if the E-values were $<10^{-10}$ and the sequence similarity >50% (see Materials and Methods, Ch. 2.5). E, Expectation-value; I, amino acid sequence identity; S, amino acid sequence similarity.
[b] F4810/72, *B. cereus* AH187 (NCBI TaxID: 405534).
[c] BSU168, *B. subtilis* subsp. *subtilis* str. 168 (NCBI TaxID: 224308).

Retrieval of BeTs and prediction of orthologs was unambiguous for PerR, CodY, ComK, HrcA, MntR, and SinR (Table 16). However, a TnrA ortholog is obviously absent in *B. cereus* F4810/72, and several paralogs of the response regulators DegU and ComA were found, making the prediction of functional equivalence uncertain.

3.4.2 *In vitro ces* promoter binding analyses

Transcription factor orthology as predicted by the BRH method is usually not sufficient to unambiguously assign a role in transcriptional regulation. Thus, CcpA, CodY, ComK, PerR, and SinR of *B. cereus* as well as DegU of *B. subtilis* were further analyzed regarding their *in vitro* binding ability towards various stretches of the *ces* promoter region (Fig. 14). Transcription factors were heterologously expressed as soluble polyhistidine-tag fusion proteins and used for non-radioactive gel mobility shift experiments. To ensure that the purified proteins were functional, the His_6-tag was fused to the protein terminus devoid of the DNA binding motif. Furthermore, a promoter region to which binding had been verified for *B. subtilis* was included as positive control.

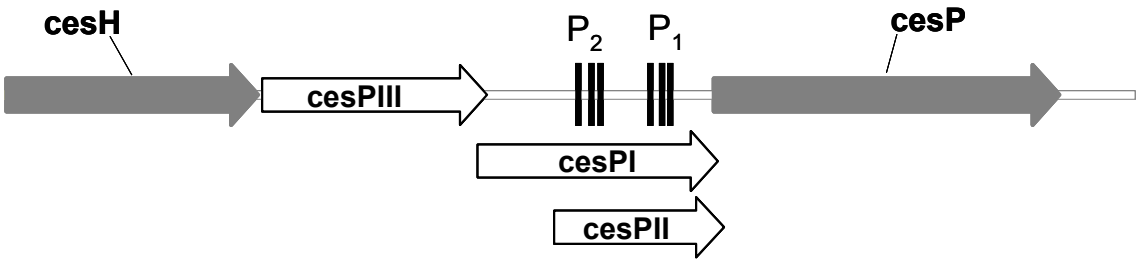

Figure 14: Features of DNA probes used for *in vitro* binding studies with various *B. cereus* transcription factors. Fragments of the non-coding region between the *cesH* and *cesP* genes (grey arrows) were amplified by PCR, purified and applied for gel mobility shift assays. The positions of the main *ces* operon promoter P_1 and the second promoter P_2 are denoted by three black bars, which represent the -35 and the -10 boxes as well as the transcription start (+1). cesPI designates a 523-bp fragment that covers both promoters, while the second half of the non-coding region is covered by cesPIII (488 bp). The cesPII probe is a 368-bp fragment of P_1 and P_2, but with shorter upstream region than cesPI.

Optimization of gel shift conditions for the global transition state regulator CodY was performed with the promoter of *ilvB*, a gene involved in biosynthesis of branched-chain amino acids in *B. subtilis*, which is repressed by CodY. *In vitro* DNA binding experiments were carried out in the presence of L-isoleucine, L-leucine, and L-valine (ILV) and GTP in the binding and running buffers, which are putative ligands of the protein. As shown in Figure 15, addition of CodY-His_6 to a DNA probe containing the *B. subtilis ilvB* promoter region led to the formation of protein-DNA-complexes and a slower migrating band on the native PAA gels. The apparent equilibrium constant [K_D] was estimated to be around 150 nM. By contrast, binding was weaker (K_D ≈500 nM) when ILV were omitted from assay buffers (data not shown), indicating that the ligands enhanced the DNA binding capacity of *B. cereus* CodY *in vitro*. Binding to P_{ilvB} was specific, since the competitive negative control DNA was not shifted.

Moreover, incubation with two different DNA fragments randomly amplified from *B. cereus* genomic DNA did not lead to DNA/protein complex formation (Fig. 15). Importantly, gel shifts revealed that CodY bound with high affinity (K_D ≈50 nM) to the 3´ area of the non-coding region between *cesH* and *cesP* (probes: cesPI and cespII), but not to the 5´ area lacking the main promoter region (cesPIII probe).

A targeted *in silico* prediction of the position of putative CodY-boxes was perfomed using the xBASE 2.0 server (for details, see Materials and Methods). In accordance with the gel shift assays, one 15-bp sequence with three mismatches to the *B. subtilis* CodY consensus motif was found in direct proximity to the -35 region of the $cesP_1$ promoter, covering the bases -55 to -41 relative to the transcriptional start site of *cesP*. Likewise, a putative CodY-box with three mismatches was predicted to lie within the intracistronic *cesB* promoter of the *ces* gene cluster. However, CodY bound with weak affinity to P_{cesB} and the K_D was higher than 521 nM (Fig. 15).

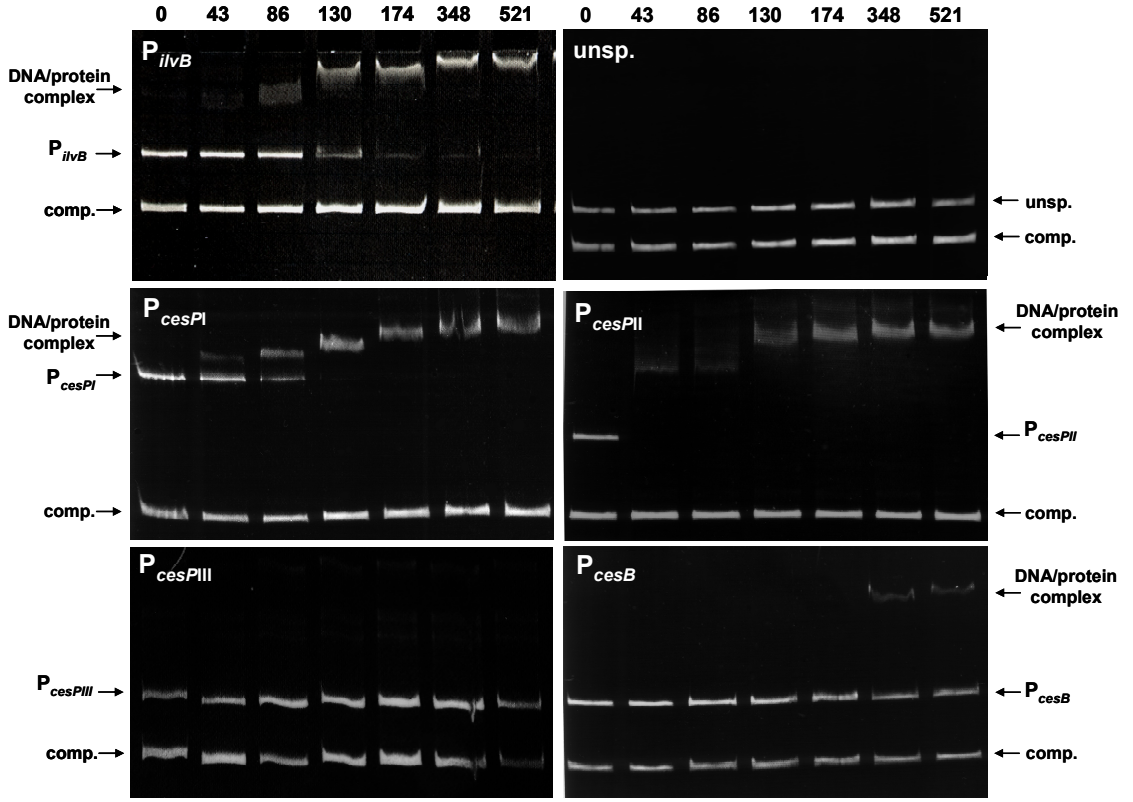

Figure 15: Gel shift analysis of CodY binding to different promoter regions. The non-radioactive gel mobility assays were performed by incubating PCR-generated DNA fragments containing the regulatory regions of *ilvB*, *cesP*, *cesB,* and randomly amplified DNA (unsp.) with a competitive, negative control DNA fragment (comp.) and increasing amounts of purified CodY-His_6 in the presence of branched-chain amino acids and GTP. On top of the panels, CodY concentrations are indicated in nM with respect to the monomer. The leftmost lane of each panel corresponds to free DNA. Gel electrophoresis was performed on 10% native TBE polyacrylamide gels and DNA was detected with ethidium bromide staining. Representative images of at least three independent experiments are shown.

Cereulide synthesis peaks during the transition from vegetative to stationary phase. Therefore, *ces* promoter binding capability of SinR and ComK regulators, which are active during the transition state, was analyzed. In *B. subtilis*, SinR regulates differentiation processes such as biofilm formation, whereas ComK is the master regulator of competence development.

While SinR bound specifically and with high affinity ($K_D \approx 20$ nM) to the control promoter of the *epsA* exopolysaccharide formation operon (Table 17), even 10-fold higher protein concentrations did not lead to the formation of DNA/protein complexes with the DNA probes cesPI, cesPII, and cesPIII (Fig. 16 and Table 17). These results demonstrate that SinR has no *in vitro* affinity to the cereulide synthetase promoter.

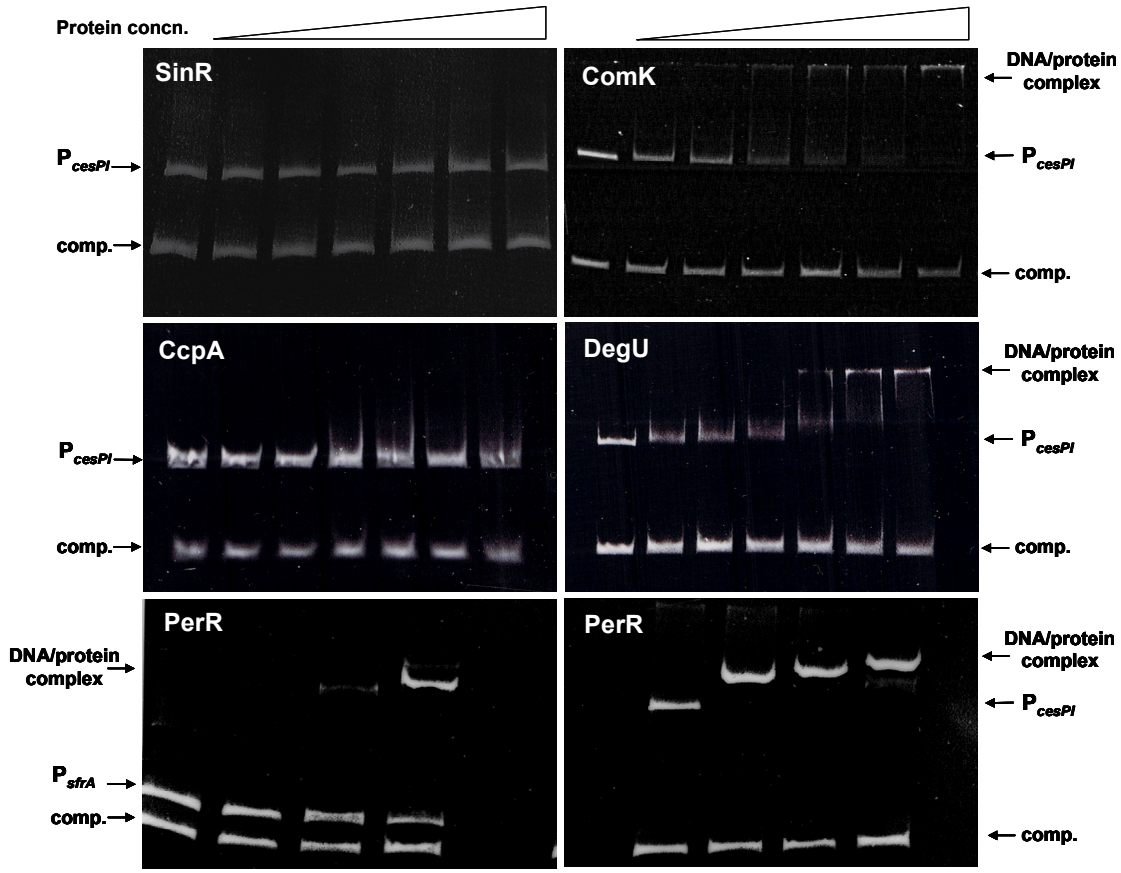

Figure 16: *In vitro* binding analysis of different transcription factors to the *cesP* promoter region of the cereulide biosynthesis operon. His_6-tagged CcpA, DegU, SinR, ComK, and PerR were purified and incubated with the cesPI DNA probe and a competitive, negative control DNA fragment (comp.). Triangles on top of the panels indicate increasing protein concentrations. Additionally, binding analysis of PerR to the *srfA* promoter of the surfactin biosynthesis operon of *B. subtilis* is shown. The non-radioactive gel shift experiments were performed with varying buffers and native gel concentrations as described in the Materials and Methods section. Representative images of at least three independent experiments are shown.

Table 17: Estimated equilibrium constants [K_D] obtained by gel mobility shift analyses with various transcription factors and control promoter regions as well as three different DNA probes covering the cereulide synthetase promoter region[a]

	Apparent equilibrium constant K_D [nM] of binding to			
Transcription factor	Positive control promoter[b]	cesPI	cesPII	cesPIII
CodY	150 (*ilvB*)	50	50	NB
SinR	20 (*epsA*)	NB	NB	NB
ComK	660 (*comK*)	878	2,200	NB
CcpA	1,020 (*ilvB*)	NB[c]	NB	NB
DegU(~P)	1,450 (*comK*; *B. subtilis*)	1,930	3,870	1,930
PerR	1,550 (*sfrA*; *B. subtilis*)	780	ND[d]	ND

[a] Features of the *cesP* promoter probes I, II, and III are described in the Results section.
[b] Gene is given in parenthesis. [c] NB, no binding observed. [d] ND, not determined.

The ComK protein was found to bind with an estimated K_D of 660 nM to its own promoter region and with slightly weaker affinity to the 523-bp cesPI probe ($K_D \approx$ 878 nM; Fig. 16), but not to the cesPIII probe lacking the core promoter elements (Table 17). Binding to the shorter, 368-bp fragment cesPII was 2.5-fold weaker than towards cesPI. This might indicate that a second ComK binding motif is situated upstream of cesPII, which is covered by the 155-bp extension of the cesPI fragment.

Although binding motifs for the catabolite control protein A (CcpA) were not predicted by DBTBS *in silico* analyses, CcpA was chosen for binding assays, because previous qPCR experiments revealed that *ces* gene transcription was downregulated the presence of D-glucose (Dommel 2008). However, although gel shift conditions could be optimized to achieve an efficient binding to the *ilvB* promoter (Table 17), interaction of His_6-tagged CcpA with the three *cesP* promoter fragments was not observed. Additionally, presence of the effector molecule glucose-6-phosphate did not stimulate binding to cesPI, II, and III.

To study the impact of two-component system-mediated transcriptional regulation on cereulide synthesis, the DegU response regulator of the DegS/DegU system was selected. Since F4810/72 encodes five regulators with moderate similarity to DegU from *B. subtilis* (30 to 42% amino acid identity; Table 16), the *B. subtilis* homolog was used to initially elucidate a possible role of DegU-like proteins in *ces* gene transcription. The DegU-His_6 protein bound with similar affinity to the promoter region of *comK* and the probes cesPI and cesPIII (Table 17 and Fig. 16). Binding to the shorter cesPII probe was approximately 2-fold weaker, suggesting that the longer promoter fragment contained a higher number of DNA stretches that allowed interaction with the transcription factor. Phosphorylation of DegU did not influence the DNA binding efficiency. Thus, DegU might bind in its phosphorylated and unphosphorylated form to the core *ces* promoter and to the distal promoter area (cesPIII).

To elucidate the importance of metalloregulators in regulation of cereulide biosynthesis, PerR was chosen from the group of PerR, Zur, and MntR, whose regulons are interconnected due to the response to an overlapping set of metal ion ligands (Herbig and Helmann 2002). After pre-

incubation with manganese (see Ch. 2.8.5) PerR-His_6 bound to the positive control promoter of the surfactin NRPS operon (P_{srfA}) with an estimated apparent equilibrium constant K_D of 1,560 nM (Fig. 16 and Table 17). By contrast, the cesPI DNA probe was shiftet at 780 nM, showing that PerR bound with higher affinity to the *ces* operon promoter region.

Taken together, the *in vitro* binding experiments indicate that CodY, PerR, ComK, and, if encoded in *B. cereus,* a DegU homolog might bind to the *cesP* promoter region and participate in the regulation of cereulide biosynthesis in *B. cereus* F4810/72, while a specific *in vitro* interaction of CcpA and SinR was not observed.

3.5 The role of CodY in virulence gene regulation of emetic *B. cereus*

3.5.1 Influence of CodY on cereulide synthesis

Due to its ability to bind to the *ces* promoter region and due to the observation that the cereulide precursor L-valine possibly act as a co-repressors of CodY, the transcriptional regulator was chosen to study its *in vivo* function in the regulation of cereulide synthesis.

For this purpose, a *codY*-null mutation was introduced into *B. cereus* F4810/72 by allelic replacement of the CodY encoding sequence with a spectinomycin-resistance cassette. Non-polar and complete gene inactivation was verified with PCR and qPCR (data not shown). During growth in LB medium at 30°C, the Δ*codY* mutant strain exhibited a prolonged lag-phase and a slightly lowered maximal optical density as compared to the wild type (Fig. 17). On selective agar, the overall colony morphology was similar to the wild type, but activity of PI- and PC-specific phospholipases was strongly reduced (Fig. 17; inset). Since these enzymes usually lead to turquoise colored colonies on BCM agar and to a zone of egg yolk precipitation on MYP agar, findings indicated that deletion of *codY* caused considerable changes in the secretome of *B. cereus* F4810/72.

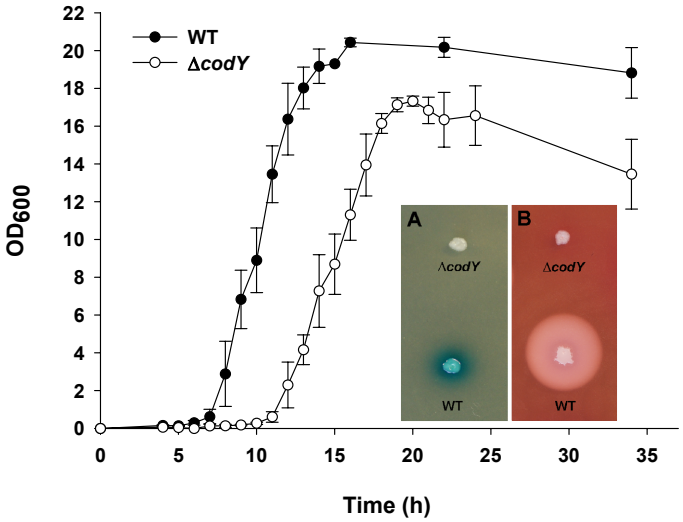

Figure 17: Growth behavior and colony phenotypes of the emetic *B. cereus* strain F4810/72 (WT) and the isogenic *codY* null mutant (Δ*codY*). Strains were cultivated in LB medium at 30°C and growth was monitored at an optical density of 600 nm. Standard deviations are derived from three independent measurements. The small inset shows the colony morphology on (A) BCM agar and (B) MYP agar, on which the bacterial PI-PLC or PC-PLC enzyme activity can be detected by turquoise color development or egg yolk precipitation zones, respectively.

To examine whether CodY acts as a repressor or activator of cereulide synthesis, *cesA* transcription was monitored throughout all growth phases by qPCR. To compensate for the slight growth delay of the Δ*codY* mutant compared to its parent, RNA was isolated from culture samples harvested at identical optical densities. In comparison to the wild type strain, absence of *codY* led to a 30- to 60-fold enhanced synthesis of *cesA* mRNA during early phases of growth, approximately until the mid-exponential growth phase (Fig. 18).

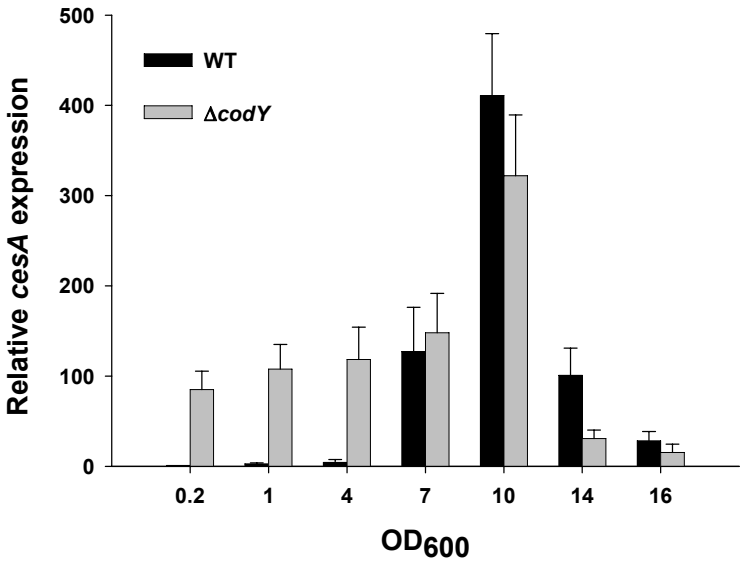

Figure 18: Cereulide synthetase gene transcription is derepressed upon *codY* inactivation. Total RNA was extracted from LB grown cultures of *B. cereus* F4810/72 (WT) and the isogenic *codY* null mutant (Δ*codY*) harvested at indicated optical densities. After reverse transcription, *cesA* mRNA levels were determined by qPCR and normalized to the 16S *rrn* levels of the same sample preparations.

The temporal derepression enhanced cereulide production by 40%, as quantified with the HEp-2 cytotoxicity assay (Fig. 19A). To ensure that enhanced toxin synthesis was a specific effect attributable to the absence of *codY*, the toxin phenotype was further tested after over-expressing

the regulator in F4810/72. Therefore, the promoterless *codY* gene was fused to the xylose-inducible promoter of the multicopy expression vector pWH1520 and transferred to F4810/72. Overexpression of *codY* decreased cereulide amounts by 10% to 95% (Fig. 19A), which in turn correlated roughly with the amount of expressed CodY protein, as observed by immunoblotting (Fig. 19B).

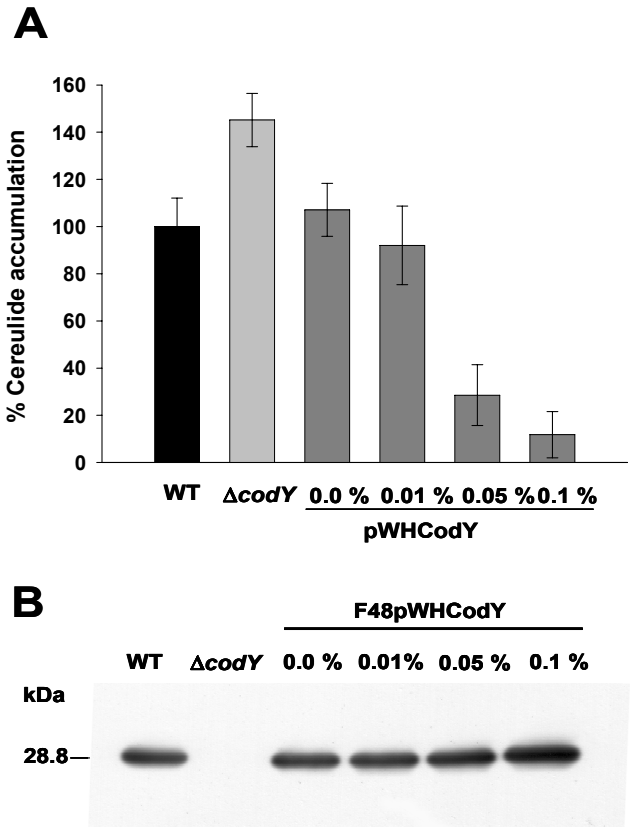

Figure 19: Cereulide synthesis is repressed by CodY. (**A**) *B. cereus* F4810/72 (WT), the isogenic codY mutant strain (Δ*codY*), and the CodY-overproducing F48pWHCodY strain were grown in LB medium until the late stationary phase. Overexpression of *codY* was induced by the addition of 0.01 to 0.1% xylose. Cytotoxicity of autoclaved culture samples was determined with a HEp-2 cell-based bioassay. The toxicity of one wild type samples was set to 100% as reference value. (**B**) Western blot analysis of CodY expression in whole cell lysates using a polyclonal anti-CodY antibody. Strains were cultured in LB to an optical density of 10. To gradually induce CodY overproduction in F48pWHCodY, xylose was added to the indicated concentrations. Identical amounts of total protein preparations were subjected to SDS-PAGE.

To test whether CodY controls cereulide synthesis indirectly, transcription of *abrB* and *spo0A* was compared in the Δ*codY* mutant strain and its parent. However, qPCR analysis showed no differences in the transcript levels of the two genes in the wild type strain and the deduced mutant throughout all phases of growth (data not shown). Furthermore, gel mobility shifts conducted with DNA fragments containing the putative promoter regions of *abrB* and *spo0A* revealed no specific binding of CodY-His_6 (data not shown).

Gel mobility shift assays indicated that GTP and BCAAs are putative effector molecules of F4810/72 CodY (Ch. 3.4). To monitor whether the metabolites enhance the repressor activity of the protein, F4810/72 and the Δ*codY* mutant were grown in chemically defined MOD medium that basically contained a mixture of 15 amino acids (including 5 mM L-isoleucine, 5 mM L-leucine, and 7 mM of L-valine) and glucose as the carbon source. The MOD medium was either depleted of L-isoleucine, L-leucine, or L-valine, respectively, or one of the BCAAs was fed in

an excess of 20 mM. Whereas the mutant grew in all MOD variations, growth was not observed for its parental strain without either L-valine or L-leucine (Table 18). However, HEp-2 measurements revealed that in comparison to the L-leucine depleted medium, addition of BCAAs reduced cereulide synthesis in the wild type strain by 3- to 6-fold, with L-leucine being the most potent amino acid. By contrast, toxin production was unaffected by BCAA surplus in absence of CodY (Table 18).

Table 18: Comparison of cereulide synthesis by the *codY* mutant and its parental strain *B. cereus* F4810/72 under influence of branched-chain amino acids in defined MOD medium[a]

Growth condition[a]	Cereulide amount (VE/OD_{600}) ± SD[b]	
	F4810/72	F48ΔcodY
MOD	13.1 ± 2.0	29.1 ± 3.7
MOD + Ileu	8.4 ± 1.2	31.8 ± 8.4
MOD + Leu	4.3 ± 1.0	36.2 ± 8.0
MOD + Val	6.6 ± 0.2	27.3 ± 4.7
MOD - Ileu	27.1 ± 4.8	28.6 ± 7.8
MOD - Leu	NG[c]	30.4 ± 6.0
MOD - Val	NG[c]	29.2 ± 2.5

[a] (+) indicates addition of L-valine, L-isoleucine, or L-leucine, respectively, to a final concentration of 20 mM.
(-) indicates that the respective amino acid was omitted from the growth medium.
[b] Cereulide amounts were measured with the HEp-2 assay and are given as valinomycin-equivalents (VE) normalized to the optical density at the time point of culture sampling.
[c] NG, no growth.

To assess the effect of GTP depletion on cereulide synthesis, both, wild type *B. cereus* and the Δ*codY* mutant were exposed to decoyinine, a specific GMP synthase inhibitor. LB grown cultures were split at an OD_{600} of 0.5 and exposed to either 1.8 mM decoyinine or to KOH, which was used as decoyinine solvent. Decoyinine addition did not affect the growth rates of the strains (data not shown). However, qPCR revealed enhanced *cesA* mRNA levels during phases of rapid growth in the wild type strain, while the addition of decoyinine had no additional derepressing effect in the mutant strain (data not shown). Furthermore, no obvious change in transcription of *codY* itself was observed after decoyinine addition (data not shown). These results correlated with the determined toxin amounts, which were similar in the decoyinine-treated wild type cultures and in Δ*codY* mutant cultures (Fig. 20). Thus, lowering of GTP levels mimicked a *codY*-deficient phenotype.

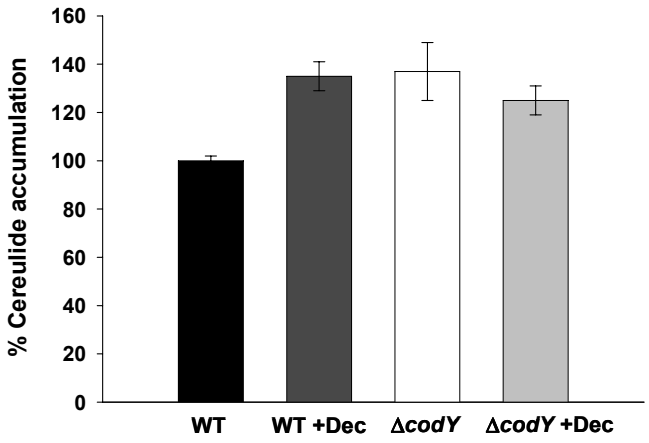

Figure 20: Decoyinine-induced GTP-depletion mimics a *codY* null phenotype. *B. cereus* F4810/72 and the isogenic *codY* mutant were exposed to the GMP synthase inhibitor decoyinine (WT+Dec/Δ*codY*+Dec) or to the decoyinine solvent KOH (WT/ Δ*codY*). Cereulide accumulation was determined with a HEp-2 cell-based biotoxicity assay. The toxicity of one wild type sample was set to 100% as reference value.

3.5.2 Influence of CodY on transition and stationary phase virulence factors

CodY is well known to control transition and stationary phase gene expression in a variety of gram-positive pathogens. The initial phenotypical analysis of the Δ*codY* mutant on selective media indicated that the synthesis of virulence-associated factors, such as the phospholipases that are secreted with increasing cellular density, was strongly reduced (Fig. 17). Thus, *B. cereus* F48ΔcodY was further characterized with respect to the impact of a *codY* deletion on the expression of selected virulence determinants.

Figure 21 illustrates that the chosen genes were partially subject to CodY-mediated repression, while others were in turn subject to induction, as explored by qPCR. *ilvE*, a BCAA aminotransferase, was included as a control, since this is a strongly CodY-regulated gene in *B. subtilis* (where it is termed *ybgE*). As expected, *ilvE* transcription was up to 1,800-fold upregulated in the *codY* deletion mutant.

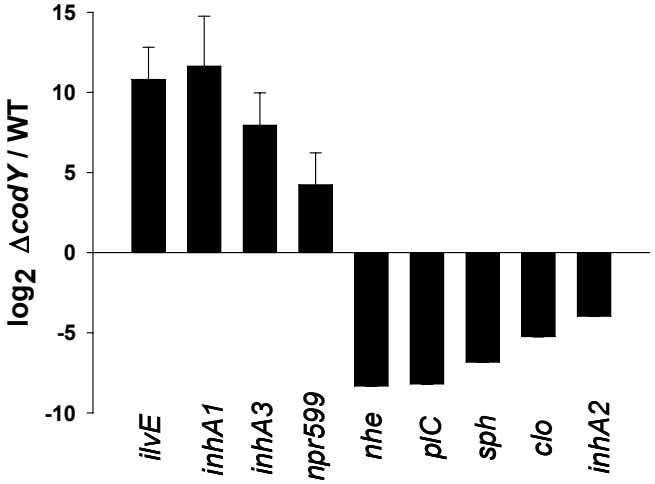

Figure 21: Effect of a *codY* mutation on the transcription of selected virulence-associated factors in *B. cereus* F4810/72. The change in mRNA levels of the Δ*codY* mutant is shown relative to the wild type (WT), as analyzed by qPCR. Bars represent means from at least two independent cultures and six indepen-dent qPCR measurements. The relative gene expression is given in log-2 scale.

Similarly, mRNA levels of the immune-inhibitor metalloprotease InhA1 encoding *inhA1* gene were significantly enhanced (up to 3,200-fold) in the absence of *codY*. An *in silico* analysis performed with the xBASE2.0 program revealed that the regulatory region of *inhA1* contains three putative CodY binding sequences (with three mismatches to the CodY consensus sequence, each). Consistently, purified CodY-His_6 showed high *in vitro* affinity towards the *inhA1* promoter region and bound with an estimated K_D of 100 nM (Fig. 22).

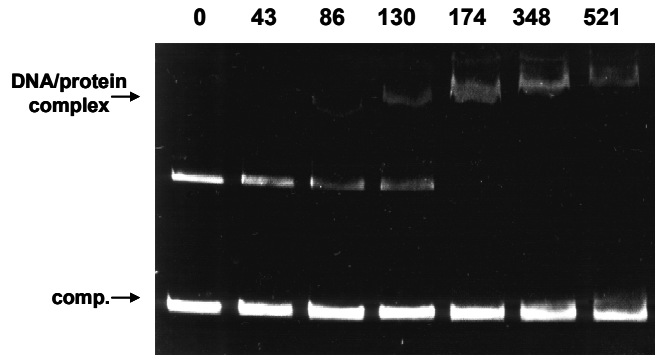

Figure 22: Gel mobility shift analysis of CodY-His_6 binding to the putative promoter region of the immune inhibitor metalloprotease 1 (InhA1) of *B. cereus* F4810/72. Numbers on the top of the figure denote the used CodY concentrations, which are given in nM with respect to the protein monomer. Comp. designates the competitive negative control DNA.

In addition, other protease encoding genes, such as immune-inhibitor metalloprotease 3 (*inhA3*), and neutral protease 599 (*npr599*) were subject to moderate CodY repression in the wild type (19- to 250-fold; Fig. 21). However, CodY did not bind to the respective promoter regions (data not shown). By contrast, transcription of several virulence genes belonging to the PlcR quorum sensing regulon, including the non-hemolytic enterotoxin (*Nhe*), and PC-specific phospholipase C (*PC-plC*), was found to be downregulated in the Δ*codY* mutant (290-fold and 320-fold, respectively). Similarly, expression of sphingomyelinase (*sph*), cereolysin O (*clo*), and immune-inhibitor metalloprotease 2 (*inhA2*) genes was significantly decreased (in the range of 15-fold to 115-fold), suggesting that CodY is an important positive regulator for this group of genes (Fig. 21). To confirm the qPCR results for a distinct subset of virulence determinants, tests were performed for phenotypical verification.

To estimate the degree of CodY regulation on the synthesis of the non-hemolytic enterotoxin Nhe, toxin accumulation was quantified with a Vero cell-based cytotoxicity assay. According to the downregulation observed in qPCR, enterotoxin titer were 5- to 20-fold lower upon *codY* deletion (Fig. 23). Some *B. cereus* F48ΔcodY supernatant samples remained completely non-toxic towards the Vero cell line. However, overexpression of CodY enhanced Nhe titer up to 3-fold, strongly indicating that the effect was attributable to CodY-mediated regulation (Fig. 23).

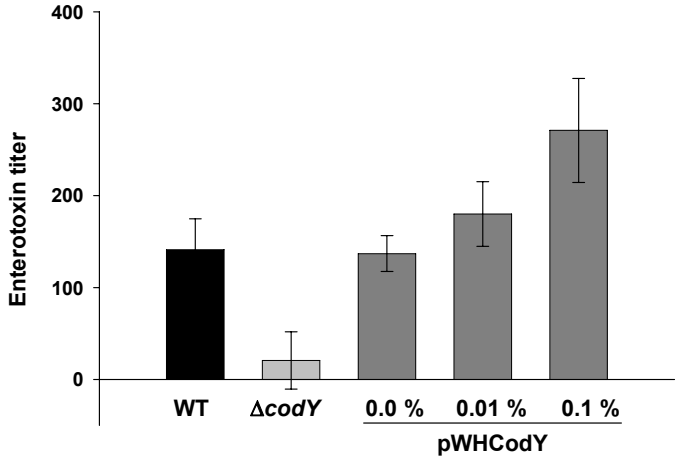

Figure 23: Non-hemolytic enterotoxin (Nhe) synthesis is induced by CodY. Vero cells were incubated with culture supernatants of *B. cereus* F4810/72 (WT), the isogenic Δ*codY* null mutant and the CodY-overproducing *B. cereus* F48pWHCodY. All strains were grown in BHI medium to an OD_{600} of 10. Overexpression of *codY* was induced by the addition of 0.01 to 0.1% xylose. The enterotoxin titer is expressed as the reciprocal value of the supernatant dilution, at which 50% cytotoxicity towards Vero cells was observed.

To test whether the reduced transcription of genes encoding the lipolytic enzymes phospholipase C and shingomyelinase also led to a reduced enzyme synthesis, the enzymatic activities were quantified in culture supernatants of *B. cereus* F4810/72 and of the *codY* null strain, which .were harvested at various phases of growth (Fig. 24A and B). In accordance with the qPCR analysis (Fig. 21), deletion of *codY* led to a substantial loss of PC-PLC and SPH activities throughout the growth cycle and the enzyme activities were reduced up to 97%, suggesting that CodY has a key role in activating, either directly or indirectly, expression of these secreted virulence factors.

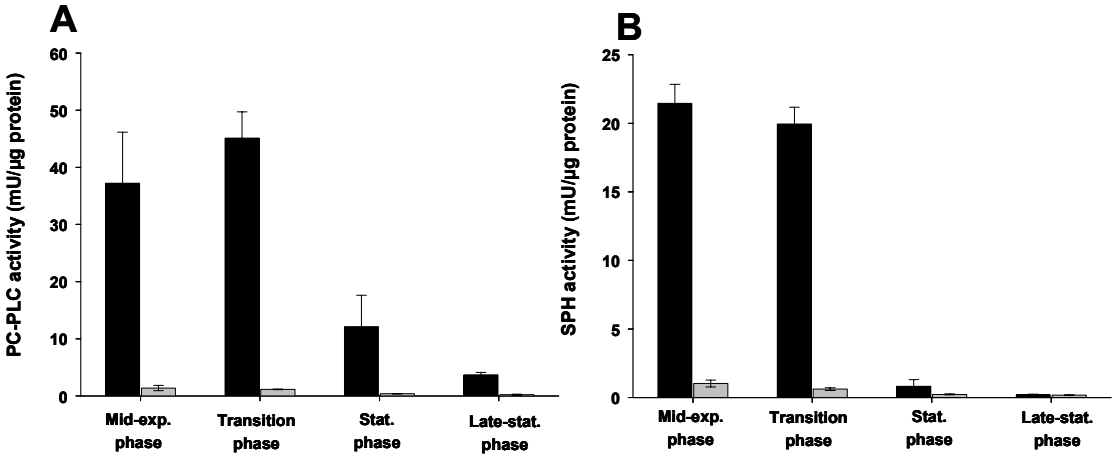

Figure 24: Effect of a *codY* deletion on the expression of phosphatidylcholine-specific phospholipase C (**A**) and sphingomyelinase (**B**) in *B. cereus* F4819/72 (black bars) and the isogenic *codY* null mutant (grey bars). The enzymatic activities of the culture supernatants were normalized to the total concentration of extracellular protein at indicated growth phases.

To quantify the impact of a *codY* deletion on the hemolytic activity of *B. cereus,* which is attributed to the simultaneous action of several secreted virulence factors such as cereolysin O (*clo*), phospholipase C, and shingomyelinase, horse erythrocytes were exposed to supernatants of transition phase cultures of the Δ*codY* mutant and its parental strain. As comparative samples, supernatants of a *plcR*-deficient strain were included in the assay. Compared to their parental strain, supernatants of Δ*codY* and Δ*plcR* mutants were only weakly hemolytic towards horse erythrocytes (Fig. 25) and cytolysis was reduced up to 22-fold and 32-fold, respectively.

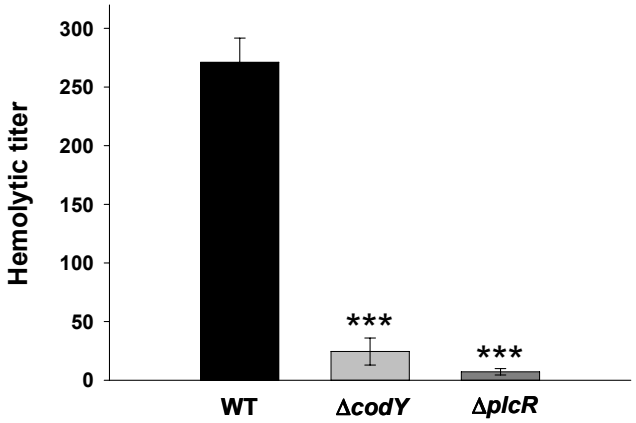

Figure 25: Effect of *codY* and *plcR* inactivation on the hemolytic activity of *B. cereus* F4810/72 supernatants towards horse red blood cells (RBCs). Cultures of *B. cereus* F4810/72 (WT), and of the isogenic *codY* and *plcR* null mutants were harvested at an optical density of 10. The hemolytic titer is expressed as the reciprocal of the supernatant dilution, at which 50% hemolysis of RBCs was observed. Significance of differences ($p < 0.001$) between the WT strain and the respective mutant strain was calculated with the paired Student´s t-test.

To finally assess whether the CodY-mediated activation of virulence factors assigned to the PlcR regulon could be attributed to a direct interaction of CodY with the respective promoter regions, *in silico* prediction of CodY motifs was performed. Putative CodY binding sequences were only found in the upstream regions of *clo* and *inhA2*. In both cases, the 15-bp sequence exhibited 3 mismatches difference to the consensus CodY-box. However, subsequently performed gel mobility shift assays did not reveal *in vitro* binding (data not shown). Moreover, CodY-His_6 showed no binding activity towards the promoter regions of *nhe* and *PC-plC*, as expected due to missing CodY-type recognition sequences (data not shown). This further raised the possibility that CodY might be a direct activator of *plcR* transcription. However, *plcR* mRNA levels were only modestly decreased (around 5-fold) in the *codY* strain. The effect was temporary and restricted to the mid-exponential growth phase, which is rather atypical for a direct CodY-mediated repression. Furthermore, CodY-His_6 did not bind to the *plcR* promoter region *in vitro*, which is consistent with the failure to predict a CodY box *in silico*. Nevertheless, data show that CodY profoundly influences the virulence of *B. cereus* F4810/72 by acting as an indirect activator of a broad range of virulence factors, including the important enterotoxin Nhe.

3.6 Subproteome analysis of *B. cereus* F4810/72 and its derivatives

The involvement of CodY (Ch. 3.5) and other chromosomally encoded transcription factors (Ch. 3.4) in *ces* gene regulation demonstrates the tight communication between chromosomal and pCER270-encoded elements in *B. cereus* F4810/72. To gain further insights into this global interrelation and to determine whether plasmid-borne regulators might additionally affect cereulide synthesis, *ces* promoter activity and subproteomes of *B. cereus* F4810/72, the plasmid-cured F48(pCER270-) strain, and the *ces* operon-deficient F48ΔcesP/polar mutant were compared.

The response of the main promoter of the *ces* operon (P_{cesP1}) was assessed in different genetic backgrounds with bioluminescence measurements. For this purpose, strains were transformed with the luciferase-based reporter plasmid pMDX[P_1/*lux*] and further grown at 30°C in LB medium containing 5 µg ml^{-1} chloramphenicol to ensure plasmid maintenance. The activity of P_{cesP1} was measured with a bioluminescence reader and was further normalized to the optical density at all sampling time points. The mutant strains did not exhibit growth deficiencies compared to the wild type strain (data not shown). As expected, promoter activity was strict temporally regulated in the wild type background (Fig. 27). Maximum activity was detected during the late exponential growth phase, which is reached approximately 18 hours after inoculation of the culture in LB-Cm5 medium (Fig. 27). Compared to the wild type, promoter activity levels were up to 75% reduced in a pCER270- background throughout all phases of growth, pointing towards a substantial impact of pCER270 on the P_{cesP1} activity. Interestingly, polar disruption of the *ces* gene operon also significantly reduced activity of the promoter, albeit at a lower rate. Moreover, Figure 27 illustrates that the temporal manner of *ces* gene expression was not altered, since maximum transcription occurred during the logarithmic phase of growth.

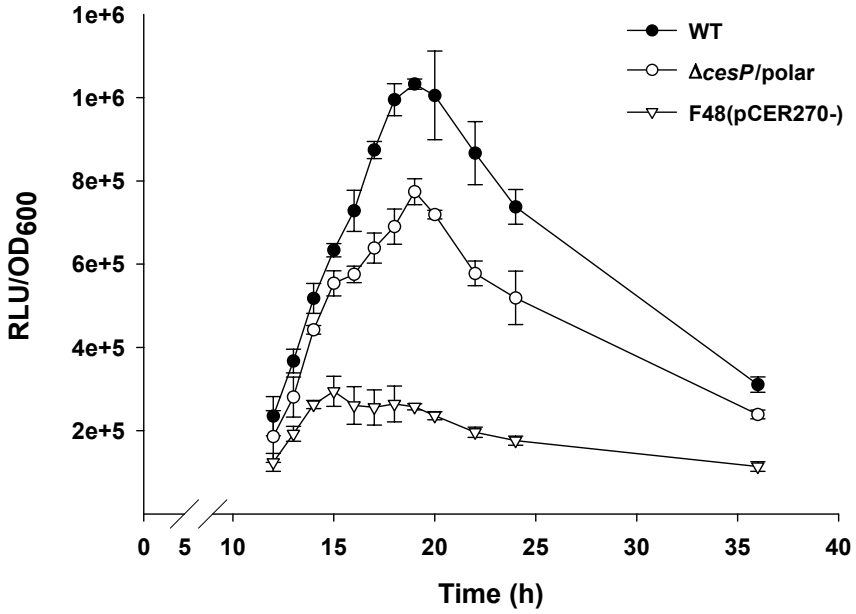

Figure 27: Influence of genetic background mutations on *ces* promoter activity. *B. cereus* F4810/72 wild type (closed circles, •), *B. cereus* F48ΔcesP/polar (open circles, o) and the megaplasmid-deficient *B.cereus* F48(pCER270-) (open triangles, ∇) harboring an episomal *ces* promoter-*lux* fusion construct (pMDX[P1/*lux*]) were grown in LB medium at 30°C. Promoter activity was recorded as relative bioluminescence units (RLU) and normalized to the optical density at 600 nm (OD_{600}). Mean values and the respective standard deviations of three independent experiments are shown.

To examine the influence of a deletion of the cereulide synthetase operon and the loss of the virulence plasmid pCER270 on a proteomic level, intracellular and extracellular subproteomes of F4810/72, F48ΔcesP/polar, and F48(pCER270-), which were harvested from LB medium in the mid-exponential phase of growth, were compared.

Differentially expressed proteins of the cytosolic and secreted protein fractions were identified by two-dimensional differential gel electrophoresis (2-D DIGE). Within a pH range of 4 to 7, a total of 2113 spots were detected in the cytosolic fraction and 2344 spots were detected in the secreted subproteome. A statistical false-discovery rate (FDR) analysis using a 5% cut-off threshold revealed that only a few proteins were significantly up- or downregulated in the cytosol of the mutant strains (Table 19). In comparison, *ces* gene inactivation and absence of pCER270 profoundly influenced the extracellular protein patterns of *B. cereus*, and a total of 151 or 199 differentially regulated spots was detected, respectively.

Table 19: 2-D DIGE-based analysis of differentially regulated protein spots upon *ces* gene cluster inactivation or upon pBCER270 plasmid-curing in comparison to *B. cereus* F4810/72 wild type[a]

	F48ΔcesP/polar		F48(pCER270-)	
	Cytosol[b]	Secretome[c]	Cytosol[b]	Secretome[c]
Number of upregulated or appeared spots	4	99	10	123
Number of downregulated or disappeared spots	4	52	10	76

[a]Image processing, spot detection and initial statistical analysis was performed with the DeCyder software (GE Healthcare). Changes in the spot volume were considered significant on the basis of false-discovery rate (FDR) calculations using the R-software program (http://www.r-project.org/) with a a significance p-value cutoff of 0.05.

FDR corrected spots exhibiting a regulated ≤1.5-fold were further selected for identification by MALDI-TOF mass spectrometry. A comprehensive list of identified proteins and of the regulation patterns comparing the subproteomes of pCER270/WT, ces/WT, and ces/pCER270 is provided in the Appendix (Table A2).

Upon comparison of the cytosolic and secreted subproteomes of *B. cereus* wild type and the plasmid-cured strain, 26 differentially regulated protein spots were identified that corresponded to 17 different proteins (Figs. 28A/29A, and Table 20). Among the down-regulated proteins, an FtsZ-domain containing protein (RepX), and two novel proteins, a putative chitinase (chitin-binding domain protein) and a protein annotated as hypothetical metallopeptidase were identified, which are encoded on the virulence plasmid, and hence, are absent in the mutant strain (Table 20). A BLASTP analysis revealed that the metallopeptidase shares 43% amino acid similarity to the neutral protease B (NprB) of certain *B. cereus* group strains, which is involved in maturation of the quorum sensing peptide PapR. This protein was designated NprC38. Furthermore, chromosomally encoded proteins were affected by plasmid curing, for instance proteins of structural components of the cell surface (EA1 and a SAP-like crystal protein), a lipoprotein with 99% similarity to vancomycin B-type resistance proteins previously detected in *B. anthracis* RA3, and enzymes involved in oxidative stress response and in the cellular core metabolism.

By contrast, absence of pCER270 induced the upregulation of several chromosomally encoded proteins, including the metalloendopeptidase NprP2, flagellin A, and an isoform of succinate dehydrogenase (SdhA) (Table 20). Moreover, several virulence factors were stronger expressed as in the *B. cereus* wild type strain, namely the enterotoxin components NheA and NheB, cereolysin O and phospholipase C. Interestingly, among the 11 overexpressed proteins, 6 were members of the PapR-PlcR quorum sensing regulon and possessed a PlcR consensus motif upstream of the encoding ORFs (Table 20).

Table 20: Differentially expressed proteins upon pCER270-curing of *B. cereus* F4810/72 as revealed by 2-D DIGE analysis[a]

Accession number (NCBI)	Desig-nation	Functional annotation	Fold regula-tion[a]	Locali-zation[b]	Signal Peptide[c]	Plamid encoded	PlcR re-gulated[d]
Downregulated or absent spots in absence of pCER270							
C0036		Chitin-binding protein	-186.9	S	●	●	
C0036		Chitin-binding protein	-121.3	S	●	●	
C0036		Chitin-binding protein	-24.2	S	●	●	
C0038	NprC38[e]	Putative metallopeptidase	-13.5	S	●	●	
C0038	NprC38	Putative metallopeptidase	-14.0	S	●	●	
C0096	RepX	Plasmid replication protein	-7.1	C		●	
A1065	EA1	S-layer protein	-11.2	C	●		
A1064	SAP	Crystal protein	-3.1	S	●		
A1064	SAP	Crystal protein	-3.4	S	●		
A3551	VanW[f]	Putative lipoprotein	-1.9	S	●		
A0439	AhpC#	Peroxiredoxin	-2.0	S			
A4645	SdhA*	Succinate dehydrogenase flavoprotein subunit	-6.7	C			
A4645	SdhA*	Succinate dehydrogenase flavoprotein subunit	-7.5	C			
Upregulated spots in absence of pCER270							
A2787	NprP2	Metalloendopeptidase	9.6	S	●		●
A2787	NprP2	Metalloendopeptidase	2.7	S	●		●
A1995	NheA	Non-hemolytic enterotoxin, subunit A	1.7	S	●		●
A1996	NheB	Non-hemolytic enterotoxin, subunit B	1.6	S	●		●
A1996	NheB	Non-hemolytic enterotoxin, subunit B	1.5	S	●		●
A0684	ColC	Microbial collagenase	1.8	S	●		●
A3327	Clo	Anthrolysin O; pore-forming toxin	1.6	S	●		●
A0804	PC-plC	PC-dependent phospholipase C	1.5	S	●		●
A1835	FlgA	Flagellin A	5.4	S			
A4357	GcvP	Glycine dehydrogenase subunit 1	2.0	S			
A4358	GcvT	Glycine cleavage system, aminotransferase T	1.7	S			
A4906	PckA*	Phosphoenolpyruvate carboxykinase	1.5	S			
A4645	SdhA*	Succinate dehydrogenase flavoprotein subunit	2.3	C			

[a] Fold regulation denotes the average in-/decrease of spot abundance of F48pCER270- proteins compared to wild type proteins. Proteins were identified by MALDI-MS/MS or PMF (see Materials and Methods). Underlined proteins are also differentially regulated upon *ces* cluster inactivation (Table 21). Proteins involved in oxidative stress response are marked with a sharp (#). Proteins involved in C- metabolism pathways are marked with an asterisk (*).
[b] Protein was identified in the C, cytosol or S, secretome fraction. [c] Presence of a signal peptide was predicted on the SignalIP 3.0 server (see Material and Methods). [d] Regulation by PlcR was inferred from previous studies (e.g. Gohar *et al.* 2008; Sastalla *et al.* 2010), and deduced from the absence or presence of a PlcR consensus box in the putative promoter region. [e] Novel protein; hereafter referred to as NrpC38; 52% similarity to a neutral protease (bacillolysin) of *B. cereus* ATCC10987 and *B. anthracis* CI, and 43% similarity to NprB of *B. cereus* ATCC14579.
[f] 99% identity to *B. anthracis* Ames (RA3) vancomycin B-type resistance protein VanW.

While most of the identified secretome proteins of the pCER270 mutant were degradative enzymes or virulence factors, the majority of differentially expressed proteins in the F48ΔcesP/polar strain has assigned functions in the central carbon metabolism (Figs 28B/29B, and Table 21). These include for instance phoyphopyruvate hydratase (Eno), malate dehydrogenase (MalS) and glucose-6-phosphate isomerase (Pgi). Moreover, three enzymes of nitrogen metabolic pathways (GcvT, Pyn2, and PyrG), and proteins involved in the response to oxidative stress and cellular deteoxification (SodA1, PdhD, AhpF, and AhpC) were upregulated due to the absence of the *ces* operon. The flavoprotein subunit of the succinate dehydrogenase complex was detected in a spot-train with three different pI values, which points towards posttranslational modifications. Two of the spots were detected in 8- to 9-fold lower abundance and one in 2-fold higher abundance compared to the wild type strain (Table 21). The occurrence of three isoforms of SdhA and their differential regulation was also observed in the plasmid-cured mutant (Table 20), indicating that the absence of the *ces* operon had a specific effect on SdhA expression and modification. Also, GcvT and PckA were up-regulated in absence of pCER270 and upon *ces* inactivation, and VanW expression was down-regulated in a similar manner in both mutants, suggesting a *ces* gene cluster-attributed effect in these cases.

Table 21: Differentially expressed proteins upon *ces* operon inactivation of *B. cereus* F4810/72 as revealed by 2-D DIGE analysis[a]

Accession number (NCBI)[a]	Desig-nation	Functional annotation	Fold regula-tion[a]	Locali-zation[b]	Signal Peptide[c]	Plasmid encoded	PlcR re-gulated[d]
Down-regulated spots in absence of the *ces* operon							
A3551	VanW[f]	Putative lipoprotein	-1.9	S	●		
A4645	SdhA*	Succinate dehydrogenase flavoprotein subunit	-8.7	C			
A4645	SdhA*	Succinate dehydrogenase flavoprotein subunit	-8.8	C			
Up-regulated spots in absence of the *ces* operon							
A4645	SdhA*	Succinate dehydrogenase flavoprotein subunit	2.3	C			
A4906	PckA*	Phosphoenolpyruvate carboxykinase	2.0	S			
A4358	GcvT*#	Glycine cleavage system, aminotransferase T	1.6	S			
A5284	Eno*	Enolase (phosphopyruvate hydratase)	2.2	S			
A5285	GpmI*	Phosphoglyceromutase	1.7	S			
A5042	Pgi*	Glucose-6-phosphate isomerase	1.7	S			
A1922	MalS*	Malate dehydrogenase	1.7	S			
A5064	ManB*	Phosphoglucomutase / phosphomannomutase family protein	1.9	S			
A4088	PdhD*	Dihydrolipoamide dehydrogenase	2.0	S			
A4218	Pyn2	Pyrimidine-nucleoside phosphorylase	1.7	S			
A5516	PyrG	CTP synthetase	1.9	S			
A4408	SodA1#	Superoxide dismutase, Mn	1.6	S			
A0438	AhpF#	Alkyl hydroperoxide reductase, F subunit	1.6	S			
A0439	AhpC#	Peroxiredoxin	1.9	S			
A4293	BfmbC*#	Dihydrolipoamide dehydrogenase	1.9	S			

[a] Fold regulation denotes the average in-/decrease of spot abundance of F48ΔcesP/polar proteins compared to wild type proteins. Proteins were identified by MALDI-MS/MS or PMF (see Materials and Methods). Underlined proteins are also differentially regulated upon pCER270 plasmid-curing (Table 20). Proteins involved in oxidative stress response are marked with a sharp (#). Proteins involved in C- metabolism pathways are marked with an asterisk (*).
[b] Protein was identified in the C, cytosol or S, secretome fraction.
[c] Presence of a signal peptide was predicted on the SignalIP 3.0 server (see Material and Methods).
[d] Regulation by PlcR was inferred from previous studies (e.g. Gohar *et al.* 2008; Sastalla *et al.* 2010), and deduced from the absence or presence of a PlcR consensus box in the putative promoter region.

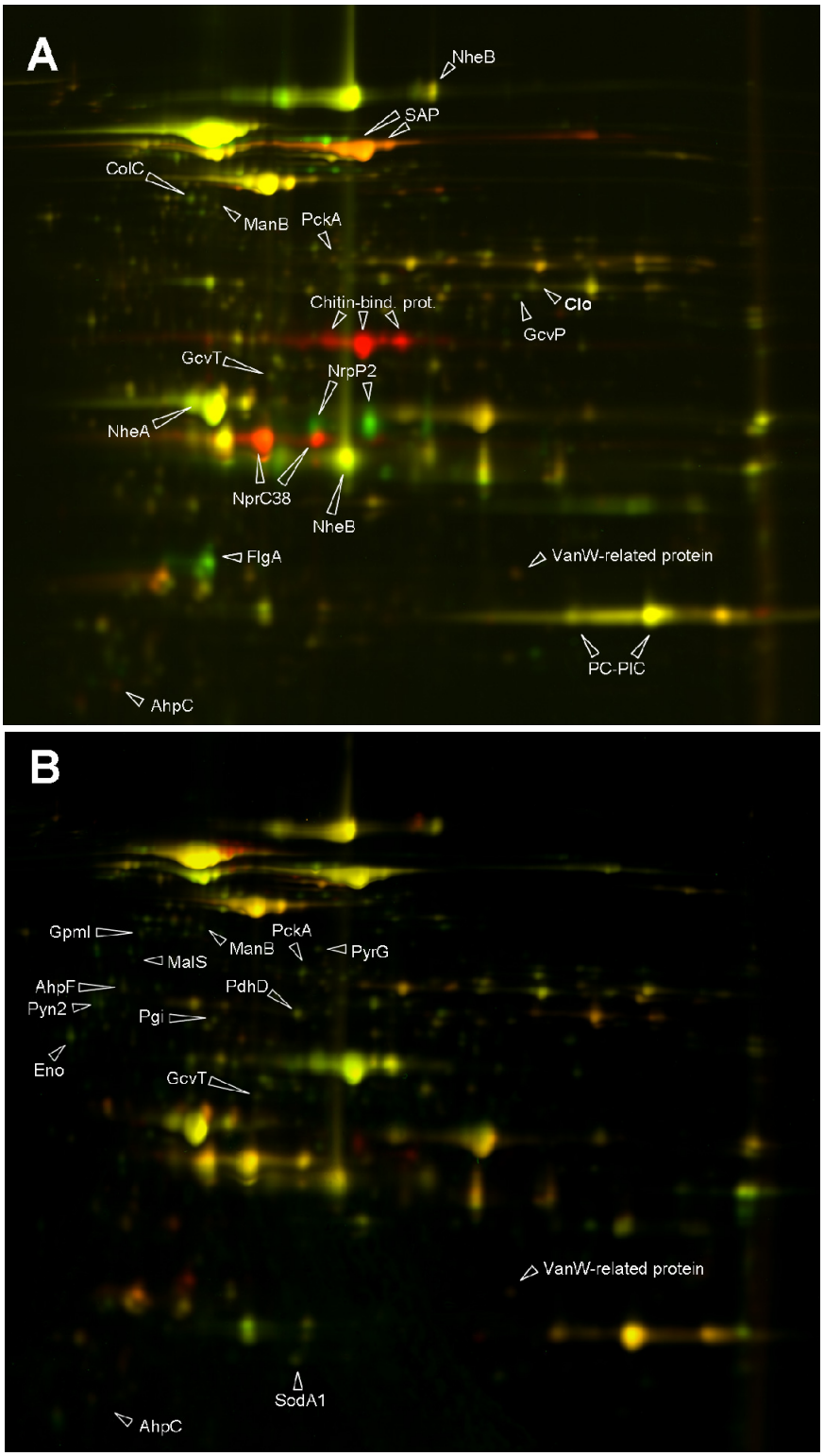

Figure 28: 2-D DIGE analysis of differentially expressed proteins in the extracellular proteome after complete curing of the pCER270 virulence plasmid of *B. cereus* F4810/72 (**A**) or after inactivation of the cereulide biosynthetic gene cluster (**B**). Representative dual-channel overlay images are shown. Proteins present in higher levels in the wild type are depicted in red (Cy5), whereas higher abundance in the F48(pCER270-) strain or in the F48ΔcesP/polar mutant is indicated by green spots (Cy3). Unchanged protein levels are indicated by yellow spots. The up-regulated or down-regulated proteins identified by MALDI-TOF mass spectrometry are marked with an arrow.

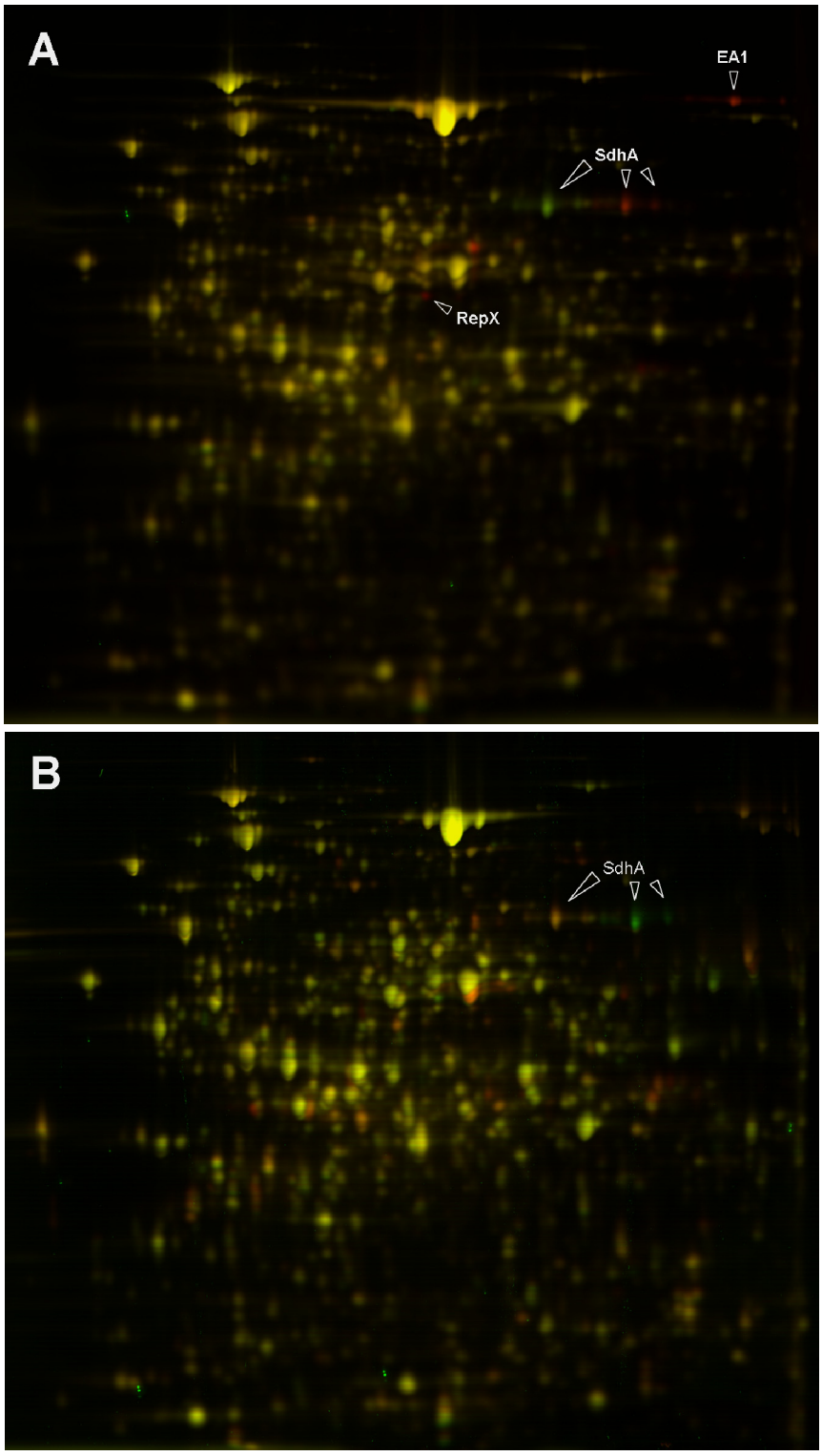

Figure 29: 2-D DIGE analysis of differentially expressed proteins in the cytosolic proteome after complete curing of the pCER270 virulence plasmid of *B. cereus* F4810/72 (**A**) or after inactivation of the cereulide biosynthetic gene cluster (**B**). Representative dual-channel overlay images are shown. (**A**) Wild type proteins were labelled with Cy3 (green spots) and F48(pCER270-) proteins with Cy5 (red spots). (**B**) Wild type proteins were labelled with Cy5 (red spots) and F48ΔcesP/polar proteins with Cy3 (green). The up-regulated or down-regulated proteins identified by MALDI-TOF mass spectrometry are marked with an arrow.

3.7 Cell population heterogeneity in *B. cereus* F4810/72

The first tools for monitoring *ces* gene promoter activity in *B. cereus* F4810/72 were based on the replicative, episomal plasmid pXen1 (Ch. 3.2). However, it would be desirable to monitor *ces* gene transcription at the native locus on the megaplasmid pCER270 to allow an unbiased monitoring of *ces* operon promoter activity on a single cell level. Therefore, a transcriptional fusion of the main *cesP* promoter region with a *gfpmut3a-spc* cassette was integrated on the pCER270 plasmid *via* homologous recombination (see Fig. 4 in Materials and Methods).

After heterogramic conjugation only one brightly fluorescing colony was found, indicating the low frequency of double homologous recombination events into pCER270. The first hint regarding a heterogenous expression of the *ces* gene in *B. cereus* F4810/72 cells came from the observation that re-streaking of the colony resulted in daughter-colonies consisting of fluorescent and non-fluorescent cells (Fig. 30).

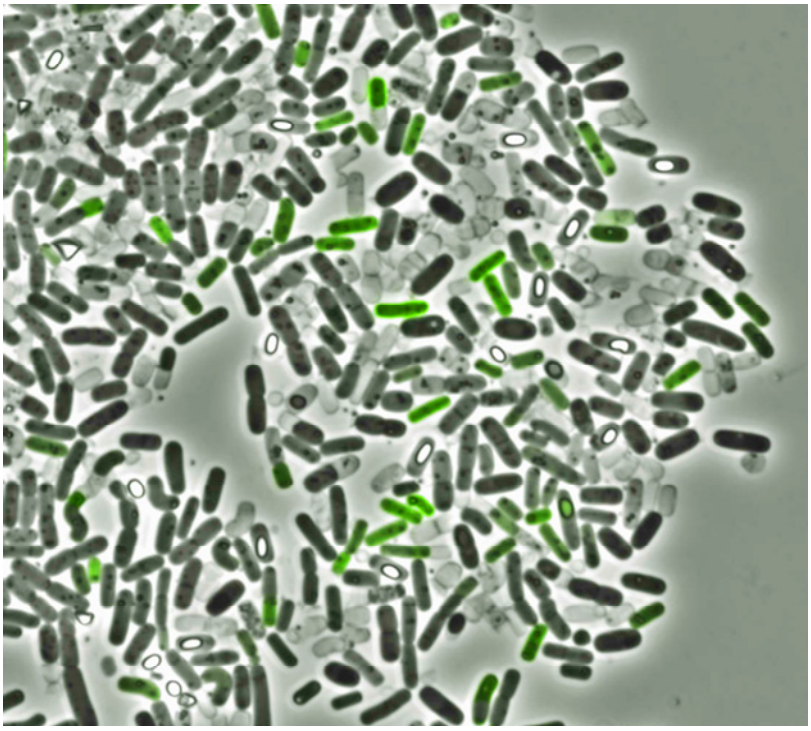

Figure 30: Heterogeneity in *ces* synthetase gene expression in single cells of emetic *B. cereus*. Depicted are cells isolated from various sites of a colony of the reporter strain F48icesGFP that carries a *gfp-spc* fusion at the native *ces* operon locus on pCER270. The strain was constructed by homologous recombination as described in Materials and Methods. The colony was grown at 30°C on selective LB medium containing 150 µg ml^{-1} spectinomycin. Fluorescence and phase-contrast pictures were taken with an Olympus microscope and overlaid. Magnification is 1,000-fold. A representative image is shown.

To ensure that all cells of a single colony contained the GFP fusion, an overnight culture was serially diluted and spread on LB plates with or without 150µg ml^{-1} spectinomycin to compare the numbers of resistant clones. One hundred colonies of different dilution steps were screened by PCR for the presence of the *spc* cassette, the *gfp* cassette, and the appropriate integration site on pCER270. All colonies turned out to harbor the desired *gfp* construct and one was chosen for further examination.

To determine whether heterogenous GFP/cereulide gene expression would also occur under the cultivation conditions routinely used throughout this study, the reporter strain was grown in LB medium containing 150 µg ml^{-1} spectinomycin. To ensure a homogenous population age, F48icesGFP was synchronized regarding the sporulation process by repeated 1:1,000-dilution of vegetative phase cells. After the third round of pre-culturing, examination started directly after inoculation, setting this time point as "zero" for the analyses. Per time point, 800 to 1,000 cells were analyzed by phase-contrast and fluorescence microscopy, thereby counting cells as individuals that showed a clear septation. The reporter strain did not exhibit GFP signals during early vegetative, rapid growth. However, all cells showed marginal levels of background fluorescence, which was also observed in the wild type *B. cereus* F4810/72 control culture lacking a GFP construct (data not shown). Therefore, the low level fluorescent population was referred to as non-expressing or non-fluorescing cells (*ces*-OFF cells; Fig. 31). During the mid-exponential growth phase ($OD_{600}\approx 7$), a bifurcation into distinct groups of non-expressing cells and *gfp* expressing, fluorescing cells (*ces*-ON cells) was observed (Fig. 31 and Fig. 32). It is noteworthy that this pattern was not bimodal in a strict sense, since a small fraction of cells developed within the following division cycles, which was highly fluorescent (termed *ces*-ON^+ cells).

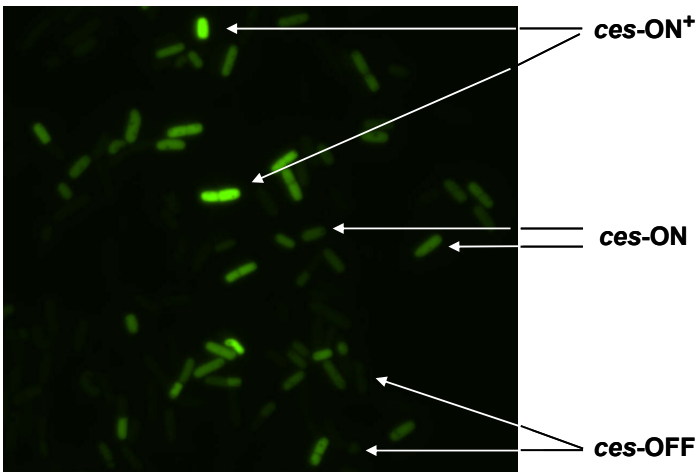

Figure 31: Fluorescence image of synchronized cells of the GFP-based cereulide reporter strain *B. cereus* F48icesGFP grown in LB medium. Heterogenous *gfp* expression driven by the *cesP* promoter on the native pCER270 locus results in brightly fluorescing (*ces*-ON^+), medium fluorescing (*ces*-ON), and non-fluorescing (*ces*-OFF) cells.

The high-expressing subgroup was visually distinguishable from the intermediate expressing cells and constituted 1 to 4% of the whole population. However, by referring to a bimodal distribution in the classical sense, all ON cells constituted about 7 to 16% of the total population. As illustrated in Figure 32, this distribution remained largely unchanged during the growth cycle. Furthermore, it was repeatedly observed that, although cells entered the stationary phase of growth, the culture did not sporulate uniformly. The lower panels of Figure 32 and Figure 33 show the coexistence of vegetative cells, forespore-forming as well as cells containing phase-bright endospores.

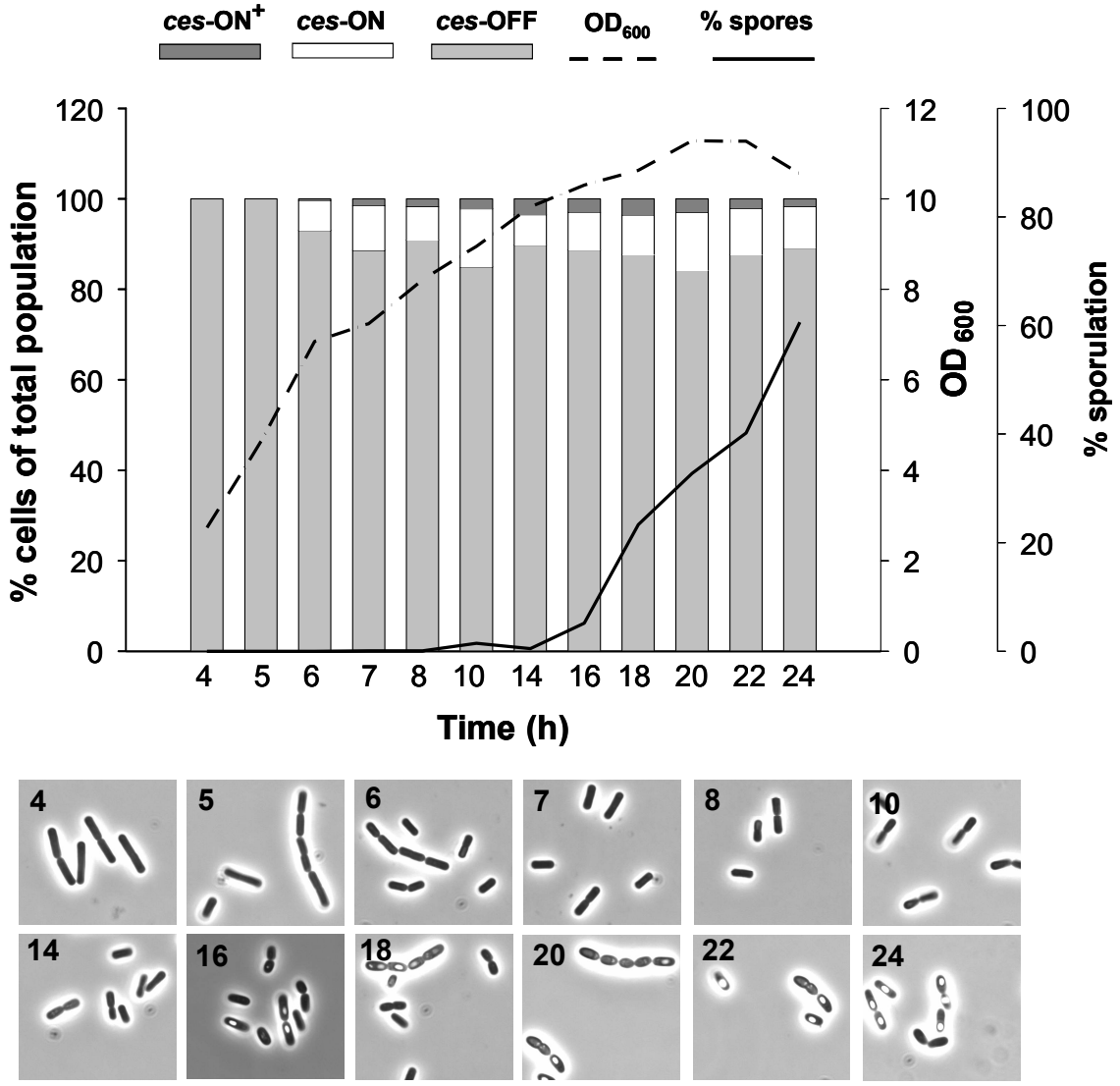

Figure 32: Heterogenous distribution of *ces* operon promoter activity in single cells of an isogenic culture of *B. cereus* F48icesGFP. Reporter cells were synchronized to minimize growth phase-dependent effects and further cultured at 30°C in LB medium supplemented with spectinomycin as selectable marker. The GFP signal was analyzed by fluorescence microscopy (see Materials and Methods). Heterogenous GFP accumulation indicates that the *ces* promoter is inactive in a large part of the population (*ces*-OFF cells; pale grey bars), whereas two smaller subpopulations exhibited medium (*ces*-ON cells; white bars) and high (*ces*-ON$^+$ cells; dark grey bars) GFP signal intensities. Growth was recorded as optical density at 600 nm (OD_{600}; dashed line) and spore numbers (solid line) were recorded by counting phase-bright forespores and endospores. Depicted are the mean values of two independent experiments. The lower panels 4 to 24 show representative phase-contrast images of F48icesGFP cells taken at the respective time points after inoculation of the culture.

While the intermediate GFP signals were randomly distributed between cell chains, cell doublets, single cells, and endospores, the high-expressing cells were mainly associated in cell chains, especially during the late growth phases (Fig. 33). These cells did not form endospores, indicating that they were arrested in a developmental stage resembling the vegetative phase of growth.

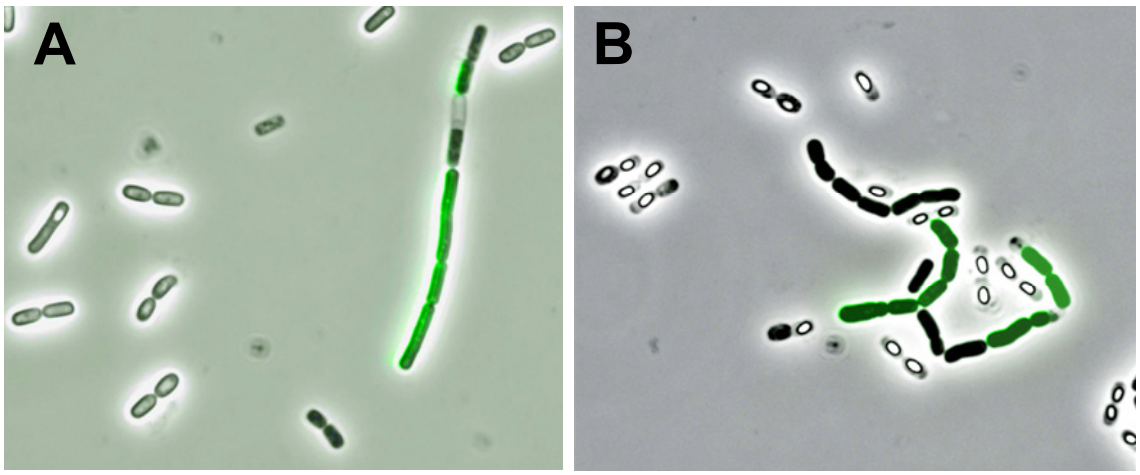

Figure 33: Cereulide synthesis might be preferentially turned on in a certain, hitherto uncharacterized developmental stage of a *B. cereus* subpopulation. Fluorescence images of the synchronized *B. cereus* reporter strain F48icesGFP were taken (A) 16 hours and (B) 24 hours after growth in LB medium supplemented with 150µg ml^{-1} spectinomycin. During late growth phases, the GFP signal is turned on in spatially connected and chained cells, but is broadly absent in the endospore-forming subpopulation.

In summary, data presented here provide strong evidence for a heterogeneous induction of cereulide synthetase gene expression in an isogenic population of *B. cereus* F4810/72 under the chosen culture conditions.

4 Discussion

4.1 Emetic *B. cereus*: emerging foodborne pathogens

4.1.1 Incidence of emetic *B. cereus* and cereulide in dairy-based foods

Cereulide producing emetic *Bacillus cereus* is increasingly recognized as the causative agent of usually mild, but occasionally lethal food-borne intoxications of humans. Until now, comprehensive food screening surveys targeting at both, the detection of emetic strains and the detection of the toxin have not been conducted. Therefore, a polyphasic approach combining a routine diagnostic method for enumeration of presumptive *B. cereus* (MPN technique according to EN ISO 21871) with PCR-based (real-time) assays (Ehling-Schulz *et al.* 2004; Fricker *et al.* 2007), and a HEp-2 cell based cereulide detection assay was used to assess the incidence of emetic *B. cereus* and cereulide in dairy-based products and their ingredients (Fig. A1, Appendix).

Presumptive *B. cereus* was found in 48% of the ingredients and in 50% of food samples, albeit at low cell counts ranging from 0.3 to 480 CFU per gram (Table 9). These values do not exceed international tolerance levels for *B. cereus*, which are typically set to 10^3-10^4 CFU per gram (Becker 2005) and are in accordance with previous studies reporting on the occurrence of *B. cereus* in milk-derived products (see e.g. Becker *et al.* 1994; Reyes *et al.* 2007). Nevertheless, this study revealed that emetic strains were natural contaminants in 8% of the retail foods and in 14% food of the ingredients. In comparison to the MPN/colony PCR-approach, emetic strains were more frequently detected with the real-time PCR assay. It can thus be assumed that emetic strains occasionally can be outcompeted by other *B. cereus* group organisms during the MPN enrichment procedure (see e.g. whole milk powder, Table 11) and that emetic strains were present during the manufacturing process, but are absent in the end-product (see e.g. condensed milk, Table 11). These results emphasize the need for targeted strategies to inhibit cereulide toxin production in early steps of the product processing line that might be favorable for *B. cereus* growth. Cereulide is extremely stable and withstands a broad pH range and enzymatic cleavage, as well as inactivation by filtration or thermal processing during food manufacturing or reheating of prepared foods (Agata *et al.* 2002; Rajkovic *et al.* 2008). It is therefore highly important to prevent the synthesis of the toxin and to prevent its introduction into the food chain by food ingredients.

Cereulide was detected in 3% of the retail products and in 10% of the ingredients in quantities of 0.14 to 0.72 µg per gram of food, underscoring that food ingredients, such as thickening agents, fruit preparations, milk and whey powder, as well as rice and pasteurized liquid egg can not only act as vehicles for toxin producer but also for cereulide (Table 11). These data stress the point that the risk to the consumer should not be solely judged by the cell count or the

presence of emetic strains, especially as concentrations as low as 0.01-0.03 µg/g food have been implicated in emetic intoxication cases (Essen *et al.* 2000; Agata *et al.* 2002).

The analysis of suspicious foods showed that around 35% were contaminated with emetic *B. cereus* and cereulide. The clinical manifestation of emetic intoxications resembles staphyloenterotoxicosis (Drobniewski 1993). Since public health facilities are more aware of *S. aureus*, the true incidence of *B. cereus* poisoning cases is largely unknow and presumingly underestimated (Ehling-Schulz *et al.* 2004). The data of the present survey indicate that incidence rates for emetic food poisonings caused by *B. cereus* contaminating dairy-products might be higher as hitherto anticipated. Indeed, milk, milk powder, and milk powder-based hot chocolate from vending machines have already been implicated in emetic *B. cereus* outbreaks and food-borne illnesses (Holmes *et al.* 1981; van Netten *et al.* 1990; Shinagawa 1993; Nelms *et al.* 1997).

This work shows that cereulide and emetic strains are common contaminants of dairy-based foods and their ingredients, and that their prevalence was hitherto apparently underestimated. However, a broad-scale screening is currently hindered by the time-consuming and laborious extraction procedures necessary to assess cereulide levels in complex matrices. The extraction of the highly lipophilic cereulide molecule, especially from fat-rich foods is often error-prone, e.g. the toxin recovery rate from different food matrices varies from 10% to 100% (Frenzel and Ehling-Schulz, unpublished data) and matrix specific extraction protocols are often required (Shaheen *et al.* 2006). Thus, although the European Food Safety Authority stressed the necessity of identifying categories of foodstuffs that may pose a risk to human health with respect to cereulide contamination (Anonymous 2005), alternative strategies to quantify the risk of toxin production, e.g. the *lux*-based reporter strain system presented in Chapter 3.2, are needed.

4.1.2 A *lux*-based reporter strain as novel tool to enhance *B. cereus* food safety

Emetic intoxications are frequently associated with starchy and farinaceous foods (Kramer and Gilbert 1989; Ehling-Schulz *et al.* 2004). However, a basic categorization scheme or a rapid risk analysis method regarding the potential of different types of foods to support cereulide synthesis is not available yet. Therefore, the suitability of a luciferase-based *B. cereus* reporter strain to reflect varying degrees of toxin synthesis was evaluated. The *in situ* application of the luciferase-based *B. cereus* F4810/72[P_1/*lux*] reporter strain allowed a direct monitoring of *ces* gene promoter activity in complex environments. The results from various growth media and foods illustrate that the influence of external parameters is reflected by gradual promoter responses, which were displayed by the varying intensity of bioluminescence signals (Table 12, Fig. 6, and Fig. 7). Furthermore, *lux* signals emitted by two recently isolated emetic strains transformed with pMDX[P_1/*lux*] had a similar intensity, suggesting that the genetical background of the F4810/72 reporter strain has not been altered by laboratory domestication (Fig. 8).

The activity of the P_1 promoter was strongly dependent on the nutrients provided. Thus, the *lux* reporter system described here visualizes the findings of previous studies reporting substantial variances in cereulide production on different growth media (Szabo *et al.* 1991; Rajkovic *et al.* 2006). Media routinely used for *B. cereus* detection and experimental procedures (MYP, PC, and LB and BCM) showed higher P_{cesP1} activity than protein enriched media such as Columbia blood, TSA and BHI agar (Fig. 6). However, blood, TSA or BHI agar are still frequently used to study cereulide production by emetic *B. cereus*, though it was reported earlier that less toxin was detected in contrast to e.g. skim milk or rice based media (Szabo *et al.* 1991; Finlay *et al.* 1999).

The system was further adapted for the application in foods. A set of 115 retail products was inoculated with F4810/72[P_1/*lux*] and incubated for 24 hours at 24°C, the temperature reported to be optimum for cereulide production (Häggblom *et al.* 2002). The luciferase signals were quantified with a software-assisted region-of-interest (ROI) and results were used to establish a categorization system, which served to classify foods to be at high risk, risk, or low risk regarding the toxin formation capability (Table 13 and Fig. 7). Food characteristics commonly observed in the three different categories are shown in Figure 34.

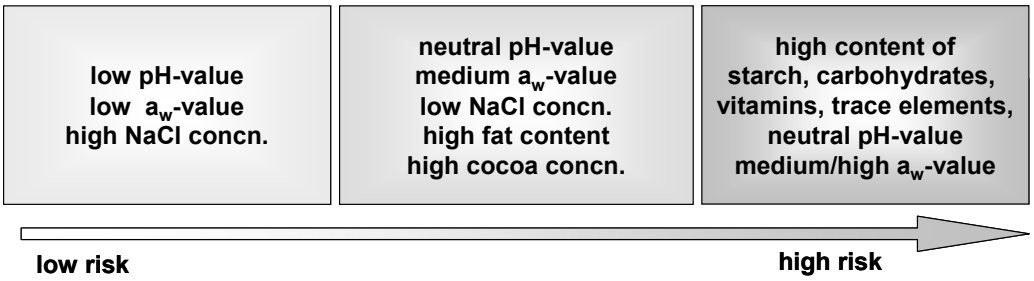

Figure 34: Indicative scheme for abiotic factors influencing the activity of the cereulide synthetase promoter driving the expression of the NRPS encoding *cesPTABCD* cluster. The parameters were deduced from the examination of 115 foods and food ingredient using an emetic *lux* reporter strain (Ch. 3.2). The arrow denotes the increasing toxin formation capability with respect to the food composition.

As shown by cereulide quantification, the amount of toxin produced correlated to the signal intensity of the *ces* promoter driven *lux* gene expression (Table 13). In accordance to the results obtained on growth media, high promoter activity was detected in the carbohydrate rich cooked rice, while only intermediate promoter activity was observed in the proteinaceous camembert cheese (Fig. 7 and Table 13), although final cell numbers of the *lux* reporter strain in both model food systems did not significantly differ. These findings correlate with reports of emetic food poisoning cases that implicate farinaceous, rather than proteinaceous foods (Essen *et al.* 2000; Agata *et al.* 2002; Ehling-Schulz *et al.* 2004; Fricker *et al.* 2007) and underscore the risk of emetic intoxications, for instance, in mass catering quantities of rice- or pasta-based dishes that have been improperly cooled.

It is interesting to note that the group of high risk products comprised foods, which are frequently associated with food poisonings, outbreaks, or frequently contaminated with emetic *B. cereus*: pasta, rice, milk powder, and infant formulae (Holmes *et al.* 1981; Mahler, 1997;

Andersson *et al.* 2004; Dierick *et al.* 2005; Duc *et al.* 2005; Ehling-Schulz *et al.* 2005; Pirhonen *et al.* 2005).

Besides this classical outbreak related food, the system revealed other products to be potentially at risk to support the production of hazardous cereulide concentrations, such as a sweetened dairy-based dessert and camembert cheese. Indeed, cereulide was detected in a retail camembert cheese sample investigated previously (Rajkovic *et al.* 2007). The proposed risk group classification is further supported by the fact, that around 8-10 µg cereulide per kg of body weight must be consumed by healthy individuals to provoke a clinical manifestation of the emetic syndrome (Shinagawa *et al.* 1995; Jääskeläinen *et al.* 2003). Thus, foods containing > 1 µg g^{-1} cereulide would be hazardous to a child of 10 kg body weight, if about 100 g were consumed. Indeed, foods related to emetic poisoning contained about 1-13 µg g^{-1} cereulide (Essen *et al.* 2000; Agata *et al.* 2002; Jääskeläinen *et al.* 2003). Nevertheless, the risk group foods should also be considered critical, as it was also shown that food poisoning cases implicated meals which contained as little as 0.01 µg g^{-1} of the toxin (Essen *et al.* 2000; Agata *et al.* 2002).

The assay presented here offers the advantage of a high throughput system for a basic categorization of foods regarding the risk of cereulide production. Furthermore, risky food ingredients might be excluded from the food production line to elevate the safety of the end-product. The advantage of this bioluminescence-based system is conclusively substantiated by the short duration of this analysis method. In contrast to time consuming extraction methods for the detection of cereulide itself, data can be achieved within 24 hours. Thus, the real-time monitoring of *ces* gene expression might have the potential as an industrial application to support hazard identification in terms of HACCP concepts, and offers the possibility to basically identify a potential source of risk to the consumer.

4.1.3 Initial steps towards targeted hurdle concepts in *B. cereus* food safety

Data presented in this study as well as data of previous studies (Agata *et al.* 2002; Rajkovic *et al.* 2007) highlight the potential of emetic *B. cereus* and the stable toxin cereulide to contaminate a variety of retail products. In addition, this work showed that food ingredients represent an important contamination source probably underestimated in the past. Thus, effective measures to prevent toxin formation in food production are needed. A broad variety of food types was found to support cereulide formation (Ch. 3.2). However, data of Chapter 3.3 indicate that the usage of long-chain polyphosphates (polyPs), which are extensively applied as functional food additives in the dairy and meat industry (Shelef and Seiter 1993; Prakash 2000), have the potential and might contribute to enhance *B. cereus* food safety, for instance as part of a hurdle concept. PolyPs are straight-chain polymers of condensed orthophosphoric acid residues. PolyPs and derived orthophosphate blends are classified as GRAS (generally recognized as safe) and therefore widely applicable (Molins 1991). A previous study on the influence of long-chain polyphosphates (polyPs) on cell division in non-emetic *B. cereus* (Maier

et al. 1999) raised the question of whether these substances could also have an impact on cereulide production in emetic strains.

The inhibitory potential of polyPs was assessed in reconstituted infant food, since this substrate is known to allow the production of exceptionally large quantities of cereulide when spoilage under temperature abuse conditions is simulated (Shaheen *et al*. 2008). Moreover, infant formulae are frequently contaminated with *B. cereus* (Ch. 3.1 and (Becker *et al.* 1994; Shaheen *et al.* 2006). Simulation of food spoilage at room temperature revealed that the antimicrobial activity and toxin inhibition efficiency differed depending on the type of polyP blend used. In comparison to broth culture experiments, higher polyP concentrations (5 vol%) were necessary to achieve growth inhibition (Fig. 9 and Table 14). This is in agreement with data from previous studies, which demonstrated that the efficiency of polyPs in culture media with comparably simple compositions is not necessarily matched by the activity in complex food matrices (Shelef and Seiter 1993; Prakash 2000). Thus, the outcome of growth inhibition strongly depends on the complexity of the environment (Zessin and Shelef 1988; Lee *et al.* 1994), and the analyzed infant formula was enriched with proteins and vitamins. PolyP blend 2 displayed enhanced inhibitory effects and prevented the outgrowth of the initial cell inoculum in the infant formula but not in PC broth and oat milk. This might be explained by the finding that the antimicrobial activity of foodgrade phosphates is modulated in response to different food matrices or ingredients (Shelef *et al.* 1989; Glass and Johnson 2004). PolyP 1, the blend with the highest orthophosphate content, did not influence cell growth (Table 14). However, cereulide titers were reduced by 70%, which strengthens the assumption that the cereulide synthesis process sensitively reacts to the presence of polyphosphates. PolyP 3 most efficiently inhibited toxin production by 98%, albeit at a concentration (5 vol-%, corresponding to approximately a 3.5% P_2O_5 content), which is somewhat above the legal limit for this food additive. Considering the high initial inoculation level, it should be noted, however, that this might not necessarily reflect naturally occurring food spoilage cases. Different studies of the prevalence of *B. cereus* in powdered infant foods showed that the pathogen is usually found in quantities below 10^3 CFU g^{-1} (for a recent report, see Haughton *et al.* 2010). Therefore, lower polyP concentrations may be sufficient to prevent toxin synthesis under common household conditions even in sensitive foods such as infant formulas. Data comparing the effects of 0.1 to 0.5% of the three polyP blends in the model food oat milk are summarized in Table 15. Most importantly, the use of 0.5 vol-% polyPs (approximately 0.35% P_2O_5) completely prevented toxin formation within concentrations commonly used in the food industry worldwide (0.2 to 0.8% P_2O_5 content) (Akhtar *et al.* 2008). Furthermore, these concentrations are within the maximum use level of 0.5 to 2% P_2O_5 for dairy products prescribed by the European Scientific Committee on Food (SCF) (http://ec.europa.eu/food/fs/sc/scf/reports_en.html) and the joint FAO/WHO Codex Alimentarius Commission (CAC) (codex general standard for food additives 192-1995, version 2009 (Anonymous 2009)).

In conclusion, this study indicates that the use of commercial polyphosphate blends could serve as one module of a food safety hurdle concept, which is targeted at the inhibition of cereulide synthesis in food ingredients or foods, especially where *B. cereus* spores can not be excluded or

inactivated during processing or preparation steps. Considering their broad applicability in the food industry (Prakash 2000), polyPs may also contribute to control cereulide synthesis in other food systems. However, before a firm conclusion on the practical suitability of polyPs can be drawn, the efficiency of the food additives must be validated with additional model foods and pilot studies. One should also bear in mind that the effective control of cereulide contamination in complex food matrices requires a well-balanced adjustment of several factors, including water activity (a_w value), pH value, nutrient composition, and temperature, which jointly affect toxin synthesis (Fig. 34). However, this study not only presents the first data concerning the inhibitory action of polyPs on a nonribosomally synthesized peptide toxin, but also presents the first successful attempt of a targeted inhibition of cereulide production in foods.

4.2 Cereulide synthesis: regulation at the intersection of metabolism and virulence

4.2.1 Cellular phosphate status is crucial for cereulide synthesis

The food industry uses polyPs owing to their functional aspects regarding emulsification, stabilization, oxidation prevention, and flavor protection, but also as antimicrobial substances (Molins 1991; Shelef and Seiter 1993). Due to their polyanionic nature, polyPs sequester divalent cations and render them unavailable to microorganisms, which is often assumed to be a cause of their antimicrobial activity, leading to loss of membrane integrity and cell lysis (Wagner 1986; Shelef and Seiter 1993; Lee *et al.* 1994; Maier *et al.* 1999). However, more-specific effects have also been reported, including interference with ATP generation, protein folding, or enzyme activities (Wagner and Busta 1985; Chambert and Petit-Glatron 1999; Prakash 2000), which undelines that the knowledge concerning the molecular effects of polyPs is still limited. Interestingly, the chemically manufactured polyP molecules have natural analogues synthesized in all bacteria and fullfill manifold physiological functions (recently reviewed by (Rao *et al.* 2009). While the role of intracellular polyPs in *B. cereus* biofilm formation, sporulation and motility was demonstrated (Shi *et al.* 2004), the fate of exogenously added polyP has not been dissected so far. Endogenous polyP concentrations are strictly regulated in prokaryotes. The concentration is low during rapid growth but increases under conditions of nutritional imbalance unfavourable for growth (Wagner 1986). As *B. cereus* usually does not accumulate high polyP levels (Shi *et al.* 2004) the presence of exogenous polyPs might increase the intracellular concentration, which may result in imbalances affecting numerous cellular processes.

In accordance to previous studies, sublethal, non-lytic polyP concentrations caused bacteriostasis and defective cell division (Fig. 10) (Wagner and Busta 1985; Zaika *et al.* 1997; Maier *et al.* 1999). It was assumed that sequestration of divalent cations caused the defect in septum formation due to an indirect effect of the cation deprivation on the GTPase activity of

FtsZ proteins (Maier *et al.* 1999). However, in the current study, the vegetative cell shape normalized after the commencement of a delayed exponential growth phase (Fig. 10), indicating that polyP is slowly degraded to orthophosphate (P_i) residues lacking antimicrobial activity (Shelef and Seiter 1993). Consistently, a BLAST analysis revealed that all key enzymes for polyP hydrolysis and synthesis (polyP kinase [PPK], polyP/AMP phosphotransferase [PAP], and exopolyphosphatase [PPX]) are present in *B. cereus* F4810/72, stressing the point that regulation of the internal polyP level is crucial for this organism.

The qPCR data indicate that polyPs interfere with early stages of the toxin formation process by delaying and reducing *ces* gene transcription, and hence, cereulide synthesis (Fig. 11). Interestingly, polyP-induced delay of toxicity despite vegetative growth has also been reported for the nonribosomal synthesis of aflatoxin B1 and G1 by *Aspergillus* spp. (Marsh *et al.* 1996). However, the influence on transcription or activity of the polyketide synthase enzyme was not determined, though the underlying effect was remotely attributed to disturbances of primary metabolic pathways. Similarly, a feedback inhibition by phosphorylated intermediates to biosynthetic pathways was taken into account to explain the polyP-induced effects leading to aflatoxin synthesis inhibition (Luchese and Harrigan 1993).

Intriguingly, subinhibitory concentrations had a stronger effect on the toxin synthesis mechanism than on other cellular processes, such as binary fission (Fig. 12). This finding suggests that cereulide synthesis has a much narrower tolerance range for phosphate than the vegetative growth of the organism. Thus, polyP-mediated chelation of metal ions might not be the ultimate cause of reduced toxin synthesis, as main cellular functions like binary fission, which is highly dependent on cations (Margolin 2005), apparently were not influenced.

PolyPs are potent phosphorylating agents that likely participate in protein phosphorylation and thus are influencing metabolic regulation in microorganisms (reviewed by (Kulaev *et al.* 1999; Rao *et al.* 2009). One might speculate that polyPs modulate the phosphorylation status of regulatory proteins of the cereulide synthesis network, e.g. transcription factors. In *B. anthracis*, AtxA, a global virulence regulator, is subjected to phosphorylation by the phosphotransferase system (Tsvetanova *et al.* 2007). Interestingly, it has also been reported that CodY, a transcriptional repressor of cereulide synthesis (Ch. 3.5.1), is phosphorylated *in vivo* (Macek *et al.* 2007). In *Mycobacterium tuberculosis*, polyPs directly act as phosphate donors to the MprA/B TCS, which activates the synthesis of the alarmone (p)ppGpp (guanosine 5´-diphosphate 3´-diphosphate). In turn, ppGpp is necessary to activate the expression of nonribosomal polyketide synthases, which are important virulence factors in MTB (Dahl *et al.* 2003). Strikingly, ppGpp also activates the nonribosomal synthesis of bacilysin, actinorhodin, and undecylprodigiosin in *B. subtilis* and *Streptomyces* spp., respectively (Hu *et al.* 2002; Inaoka *et al.* 2003). In the majority of microorganisms, the metabolites polyP, GTP, ATP, and ppGpp are inherently connected, because polyP and ppGpp are synthesized from the GTP and ATP pool (Rao *et al.* 2009). Thus, polyP might also modulate *ces* synthesis *via* ppGpp, or *via* GTP, which is sensed by CodY (Ch. 3.5.1).

Moreover, imbalances in the intracellular polyP/P_i ratio might interfere with the phosphoryl flux through the phosphorelay which would result in altered Spo0A activity, and hence, *ces* gene

transcription. Indeed, Spo0A is likely to be a direct target of inherent polyP regulation in *B. cereus*, since elevated polyP accumulation in a Δ*ppx* mutant prevented sporulation, whereas the decrease of polyP levels in wild type cells triggered sporulation (Shi *et al.* 2004). This hypothesis is supported by the observation that extracellular polyP application on swarming agar impaired swarming and sporulation of *B. cereus* F4810/72 (Frenzel, unpublished data). Both cellular differentaition processes are initiated by Spo0A~P (Banse *et al.* 2008).

Alternatively, phosphate imbalance might affect catalytic processes of NRPS modules posttranslationally, e.g., by interfering with the activation of the NRPS modules by the phosphopanteteinyl transferase. Additionally, it was demonstrated that a NRPS of *Bacillus brevis* not only synthesizes the antibiotic tyrocidine but also (di)adenosine polyphosphates (Dieckmann *et al.* 2001). It is therefore tempting to speculate that the exogenous polyP overflow leads to a dysfunction of the NRPS enzyme complex.

The underlying mechanism leading to the inhibitory effect of polyPs on cereulide synthesis remains unknown. Nevertheless, it is reasonable to assume that nonribosomal toxin formation is impaired under elevated phosphate levels by a multi-factorial mechanism due to a narrow tolerance range regarding external and internal phosphate concentrations.

4.2.2 A network of regulators fine-tunes transcription of the *ces* operon

Environmental cues substantially modulate the outcome of cereulide synthesis (Ch. 3.2 and Ch. 3.3), but less is known about how these signals are transmitted to affect transcriptional control of *ces* gene expression. The majority of transcriptional regulators directing cereulide synthesis has not been identified yet. In the frame of this work, several transcription factor homologs of F4810/72 were identified, heterologously expressed, and tested regarding their affinity towards different regions of the *ces* promoter area (Ch. 3.4), to decipher the mechanisms controlling *ces* gene transcription.

ComA~P activates the transcription of NRPSs operons for surfactin, bacilysin, lichenysin A, and bacillomycin D, produced by several *B. subtilis* group strains (Roggiani and Dubnau 1993; Yakimov and Golyshin 1997; Yazgan *et al.* 2001; Koumoutsi *et al.* 2007). However, *B. cereus* F4810/72 lacks a ComA ortholog (Table 16). A BRH approach on the cognate histidine-kinase of ComA, namely ComP, revealed that the putative ComP homolog is N-terminally truncated in F4810/72 (data not shown). This might explain the difficulty in predicting a ComA homolog in F4810/72, as it could be obsolete if the signal-receiving sensory domain of ComP is absent. In *B. subtilis*, the ComP/A TCS is part of the *comQXPA* cluster that directs competence development and surfactin synthesis in a quorum sensing dependent manner (Hamze *et al.* 2009). Because F4810/72 also lacks *comX* and *comQ*, these findings suggest that cereulide synthesis is not controlled by a *comQXPA*-like quorum sensing locus.

In vitro DNA-binding experiments with purified CodY, a global regulator of stationary phase adaptation (Sonenshein 2005), showed a specific interaction with two DNA probes covering the core promoter region of the *ces* operon (Fig. 14, Fig. 15, and Table 17). The apparent K_D for

cesPI and cesPII was estimated to be around 50 nM, which is in exellent agreement with earlier publihed gel retardation assays conducted with CodY homologs of other gram-positive bacteria and is furthermore indicative for the presence of high affinity CodY-binding sites (Shivers *et al.* 2006; Dineen *et al.* 2010; Majerczyk *et al.* 2010). Moreover, CodY bound to the internal *cesB* promoter of the *ces* gene cluster, albeit with 10-fold lower affinity (Fig. 15). Although the function of this intracistronic promoter in *ces* operon expression is yet unknown, data presented here indicate that P_{cesB} is, similar to the main promoter, controlled by CodY. As P_{cesB} is approximately 5-fold less active than the main promoter region (Dommel *et al.* 2010), a low-affinity binding site would presumably be sufficient for a CodY-mediated activation or repression of the distal genes. Indeed, it has been shown for *B. subtilis* that the expression of CodY regulon genes is not simply turned on by ceasing co-repressor levels, but is rather sophisticatedly fine-tuned through the number and existence of low and high affinity *cis* acting elements that determine the gene-specific strength of repression (Brinsmade *et al.* 2010; Belitsky and Sonenshein 2011).

Gel mobility shift assay indicated that *B. cereus* CodY binds, like the *B. subtilis* homolog, GTP and branched-chain amino acids (BCAAs) as ligands that enhance the DNA affinity of the protein (Ratnayake-Lecamwasam *et al.* 2001; Shivers and Sonenshein 2004). Moreover, CodY bound specifically to the promoter of *ilvB*, a gene involved in the synthesis of BCAAs (Sonenshein 2007). The apparent equilibrium constant [K_D] of around 150 nM is in excellent agreement with previously published *ilvB* promoter gel retardation assay with *B. subtilis* CodY (apparent $K_D \approx$ 200-250 nM) (Molle *et al.* 2003). This might indicate that CodY controls a similar regulon as its *B. subtilis* counterpart and is involved in nitrogen metabolism (Sonenshein 2007). Thus, in the case of emetic *B. cereus*, CodY would not only control cereulide synthesis but also the synthesis of precursor molecules of the dodecadepsipeptide (i.e. L-valine and α-ketoacids). A detailed discussion on the *in vivo* function of CodY in *B. cereus* pathogenicity is provided in Chapter 4.2.3.

In contrast, SinR and CcpA did not interact with the *ces* promoter probes (Fig. 16 and Table 17). Hence, it seems rather unlikely that these transcription factors directly participate in transcriptional control of the *ces* biosynthesis operon.

The carbon control protein CcpA was tested because (i) previous studies showed that glucose caused a downregulation of *ces* gene transcription in F4810/72 (Dommel 2008; Lücking 2009), and (ii) cereulide levels were 6-fold lower when *B. cereus* was grown in defined MOD medium with glucose as the sole carbon source, instead of fructose, respectively (Frenzel, unpublished data). These finding are in agreement with a previous study, which showed that in *B. subtilis* glucose causes a stronger CcpA-mediated carbon catabolite gene repression (CCR) than fructose (Singh *et al.* 2008). Thus, CcpA possibly influences cereulide synthesis indirectly. One explanation might be that glucose stimulates CcpA to increase the synthesis of BCAAs by inducing the *ilv-leu* operon, thereby increasing the ligand pool for CodY (Sonenshein 2007). This would imply that CodY acts as a repressor of cereulide synthesis. This hypothesis is supported by the observation that cereulide levels were not influenced when a *codY*-deficient F4810/72 mutant was cultivated with different C-sources (Frenzel, unpublished data). Hence,

CcpA could be a player in the cereulide synthesis regulon that connects the central carbon and nitrogen metabolism *via* CodY to cereulide toxin expression.

By contrast, ComK was found to bind specifically to DNA probes carrying the $cesP_1$ and $cesP_2$ promoters (Fig. 16 and Table 17). In *B. subtilis*, ComK acts as an auto-stimulating regulator of competence development that activates the transcription of late competence genes including the machinery for DNA-uptake and -integration (reviewed by (Hamoen *et al.* 2003; Schultz *et al.* 2009). Recently, similar physiological functions have been proposed for the ComK homolog of the non-emetic *B. cereus* strain ATCC14579 (Mironczuk *et al.* 2008). In the present study, F4810/72 ComK bound to its own promoter region (Table 17), illustrating that the transcription factor might act auto-regulatory on its own synthesis. In *B. subtilis*, ComK expression is temporally limited: basal expression levels increase exponentially before entry into the stationary phase, but cease towards undetectable levels in stationary phase (Leisner *et al.* 2007). Assuming a similar activity pattern in *B. cereus*, it is tempting to speculate that ComK could activate *ces* gene transcription, which would be amplified by the auto-stimulatory loop of ComK expression. This might contribute to the rapid increase of *ces* transcript levels during late exponential growth, which was observed in previous studies (Lücking *et al.* 2009; Dommel *et al.* 2011; Frenzel *et al.* 2011).

Two-component systems (TCSs) are frequently involved in the control of virulence factor expression (Beier and Gross 2006). Since the *in silico* approach predicted seven possible binding sites for DegU, and since DegU is a direct activator of bacillomycin D NRPS expression (Koumoutsi *et al.* 2007), this response regulator was selected for analysis. However, due to the ambiguity in identifying a F4810/72 homolog, the *B. subtilis* protein was used as a model in the gel shift experiments. According to the *in silico* prediction, DegU interacted with all three DNA probes (Table 17), suggesting that a DegU-like protein might be crucial for cereulide synthesis. However, targeted bioinformatic and experimental approaches will be necessary to identify a functional ortholog in *B. cereus* F4810/72.

Also, PerR bound to the cesPI probe covering the P_1 and P_2 promoter elements (Fig. 16). As predicted by DBTBS *in silico* footprinting, PerR possibly interacts with a binding site that covers the -10 box and the transcriptional start site of P_2, whereas a second binding site is situated 9 bp upstream of the -35 box of P_1 (data not shown). Likewise, the promoter region of the surfactin synthesizing NRPS of *B. subtilis* harbors two tandemly arranged PerR binding sites (Hayashi *et al.* 2005). PerR is a metal-binding transcription factor that senses H_2O_2 by iron-catalyzed histidine oxidation (see Fig. 5) (recently reviewed by (Zuber 2009; Duarte and Latour 2010). H_2O_2 binding leads to inactivation of PerR and promotes the synthesis of enzymes for oxidative stress response and detoxification (Bsat *et al.* 1996). Activation of the purified *B. cereus* PerR protein by manganese (Ch. 2.8.5) and the presence of amino acid residues necessary for coordinating the metal ion ligands (Fig. 35) strongly indicate that PerR of *B. cereus* F4810/72 executes the same *in vivo* functions as the *B. subtilis* homolog and senses H_2O_2 (Lee and Helmann 2006)

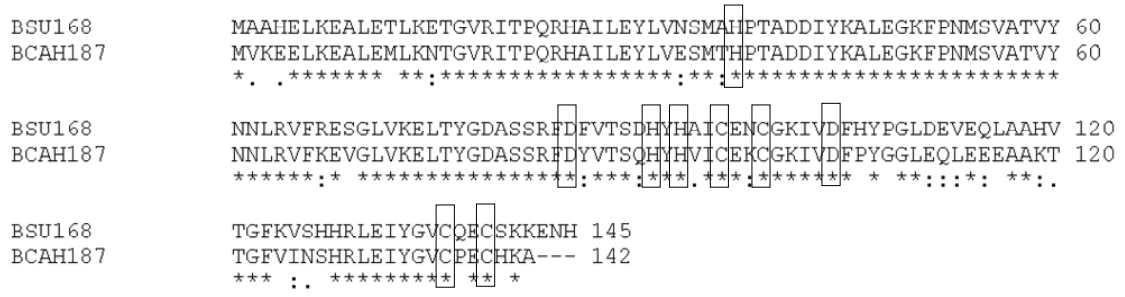

Figure 35: Alignment of amino acid sequences of PerR metalloregulators encoded in *B. subtilis* 168 (BSU168) and *B. cereus* F4810/72 (BCAH187). The amino acids residues coordinating the regulatory and structural Fe^{2+}/Mn^{2+} and Zn^{2+} ions are boxed.

These results point towards a connection between toxin synthesis and oxidative stress levels encountered by the cell. Indeed, cereulide synthesis demands the presence of oxygen, but toxin levels are highest under low oxygen tensions (Finlay *et al.* 2002; Jaaskelainen *et al.* 2004), suggesting that aerobic respiration and the cellular redox state are crucial factors influencing the cereulide synthesis network. It has been proposed that enhanced endogenous H_2O_2 concentrations arise during increased tricarboxylic acid (TCA) cycle activity, i.e., within the onset of stationary phase (Somerville and Proctor 2009), and are further induced by external stressors, such as high salt concentrations, acid shock, and antibiotics that perturb the electron transfer chain (Kohanski *et al.* 2007; Mols *et al.* 2010; Mols and Abee 2011). Thus, it might be speculated, however, that PerR acts as a transcriptional activator of cereulide synthesis, which is inactivated by H_2O_2 stress. This hypothesis is further strengthened by the observation that salt exposure significantly reduced cereulide synthesis on a transcriptional and expressional level, although the growth rate of F4810/72 was not affected (Dommel *et al.* 2011).

According to the *in vitro* binding experiments, cereulide synthesis seems to be co-regulated by several transcription factors in a highly complex manner (Fig. 36). As the transcription factors belong to distinct regulatory circuitries that perceive and respond to various stimuli, such as GTP, BCAAs and H_2O_2, it seems reasonable that transcription of the *ces* operon is strictly temporally limited and tightly controlled. Notably, multifaceted transcriptional regulation is common for NRPS of *Bacillus* spp. (for examples, see (Marahiel *et al.* 1993; Yazgan *et al.* 2001). Considering the absence of a *comQXPA* quorum sensing locus in F4810/72, it might be speculated, that a generalized transcription factor network directing NRPS regulation does not exist in *Bacilli* and that regulation is -at least partially- regulated in a specific manner depending on the strain and on the NRP. For instance, surfactin synthesis is repressed by CodY in *B. subtilis* 168, but not in *B. subtilis* ATCC6633 (Duitman *et al.* 2007). Considering this complexity, and considering that the *in silico* footprinting analysis predicted binding sites for additional transcriptional regulators (Table A1, Appendix), it is expected that extensive research is required to understand the transcriptional co-regulation of cereulide synthesis. Also, further studies are necessary to prove the *in vivo* contribution of PerR, ComK, and DegU-like response regulators to the regulatory networks governing cereulide synthesis.

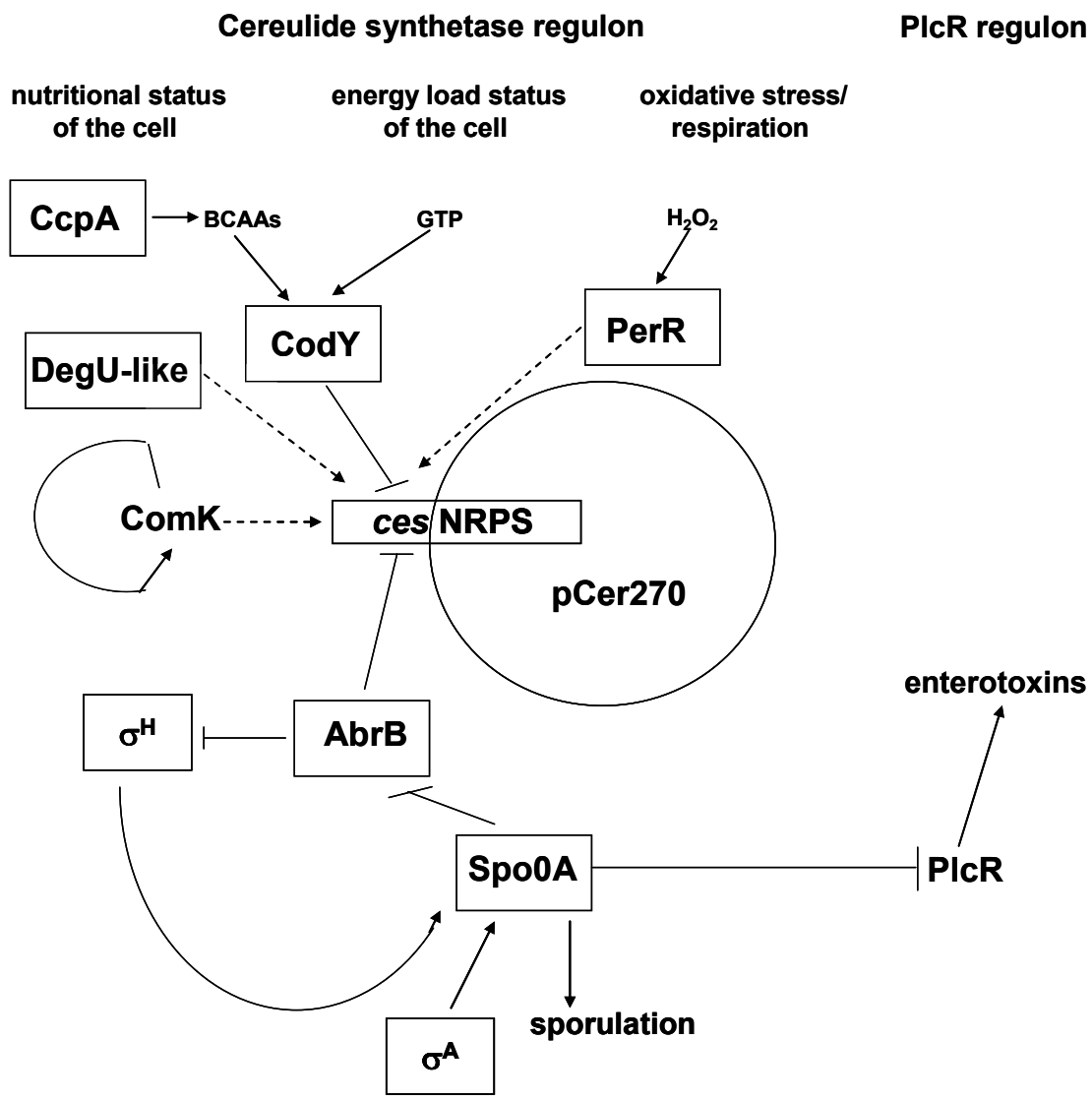

Figure 36: Tentative scheme of transcriptional regulatory circuitries involved in regulation of cereulide synthesis. Information on single transcription factors are provided in text. Dashed arrows denote that the transcription factors bound *in vitro* to the *ces* promoter area, but that the *in vivo* function must yet be examined by mutagenesis studies.

4.2.3 CodY: a central regulator of virulence

4.2.3.1 CodY represses cereulide toxin synthesis

To analyze the *in vivo* influence of CodY on cereulide synthesis, a *codY* null mutant strain of *B. cereus* F4810/72 was constructed (Chapter 3.5.1). In the Δ*codY* mutant, *cesA* transcription was strongly derepressed in early to mid-exponential growth phases (Fig. 18), strongly indicating that CodY acts as a repressor of the *ces* operon. However, transcription was still

subject to growth-phase-dependent regulation, reflecting the co-regulation by additional transcription factors. Consistently, deletion of *codY* did not alter the expression of *abrB* and *spo0A*, which were previously identified as *ces* regulatory elements (Lücking *et al.* 2009).

A direct repressor function was further supported by the observation that overexpression of CodY significantly reduced cereulide synthesis (Fig. 19). Also, the localization of a predicted CodY-box in proximity to the RNAP binding site (Ch. 3.4.2) supported the likeliness of a repressor function *in vivo*, as binding motifs in *B. subtilis* are frequently found immediately upstream of the -35 promoter region (Belitsky and Sonenshein 2008).The presence of BCAAs not only enhanced specific binding of purified CodY to the *ces* promoter *in vitro*, but also significantly repressed cereulide production in the wild type strain *in vivo*, whereas the *codY* mutant was not affected (Table 18). This strengthens the hypothesis that BCAAs are effector molecules of the metabolite-responsive regulator in emetic *B. cereus*. This is also indirectly reflected by the observation that *codY* inactivation suppressed the partial BCAA auxotrophic phenotype of *B. cereus* F4810/72 (Table 18). An explanation might be that the presence of L-isoleucine, which is supposed to be the most potent co-repressor of CodY (Shivers and Sonenshein 2004; den Hengst *et al.* 2005), was sufficient to block the *de novo* synthesis of BCAAs in the wild type strain. This repression was rescued by a *codY* disruption and, hence, the mutant strain was able to grow without either L-valine, L-isoleucine or L-leucine, which partially share enzymes in their biosynthesis pathways (Fink 1993). The dual role of L-valine in being both, toxin monomer and CodY-activating signaling metabolite, highlights the tight embedding of nonribosomal, plasmid-borne cereulide synthesis in the primary metabolism of emetic *B. cereus*. Data presented here also suggest that GTP is an *in vivo* ligand of CodY, because decoyinine-treatment of wild type cultures led to enhanced toxin synthesis (Fig. 20). This indicates that GTP can affect the CodY activity independently from the BCAAs, similar to the *B. subtilis* protein (Shivers and Sonenshein 2004).

The depletion of intracellular GTP and BCAA pools correlates with the entry into transition and stationary phase of growth and with the onset of sporulation (Soga *et al.* 2003; Sonenshein 2005). This implies that CodY functions as a timing regulator that links the onset of cereulide synthesis to growth phases hallmarked by unfavourable enegetic and nutritional conditions. This tightly temporal control seems to be crucial for *B. cereus*, as repression by the transition state regulator AbrB additionally secures timing of *ces* gene expression (Fig. 36). Comparatively, CodY and AbrB homologs jointly control the expression of the surfactin-producing NRPS in *B. subtilis*, thereby functionally linking surfactin synthesis to the onset of competence development, biofilm formation, and the development of multicellularity (Nakano *et al.* 1991; Serror and Sonenshein 1996; Lopez *et al.* 2009; Lopez and Kolter 2010).

Lastly, the enhanced repression of *ces* gene transcription by a surplus of amino acids might be a reason why proteinaceous foods are commonly poor substrates for cereulide synthesis (Ch. 3.2).

4.2.3.2 CodY activates transition and stationary phase virulence factors

The virulence potential of emetic and non-emetic *B. cereus* strains is highest during transition to the stationary phase, when the master regulators PlcR ad Spo0A induce the synthesis and secretion of several virulence determinants, including the medically important enterotoxins (Gohar *et al.* 2008) and cereulide (Lücking *et al.* 2009). At the same time, nutrient limitation progresses, and it is expected that CodY-repressed genes are upregulated (Sonenshein 2005). Only recently, it has been shown for several low-GC gram-positive pathogens that CodY controls the expression of virulence factors (see e.g. Majerczyk *et al.* 2008; van Schaik *et al.* 2009; Dineen *et al.* 2010). However, the functional role of CodY in *B. cereus* pathogenicity has not been studied so far. The data presented in Chapter 3.5.2 support the nature of the pleiotropic regulator in being a key regulator of bacterial pathogenicity.

In contrast to the observed upregulation of *ces* gene expression (Ch. 3.5.1), deletion of *codY* in *B. cereus* F4810/72 resulted in a significant downregulation of genes encoding the cytolytic proteins cereolysin O, phospholipase C, sphingomyelinase, immune inhibitor metalloprotease 2, and the enterotoxin Nhe (Fig. 21), which contribute to local and systemic infections and presumably counteract the host immune system (reviewed by (Kotiranta *et al.* 2000; Stenfors Arnesen *et al.* 2008; Bottone 2010). This finding was rather unexpected, as these virulence-associated factors belong to the group of genes, which were since now regarded to be pimarily regulated by the global PapR-PlcR quorum sensing regulon of *B. cereus* that acts independently from the regulatory circuits of cereulide synthesis (Gohar *et al.* 2008; Lücking *et al.* 2009). However, the hemolytic activity was profoundly impaired (Fig. 25), and enzymatic PC-PLC and SPH activities were nearly abolished in supernatants of the Δ*codY* mutant (Fig. 24). In addition, Nhe was almost undetectable in the Vero cell cytotoxicity assay (Fig. 23). As overexpression of CodY resulted in enhanced Nhe production (Fig. 23), the effect was clearly attributable to CodY. However, purified CodY did not exhibit *in vitro* affinity to any of the putative promoter regions of the PlcR regulon genes, which indicates that CodY is an indirect activator of some PlcR quorum sensing-dependent virulence genes of emetic *B. cereus.*

A direct repressor function of CodY was previously solely shown for *S. aureus* toxin genes (Majerczyk *et al.* 2010), whereas indirect regulation through targeting the expression of downstream regulators seems to occur more frequently. For instance, CodY represses *tdcR* sigma factor expression necessary for toxin synthesis in *Clostridium difficile* (Dineen *et al.* 2007). However, as *plcR* mRNA levels were not significantly altered in the Δ*codY* mutant, one might speculate that PlcR activity is modulated posttranslationally, as it was hypothesized for the central virulence regulator AtxA in *B. anthracis* (van Schaik *et al.* 2009). Alternatively, PlcR might be regulated posttranscriptionally by the action of CodY-induced synthesis of small regulatory RNAs, as recently shown for the AhrC regulator in *B. subtilis* (Preis *et al.* 2009). Furthermore, it cannot be excluded that CodY acts on the expression of factors that additionally control production of the virulence factors examined in this study. Nevertheless, the present data demonstrate that CodY is important for activating the production of quorum sensing induced virulence factors, such as the enterotoxin Nhe, sphingomyelinase and of phospholipase C. This

further implies that these genes are controlled in a complex manner in emetic *B. cereus*, underlying both, quorum sensing and nutrient-sensing mechanisms. However, the mechanisms causing a partial congruency of the CodY and PlcR regulons and the impact of CodY on the quorum sensing network must be elucidated in further in-depth studies.

Comparative qPCR analysis also revealed that CodY strongly repressed *ilvE*, a core metabolic gene involved in BCAA synthesis (Fink 1993) (Fig. 21). This is in agreement with previous studies, which demonstrated the key role of CodY in anabolic and catabolic nitrogen metabolism, including the induction of proteases and suitable permeases in several low-GC gram-positive bacteria (Molle *et al.* 2003; den Hengst *et al.* 2005; Guedon *et al.* 2005; Hsueh *et al.* 2008; Pohl *et al.* 2009; Majerczyk *et al.* 2010). Likewise, qPCR data show that the expression of the proteases InhA1, InhA3, and Npr599 was strongly upregulated in the Δ*codY* mutant (Fig. 21). Moreover, *in vitro* binding analyses revealed that CodY interacts with the promoter of *inhA1* (Fig. 22), which does not belong to the PlcR regulon (Guillemet *et al.* 2010), and is therefore consistent with the exceptionally strong derepression in the *codY*-deletion strain (Fig. 21). InhA metalloproteases are important virulence factors that contribute to counteract the host immune system (Guillemet *et al.* 2010). For instance, InhA1, which is both, secreted and spore surface-bound, was found to induce tissue degeneration by degrading tissue proteins, and to effect macrophage escape of internalized spores (Ramarao and Lereclus 2005; Chung *et al.* 2006). CodY might time the expression of InhA1 to allow its association with the exosporium during ongoing nutrient limitation. Furthermore, this supports the role of CodY in directly linking *B. cereus* nitrogen metabolism to pathogenicity, as it was discussed for the cereulide synthesis network in Chapter 4.2.3.1.

Recently, the invertebrate *Galleria mellonella* has become a popular alternative model system to study the virulence of human pathogens, since the *G. mellonella* immune responses functionally resemble mammalian innate immune responses to microbial infections (Mukherjee *et al.* 2010; Michaux *et al.* 2011; Senior *et al.* 2011). We observed that *codY* inactivation resulted in a severe virulence defect in this infection model (V. Doll, E. Frenzel, and M. Ehling-Schulz, unpublished data). This strongly indicates that *codY* is necessary to establish a rapid and severe course of *B. cereus* infections and highlights the profound role of *codY* in the overall pathogenicity of *B. cereus*, presumably also concerning human hosts.

In conclusion, this study provides the first evidence that the global regulator CodY is essential for virulence of both, emetic and of non-emetic *B. cereus* strains, since it controls cereulide as well as enterotoxin synthesis. CodY exerts a direct influence on the cereulide regulon and an, yet uncharacterized, indirect effect on the quorum sensing-dependent PlcR regulon, which were considered to operate independently up to now. Due to its ability to sense the nutritional and energy status of the cell by "monitoring" the GTP and BCAA levels, CodY functions as a timing regulator, possibly allowing the development of pathogenic traits in eligible host environments.

4.2.4 Plasmid-chromosome crosstalk in *B. cereus* F4810/72

The cross-talk between the chromosomally encoded transcription factors and the plasmid-borne cereulide operon suggests that the pXO1-like virulence plasmid pCER270 is tightly embedded in core metabolic processes rather than constituting an autarchic element (Ch. 4.2.2 and Ch. 4.2.3). To screen for putative cross-regulatory elements located on pCER270 that might act on cereulide synthesis and on the expression of chromosomally encoded proteins, luciferase measurements and 2-D DIGE anayses of *B. cereus* F4810/72 and its plasmid-cured and *ces* cluster inactivation derivatives were performed (Ch. 3.6).

Measuring of the *ces* promoter response in the different genetic backgrounds revealed that the promoter was slightly (F48ΔcesP/polar), or significantly (F48(pCER270-)) less active, respectively (Fig. 27). One possibility might be that pCER270 encodes regulatory elements that act directly or indirectly to activate transcription of the *ces* gene cluster or repress a direct *ces* operon repressor, respectively. Currently 10 putative transcriptional regulators and one TCS of unknown function are annotated on pCER270 (Rasko *et al.* 2007). Their functional analysis will help to clarify a possible role in the cereulide synthesis network. Similarly, the *ces* promoter response decreased upon inactivation of the Ces NRPS encoding *cesAB* genes and the adjacent ABC-type transporter (*cesCD*). This might point towards an autoregulation of the *ces* gene cluster or a feedback-inhibition due to a tailback of cereulide precursors, e.g., elevated L-valine levels might enhance the activity of the *ces* gene repressor CodY (compare Ch. 3.5.1). Alternatively, the possibility exists that hitherto unidentified regulatory elements are encoded within the *ces* gene cluster itself. For instance, in *B. subtilis* and *B. licheniformis*, the ORF of the valine-activating domain of the SrfAB module responsible for nonribosomal surfactin biosynthesis harbors *comS*, an overlapping gene, which is out of frame with *srfAB1* and regulates competence development (D'Souza *et al.* 1994; Hamoen *et al.* 1995; Hoffmann *et al.* 2011).

As the results of the *lux* assays indicated the existence of cross-talk mechanisms between pCER270 encoded elements and the *ces* gene operon or chromosomal genes, putative cross-regulatory mechanisms were further analyzed on the proteomic level. DIGE-based comparative proteomics of the wild type and the virulence-plasmid cured strain resulted in the identification of three proteins that are encoded on pCER270: The FtsZ-protein domain containing replication protein RepX, and two novel, strongly expressed enzymes, the chitin-binding domain protein and a metallopeptidase (Fig. 28A/29A and Table 20). Production of the chitin degrading enzyme might be indicative for an insect- and/or soil-associated lifestyle of *B. cereus* F4810/72, as it is discussed for *B. cereus* strains in general (Ivanova *et al.* 2003; Stenfors Arnesen *et al.* 2008). The comparatively high expression of a plasmid-born protease further shows that *B. cereus* is more acquisitive for proteins and peptides, rather than for polysaccharides and sugar sources, as stated previously (Ivanova *et al.* 2003). Interestingly, the metallopeptidase termed NrpC38, shows 43% homology to NrpB, also termed bacillolysin, a protease involved in the maturation of the PapR signaling peptide of the PapR-PlcR quorum sensing system. In *B. cereus* ATCC14579 and related strains such as *B. cereus* G569, and *B. thuringiensis* 407 Cry$^-$, the QS-

mediating proteins are encoded in direct vicinity: the signaling peptide binding PlcR regulator, the PapR propeptide, and the extracellular propeptide processing protease NprB (Gohar *et al.* 2008; Pomerantsev *et al.* 2009). It is important to note that the PapR-PlcR operon associated NprB protease of F4810/72 is truncated and might be non-functional, and the emetic-like strain ATCC10987 as well as *B. anthracis* strains are devoid of NprB, which indicates that the signal peptide must be processed in a different way. It is tempting to assume that the plasmid-related protease might constitute a signaling peptide processing protein in F4810/72.

Notably, plasmid-curing caused a strong downregulation of two chromosomally encoded surface (S)-layer proteins: EA1 and a Sap-like protein. The existence of an S-layer has not been reported for F4810/72 yet. However, S-layer are only present in a genetically clustered subgroup of *B. cereus* strains exhibiting a close relationship to *B. anthracis* (Mignot *et al.* 2001), which highlights the phylogenetic kinship of F4810/72 and the latter. In *B. anthracis*, the *eag* and *sap* genes are induced and repressed, respectively, by the pXO1-plasmid borne regulator PagR (Mignot *et al.* 2004). Interestingly, pCER270 encodes a PagR-type regulator (BCAH187_C0268), which displays significant (70%) sequence similarity with the *B. anthracis* protein (data not shown). It therefore seems reasonable that the PagR-type protein encoded on pCER270 is necessary to activate S-layer synthesis in F4810/72. In *B. anthracis*, PagR synthesis, in turn, is under control of the main virulence regulator AtxA, encoded on pXO1 (Fouet and Mock 2006). However, F4810/72 lacks an AtxA homolog, which might explain the differential regulation of the tandemly encoded surface proteins in comparison to *B. anthracis*.

In contrast, pCER270-curing led to enhanced expression of several proteases and virulence factors, which are controlled by the PapR-PlcR quorum sensing virulence regulon in the non-emetic *B. cereus*: the metalloendopeptidase NrpP2, enterotoxin Nhe, cereolysin O, phosphatidylcholine-specific phospholipase C, and microbial collagenase (Table 20) (Gohar *et al.* 2008). One might speculate that the elevated expression of PlcR group virulence factors is induced due to a missing plasmid-born repressor that either acts directly to control the transcription of PlcR group genes, or indirectly by controlling PlcR transcription or activity. With the exception of NprP2, only a moderate upregulation of the expression of PlcR regulon proteins was observed (around 2-fold). This might rather indicate an indirect effect on the PlcR regulator, which in turn is repressed by the phosphorylated form of Spo0A. A BLASTP analysis revealed that pCER270 encodes a Rap-Phr system (BCAH187_C0264/5; currently annotated as tetratricopeptide repeat domain protein and hypothetical protein) 90% identical to the pXO1-borne Cot43/BXA0205 system of *B. anthracis*, which affects sporulation and protease secretion by modulating the phosphorylation status of Spo0A (Aronson *et al.* 2005; Bongiorni *et al.* 2006). It seems that BCAH187_C0264/5 is involved in Spo0A phosphorylation control, because biofilm formation is heavily impaired in F4810/72 upon plasmid curing (Lücking 2009), and biofilm formation depends on the phosphorylation status of Spo0A (Banse *et al.* 2008). Likewise, it was recently reported that plasmid curing of *B. subtilis* NCIB3610 leads to reduced biofilm synthesis because of the absence of a plasmid-borne Rap-Phr system: RapP (McLoon *et al.* 2011). In summary, there is strong evidence that BCAH187_C0264/5, now designated as RapP270/Phr270, is one of the phosphatases that jointly control the phosphorylation status of

Spo0A and thus indirectly the secretion of PlcR group proteins. Additionally, this might explain the upregulation of flagellin (Table 20), which harbors a Spo0A consensus sequence in the promoter region. An alignment of plasmid-borne Rap proteins is shown in Figure 37.

```
BCAH187         MIASIKGNEQITKMLNDWYIEIRARHIGKAHKLKLEIDQKIHNIEEDQNLLLYYSLLDFR 60
BAN2012         MIVSVKGNEQITKMLNDWYIEIRARHVGKAHNLKLEIDQKIHNIEEDQNLLLYYALLDFR 60
BSU3610         MKSGVIPSSAVGQKINEWYRYIRTFSVPDAEVLKAEIQQELKHMQHDSNLLLYYSLMEFR 60
                *  .:  .. : : :*:**  **:  : .*. ** **:*:::::::.*.******:*::**

BCAH187         HQYMVDSLSIGKDS-----------FDKVESLEVPADQFLSYYYHFFKAIHSNITGNFTS 109
BAN2012         HQYMLDSLSIGKDS-----------FDKVDSLGVPADQFLQYYYHFFKAIHSNITGDFTS 109
BSU3610         HQLMLDYLEPLEKLNIEDQPSLSELSRNIDSNQADLKGLLDYYVNFFRGMYEFDKREFIS 120
                ** *:* *.  :.              :::*  .  . :*.** :**:.::.  . :* *

BCAH187         AKEHYNKAEELLNHIPDEVEHGEFYFKLSTFHYHIYKPLAAIKEATKAKEIFKKHAGYEA 169
BAN2012         AKEHYNQAELLLKHIPDEIEHAEFRFKLSTFHYHIYKPLAAIKEATKAKDIFKKHAGYET 169
BSU3610         AITYYKQAEKKLSFVADHIERAEFYFKIAEAYYYMKQTYFSLINIKNAYEIYVEQETYNV 180
                *  :*::**  *..:.*.:*:.** **::  :*:: :.  :: : .:* :*: ::  *:.

BCAH187         TIALCDNLIGLACTHLKQFEEAEEHFITAINTFKKSGEEKFITFVRHNLGLMYAGQNLSE 229
BAN2012         NIGLCDNLIGLACTHLKQFEEAEEHFITAINTFKKSGKEKNITFVRHNLGLMYSGQNLSE 229
BSU3610         RIIQCHFVFGVNLMDERNFEQAARHFKLALNMAQAEQKAQLVGRAYYNLGLCYYNQDLLD 240
                 *  *. ::*:   . ::**:* .**  *:*  : . : : :  . :**** * .*:* :

BCAH187         LAIRYLSEVIQELPKD------YKAIFIKAREHMEMGDSEETSNLIDKGLEVCKELKNEE 283
BAN2012         LAIRYLSEVTQELPKD------YKAIFIKAREHMKIGESKETYNLIVKGLEICKELKNEE 283
BSU3610         PAIDYFEKAVSTFESSRIVNSLPQAYFLITLIYYKQGKHDKASEYHKRGYEYAKETDDAD 300
                 ** *:.:. . : ..       :* *: :  : : *. .:: :   :* * .** .: :

BCAH187         YEHHFWILEKLNQKVTADELEKTIKTGISYFERENLHEYVQEYAKKLAVLFHQENNRSKA 343
BAN2012         YEHHFLILEKLNQKVSADELEKTIKTGISYFKRENLHEYVQEYAKKLAVLFHQENNRSKA 343
BSU3610         YAVKFEFLQSLYLDQPN---EEGIERCFQYLKNKNMYADIEDLALEVAKYYYEQKWFKLS 357
                *  :* :*:.*  . .    *: *:  :.*::.:*::  ::: * ::*  :::::  . :

BCAH187         SDYFYLSHQAEEKNFEKEALK---- 364
BAN2012         SDYFYLSHQAEEQNFEKEALK---- 364
BSU3610         ASYFLQVEEARKQIQRSEGLYEIEI 382
                :.**   .:*.::  ..*.*
```

Figure 37: Clustal W alignment of plasmid-born Rap-Phr homologs of *B. cereus* F4810/72 (BCAH187), *B. anthracis* A2012 (BAN2012) and *B. subtilis* NCIB3610 (BSU3610).

The present data indicate that maintenance of pCER270 is more advantageous for F4810/72 than higher expression of virulence factors and other PlcR controlled proteins. This is strengthened by the observation that F4810/72 encodes only one PlcR paralog (data not shown), whereas the non-emetic ATCC14579 encodes three PlcR paralogs that might be activated by the PapR signaling peptide (Ivanova *et al.* 2003). Since pCER270 carries genes for secreted proteins that are highly expressed (Table 20 and Fig. 28A), the RapP270/Phr270 system might temper the synthesis of less beneficial secreted proteins that are chromosomally encoded. Perhaps, this observation is also important to understand the evolution of the proposed incompatibility of the pXO1-related AtxA regulon and the PapR-PlcR regulon in *B. anthracis* strains (see Introduction).

A subset of proteins detected in the "secretome" does not possess a recognisable signal sequence, as is the case for AhpC, AhpF, enolase (Eno), SodA1, and glucose-6-phosphate isomerase (Pgi) (Table 21). These proteins have been previously detected in the extracellular fractions of *B. cereus* and *B. anthracis* proteomes (Antelmann *et al.* 2005; Gohar *et al.* 2005; Chitlaru *et al.* 2006). Several authors speculated that the occurrence was linked to cell lysis of the strains (Antelmann *et al.* 2005; Gohar *et al.* 2008). However, a recent study showed that *B. anthracis* releases bilayered, membrane-derived vesicles, suggesting that besides the common Sec system alternative secretory pathways exist in this organism (Rivera *et al.* 2010). Intriguingly, these vesicles not only contained virulence components such as anthrolysin O, but also enzymes of the central metabolism, including Pgi, Eno, and dihydrolipoamide dehydrogenase. As the latter were observed to be upregulated upon *ces* cluster inactivation (Table 21 and Fig. 28B), it is tempting to speculate that vesicle-shedding was enhanced in the mutant strain. Indeed, *B. cereus* ATCC14579 was found to produce membrane-derived vesicles in a previous study (Dorward and Garon 1990).

By contrast, *ces* cluster inactivation caused the downregulation of a putative lipoprotein that shows similarity to VanW, a protein encoded in vancomycin B-type resistance cassettes of enterococci (Reynolds and Courvalin 2005). The detection of a VanW-related protein has been described in different *B. anthracis* proteome surveys (Antelmann *et al.* 2005; Lamonica *et al.* 2005; Chitlaru *et al.* 2006), but not in *B. cereus* or *B. thuringiensis* studies so far. The biological function of this lipoprotein is unknown, but it seems to be membrane-associated in *B. anthracis* (Chitlaru *et al.* 2006) and is downregulated upon pXO1-curing (Lamonica *et al.* 2005), similar to the downregulation observed in this study. In *B. anthracis*, membrane-associated lipoproteins are linked to oxidative stress resistance and are occasionally part of metal-ion ABC-transporters (Fouet 2009). Thus it is tempting to speculate that the lipoprotein might be anchored in spatial position to the *ces* NRPS, or to the CesCD-ABC-transporter. However, the reason why the VanW-like protein is less expressed upon *ces* cluster inactivation remains puzzling.

Upon inactivation of the *ces* cluster, several enzymes participating in glycolysis/gluconeogenesis and in the TCA cycle were moderately upregulated, indicating that the observed effect was specific and no artifact (Fig. 38). The reason for this upregulation, however, is not readily explained, as removal of the complete plasmid offsets this effect (compare Tables 20 and 21). Nevertheless, for the F48ΔcesP/polar mutant, one might speculate that the backlog of cereulide precursors leads to a dysregulation or redirection of the TCA cycle and the gluconeogenesis/glycolysis pathway, reflecting the tight linkage of cereulide synthesis to the primary metabolism.

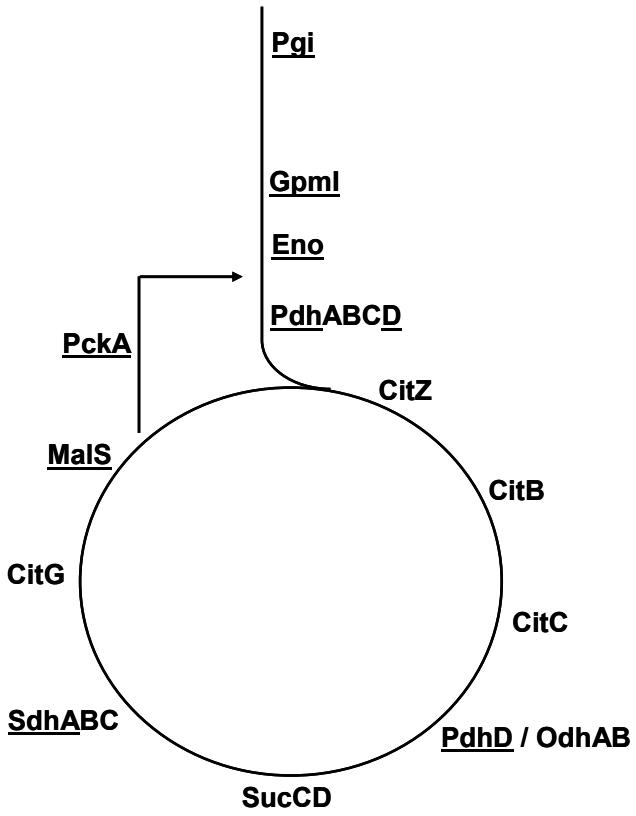

Figure 38: Schematic presentation of proteins upregulated upon *ces* cluster inactivation in *B. cereus* F4810/72 and their embedding in glycolysis/gluconeogenesis and in the TCA cycle. The underlined proteins were identified in a 2-D DIGE analysis comparing the proteomes of *B. cereus* WT and F48ΔcesP/polar (see Ch. 3.6). *Pgi*, glucose-6-phosphate isomerase; *GmpI,* phosphoglyceromutase; *Eno*, enolase; *PhdD*, dihydrolipoamide dehydrogenase, E3 subunit of the pyruvate complex; *CitZ,* citrate synthase; *CitB,* aconitase; *CitC,* isocitrate dehydrogenase; *OdhAB,* 2-oxoglutarate dehydrogenase complex; *SucCD,* succinyl-CoA-synthetase; *SdhA*, membrane-bound A sub-unit of succinate dehydrogenase complex; *CitG,* fumarase; *MalS,* malate dehydrogenase; *PckA*, phosphoenol-pyruvate carboxykinase.

In addition, upon *ces* cluster inactivation, several ROS detoxifying enzymes and dihydrolipoamide moiety containing enzymes were upregulated, whereas the succinate dehydrogenase flavoprotein subunit was downregulated. Interestingly, there seems to be a connection between the expression of NRPS and NRPS/PKS enzymes and oxidative stress resistance, because it was reported that inactivation mutants of *Cochlilobolus heterostrophus*, *Aspergillus fumigatus*, *Anabaena* sp., and *Streptococcus mutans* were (hyper)sensitive towards H_2O_2 stress or accumulated higher amounts of ROS (Oide *et al.* 2006; Reeves *et al.* 2006; Jeanjean *et al.* 2008; Wu *et al.* 2010). As mentioned in Chapter 4.2.2, elevated oxidative stress might arise via enhanced TCA cycle activity, which is in accordance to the observed upregulation of TCA and glycolysis/gluconeogenesis enzymes in the *ces* inactivation mutant (Table 21). Yet, this effect seems to be counterbalanced upon removal of the complete pCER270 plasmid in an unknown fashion. Nevertheless, superoxide dismutase (SodA1) and the alkyl hydroperoxide reductase complex (AhpCF) constitute key enzymes for scavenging and detoxifying reactive oxygen species and were upregulated upon removal of the NRPS multienzyme. Since these enzymes are part of the PerR regulon, which is induced by H_2O_2-mediated PerR-inactivation (Bsat *et al.* 1996) (Ch. 4.2.2), elevated expression is indicative for an elevated ROS level in the *ces* mutant. In light of this observation, it seems that the upregulation of dihydrolipoamide moiety containing enzyme subunits (dihydrolipoamide dehydrogenase subunits of the branched chain α-keto acid dehydrogenase complex [BfmbC], pyruvate dehydrogenase complex [PdhD], and H subunit of the glycine cleavage system [GcvH]) was no coincidence. They can function as radical scavengers, thereby preventing cell

membrane lipid peroxidation by ROS (Suzuki *et al.* 1991; Patel and Hong 1998). These data strengthen the hypothesis that the nonribosomal synthesis of cereulide is influenced by oxidative stress levels and/or the redox balance state of F4810/72 (compare Ch. 4.2.2).

The question remains why two possibly differentially phosphorylated isoforms of succinate dehydrogenase flavoprotein subunit (SdhA) (Levine *et al.* 2006; Eymann *et al.* 2007) are substantially lower expressed upon *ces* cluster inactivation in contrast to upregulation of the remaining core metabolic enzymes. As knowledge on the regulation of the expression of the *sdhA* gene/protein is limited, one can only speculate: In several bacteria including *E. coli*, *Pseudomonas aeruginosa*, *Neisseria meningitidis*, and *B. subtilis*, SdhA expression is posttranscriptionally regulated by translation-inhibition *via* sRNAs (Masse *et al.* 2005; Mellin *et al.* 2007; Gaballa *et al.* 2008). sRNA synthesis is derepressed under iron-limiting conditions due to the inactivation of the iron-binding metalloregulator Fur, a paralog of PerR. It is increasingly recognized that the Fur and PerR regulons partially overlap in controlling metal ion homeostasis and ROS detoxification, since the activity of both protein depends on a bound iron ligand and since the controlled genes encode enzymes that contain iron in their active sites, thus are susceptible to ROS inactivation by a Fenton reaction (Herbig and Helmann 2002; Helmann *et al.* 2003; Mostertz *et al.* 2004). Therefore, it might be assumed that the elevated H_2O_2 stress leads to a sRNA-mediated downregulation of *sdhA* mRNA translation. Besides, the succinate dehydrogenase complex *per se* can generate ROS, as it is the key enzyme for feeding electrons in the respiratory chain and can contribute to a misdirection of electrons to dioxygen (Imlay and Fridovich 1991; Yankovskaya *et al.* 2003; Imlay 2008).

In conclusion, this study shows that the megaplasmid pCER270 is not solely important for cereulide synthesis in the emetic strain F4810/72, but has also an impact on the expression of chromosomally encoded virulence factors, such as the enterotoxin Nhe. pCER270 encodes degradative enzymes and thus is highly likely to be involved in nutrient acquisition. Moreover, pCER270 controls the cell wall architecture (EA1 and SAP S-layer proteins), biofilm formation, flagellum synthesis, and secretion of (virulence) proteins possibly *via* the plasmid-borne RapR-Phr-type quorum sensing regulator, designated RapP270/Phr270. Furthermore, data derived from the targeted *ces* cluster inactivation indicate that the presence of the biosynthetic operon for cereulide synthesis influences the expression of a variety of core metabolic enzymes and oxidative stress responding proteins, underlining the tight embedding of the NRPS in the central metabolism of *B. cereus* F4810/72. The P_1-promoter response in the different genetic backgrounds indicates that there exist i) a NRPS- or ABC transporter-associated self-controlling mechanism and ii) activators or mutually acting repressors of cereulide synthesis, which are plasmid-borne. A tentative comprehensive regulation scheme of all observed phenomena is provided in Figure 39.

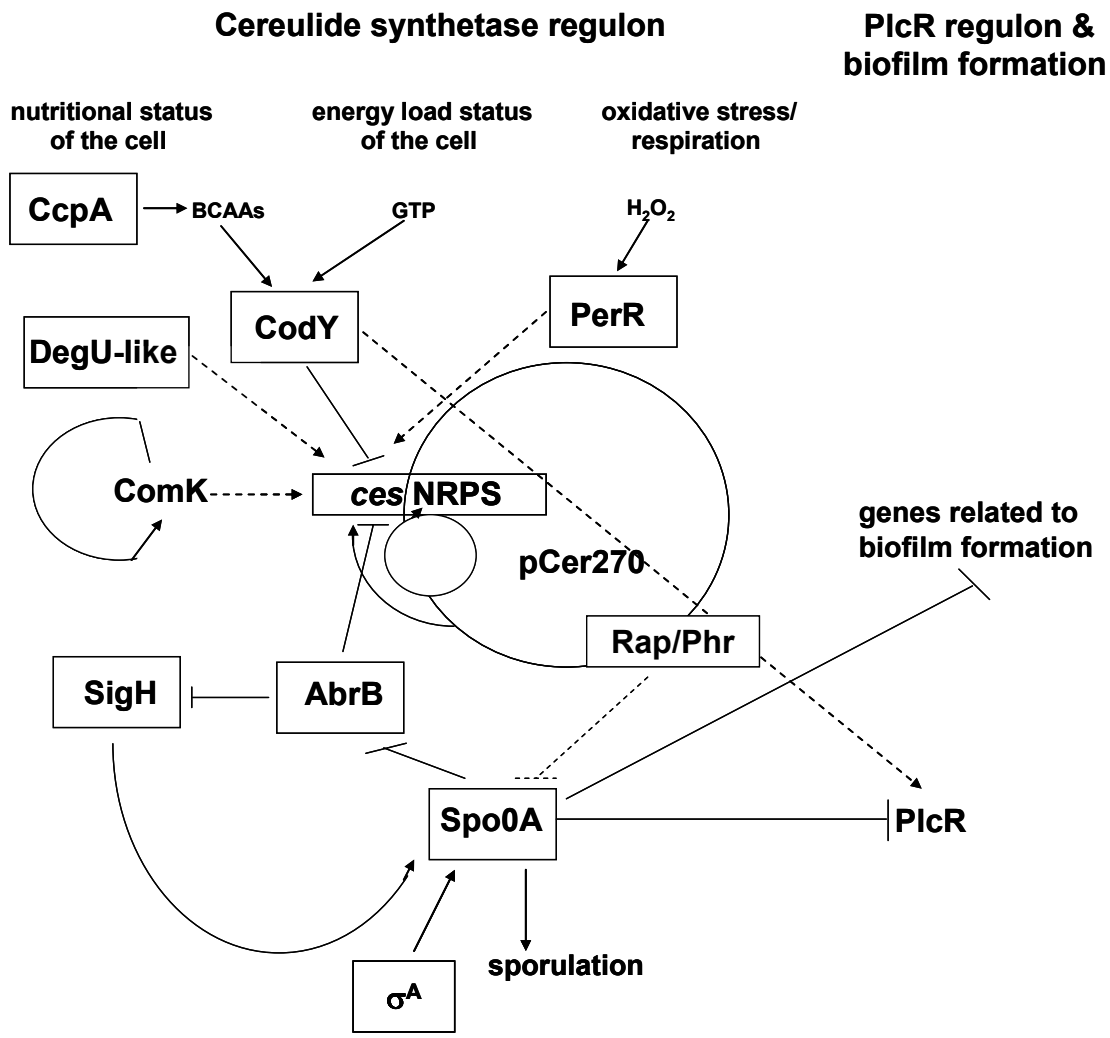

Figure 39: Tentative scheme for the regulation of cereulide synthesis and of PlcR controlled virulence factor expression in emetic *B. cereus*. For details, refer to the text section. Dashed arrows denote that the transcription factors bound *in vitro* to the *ces* promoter area, but that the *in vivo* function must yet be examined by mutagenesis studies. The dashed arrow connecting CodY and PlcR indicates that CodY excerts an indirect activating effect on the PlcR regulon genes. The effect of the plasmid-borne Rap/Phr system on Spo0A activity must be studied in detail.

4.2.5 Cereulide synthesis is a bistable phenomenon

Monitoring of the *ces* promoter activity on a single cell level revealed that only 7 to 16% of the synchronized F4810/72 population initiates cereulide synthesis (or at least expresses the $P_{ces\text{-}gfp}$ reporter; Ch. 3.7). Similar heterogenous, or bistable, expression patterns for antimicrobial compounds have been observed for the NRPS-driven synthesis of surfactin (10% of the *B. subtilis* cells are producers; Lopez *et al.* 2009), and synthesis of colicin K (3% of the *E. coli* cells are producers; Mulec *et al.* 2003).

Per definition, the term bistability denotes the existence of two alternative, stable phenotypes within an isogenic population grown in homogenous environments (Dubnau and Losick 2006). The basis of bistability is stochasticity in gene expression, also termed “noise”, which includes

random fluctuations in the transcription or translation of a protein central to the bistable phenotype, for example a transcriptional regulator (reviewed by Smits *et al.* 2006). The bistable population state commonly arises through the non-linear, amplifying effects of either a positive feedback-loop, or a double-negative feed-back loop (Ferrell 2002). Based on the proposed model for transcriptional regulation of cereulide synthesis (Fig. 36 and Fig. 39), two regulators could be involved in noise generation to establish the mechanistic basis for *ces* gene bistability: Spo0A and ComK. In *B. subtilis*, CodY, PerR and DegU proteins are weak repressors of their own synthesis or are subjected to rapid degradation (Fuangthong *et al.* 2002; Molle *et al.* 2003; Ogura and Tsukahara 2010). However, the latter are likely to provide input signals in the regulatory circuits of cereulide production that might modulate the outcome of feedback-based multistability.

Recently, three independent studies on sporulation heterogeneity in *B. subtilis* populations came to the conclusion that the autostimulatory transcription of *spo0A* is not the basis of bistable sporulation patterns, but rather the autostimulatory architecture of the complex sporulation phosphorelay that involves several kinases, phosphotransferases, and phosphatases (Veening *et al.* 2008; Chastanet *et al.* 2010; de Jong *et al.* 2010). The highly dynamic gene expression as well as the phosphate flux through the relay generates noise in the accumulation of Spo0A~P, which results in heterogenous cellular states with respect to the progression of sporulation (Chastanet *et al.* 2010; de Jong *et al.* 2010). These variances in Spo0A phosphorylation might be a cause of bimodal NRPS expression, because Spo0A~P blocks AbrB expression (Lücking *et al.* 2009). This would furthermore explain why the moderate GFP signal was detected in cells of different developmental states, since repression of *abrB* depends on the early, σ^A-promoted Spo0A expression (Lücking *et al.* 2009) and on low Spo0A~P levels (Perego *et al.* 1988), whereas the cell fate for sporulation is decided in later phases of the cell cycle by higher Spo0A~P concentrations (Fujita *et al.* 2005).

During this study, it was observed that GFP-ON cells were often associated in cell chains (Fig. 33). A similar phenomenon in *B. subtilis* led to the theory that the decision to sporulate is inherited over several cell divisions, and is therefore epigenetically programmed (Veening *et al.* 2008). As the scale of cereulide production of F4810/72 is dependent on the history of the cell inoculum (Dommel *et al.* 2011), it is tempting to speculate that a specialized population lineage "remembers" its task to produce the ionophor.

Bistability has also been extensively studied with respect to the development of natural competence in *B. subtilis* (Maamar and Dubnau 2005; Smits *et al.* 2005; Leisner *et al.* 2007; Leisner *et al.* 2008). During transition to the stationary phase, 10-20% of the cells accumulate ComK above a critical threshold level and enter a semidormant vegetative K-state, allowing the uptake of exogenous nucleic acids (Maamar and Dubnau 2005). By using a *comK-gfp* reporter, Maamar and Dubnau observed the existence of three fluorescence classes, similar to the high, intermediate and non expressing cells detected in this study (Fig. 31 and Fig. 32). It was discussed that the intermediate cell fraction either enters the high expressing state, or represents a distinct subgroup (Maamar and Dubnau 2005). Thus, competence development and cereulide expression might be more complex than a dual model would assume. However, the F4810/72

ComK protein obviously acts autostimulatory (Ch. 3.4.2) and qPCR analysis revealed that *comK* mRNA levels are highest during mid- to late exponential growth (Frenzel, unpublished data), similar to the kinetics of *ces* gene transcription. It seems thus possible that ComK triggers the phenotypic heterogeneity. Finally, this would imply that cereulide producing cells simultaneously enter the competence state and this would fit the observation that the majority of $P_{cesP\text{-}gfp}$ ON cells did not sporulate (Fig. 33).

On this basis and by analogy to the bistable surfactin synthesis that is used for intercellular signaling, the following biological function for cereulide might be assumed: In *B. subtilis*, the potassium ionophor surfactin acts as a signaling molecule that causes ion leakage in a subpopulation of surfactin-responsive cells, all of them surfactin non-producers, which then triggers the production of an extracellular matrix (Lopez and Kolter 2010). Since cereulide, like surfactin, is a potassium ionophore, it might also induce the cellular differentiation of a subpopulation to produce a biofilm matrix (Fig. 40). Moreover, it was recently shown that cereulide acts bacteriolytic and has antifungal activity (Ladeuze *et al.* 2011; Tempelaars *et al.* 2011). Therefore, it might be possible that DNA is shed into the biofilm, which is a matrix that promotes the uptake of exogenous DNA relased by lysing siblings or competitors (Spoering and Gilmore 2006). The high ComK levels in the cereulide producing cells concomitantly induce the expression of DNA-uptake and –integration machineries. Thus, it is tempting to speculate that cereulide synthesis, biofilm formation and DNA uptake are interconnected phernomena in emetic *B. cereus*, which are activated in distinct cellular subpopulations.

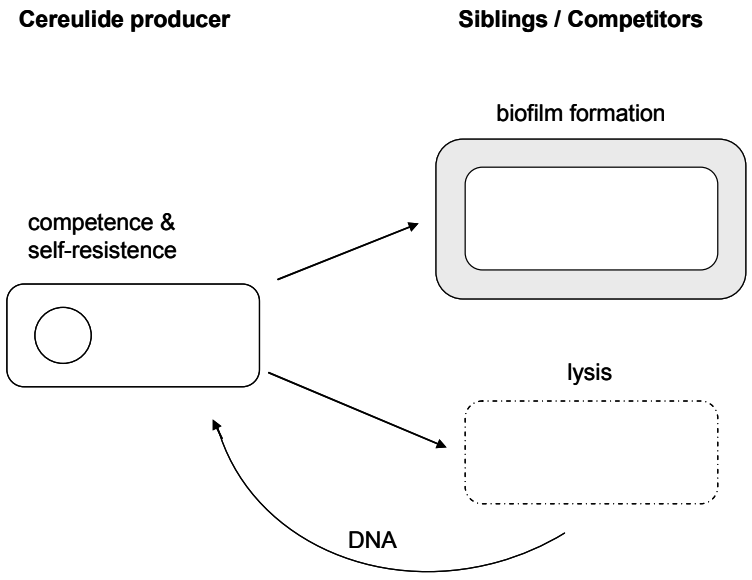

Figure 40: Tentative scheme for a connection between competence development and cereulide synthesis in emetic *B. cereus*. A subpopulation initiates cereulide synthesis and enters the natural competence state, thereby expressing genes for DNA uptake and integration. These cells are resistent against cereulide, since they concomitantly express the CesCD ABC-transporter that might serve as an efflux system. As is the case of surfactin-induced multicellularity in *B. subtilis* (Lopez and Kolter 2010), the potassium ionophor cereulide could trigger biofilm synthesis in a different *B. cereus* subpopulation and cause the lysis of siblings and/or competitors, that do not express the *ces* cluster genes. In the biofilm matrix, the released exogenous DNA is taken up by the cereulide producing subpopulation.

However, several aspects of these hypotheses need to be studied in greater detail before a firm conclusion can be drawn. Nonetheless, the data presented here show that cereulide synthesis is not initiated uniformly under the chosen conditions. This might -at least partially- be a reason for the existence of low, medium and high cereulide producing *B. cereus* strains: As emetic strains do not exhibit nucleotide polymorphisms in the *ces* promoter region or in the primary sequence of the NRPS encoding genes (Dommel 2008; Dommel *et al.* 2011), their differing toxigenic potentials might be based on different noise levels of transcription factors controlling *ces* gene expression. This finding might contitute a basis for the differentiation of low and highly virulent emetic *B. cereus* strains in the future.

5 Concluding Remarks and Perspectives

This study revealed that the biosynthesis of cereulide in emetic *B. cereus* is governed by a highly complex network involving intrinsic as well as extrinsic factors. It was shown that environmental stimuli, such as the food matrix and food additives, profoundly influence the activity of the cereulide synthetase promoter and the level of toxin synthesis. The elucidation of how the extrinsic signals are sensed (for example by deletion studies of two-component systems) and become integrated on a transcriptional level will be an important step to unravel the varying potentials of different types of food to promote toxin production. The data presented in this work provide a first hint that the pleiotropic transcriptional regulator CodY acts as a molecular connector between the plasmid-borne, nonribosomal toxin synthesis and the primary metabolism. This sensor of the metabolic and energetic cell status was furthermore found to play a key role in the overall pathogenicity of *B. cereus* by repressing *ces* gene expression and by activating the synthesis of medically important enterotoxins, which were formerly thought to be controlled by independent regulatory circuitries. An in-depths analysis of the CodY regulon, for instance by microarrays, proteomic surveys, and *via* identification of small regulatory RNAs, would provide imporant insights into the mechanisms causing a partial congruency of the CodY and PlcR virulence regulons.

The preliminary conceptual framework developed for transcriptional control of cereulide synthetase gene expression (Fig. 36) should facilitate future investigations on the *in vivo* contribution of single regulators and environmental cues to the toxin synthesis network. However, the single-cell approach employed in this thesis emphasis that averaging techniques, such as qPCR, cannot capture physiological cell heterogeneity, which possibly leads to a non-consideration of important clues. For instance, different noise levels of bistability-generating transcription factors seem to be a promising idea of how highly and low toxigenic cereulide producing strains might arise. Currently, flow cytometry and mathematic modeling of cellular networks are two methods of choice to study stochastic fluctuation dynamics in (virulence) gene expression (Rao *et al.* 2002; Smits *et al.* 2006). Thus, flow cytometry studies with additional *gfp*-tagged emetic strains might be a promising tool for providing insight into the molecular heterogeneity of toxin synthesis, which is of high importance to improve the knowledge on the development of human pathogenicity in emetic *B. cereus* and is further important with respect to food safety issues. However, since the metabolic cell status, such as the polyP/P_i ratio and branched-chain amino acids levels, profoundly influence cereulide synthesis, it might be further interesting to compare the metabolomes and metabolic capacity of low and high cereulide producers. Metabolic fingerprinting studies might be conducted to assess whether certain (groups of) metabolites can be traced back to highly virulent emetic strains. Vice versa, this might allow a conclusion on key metabolic intermediates that, for instance, act as ligands of central transcriptional regulators of toxin synthesis and in turn affect the highly complex cereulide biosynthesis network.

6 References

Abee, T., Groot, M. N., Tempelaars, M., Zwietering, M., Moezelaar, R. and van der Voort, M. (2011). Germination and outgrowth of spores of *Bacillus cereus* group members: diversity and role of germinant receptors. Food Microbiol 28(2): 199-208.

Agata, N., Mori, M., Ohta, M., Suwan, S., Ohtani, I. and Isobe, M. (1994). A novel dodecadepsipeptide, cereulide, isolated from *Bacillus cereus* causes vacuole formation in HEp-2 cells. FEMS Microbiol Lett 121(1): 31 - 34.

Agata, N., Ohta, M., Mori, M. and Isobe, M. (1995). A novel dodecadepsipeptide, cereulide, is an emetic toxin of *Bacillus cereus*. FEMS Microbiol Lett 129(1): 17-20.

Agata, N., Ohta, M. and Yokoyama, K. (2002). Production of *Bacillus cereus* emetic toxin (cereulide) in various foods. Int J Food Microbiol 73(1): 23-27.

Akhtar, S., Paredes-Sabja, D. and Sarker, M. R. (2008). Inhibitory effects of polyphosphates on *Clostridium perfringens* growth, sporulation and spore outgrowth. Food Microbiol 25(6): 802-808.

Altschul, S., Madden, T., Schaffer, A., Zhang, J., Zhang, Z., Miller, W. and Lipman, D. (1997). Gapped BLAST and PSI-BLAST: a new generation of protein database search programs. Nucleic Acids Res 25(17): 3389 - 3402.

Altschul, S. F., Gish, W., Miller, W., Myers, E. W. and Lipman, D. J. (1990). Basic local alignment search tool. J Mol Biol 215(3): 403-10.

Altschul, S. F., Madden, T. L., Schaffer, A. A., Zhang, J., Zhang, Z., Miller, W. and Lipman, D. J. (1997). Gapped BLAST and PSI-BLAST: a new generation of protein database search programs. Nucleic Acids Res 25(17): 3389 - 3402.

Andersson, A., Ronner, U. and Granum, P. E. (1995). What problems does the food industry have with the spore-forming pathogens *Bacillus cereus* and *Clostridium perfringens*? Int J Food Microbiol 28(2): 145-155.

Andersson, M. A., Hakulinen, P., Honkalampi-Hamalainen, U., Hoornstra, D., Lhuguenot, J. C., Maki-Paakkanen, J., Savolainen, M., Severin, I., Stammati, A. L., Turco, L., Weber, A., von Wright, A., Zucco, F. and Salkinoja-Salonen, M. (2007). Toxicological profile of cereulide, the *Bacillus cereus* emetic toxin, in functional assays with human, animal and bacterial cells. Toxicon 49(3): 351-367.

Andersson, M. A., Jaaskelainen, E. L., Shaheen, R., Pirhonen, T., Wijnands, L. M. and Salkinoja-Salonen, M. S. (2004). Sperm bioassay for rapid detection of cereulide-producing *Bacillus cereus* in food and related environments. Int J Food Microbiol 94(2): 175-83.

Anonymous (2005). Opinion of the Scientific Panel on Biological Hazards on *Bacillus cereus* and other *Bacillus* spp. in foodstuffs. The EFSA Journal 175: 1-48.

Anonymous (2009). The Community Summary Report on Food-borne Outbreaks in the European Union in 2007. The EFSA Journal 271: 1-128.

Anonymous (2009). Joint FAO/WHO food standards programme. Codex Alimentarius Commission, Rome, Italy. http://www.who.int/foodsafety/codex/en/.

Anonymous (2010). The Community Summary Report on Trends and Sources of Zoonoses, Zoonotic Agents and food-borne outbreaks in the European Union in 2008. The EFSA Journal 8: 283-297.

Antelmann, H., Williams, R. C., Miethke, M., Wipat, A., Albrecht, D., Harwood, C. R. and Hecker, M. (2005). The extracellular and cytoplasmic proteomes of the non-virulent *Bacillus anthracis* strain UM23C1-2. Proteomics 5(14): 3684-3695.

Apetroaie, C., Andersson, M. A., Sproer, C., Tsitko, I., Shaheen, R., Jaaskelainen, E. L., Wijnands, L. M., Heikkila, R. and Salkinoja-Salonen, M. S. (2005). Cereulide-producing strains of *Bacillus cereus* show diversity. Arch Microbiol 184(3): 141-51.

Aronson, A. I., Bell, C. and Fulroth, B. (2005). Plasmid-encoded regulator of extracellular proteases in *Bacillus anthracis*. J Bacteriol 187(9): 3133-8.

Aronson, A. I. and Shai, Y. (2001). Why *Bacillus thuringiensis* insecticidal toxins are so effective: unique features of their mode of action. FEMS Microbiol Lett 195(1): 1-8.

Ash, C., Farrow, J. A., Dorsch, M., Stackebrandt, E. and Collins, M. D. (1991). Comparative analysis of *Bacillus anthracis*, *Bacillus cereus*, and related species on the basis of reverse transcriptase sequencing of 16S rRNA. Int J Syst Bacteriol 41(3): 343-346.

Ausubel, F. M., Brent, R., Kingston, R. E., Moore, D. D., Seidmann, J. G., Smith, J. A. and Struhl, K. (1987). Current Protocols in Molecular Biology (ed. Ausubel, F. M.). New York, John Wiley & Sons.

Banse, A. V., Chastanet, A., Rahn-Lee, L., Hobbs, E. C. and Losick, R. (2008). Parallel pathways of repression and antirepression governing the transition to stationary phase in *Bacillus subtilis*. Proc Natl Acad Sci U S A 105(40): 15547-15552.

Barbe, V., Cruveiller, S., Kunst, F., Lenoble, P., Meurice, G., Sekowska, A., Vallenet, D., Wang, T., Moszer, I., Medigue, C. and Danchin, A. (2009). From a consortium sequence to a unified sequence: the *Bacillus subtilis* 168 reference genome a decade later. Microbiology 155(Pt 6): 1758-75.

Becker, B. (2005). Milchindustrie. p. 71-72. *In* Pathogene Mikroorganismen: *Bacillus cereus*. B. Becker (ed.), B. Behr´s Verlag GmbH Co. KG, Hamburg.

Becker, B. (2005). Richt- und Warnwerte. p. 77-80. *In* Pathogene Mikroorganismen: *Bacillus cereus*. B. Becker (ed.), B. Behr´s Verlag GmbH Co. KG, Hamburg.

Becker, H., Schaller, G., von Wiese, W. and Terplan, G. (1994). *Bacillus cereus* in infant foods and dried milk products. Int J Food Microbiol 23(1): 1-15.

Beecher, D. J. and Macmillan, J. D. (1991). Characterization of the components of hemolysin BL from *Bacillus cereus*. Infect Immun 59(5): 1778-1784.

Beecher, D. J., Olsen, T. W., Somers, E. B. and Wong, A. C. (2000). Evidence for contribution of tripartite hemolysin BL, phosphatidylcholine-preferring phospholipase C, and collagenase to virulence of *Bacillus cereus* endophthalmitis. Infect Immun 68(9): 5269-5276.

Beecher, D. J. and Wong, A. C. (2000). Cooperative, synergistic and antagonistic haemolytic interactions between haemolysin BL, phosphatidylcholine phospholipase C and sphingomyelinase from *Bacillus cereus*. Microbiology 146 Pt 12: 3033-3039.

Beier, D. and Gross, R. (2006). Regulation of bacterial virulence by two-component systems. Curr Opin Microbiol 9(2): 143-152.

Belitsky, B. R. and Sonenshein, A. L. (2008). Genetic and biochemical analysis of CodY-binding sites in *Bacillus subtilis*. J Bacteriol 190(4): 1224-36.

Belitsky, B. R. and Sonenshein, A. L. (2011). Contributions of multiple binding sites and effector-independent binding to CodY-mediated regulation in *Bacillus subtilis*. J Bacteriol 193(2): 473-84.

Bendtsen, J. D., Nielsen, H., von Heijne, G. and Brunak, S. (2004). Improved prediction of signal peptides: SignalP 3.0. J Mol Biol 340(4): 783-795.

Berry, C., O'Neil, S., Ben-Dov, E., Jones, A. F., Murphy, L., Quail, M. A., Holden, M. T., Harris, D., Zaritsky, A. and Parkhill, J. (2002). Complete sequence and organization of pBtoxis, the toxin-coding plasmid of *Bacillus thuringiensis* subsp. *israelensis*. Appl Environ Microbiol 68(10): 5082-5095.

Bongiorni, C., Stoessel, R., Shoemaker, D. and Perego, M. (2006). Rap phosphatase of virulence plasmid pXO1 inhibits *Bacillus anthracis* sporulation. J Bacteriol 188(2): 487-98.

Bottone, E. J. (2010). *Bacillus cereus*, a volatile human pathogen. Clin Microbiol Rev 23(2): 382-398.

Brinsmade, S. R., Kleijn, R. J., Sauer, U. and Sonenshein, A. L. (2010). Regulation of CodY activity through modulation of intracellular branched-chain amino acid pools. J Bacteriol 192(24): 6357-6368.

Bsat, N., Chen, L. and Helmann, J. D. (1996). Mutation of the *Bacillus subtilis* alkyl hydroperoxide reductase (*ahpCF*) operon reveals compensatory interactions among hydrogen peroxide stress genes. J Bacteriol 178(22): 6579-6586.

Caboche, S., Leclere, V., Pupin, M., Kucherov, G. and Jacques, P. (2010). Diversity of monomers in nonribosomal peptides: towards the prediction of origin and biological activity. J Bacteriol 192(19): 5143-5150.

Caboche, S., Pupin, M., Leclere, V., Fontaine, A., Jacques, P. and Kucherov, G. (2008). NORINE: a database of nonribosomal peptides. Nucleic Acids Res 36: D326-331.

Cadot, C., Tran, S. L., Vignaud, M. L., De Buyser, M. L., Kolsto, A. B., Brisabois, A., Nguyen-The, C., Lereclus, D., Guinebretiere, M. H. and Ramarao, N. (2010). InhA1, NprA, and HlyII as candidates for markers to differentiate pathogenic from nonpathogenic *Bacillus cereus* strains. J Clin Microbiol 48(4): 1358-1365.

Callegan, M. C., Cochran, D. C., Kane, S. T., Gilmore, M. S., Gominet, M. and Lereclus, D. (2002). Contribution of membrane-damaging toxins to *Bacillus* endophthalmitis pathogenesis. Infect Immun 70(10): 5381-5389.

Carlin, F., Fricker, M., Pielaat, A., Heisterkamp, S., Shaheen, R., Salonen, M. S., Svensson, B., Nguyen-the, C. and Ehling-Schulz, M. (2006). Emetic toxin-producing strains of *Bacillus cereus* show distinct characteristics within the *Bacillus cereus* group. Int J Food Microbiol 109(1-2): 132-138.

Chambert, R. and Petit-Glatron, M. F. (1999). Anionic polymers of *Bacillus subtilis* cell wall modulate the folding rate of secreted proteins. FEMS Microbiol Lett 179(1): 43-47.

Chastanet, A., Vitkup, D., Yuan, G. C., Norman, T. M., Liu, J. S. and Losick, R. M. (2010). Broadly heterogeneous activation of the master regulator for sporulation in *Bacillus subtilis*. Proc Natl Acad Sci U S A 107(18): 8486-8491.

Chaudhuri, R. R., Loman, N. J., Snyder, L. A., Bailey, C. M., Stekel, D. J. and Pallen, M. J. (2008). xBASE2: a comprehensive resource for comparative bacterial genomics. Nucleic Acids Res 36(Database issue): D543-6.

Chitlaru, T., Gat, O., Gozlan, Y., Ariel, N. and Shafferman, A. (2006). Differential proteomic analysis of the *Bacillus anthracis* secretome: distinct plasmid and chromosome CO2-dependent cross talk mechanisms modulate extracellular proteolytic activities. J Bacteriol 188(10): 3551-3571.

Chothia, C. and Lesk, A. M. (1986). The relation between the divergence of sequence and structure in proteins. The EMBO Journal 5(4): 823-826.

Christiansson, A., Naidu, A. S., Nilsson, I., Wadstrom, T. and Pettersson, H. E. (1989). Toxin production by *Bacillus cereus* dairy isolates in milk at low temperatures. Appl Environ Microbiol 55(10): 2595-2600.

Chung, M. C., Popova, T. G., Millis, B. A., Mukherjee, D. V., Zhou, W., Liotta, L. A., Petricoin, E. F., Chandhoke, V., Bailey, C. and Popov, S. G. (2006). Secreted neutral metalloproteases of *Bacillus anthracis* as candidate pathogenic factors. J Biol Chem 281(42): 31408-31418.

Cormack, B. P., Valdivia, R. H. and Falkow, S. (1996). FACS-optimized mutants of the green fluorescent protein (GFP). Gene 173(1): 33-38.

D'Souza, C., Nakano, M. M. and Zuber, P. (1994). Identification of *comS*, a gene of the *srfA* operon that regulates the establishment of genetic competence in *Bacillus subtilis*. Proc Natl Acad Sci U S A 91(20): 9397-9401.

Dahl, J. L., Kraus, C. N., Boshoff, H. I., Doan, B., Foley, K., Avarbock, D., Kaplan, G., Mizrahi, V., Rubin, H. and Barry, C. E., 3rd (2003). The role of RelMtb-mediated adaptation to stationary phase in long-term persistence of *Mycobacterium tuberculosis* in mice. Proc Natl Acad Sci U S A 100(17): 10026-10031.

de Jong, I. G., Veening, J. W. and Kuipers, O. P. (2010). Heterochronic phosphorelay gene expression as a source of heterogeneity in *Bacillus subtilis* spore formation. J Bacteriol 192(8): 2053-2067.

Declerck, N., Bouillaut, L., Chaix, D., Rugani, N., Slamti, L., Hoh, F., Lereclus, D. and Arold, S. T. (2007). Structure of PlcR: Insights into virulence regulation and evolution

of quorum sensing in Gram-positive bacteria. Proc Natl Acad Sci U S A 104(47): 18490-18495.

den Hengst, C. D., Curley, P., Larsen, R., Buist, G., Nauta, A., van Sinderen, D., Kuipers, O. P. and Kok, J. (2005). Probing direct interactions between CodY and the *oppD* promoter of *Lactococcus lactis*. J Bacteriol 187(2): 512-521.

den Hengst, C. D., van Hijum, S. A., Geurts, J. M., Nauta, A., Kok, J. and Kuipers, O. P. (2005). The *Lactococcus lactis* CodY regulon: identification of a conserved cis-regulatory element. J Biol Chem 280(40): 34332-34342.

Di Franco, C., Beccari, E., Santini, T., Pisaneschi, G. and Tecce, G. (2002). Colony shape as a genetic trait in the pattern-forming *Bacillus mycoides*. BMC Microbiol 2: 33.

Didelot, X., Barker, M., Falush, D. and Priest, F. G. (2009). Evolution of pathogenicity in the *Bacillus cereus* group. Syst Appl Microbiol 32(2): 81-90.

Dieckmann, R., Neuhof, T., Pavela-Vrancic, M. and von Dohren, H. (2001). Dipeptide synthesis by an isolated adenylate-forming domain of non- ribosomal peptide synthetases (NRPS). FEBS Lett 498(1): 42-45.

Dierick, K., Van Coillie, E., Swiecicka, I., Meyfroidt, G., Devlieger, H., Meulemans, A., Hoedemaekers, G., Fourie, L., Heyndrickx, M. and Mahillon, J. (2005). Fatal family outbreak of *Bacillus cereus*-associated food poisoning. J Clin Microbiol 43(8): 4277 - 4279.

Dietrich, R., Fella, C., Strich, S. and Märtlbauer, E. (1999). Production and characterization of monoclonal antibodies against the hemolysin BL enterotoxin complex produced by *Bacillus cereus*. Appl Environ Microbiol 65(10): 4470-4474.

Dineen, S. S., McBride, S. M. and Sonenshein, A. L. (2010). Integration of metabolism and virulence by *Clostridium difficile* CodY. J Bacteriol 192(20): 5350-5362.

Dineen, S. S., Villapakkam, A. C., Nordman, J. T. and Sonenshein, A. L. (2007). Repression of *Clostridium difficile* toxin gene expression by CodY. Mol Microbiol 66(1): 206-219.

Dommel, M. K. (2008). Molecular characterization of the genetic locus responsible for cereulide toxin production in emetic *Bacillus cereus*. PhD thesis, Technische Universität München.

Dommel, M. K., Frenzel, E., Strasser, B., Blöchinger, C., Scherer, S. and Ehling-Schulz, M. (2010). Identification of the main promoter directing cereulide biosynthesis in emetic *Bacillus cereus* and its application for real-time monitoring of *ces* gene expression in foods. Appl Environ Microbiol 76(4): 1232-1240.

Dommel, M. K., Lücking, G., Scherer, S. and Ehling-Schulz, M. (2011). Transcriptional kinetic analyses of cereulide synthetase genes with respect to growth, sporulation and emetic toxin production in *Bacillus cereus*. Food Microbiol 28(2): 284-290.

Dorward, D. W. and Garon, C. F. (1990). DNA is packaged within membrane-derived vesicles of Gram-negative but not Gram-positive bacteria. Appl Environ Microbiol 56(6): 1960-1962.

Drobniewski, F. A. (1993). *Bacillus cereus* and related species. Clin Microbiol Rev 6(4): 324-338.

Duarte, V. and Latour, J. M. (2010). PerR vs OhrR: selective peroxide sensing in *Bacillus subtilis*. Mol Biosyst 6(2): 316-323.

Dubnau, D. and Losick, R. (2006). Bistability in bacteria. Mol Microbiol 61(3): 564-572.

Duc, L. H., Dong, T. C., Logan, N. A., Sutherland, A. D., Taylor, J. and Cutting, S. M. (2005). Cases of emesis associated with bacterial contamination of an infant breakfast cereal product. Int J Food Microbiol 102(2): 245-251.

Duitman, E. H., Wyczawski, D., Boven, L. G., Venema, G., Kuipers, O. P. and Hamoen, L. W. (2007). Novel methods for genetic transformation of natural *Bacillus subtilis* isolates used to study the regulation of the mycosubtilin and surfactin synthetases. Appl Environ Microbiol 73(11): 3490-3496.

Dunn, A. K. and Handelsman, J. (1999). A vector for promoter trapping in *Bacillus cereus*. Gene 226(2): 297-305.

Duport, C., Zigha, A., Rosenfeld, E. and Schmitt, P. (2006). Control of enterotoxin gene expression in *Bacillus cereus* F4430/73 involves the redox-sensitive ResDE signal transduction system. J Bacteriol 188(18): 6640-6651.

Durfee, T., Nelson, R., Baldwin, S., Plunkett, G., 3rd, Burland, V., Mau, B., Petrosino, J. F., Qin, X., Muzny, D. M., Ayele, M., Gibbs, R. A., Csorgo, B., Posfai, G., Weinstock, G. M. and Blattner, F. R. (2008). The complete genome sequence of *Escherichia coli* DH10B: insights into the biology of a laboratory workhorse. J Bacteriol 190(7): 2597-606.

Ehling-Schulz, M., Fricker, M., Grallert, H., Rieck, P., Wagner, M. and Scherer, S. (2006). Cereulide synthetase gene cluster from emetic *Bacillus cereus*: structure and location on a mega virulence plasmid related to *Bacillus anthracis* toxin plasmid pXO1. BMC Microbiol 6: 20.

Ehling-Schulz, M., Fricker, M. and Scherer, S. (2004). *Bacillus cereus*, the causative agent of an emetic type of food-borne illness. Mol Nutr Food Res 48(7): 479-487.

Ehling-Schulz, M., Fricker, M. and Scherer, S. (2004). Identification of emetic toxin producing *Bacillus cereus* strains by a novel molecular assay. FEMS Microbiol Lett 232(2): 189-195.

Ehling-Schulz, M., Guinebretiere, M.-H., Monthan, A., Berge, O., Fricker, M. and Svensson, B. (2006). Toxin gene profiling of enterotoxic and emetic *Bacillus cereus*. FEMS Microbiology Letters 260(2): 232-240.

Ehling-Schulz, M., Knutsson, R. and Scherer, S. (2011). *Bacillus cereus*. p. 147-164. *In* P. Fratamico, Y. Liu, and S. Kathariou (eds), Genomes of Foodborne and Waterborne Pathogens. ASM Press, Washington, D.C.

Ehling-Schulz, M., Messelhäusser, U. and Granum, P. E. (2011). *Bacillus cereus* in milk and dairy products. p. 275-289. *In* J. Hoorfar (ed), Rapid Detection, Identification, and Quantification of Foodborne Pathogens. ASM Press, Washington, D.C.

Ehling-Schulz, M., Svensson, B., Guinebretiere, M. H., Lindbäck, T., Andersson, M., Schulz, A., Fricker, M., Christiansson, A., Granum, P. E., Märtlbauer, E., Nguyen-The, C., Salkinoja-Salonen, M. and Scherer, S. (2005). Emetic toxin formation of *Bacillus cereus* is restricted to a single evolutionary lineage of closely related strains. Microbiology 151(Pt 1): 183-197.

Ehling-Schulz, M., Vukov, N., Schulz, A., Shaheen, R., Andersson, M., Märtlbauer, E. and Scherer, S. (2005). Identification and partial characterization of the nonribosomal peptide synthetase gene responsible for cereulide production in emetic *Bacillus cereus*. Appl Environ Microbiol 71(1): 105-113.

Essen, R., de Ruiter, C. and de Wit, M. (2000). Massale voedselvergiftiging in het Kotterbos te Almere. Infectieziekten Bulletin 11: 205-207.

Eymann, C., Becher, D., Bernhardt, J., Gronau, K., Klutzny, A. and Hecker, M. (2007). Dynamics of protein phosphorylation on Ser/Thr/Tyr in *Bacillus subtilis*. Proteomics 7(19): 3509-3526.

Fagerlund, A., Brillard, J., Furst, R., Guinebretiere, M.-H. and Granum, P. (2007). Toxin production in a rare and genetically remote cluster of strains of the *Bacillus cereus* group. BMC Microbiol 7(1): 43.

Ferrell, J. E., Jr. (2002). Self-perpetuating states in signal transduction: positive feedback, double-negative feedback and bistability. Curr Opin Cell Biol 14(2): 140-148.

Fink, P. S. (1993). Biosynthesis of the branched-chain amino acids, p.307-317. *In* A.L. Sonenshein, J.A. Hoch, R. Losick (eds), *Bacillus subtilis* and other gram-positive bacteria: biochemistry, physiology, and molecular genetics. 1st ed. ASM Press, Washington, D.C.

Finking, R. and Marahiel, M. A. (2004). Biosynthesis of nonribosomal peptides. Annu Rev Microbiol 58: 453-488.

Finlay, W. J., Logan, N. A. and Sutherland, A. D. (1999). Semiautomated metabolic staining assay for *Bacillus cereus* emetic toxin. Appl Environ Microbiol 65(4): 1811-1812.

Finlay, W. J., Logan, N. A. and Sutherland, A. D. (2002). *Bacillus cereus* emetic toxin production in relation to dissolved oxygen tension and sporulation. Food Microbiol 19(5): 423-430.

Fouet, A. (2009). The surface of *Bacillus anthracis*. Mol Aspects Med 30(6): 374-385.

Fouet, A. and Mock, M. (2006). Regulatory networks for virulence and persistence of *Bacillus anthracis*. Curr Opin Microbiol 9(2): 160-166.

Francis, K. P., Joh, D., Bellinger-Kawahara, C., Hawkinson, M. J., Purchio, T. F. and Contag, P. R. (2000). Monitoring bioluminescent *Staphylococcus aureus* infections in living mice using a novel *luxABCDE* construct. Infect Immun 68(6): 3594-3600.

Frenzel, E., Letzel, T., Scherer, S. and Ehling-Schulz, M. (2011). Inhibition of cereulide toxin synthesis by emetic *Bacillus cereus* via long-chain polyphosphates. Appl Environ Microbiol 77(4): 1475-1482.

Fricker, M., Messelhausser, U., Busch, U., Scherer, S. and Ehling-Schulz, M. (2007). Diagnostic real-time PCR assays for the detection of emetic *Bacillus cereus* strains in foods and recent food-borne outbreaks. Appl Environ Microbiol 73(6): 1892-1898.

Fuangthong, M., Herbig, A. F., Bsat, N. and Helmann, J. D. (2002). Regulation of the *Bacillus subtilis fur* and *perR* genes by PerR: not all members of the PerR regulon are peroxide inducible. J Bacteriol 184(12): 3276-3286.

Fujita, M., Gonzalez-Pastor, J. E. and Losick, R. (2005). High- and low-threshold genes in the Spo0A regulon of *Bacillus subtilis*. J Bacteriol 187(4): 1357-1368.

Gaballa, A., Antelmann, H., Aguilar, C., Khakh, S. K., Song, K. B., Smaldone, G. T. and Helmann, J. D. (2008). The *Bacillus subtilis* iron-sparing response is mediated by a Fur-regulated small RNA and three small, basic proteins. Proc Natl Acad Sci U S A 105(33): 11927-11932.

Galvez, A., Abriouel, H., Lopez, R. L. and Ben Omar, N. (2007). Bacteriocin-based strategies for food biopreservation. Int J Food Microbiol 120(1-2): 51-70.

Gharahdaghi, F., Weinberg, C. R., Meagher, D. A., Imai, B. S. and Mische, S. M. (1999). Mass spectrometric identification of proteins from silver-stained polyacrylamide gel: a method for the removal of silver ions to enhance sensitivity. Electrophoresis 20(3): 601-605.

Glass, K. A. and Johnson, E. A. (2004). Antagonistic effect of fat on the antibotulinal activity of food preservatives and fatty acids. Food Microbiol 21: 675-682.

Glatz, B. A. and Goepfert, J. M. (1976). Defined conditions for synthesis of *Bacillus cereus* enterotoxin by fermenter-grown cultures. Appl Environ Microbiol 32(3): 400-404.

Gohar, M., Faegri, K., Perchat, S., Ravnum, S., Okstad, O. A., Gominet, M., Kolsto, A. B. and Lereclus, D. (2008). The PlcR virulence regulon of *Bacillus cereus*. PLoS One 3(7): e2793.

Gohar, M., Gilois, N., Graveline, R., Garreau, C., Sanchis, V. and Lereclus, D. (2005). A comparative study of *Bacillus cereus*, *Bacillus thuringiensis* and *Bacillus anthracis* extracellular proteomes. Proteomics 5(14): 3696-3711.

Gordon, R. E., Haynes, W. C. and Hor-Nay, C. (1973). The Genus *Bacillus*. US Government Printing Office, Washington, D.C.

Granum, P. E. and Lund, T. (1997). *Bacillus cereus* and its food poisoning toxins. FEMS Microbiol Lett 157(2): 223-228.

Guedon, E., Sperandio, B., Pons, N., Ehrlich, S. D. and Renault, P. (2005). Overall control of nitrogen metabolism in *Lactococcus lactis* by CodY, and possible models for CodY regulation in Firmicutes. Microbiology 151(Pt 12): 3895-3909.

Guillemet, E., Cadot, C., Tran, S. L., Guinebretiere, M. H., Lereclus, D. and Ramarao, N. (2010). The InhA metalloproteases of *Bacillus cereus* contribute concomitantly to virulence. J Bacteriol 192(1): 286-294.

Guinebretiere, M. H. and Nguyen-The, C. (2003). Sources of *Bacillus cereus* contamination in a pasteurized zucchini puree processing line, differentiated by two PCR-based methods. FEMS Microbiol Ecol 43(2): 207-215.

Guinebretiere, M. H., Thompson, F. L., Sorokin, A., Normand, P., Dawyndt, P., Ehling-Schulz, M., Svensson, B., Sanchis, V., Nguyen-The, C., Heyndrickx, M. and De Vos, P. (2008). Ecological diversification in the *Bacillus cereus* Group. Environ Microbiol 10(4): 851-865.

Häggblom, M. M., Apetroaie, C., Andersson, M. A. and Salkinoja-Salonen, M. S. (2002). Quantitative analysis of cereulide, the emetic toxin of *Bacillus cereus*, produced under various conditions. Appl Environ Microbiol 68(5): 2479-2483.

Hamoen, L. W., Eshuis, H., Jongbloed, J., Venema, G. and van Sinderen, D. (1995). A small gene, designated *comS*, located within the coding region of the fourth amino acid-activation domain of *srfA*, is required for competence development in *Bacillus subtilis*. Mol Microbiol 15(1): 55-63.

Hamoen, L. W., Van Werkhoven, A. F., Bijlsma, J. J., Dubnau, D. and Venema, G. (1998). The competence transcription factor of *Bacillus subtilis* recognizes short A/T-rich sequences arranged in a unique, flexible pattern along the DNA helix. Genes Dev 12(10): 1539-1550.

Hamoen, L. W., Venema, G. and Kuipers, O. P. (2003). Controlling competence in *Bacillus subtilis*: shared use of regulators. Microbiology 149(Pt 1): 9-17.

Hamze, K., Julkowska, D., Autret, S., Hinc, K., Nagorska, K., Sekowska, A., Holland, I. B. and Seror, S. J. (2009). Identification of genes required for different stages of dendritic swarming in *Bacillus subtilis*, with a novel role for *phrC*. Microbiology 155(Pt 2): 398-412.

Handke, L. D., Shivers, R. P. and Sonenshein, A. L. (2008). Interaction of *Bacillus subtilis* CodY with GTP. J Bacteriol 190(3): 798-806.

Haughton, P., Garvey, M. and Rowan, N. J. (2010). Emergence of *Bacillus cereus* as a dominant organism in Irish retailed powdered infant formulae (PIF) when reconstituted and stored under abuse conditions. Journal of Food Safety 30: 814-831.

Hayashi, K., Ohsawa, T., Kobayashi, K., Ogasawara, N. and Ogura, M. (2005). The H_2O_2 stress-responsive regulator PerR positively regulates *srfA* expression in *Bacillus subtilis*. J Bacteriol 187(19): 6659-6667.

Helgason, E., Okstad, O. A., Caugant, D. A., Johansen, H. A., Fouet, A., Mock, M., Hegna, I. and Kolsto, A. B. (2000). *Bacillus anthracis*, *Bacillus cereus*, and *Bacillus thuringiensis*--one species on the basis of genetic evidence. Appl Environ Microbiol 66(6): 2627-2630.

Hellman, L. M. and Fried, M. G. (2007). Electrophoretic mobility shift assay (EMSA) for detecting protein-nucleic acid interactions. Nat Protoc 2(8): 1849-1861.

Helmann, J. D., Wu, M. F., Gaballa, A., Kobel, P. A., Morshedi, M. M., Fawcett, P. and Paddon, C. (2003). The global transcriptional response of *Bacillus subtilis* to peroxide stress is coordinated by three transcription factors. J Bacteriol 185(1): 243-253.

Herbig, A. F. and Helmann, J. D. (2001). Roles of metal ions and hydrogen peroxide in modulating the interaction of the *Bacillus subtilis* PerR peroxide regulon repressor with operator DNA. Mol Microbiol 41(4): 849-859.

Herbig, A. F. and Helmann, J. D. (2002). Metal ion uptake and oxidative stress, p. 405-414. *In* A.L. Sonenshein, J.A. Hoch, R. Losick (eds), *Bacillus subtilis* and its closest relatives: from genes to cells. 1st ed. ASM Press, Washington, D.C.

Hoffmann, K., Wollherr, A., Larsen, M., Rachinger, M., Liesegang, H., Ehrenreich, A. and Meinhardt, F. (2011). Comparative genetic analysis and manipulation of genetic competence facilitates the direct conditional knock out of essential genes in *Bacillus licheniformis* DSM13. Appl Environ Microbiol. Online ahead of print.: doi:10.1128/AEM.00660-10.

Hoffmaster, A. R., Ravel, J., Rasko, D. A., Chapman, G. D., Chute, M. D., Marston, C. K., De, B. K., Sacchi, C. T., Fitzgerald, C., Mayer, L. W., Maiden, M. C., Priest, F. G., Barker, M., Jiang, L., Cer, R. Z., Rilstone, J., Peterson, S. N., Weyant, R. S., Galloway, D. R., Read, T. D., Popovic, T. and Fraser, C. M. (2004). Identification of

anthrax toxin genes in a *Bacillus cereus* associated with an illness resembling inhalation anthrax. Proc Natl Acad Sci U S A 101(22): 8449-8454.

Holmes, J. R., Plunkett, T., Pate, P., Roper, W. L. and Alexander, W. J. (1981). Emetic food poisoning caused by *Bacillus cereus*. Arch Intern Med 141(6): 766-767.

Hsueh, Y. H., Somers, E. B. and Wong, A. C. (2008). Characterization of the *codY* gene and its influence on biofilm formation in *Bacillus cereus*. Arch Microbiol 189(6): 557-568.

Hu, H., Zhang, Q. and Ochi, K. (2002). Activation of antibiotic biosynthesis by specified mutations in the *rpoB* gene (encoding the RNA polymerase beta subunit) of *Streptomyces lividans*. J Bacteriol 184(14): 3984-3991.

Ichikawa, K., Gakumazawa, M., Inaba, A., Shiga, K., Takeshita, S., Mori, M. and Kikuchi, N. (2009). Acute encephalopathy of *Bacillus cereus* mimicking Reye syndrome. Brain Dev 32: 688-690.

Imlay, J. A. (2008). Cellular defenses against superoxide and hydrogen peroxide. Annu Rev Biochem 77: 755-776.

Imlay, J. A. and Fridovich, I. (1991). Superoxide production by respiring membranes of *Escherichia coli*. Free Radic Res Commun 12-13 Pt 1: 59-66.

Inaoka, T., Takahashi, K., Ohnishi-Kameyama, M., Yoshida, M. and Ochi, K. (2003). Guanine nucleotides guanosine 5'-diphosphate 3'-diphosphate and GTP co-operatively regulate the production of an antibiotic bacilysin in *Bacillus subtilis*. J Biol Chem 278(4): 2169-2176.

Ivanova, N., Sorokin, A., Anderson, I., Galleron, N., Candelon, B., Kapatral, V., Bhattacharyya, A. (2003). Genome sequence of *Bacillus cereus* and comparative analysis with *Bacillus anthracis*. Nature 423(5): 87-91.

Jääskelainen, E. L., Häggblom, M. M., Andersson, M. A. and Salkinoja-Salonen, M. S. (2004). Atmospheric oxygen and other conditions affecting the production of cereulide by *Bacillus cereus* in food. Int J Food Microbiol 96(1): 75-83.

Jääskeläinen, E. L., Teplova, V., Andersson, M. A., Andersson, L. C., Tammela, P., Andersson, M. C., Pirhonen, T. I., Saris, N. E. L., Vuorela, P. and Salkinoja-Salonen, M. S. (2003). In vitro assay for human toxicity of cereulide, the emetic mitochondrial toxin produced by food poisoning *Bacillus cereus*. Toxicology in Vitro 17: 737-744.

Jacquamet, L., Traore, D. A., Ferrer, J. L., Proux, O., Testemale, D., Hazemann, J. L., Nazarenko, E., El Ghazouani, A., Caux-Thang, C., Duarte, V. and Latour, J. M. (2009). Structural characterization of the active form of PerR: insights into the metal-induced activation of PerR and Fur proteins for DNA binding. Mol Microbiol 73(1): 20-31.

Jeanjean, R., Talla, E., Latifi, A., Havaux, M., Janicki, A. and Zhang, C. C. (2008). A large gene cluster encoding peptide synthetases and polyketide synthases is involved in production of siderophores and oxidative stress response in the cyanobacterium *Anabaena* sp. strain PCC 7120. Environ Microbiol 10(10): 2574-85.

Jernigan, D. B., Raghunathan, P. L., Bell, B. P., Brechner, R., Bresnitz, E. A., Butler, J. C., Cetron, M., Cohen, M., Doyle, T., Fischer, M., Greene, C., Griffith, K. S., Guarner, J., Hadler, J. L., Hayslett, J. A., Meyer, R., Petersen, L. R., Phillips, M., Pinner, R., Popovic, T., Quinn, C. P., Reefhuis, J., Reissman, D., Rosenstein, N., Schuchat, A., Shieh, W. J., Siegal, L., Swerdlow, D. L., Tenover, F. C., Traeger, M., Ward, J. W., Weisfuse, I., Wiersma, S., Yeskey, K., Zaki, S., Ashford, D. A., Perkins, B. A., Ostroff, S., Hughes, J., Fleming, D., Koplan, J. P. and Gerberding, J. L. (2002). Investigation of bioterrorism-related anthrax, United States, 2001: epidemiologic findings. Emerg Infect Dis 8(10): 1019-1028.

Joseph, P., Ratnayake-Lecamwasam, M. and Sonenshein, A. L. (2005). A region of *Bacillus subtilis* CodY protein required for interaction with DNA. J Bacteriol 187(12): 4127-4139.

Kastrup, C. J., Boedicker, J. Q., Pomerantsev, A. P., Moayeri, M., Bian, Y., Pompano, R. R., Kline, T. R., Sylvestre, P., Shen, F., Leppla, S. H., Tang, W. J. and Ismagilov,

R. F. (2008). Spatial localization of bacteria controls coagulation of human blood by 'quorum acting'. Nat Chem Biol 4(12): 742-750.

Kawamura-Sato, K., Hirama, Y., Agata, N., Ito, H., Torii, K., Takeno, A., Hasegawa, T., Shimomura, Y. and Ohta, M. (2005). Quantitative analysis of cereulide, an emetic toxin of *Bacillus cereus*, by using rat liver mitochondria. Microbiol Immunol 49(1): 25-30.

Kearns, D. B., Chu, F., Branda, S. S., Kolter, R. and Losick, R. (2005). A master regulator for biofilm formation by *Bacillus subtilis*. Mol Microbiol 55(3): 739-749.

Klee, S. R., Ozel, M., Appel, B., Boesch, C., Ellerbrok, H., Jacob, D., Holland, G., Leendertz, F. H., Pauli, G., Grunow, R. and Nattermann, H. (2006). Characterization of *Bacillus anthracis*-like bacteria isolated from wild great apes from Cote d'Ivoire and Cameroon. J Bacteriol 188(15): 5333-5344.

Kohanski, M. A., Dwyer, D. J., Hayete, B., Lawrence, C. A. and Collins, J. J. (2007). A common mechanism of cellular death induced by bactericidal antibiotics. Cell 130(5): 797-810.

Kolsto, A. B., Tourasse, N. J. and Okstad, O. A. (2009). What sets *Bacillus anthracis* apart from other *Bacillus* species? Annu Rev Microbiol 63: 451-476.

Kotiranta, A., Lounatmaa, K. and Haapasalo, M. (2000). Epidemiology and pathogenesis of *Bacillus cereus* infections. Microbes Infect 2(2): 189-198.

Koumoutsi, A., Chen, X. H., Vater, J. and Borriss, R. (2007). DegU and YczE positively regulate the synthesis of bacillomycin D by *Bacillus amyloliquefaciens* strain FZB42. Appl Environ Microbiol 73(21): 6953-6964.

Kramer, J. M. and Gilbert, R. J. (1989). *Bacillus cereus* and other *Bacillus* species. p.21-70. *In* M. P. Doyle (ed.), Food-borne pathogens. Marcel Dekker, New York, NY.

Kulaev, I., Vagabov, V. and Kulakovskaya, T. (1999). New aspects of inorganic polyphosphate metabolism and function. J Biosci Bioeng 88(2): 111-29.

Kunst, F., Ogasawara, N., Moszer, I., Albertini, A. M., Alloni, G., Azevedo, V., Bertero, M. G., Bessieres, P., Bolotin, A., Borchert, S., Borriss, R., Boursier, L., Brans, A., Braun, M., Brignell, S. C., Bron, S., Brouillet, S., Bruschi, C. V., Caldwell, B., Capuano, V., Carter, N. M., Choi, S. K., Codani, J. J., Connerton, I. F., Danchin, A. and et al. (1997). The complete genome sequence of the gram-positive bacterium *Bacillus subtilis*. Nature 390(6657): 249-256.

Ladeuze, S., Lentz, N., Delbrassinne, L., Hu, X. and Mahillon, J. (2011). Cereulide, the emetic toxin of *Bacillus cereus*, displays antifungal activity. Appl Environ Microbiol 77(7): 2555-2558.

Laemmli, U. K. (1970). Cleavage of structural proteins during the assembly of the head of bacteriophage T4. Nature 227(259): 680-685.

Lambalot, R. H., Gehring, A. M., Flugel, R. S., Zuber, P., LaCelle, M., Marahiel, M. A., Reid, R., Khosla, C. and Walsh, C. T. (1996). A new enzyme superfamily - the phosphopantetheinyl transferases. Chem Biol 3(11): 923-936.

Lammers, C. R., Florez, L. A., Schmeisky, A. G., Roppel, S. F., Mader, U., Hamoen, L. and Stülke, J. (2010). Connecting parts with processes: SubtiWiki and SubtiPathways integrate gene and pathway annotation for *Bacillus subtilis*. Microbiology 156(Pt 3): 849-859.

Lamonica, J. M., Wagner, M., Eschenbrenner, M., Williams, L. E., Miller, T. L., Patra, G. and DelVecchio, V. G. (2005). Comparative secretome analyses of three *Bacillus anthracis* strains with variant plasmid contents. Infect Immun 73(6): 3646-3658.

Laouami, S., Messaoudi, K., Alberto, F., Clavel, T. and Duport, C. (2011). Lactate dehydrogenase A promotes communication between carbohydrate catabolism and virulence in *Bacillus cereus*. J Bacteriol 193(7): 1757-1766.

Lechner, S., Mayr, R., Francis, K. P., Pruss, B. M., Kaplan, T., Wiessner-Gunkel, E., Stewart, G. S. and Scherer, S. (1998). *Bacillus weihenstephanensis* sp. nov. is a new psychrotolerant species of the *Bacillus cereus* group. Int J Syst Bacteriol 48 Pt 4: 1373-1382.

Lee, J. W. and Helmann, J. D. (2006). The PerR transcription factor senses H_2O_2 by metal-catalysed histidine oxidation. Nature 440(7082): 363-367.

Lee, R. M., Hartmann, P. A., Olson, D. G. and Williams, F. D. (1994). Metal ions reverse the inhibitory effects of selected food-grade phosphates in *Staphylococcus aureus*. J. Food. Prot. 57(4): 284-288.

Lee, R. M., Hartmann, P. A., Stahr, H. M., Olson, D. G. and Williams, F. D. (1994). Antibacterial mechanism of long-chain polyphosphates in *Staphylococcus aureus*. J. Food. Prot. 57: 289-294.

Leisner, M., Stingl, K., Frey, E. and Maier, B. (2008). Stochastic switching to competence. Curr Opin Microbiol 11(6): 553-559.

Leisner, M., Stingl, K., Radler, J. O. and Maier, B. (2007). Basal expression rate of *comK* sets a 'switching-window' into the K-state of *Bacillus subtilis*. Mol Microbiol 63(6): 1806-1816.

Lemaux, P. G. (2008). Genetically Engineered Plants and Foods: A Scientist's Analysis of the Issues (Part I). Annu Rev Plant Biol 59: 771-812.

Lereclus, D., Agaisse, H., Grandvalet, C., Salamitou, S. and Gominet, M. (2000). Regulation of toxin and virulence gene transcription in *Bacillus thuringiensis*. Int J Med Microbiol 290(4-5): 295-299.

Levine, A., Vannier, F., Absalon, C., Kuhn, L., Jackson, P., Scrivener, E., Labas, V., Vinh, J., Courtney, P., Garin, J. and Seror, S. J. (2006). Analysis of the dynamic *Bacillus subtilis* Ser/Thr/Tyr phosphoproteome implicated in a wide variety of cellular processes. Proteomics 6(7): 2157-2173.

Loessner, M. J., Maier, S. K., Schiwek, P. and Scherer, S. (1997). Long-chain polphosphates inhibit growth of *Clostridium tyrobutyricum* in processed cheese spreads. Journal of Food Protection 60: 493-498.

Lopez, D. and Kolter, R. (2010). Extracellular signals that define distinct and coexisting cell fates in *Bacillus subtilis*. FEMS Microbiol Rev 34(2): 134-149.

Lopez, D., Vlamakis, H., Losick, R. and Kolter, R. (2009). Paracrine signaling in a bacterium. Genes Dev 23(14): 1631-1638.

Luchese, R. H. and Harrigan, W. F. (1993). Biosynthesis of aflatoxin--the role of nutritional factors. J Appl Bacteriol 74(1): 5-14.

Lücking, G. (2009). Molecular characterization of cereulide synthesis in emetic *Bacillus cereus*. PhD Thesis Technische Universität München.

Lücking, G., Dommel, M. K., Scherer, S., Fouet, A. and Ehling-Schulz, M. (2009). Cereulide synthesis in emetic *Bacillus cereus* is controlled by the transition state regulator AbrB, but not by the virulence regulator PlcR. Microbiology 155(Pt 3): 922-931.

Lund, T., De Buyser, M. L. and Granum, P. E. (2000). A new cytotoxin from *Bacillus cereus* that may cause necrotic enteritis. Mol Microbiol 38(2): 254-261.

Lund, T. and Granum, P. E. (1996). Characterisation of a non-haemolytic enterotoxin complex from *Bacillus cereus* isolated after a foodborne outbreak. FEMS Microbiol Lett 141(2-3): 151-156.

Maamar, H. and Dubnau, D. (2005). Bistability in the *Bacillus subtilis* K-state (competence) system requires a positive feedback loop. Mol Microbiol 56(3): 615-624.

Macek, B., Mijakovic, I., Olsen, J. V., Gnad, F., Kumar, C., Jensen, P. R. and Mann, M. (2007). The serine/threonine/tyrosine phosphoproteome of the model bacterium *Bacillus subtilis*. Mol Cell Proteomics 6(4): 697-707.

Magarvey, N. A., Ehling-Schulz, M. and Walsh, C. T. (2006). Characterization of the cereulide NRPS hydroxy acid specifying modules: activation of keto acids and chiral reduction on the assembly line. J. Am. Chem. Soc. 128(33): 10698-10699.

Mahler, H., Pasi, A., Kramer, J. M., Schulte, P., Scoging, A. C., Bar, W. and Krahenbuhl, S. (1997). Fulminant liver failure in association with the emetic toxin of *Bacillus cereus*. N Engl J Med 336(16): 1142-1148.

Maier, S. K., Scherer, S. and Loessner, M. J. (1999). Long-chain polyphosphate causes cell lysis and inhibits *Bacillus cereus* septum formation, which is dependent on divalent cations. Appl Environ Microbiol 65(9): 3942-3949.

Majerczyk, C. D., Dunman, P. M., Luong, T. T., Lee, C. Y., Sadykov, M. R., Somerville, G. A., Bodi, K. and Sonenshein, A. L. (2010). Direct targets of CodY in *Staphylococcus aureus*. J Bacteriol 192(11): 2861-77.

Majerczyk, C. D., Sadykov, M. R., Luong, T. T., Lee, C., Somerville, G. A. and Sonenshein, A. L. (2008). *Staphylococcus aureus* CodY negatively regulates virulence gene expression. J Bacteriol 190(7): 2257-2265.

Marahiel, M. A., Nakano, M. M. and Zuber, P. (1993). Regulation of peptide antibiotic production in *Bacillus*. Mol Microbiol 7(5): 631-636.

Marahiel, M. A., Stachelhaus, T. and Mootz, H. D. (1997). Modular peptide synthetases involved in nonribosomal peptide synthesis. Chem Rev 97(7)**:** 2651 - 2673.

Margolin, W. (2005). FtsZ and the division of prokaryotic cells and organelles. Nat Rev Mol Cell Biol 6(11): 862-871.

Marsh, S. K., Myers, D. J. and Stahr, H. M. (1996). Effects of phosphate solutions on aflatoxin production in a synthetic medium and in frankfurters. J Food Prot 59: 626-630.

Martineau, F., Picard, F. J., Roy, P. H., Ouellette, M. and Bergeron, M. G. (1996). Species-specific and ubiquitous DNA-based assays for rapid identification of *Staphylococcus epidermidis*. J Clin Microbiol 34(12): 2888-2893.

Masse, E., Vanderpool, C. K. and Gottesman, S. (2005). Effect of RyhB small RNA on global iron use in *Escherichia coli*. J Bacteriol 187(20): 6962-6971.

McLoon, A. L., Guttenplan, S. B., Kearns, D. B., Kolter, R. and Losick, R. (2011). Tracing the domestication of a biofilm-forming bacterium. J Bacteriol.193(8): 2027-2034.

Mellin, J. R., Goswami, S., Grogan, S., Tjaden, B. and Genco, C. A. (2007). A novel fur- and iron-regulated small RNA, NrrF, is required for indirect fur-mediated regulation of the sdhA and sdhC genes in *Neisseria meningitidis*. J Bacteriol 189(10): 3686-3694.

Melling, J., Capel, B. J., Turnbull, P. C. and Gilbert, R. J. (1976). Identification of a novel enterotoxigenic activity associated with *Bacillus cereus*. J Clin Pathol 29(10): 938-940.

Michaux, C., Sanguinetti, M., Reffuveille, F., Auffray, Y., Posteraro, B., Gilmore, M. S., Hartke, A. and Giard, J. C. (2011). Slya Is a transcriptional regulator involved in the virulence of *Enterococcus faecalis*. Infect Immun. Published online ahead of print on 2 May 2011. doi:10.1128/IAI.01132-10.

Mignot, T., Couture-Tosi, E., Mesnage, S., Mock, M. and Fouet, A. (2004). In vivo *Bacillus anthracis* gene expression requires PagR as an intermediate effector of the AtxA signalling cascade. Int J Med Microbiol. 293(7-8): 619-624.

Mignot, T., Denis, B., Couture-Tosi, E., Kolsto, A. B., Mock, M. and Fouet, A. (2001). Distribution of S-layers on the surface of *Bacillus cereus* strains: phylogenetic origin and ecological pressure. Environ Microbiol 3(8): 493-501.

Mignot, T., Mock, M., Robichon, D., Landier, A., Lereclus, D. and Fouet, A. (2001). The incompatibility between the PlcR- and AtxA-controlled regulons may have selected a nonsense mutation in *Bacillus anthracis*. Mol Microbiol 42(5): 1189-1198.

Mikkola, R., Saris, N. E., Grigoriev, P. A., Andersson, M. A. and Salkinoja-Salonen, M. S. (1999). Ionophoretic properties and mitochondrial effects of cereulide: the emetic toxin of *B. cereus*. Eur J Biochem 263(1): 112-117.

Miller, I. and Gemeiner, M. (1992). Two-dimensional electrophoresis of cat sera: protein identification by cross reacting antibodies against human serum proteins. Electrophoresis 13(7): 450-453.

Mironczuk, A. M., Kovacs, A. T. and Kuipers, O. P. (2008). Induction of natural competence in *Bacillus cereus* ATCC 14579. Microb Biotechnol 1(3): 226-235.

Miyoshi, S. and Shinoda, S. (2000). Microbial metalloproteases and pathogenesis. Microbes Infect 2(1): 91-98.

Mock, M. and Fouet, A. (2001). Anthrax. Annu Rev Microbiol 55: 647 - 671.

Molins, R. A. (1991). Phosphates in food. CRC Press, Boca Raton, FL.

Molle, V., Nakaura, Y., Shivers, R. P., Yamaguchi, H., Losick, R., Fujita, Y. and Sonenshein, A. L. (2003). Additional targets of the *Bacillus subtilis* global regulator CodY identified by chromatin immunoprecipitation and genome-wide transcript analysis. J Bacteriol 185(6): 1911-1922.

Mols, M. and Abee, T. (2011). Primary and secondary oxidative stress in *Bacillus*. Environ Microbiol. 13(6): 1387-1394.

Mols, M., van Kranenburg, R., van Melis, C. C., Moezelaar, R. and Abee, T. (2010). Analysis of acid-stressed *Bacillus cereus* reveals a major oxidative response and inactivation-associated radical formation. Environ Microbiol 12(4): 873-885.

Morente, E. O., Abriouel, H., Lopez, R. L., Ben Omar, N. and Galvez, A. (2010). Antibacterial activity of carvacrol and 2-nitro-1-propanol against single and mixed populations of foodborne pathogenic bacteria in corn flour dough. Food Microbiol 27(2): 274-279.

Mossel, D. A., Koopman, M. J. and Jongerius, E. (1967). Enumeration of *Bacillus cereus* in foods. Appl Microbiol 15(3): 650-653.

Mostertz, J., Scharf, C., Hecker, M. and Homuth, G. (2004). Transcriptome and proteome analysis of *Bacillus subtilis* gene expression in response to superoxide and peroxide stress. Microbiology 150(Pt 2): 497-512.

Mukherjee, K., Altincicek, B., Hain, T., Domann, E., Vilcinskas, A. and Chakraborty, T. (2010). *Galleria mellonella* as a model system for studying *Listeria* pathogenesis. Appl Environ Microbiol 76(1): 310-317.

Mulec, J., Podlesek, Z., Mrak, P., Kopitar, A., Ihan, A. and Zgur-Bertok, D. (2003). A *cka-gfp* transcriptional fusion reveals that the colicin K activity gene is induced in only 3 percent of the population. J Bacteriol 185(2): 654-659.

Nakamura, L. K. (1998). *Bacillus pseudomycoides* sp. nov. Int J Syst Bacteriol 48 Pt 3: 1031-1035.

Nakano, M. M., Magnuson, R., Myers, A., Curry, J., Grossman, A. D. and Zuber, P. (1991). *srfA* is an operon required for surfactin production, competence development, and efficient sporulation in *Bacillus subtilis*. J Bacteriol 173(5): 1770-1778.

Nelms, P. K., Larson, O. and Barnes-Josiah, D. (1997). Time to *B. cereus* about hot chocolate. Public Health Rep 112(3): 240-244.

Novak, J. S., Call, J., Tomasula, P. and Luchansky, J. B. (2005). An assessment of pasteurization treatment of water, media, and milk with respect to *Bacillus* spores. J Food Prot 68(4): 751-757.

Ogura, M. and Tsukahara, K. (2010). Autoregulation of the *Bacillus subtilis* response regulator gene *degU* is coupled with the proteolysis of DegU-P by ClpCP. Mol Microbiol 75(5): 1244-1259.

Oide, S., Moeder, W., Krasnoff, S., Gibson, D., Haas, H., Yoshioka, K. and Turgeon, B. G. (2006). NPS6, encoding a nonribosomal peptide synthetase involved in siderophore-mediated iron metabolism, is a conserved virulence determinant of plant pathogenic ascomycetes. Plant Cell 18(10): 2836-2853.

Paananen, A., Mikkola, R., Sareneva, T., Matikainen, S., Hess, M., Andersson, M., Julkunen, I., Salkinoja-Salonen, M. S. and Timonen, T. (2002). Inhibition of human natural killer cell activity by cereulide, an emetic toxin from *Bacillus cereus*. Clin Exp Immunol 129(3): 420 - 428.

Patel, M. S. and Hong, Y. S. (1998). Lipoic acid as an antioxidant. The role of dihydrolipoamide dehydrogenase. Methods Mol Biol 108: 337-346.

Perego, M., Spiegelman, G. B. and Hoch, J. A. (1988). Structure of the gene for the transition state regulator, *abrB*: regulator synthesis is controlled by the *spo0A* sporulation gene in *Bacillus subtilis*. Mol Microbiol 2(6): 689-699.

Pezard, C., Berche, P. and Mock, M. (1991). Contribution of individual toxin components to virulence of *Bacillus anthracis*. Infect Immun 59(10): 3472-3477.

Pfaffl, M. W. (2001). A new mathematical model for relative quantification in real-time RT-PCR. Nucl. Acids Res. 29(9): e45.

Pfaffl, M. W., Horgan, G. W. and Dempfle, L. (2002). Relative expression software tool (REST(C)) for group-wise comparison and statistical analysis of relative expression results in real-time PCR. Nucl. Acids Res. 30(9): e36.

Pirhonen, T. J., Andersson, M. A., Jääskeläinen, E. L., Salkinoja-Salonen, M. S., Honkanen-Buzalski, T. and Johansson, T. M. (2005). Biochemical and toxic diversity of *Bacillus cereus* in a pasta and meat dish associated with a food poisoning. Food Microbiol 22: 87-91.

Pitchayawasin, S., Kuse, M., Koga, K., Isobe, M., Agata, N. and Ohta, M. (2003). Complexation of cyclic dodecadepsipeptide, cereulide with ammonium salts. Bioorg Med Chem Lett. 13(20): 3507-3512.

Pohl, K., Francois, P., Stenz, L., Schlink, F., Geiger, T., Herbert, S., Goerke, C., Schrenzel, J. and Wolz, C. (2009). CodY in *Staphylococcus aureus*: a regulatory link between metabolism and virulence gene expression. J Bacteriol 191(9): 2953-2963.

Pomerantsev, A. P., Pomerantseva, O. M., Camp, A. S., Mukkamala, R., Goldman, S. and Leppla, S. H. (2009). PapR peptide maturation: role of the NprB protease in *Bacillus cereus* 569 PlcR/PapR global gene regulation. FEMS Immunol Med Microbiol 55(3): 361-377.

Posfay-Barbe, K. M., Schrenzel, J., Frey, J., Studer, R., Korff, C., Belli, D. C., Parvex, P., Rimensberger, P. C. and Schappi, M. G. (2008). Food poisoning as a cause of acute liver failure. Pediatr Infect Dis J 27(9): 846-847.

Prakash, A. (2000). Polyphosphates, p. 725-733. *In* A.S. Naidu (ed.), Natural Food Antimicrobial Systems, 1st ed. CRC Press LLC, Boca Raton, FL, USA.

Preis, H., Eckart, R. A., Gudipati, R. K., Heidrich, N. and Brantl, S. (2009). CodY activates transcription of a small RNA in *Bacillus subtilis*. J Bacteriol 191(17): 5446-5457.

Priest, F. G. and Alexander, B. (1988). A frequency matrix for prohabilistic identification of some bacilli. J Gen Microbiol 134: 3011 - 3018.

Radwan, M., Miller, I., Grunert, T., Marchetti-Deschmann, M., Vogl, C., O'Donoghue, N., Dunn, M. J., Kolbe, T., Allmaier, G., Gemeiner, M., Muller, M. and Strobl, B. (2008). The impact of tyrosine kinase 2 (Tyk2) on the proteome of murine macrophages and their response to lipopolysaccharide (LPS). Proteomics 8(17): 3469-3485.

Rajkovic, A., Uyttendaele, M. and Debevere, J. (2007). Computer aided boar semen motility analysis for cereulide detection in different food matrices. Int J Food Microbiol 114(1): 92-99.

Rajkovic, A., Uyttendaele, M., Deley, W., Van Soom, A., Rijsselaere, T. and Debevere, J. (2006). Dynamics of boar semen motility inhibition as a semi-quantitative measurement of *Bacillus cereus* emetic toxin (cereulide). J Microbiol Methods 65(3): 525-534.

Rajkovic, A., Uyttendaele, M., Ombregt, S. A., Jaaskelainen, E., Salkinoja-Salonen, M. and Debevere, J. (2006). Influence of type of food on the kinetics and overall production of *Bacillus cereus* emetic toxin. J Food Prot 69(4): 847-852.

Rajkovic, A., Uyttendaele, M., Vermeulen, A., Andjelkovic, M., Fitz-James, I., in 't Veld, P., Denon, Q., Verhe, R. and Debevere, J. (2008). Heat resistance of *Bacillus cereus* emetic toxin, cereulide. Lett Appl Microbiol 46(5): 536-541.

Ramarao, N. and Lereclus, D. (2005). The InhA1 metalloprotease allows spores of the *B. cereus* group to escape macrophages. Cell Microbiol 7(9): 1357-1364.

Rao, C. V., Wolf, D. M. and Arkin, A. P. (2002). Control, exploitation and tolerance of intracellular noise. Nature 420(6912): 231-237.

Rao, N. N., Gomez-Garcia, M. R. and Kornberg, A. (2009). Inorganic polyphosphate: essential for growth and survival. Annu Rev Biochem 78: 605-647.

Rasko, D. A., Altherr, M. R., Han, C. S. and Ravel, J. (2005). Genomics of the *Bacillus cereus* group of organisms. FEMS Microbiol Rev 29(2): 303-329.

Rasko, D. A., Rosovitz, M. J., Okstad, O. A., Fouts, D. E., Jiang, L., Cer, R. Z., Kolsto, A.-B., Gill, S. R. and Ravel, J. (2007). Complete sequence analysis of novel plasmids

from emetic and periodontal *Bacillus cereus* isolates reveals a common evolutionary history among the *B. cereus* group plasmids including *B. anthracis* pXO1. J. Bacteriol. 189(1): 52-64.

Rasko, D. A., Rosovitz, M. J., Okstad, O. A., Fouts, D. E., Jiang, L., Cer, R. Z., Kolsto, A. B., Gill, S. R. and Ravel, J. (2007). Complete sequence analysis of novel plasmids from emetic and periodontal *Bacillus cereus* isolates reveals a common evolutionary history among the *B. cereus*-group plasmids, including *Bacillus anthracis* pXO1. J Bacteriol 189(1): 52-64.

Ratnayake-Lecamwasam, M., Serror, P., Wong, K. W. and Sonenshein, A. L. (2001). *Bacillus subtilis* CodY represses early-stationary-phase genes by sensing GTP levels. Genes Dev 15(9): 1093-1103.

Reeves, E. P., Reiber, K., Neville, C., Scheibner, O., Kavanagh, K. and Doyle, S. (2006). A nonribosomal peptide synthetase (Pes1) confers protection against oxidative stress in *Aspergillus fumigatus*. Febs J 273(13): 3038-3053.

Remm, M., Storm, C. E. and Sonnhammer, E. L. (2001). Automatic clustering of orthologs and in-paralogs from pairwise species comparisons. J Mol Biol 314(5): 1041-52.

Reyes, J. E., Bastias, J. M., Gutierrez, M. R. and Rodriguez Mde, L. (2007). Prevalence of *Bacillus cereus* in dried milk products used by Chilean School Feeding Program. Food Microbiol 24(1): 1-6.

Reynolds, P. E. and Courvalin, P. (2005). Vancomycin resistance in enterococci due to synthesis of precursors terminating in D-alanyl-D-serine. Antimicrob Agents Chemother 49(1): 21-25.

Rivera, J., Cordero, R. J., Nakouzi, A. S., Frases, S., Nicola, A. and Casadevall, A. (2010). *Bacillus anthracis* produces membrane-derived vesicles containing biologically active toxins. Proc Natl Acad Sci U S A 107(44): 19002-19007.

Roggiani, M. and Dubnau, D. (1993). ComA, a phosphorylated response regulator protein of *Bacillus subtilis*, binds to the promoter region of *srfA*. J Bacteriol 175(10): 3182-7.

Rosenfeld, E., Duport, C., Zigha, A. and Schmitt, P. (2005). Characterization of aerobic and anaerobic vegetative growth of the food-borne pathogen *Bacillus cereus* F4430/73 strain. Can J Microbiol 51(2): 149-158.

Ross, C. L. and Koehler, T. M. (2006). *plcR/papR*-independent expression of anthrolysin O by *Bacillus anthracis*. J. Bacteriol. 188(22): 7823-7829.

Russell, N. J. and Gould, G. W. (2003). Major preservation technologies, p.14-24. *In* N. J. Russell and G. W. Gould (eds.), Food Preservatives, 2nd ed. Kluwer Academic/Plenum Publishers, New York, NY.

Rygus, T. and Hillen, W. (1991). Inducible high-level expression of heterologous genes in *Bacillus megaterium* using the regulatory elements of the xylose-utilization operon. Appl Microbiol Biotechnol 35(5): 594-599.

Rygus, T., Scheler, A., Allmansberger, R. and Hillen, W. (1991). Molecular cloning, structure, promoters and regulatory elements for transcription of the *Bacillus megaterium* encoded regulon for xylose utilization. Arch Microbiol 155(6): 535-542.

Sambrook, J., Fritsch, E. F. and Maniatis, T. (1989). Molecular Cloning: a Laboratory Manual, Cold Spring Harbor, NY: Cold Spring Harbor Laboratory Press.

Sambrook, J. and Russell, D. W. (2001). Molecular Cloning: a Laboratory Manual, 3rd edn., Cold Spring Harbor, NY: Cold Spring Harbor Laboratory Press.

Sander, C. and Schneider, R. (1991). Database of homology-derived protein structures and the structural meaning of sequence alignment. Proteins: Structure, Function, and Genetics 9: 56-68.

Sastalla, I., Maltese, L. M., Pomerantseva, O. M., Pomerantsev, A. P., Keane-Myers, A. and Leppla, S. H. (2010). Activation of the latent PlcR regulon in *Bacillus anthracis*. Microbiology 156(Pt 10): 2982-2993.

Schoder, D., Zangerl, P., Manafi, M., Wagner, M., Lindner, G. and Foissy, H. (2007). *Bacillus cereus* - ein Problemkeim der Milchwirtschaft mit unterschiedlich eingeschätztem Risikopotenzial. Vet. Med. Austria / Tierärztl. Mschr. 94: 25-33.

Schoeni, J. L. and Wong, A. C. L. (2005). *Bacillus cereus* food poisoning and its toxins. J Food Prot 68(3): 636-648.

Schultz, D., Wolynes, P. G., Ben Jacob, E. and Onuchic, J. N. (2009). Deciding fate in adverse times: sporulation and competence in *Bacillus subtilis*. Proc Natl Acad Sci U S A 106(50): 21027-21034.

Schwarzer, D., Mootz, H. D., Linne, U. and Marahiel, M. A. (2002). Regeneration of misprimed nonribosomal peptide synthetases by type II thioesterases. Proc Natl Acad Sci U S A 99(22): 14083-14088.

Senior, N. J., Bagnall, M. C., Champion, O. L., Reynolds, S. E., La Ragione, R. M., Woodward, M. J., Salguero, F. J. and Titball, R. W. (2011). *Galleria mellonella* as an infection model for *Campylobacter jejuni* virulence. J Med Microbiol 60(Pt 5): 661-669.

Serror, P. and Sonenshein, A. L. (1996). CodY is required for nutritional repression of *Bacillus subtilis* genetic competence. J Bacteriol 178(20): 5910-5915.

Shaheen, R., Andersson, M. A., Apetroaie, C., Schulz, A., Ehling-Schulz, M., Ollilainen, V. M. and Salkinoja-Salonen, M. S. (2006). Potential of selected infant food formulas for production of *Bacillus cereus* emetic toxin, cereulide. Int J Food Microbiol 107(3): 287-294.

Shelef, L. A. and Seiter, J. A. (1993). Indirect antimicrobials, p. 539-569. *In* P. M. Davidson (ed.), Antimicrobials in foods, 2nd ed. Marcel Dekker, Inc., New York, N. Y.

Shelef, L. A., Wang, Z. L. and Udeogu, A. C. (1989). Growth of *Staphylococcus aureus* and enterotoxin A production in foods containing polyphosphates. J Food Safety 10(3): 201-208.

Shi, X., Rao, N. N. and Kornberg, A. (2004). Inorganic polyphosphate in *Bacillus cereus*: motility, biofilm formation, and sporulation. Proc Natl Acad Sci U S A 101(49): 17061-17065.

Shinagawa, K. (1993). Serology and characterization of *Bacillus cereus* in relation to toxin production. Bull Int Dairy Fed 287: 42-49.

Shinagawa, K., Konuma, H., Sekita, H. and Sugii, S. (1995). Emesis of rhesus monkeys induced by intragastric administration with the HEp-2 vacuolation factor (cereulide) produced by *Bacillus cereus*. FEMS Microbiol Lett 130(1): 87-90.

Shinagawa, K., Matsusaka, N., Konuma, H. and Kurata, H. (1985). The relation between the diarrheal and other biological activities of *Bacillus cereus* involved in food poisoning outbreaks. Japanese Journal of Veterinary Science 47(4): 557-565.

Shiota, M., Saitou, K., Mizumoto, H., Matsusaka, M., Agata, N., Nakayama, M., Kage, M., Tatsumi, S., Okamoto, A., Yamaguchi, S., Ohta, M. and Hata, D. (2010). Rapid detoxification of cereulide in *Bacillus cereus* food poisoning. Pediatrics 125(4): e951-955.

Shivers, R. P., Dineen, S. S. and Sonenshein, A. L. (2006). Positive regulation of *Bacillus subtilis* ackA by CodY and CcpA: establishing a potential hierarchy in carbon flow. Mol Microbiol 62(3): 811-22.

Shivers, R. P. and Sonenshein, A. L. (2004). Activation of the *Bacillus subtilis* global regulator CodY by direct interaction with branched-chain amino acids. Mol Microbiol 53(2): 599-611.

Shivers, R. P. and Sonenshein, A. L. (2005). *Bacillus subtilis ilvB* operon: an intersection of global regulons. Mol Microbiol 56(6): 1549-1559.

Sierro, N., Makita, Y., de Hoon, M. and Nakai, K. (2008). DBTBS: a database of transcriptional regulation in *Bacillus subtilis* containing upstream intergenic conservation information. Nucleic Acids Res 36(Database issue): D93-96.

Singh, K. D., Schmalisch, M. H., Stulke, J. and Gorke, B. (2008). Carbon catabolite repression in *Bacillus subtilis*: quantitative analysis of repression exerted by different carbon sources. J Bacteriol 190(21): 7275-7284.

Smits, W. K., Eschevins, C. C., Susanna, K. A., Bron, S., Kuipers, O. P. and Hamoen, L. W. (2005). Stripping *Bacillus*: ComK auto-stimulation is responsible for the bistable response in competence development. Mol Microbiol 56(3): 604-614.

Smits, W. K., Kuipers, O. P. and Veening, J. W. (2006). Phenotypic variation in bacteria: the role of feedback regulation. Nat Rev Microbiol 4(4): 259-271.

Soga, T., Ohashi, Y., Ueno, Y., Naraoka, H., Tomita, M. and Nishioka, T. (2003). Quantitative metabolome analysis using capillary electrophoresis mass spectrometry. J Proteome Res 2(5): 488-494.

Somerville, G. A. and Proctor, R. A. (2009). At the crossroads of bacterial metabolism and virulence factor synthesis in Staphylococci. Microbiol Mol Biol Rev 73(2): 233-248.

Sonenshein, A. L. (2005). CodY, a global regulator of stationary phase and virulence in Gram-positive bacteria. Curr Opin Microbiol 8(2): 203-207.

Sonenshein, A. L. (2007). Control of key metabolic intersections in *Bacillus subtilis*. Nat Rev Microbiol 5(12): 917-927.

Spoering, A. L. and Gilmore, M. S. (2006). Quorum sensing and DNA release in bacterial biofilms. Curr Opin Microbiol 9(2): 133-137.

Srivatsan, A., Han, Y., Peng, J., Tehranchi, A. K., Gibbs, R., Wang, J. D. and Chen, R. (2008). High-precision, whole-genome sequencing of laboratory strains facilitates genetic studies. PLoS Genet 4(8): e1000139.

Stenfors Arnesen, L. P., Fagerlund, A. and Granum, P. E. (2008). From soil to gut: *Bacillus cereus* and its food poisoning toxins. FEMS Microbiol Rev 32(4): 579-606.

Strieker, M., Tanovic, A. and Marahiel, M. A. (2010). Nonribosomal peptide synthetases: structures and dynamics. Curr Opin Struct Biol 20(2): 234-240.

Susanna, K. A., Mironczuk, A. M., Smits, W. K., Hamoen, L. W. and Kuipers, O. P. (2007). A single, specific thymine mutation in the ComK-binding site severely decreases binding and transcription activation by the competence transcription factor ComK of *Bacillus subtilis*. J Bacteriol 189(13): 4718-4728.

Suzuki, Y. J., Tsuchiya, M. and Packer, L. (1991). Thioctic acid and dihydrolipoic acid are novel antioxidants which interact with reactive oxygen species. Free Radic Res Commun 15(5): 255-263.

Szabo, R., Speirs, J. and Akhtar, M. (1991). Cell culture detection and conditions for production of a *Bacillus cereus* heat-stable toxin. J Food Prot 54(4): 272-276.

Te Giffel, M. C., Beumer, R. R., Granum, P. E. and Rombouts, F. M. (1997). Isolation and characterisation of *Bacillus cereus* from pasteurised milk in household refrigerators in The Netherlands. Int J Food Microbiol 34(3): 307-318.

Tempelaars, M. H., Rodrigues, S. and Abee, T. (2011). Comparative Analysis of Antimicrobial Activities of Valinomycin and Cereulide, the *Bacillus cereus* Emetic Toxin. Appl Environ Microbiol 77(8): 2755-2762.

Ter Beek, A. and Brul, S. (2010). To kill or not to kill Bacilli: opportunities for food biotechnology. Curr Opin Biotechnol 21(2): 168-174.

Thomas, C. M. and Smith, C. A. (1987). Incompatibility group P plasmids: genetics, evolution, and use in genetic manipulation. Annu Rev Microbiol 41: 77-101.

Traore, D. A., El Ghazouani, A., Ilango, S., Dupuy, J., Jacquamet, L., Ferrer, J. L., Caux-Thang, C., Duarte, V. and Latour, J. M. (2006). Crystal structure of the apo-PerR-Zn protein from *Bacillus subtilis*. Mol Microbiol 61(5): 1211-1219.

Traore, D. A., El Ghazouani, A., Jacquamet, L., Borel, F., Ferrer, J. L., Lascoux, D., Ravanat, J. L., Jaquinod, M., Blondin, G., Caux-Thang, C., Duarte, V. and Latour, J. M. (2009). Structural and functional characterization of 2-oxo-histidine in oxidized PerR protein. Nat Chem Biol 5(1): 53-59.

Trieu-Cuot, P., Carlier, C., Poyart-Salmeron, C. and Courvalin, P. (1991). An integrative vector exploiting the transposition properties of Tn*1545* for insertional mutagenesis and cloning of genes from gram-positive bacteria. Gene 106(1): 21-27.

Trieu-Cuot, P., Carlier, C., Poyart-Salmeron, C. and Courvalin, P. (1991). Shuttle vectors containing a multiple cloning site and a *lacZ* alpha gene for conjugal transfer of DNA from *Escherichia coli* to gram-positive bacteria. Gene 102(1): 99-104.

Tsvetanova, B., Wilson, A. C., Bongiorni, C., Chiang, C., Hoch, J. A. and Perego, M. (2007). Opposing effects of histidine phosphorylation regulate the AtxA virulence transcription factor in *Bacillus anthracis*. Mol Microbiol 63(3): 644-655.

Turnbull, P. C., Kramer, J. M., Jorgensen, K., Gilbert, R. J. and Melling, J. (1979). Properties and production characteristics of vomiting, diarrheal, and necrotizing toxins of *Bacillus cereus*. Am J Clin Nutr 32(1): 219-228.

van der Auwera, G. A., Timmery, S., Hoton, F. and Mahillon, J. (2007). Plasmid exchanges among members of the *Bacillus cereus* group in foodstuffs. Int J Food Microbiol 113(2): 164-172.

van der Voort, M., Kuipers, O. P., Buist, G., de Vos, W. M. and Abee, T. (2008). Assessment of CcpA-mediated catabolite control of gene expression in *Bacillus cereus* ATCC 14579. BMC Microbiol 8: 62.

van Netten, P., van De Moosdijk, A., van Hoensel, P., Mossel, D. A. and Perales, I. (1990). Psychrotrophic strains of *Bacillus cereus* producing enterotoxin. J Appl Bacteriol 69(1): 73-79.

van Schaik, W., Chateau, A., Dillies, M. A., Coppee, J. Y., Sonenshein, A. L. and Fouet, A. (2009). The global regulator CodY regulates toxin gene expression in *Bacillus anthracis* and is required for full virulence. Infect Immun 77(10): 4437-4445.

Veening, J. W., Stewart, E. J., Berngruber, T. W., Taddei, F., Kuipers, O. P. and Hamoen, L. W. (2008). Bet-hedging and epigenetic inheritance in bacterial cell development. Proc Natl Acad Sci U S A 105(11): 4393-4398.

Vilain, S., Luo, Y., Hildreth, M. B. and Brozel, V. S. (2006). Analysis of the life cycle of the soil saprophyte *Bacillus cereus* in liquid soil extract and in soil. Appl Environ Microbiol 72(7): 4970-4977.

von Döhren, H., Keller, U., Vater, J. and Zocher, R. (1997). Multifunctional peptide synthetases. Chem Rev 97(7)**:** 2675 - 2705.

Wagner, M. K. (1986). Phosphates as antibotulinal agents in cured meats: a review. J Food Prot 49(6): 482-487.

Wagner, M. K. and Busta, F. F. (1985). Inhibition of *Clostridium botulinum* 52A toxicity and protease activity by sodium acid pyrophosphate in media systems. Appl Environ Microbiol 50(1): 16-20.

Wu, C., Cichewicz, R., Li, Y., Liu, J., Roe, B., Ferretti, J., Merritt, J. and Qi, F. (2010). Genomic island TnSmu2 of *Streptococcus mutans* harbors a nonribosomal peptide synthetase-polyketide synthase gene cluster responsible for the biosynthesis of pigments involved in oxygen and H_2O_2 tolerance. Appl Environ Microbiol 76(17): 5815-5826.

Yakimov, M. M. and Golyshin, P. N. (1997). ComA-dependent transcriptional activation of lichenysin A synthetase promoter in *Bacillus subtilis* cells. Biotechnol Prog 13(6): 757-761.

Yankovskaya, V., Horsefield, R., Tornroth, S., Luna-Chavez, C., Miyoshi, H., Leger, C., Byrne, B., Cecchini, G. and Iwata, S. (2003). Architecture of succinate dehydrogenase and reactive oxygen species generation. Science 299(5607): 700-704.

Yazgan, A., Ozcengiz, G. and Marahiel, M. A. (2001). Tn10 insertional mutations of *Bacillus subtilis* that block the biosynthesis of bacilysin. Biochim Biophys Acta 1518(1-2): 87-94.

Zaika, L., Scullen, O. J. and Fanelli, J. S. (1997). Growth inhibition of *Listeria monocytogenes* by sodium phosphate as affected by polyvalent metal ions. J. Food Sci. 62: 867-869.

Zeigler, D. R., Pragai, Z., Rodriguez, S., Chevreux, B., Muffler, A., Albert, T., Bai, R., Wyss, M. and Perkins, J. B. (2008). The origins of 168, W23, and other *Bacillus subtilis* legacy strains. J Bacteriol 190(21): 6983-6995.

Zessin, K. G. and Shelef, L. A. (1988). Sensitivity of *Pseudomonas* strains to polyphosphates in media systems. J. Food Sci. 53(2): 669-670.

Zigha, A., Rosenfeld, E., Schmitt, P. and Duport, C. (2007). The redox regulator Fnr is required for fermentative growth and enterotoxin synthesis in *Bacillus cereus* F4430/73. J Bacteriol 189(7): 2813-2824.

Zuber, P. (2009). Management of oxidative stress in *Bacillus*. Annu Rev Microbiol 63: 575-597.

7 Appendix

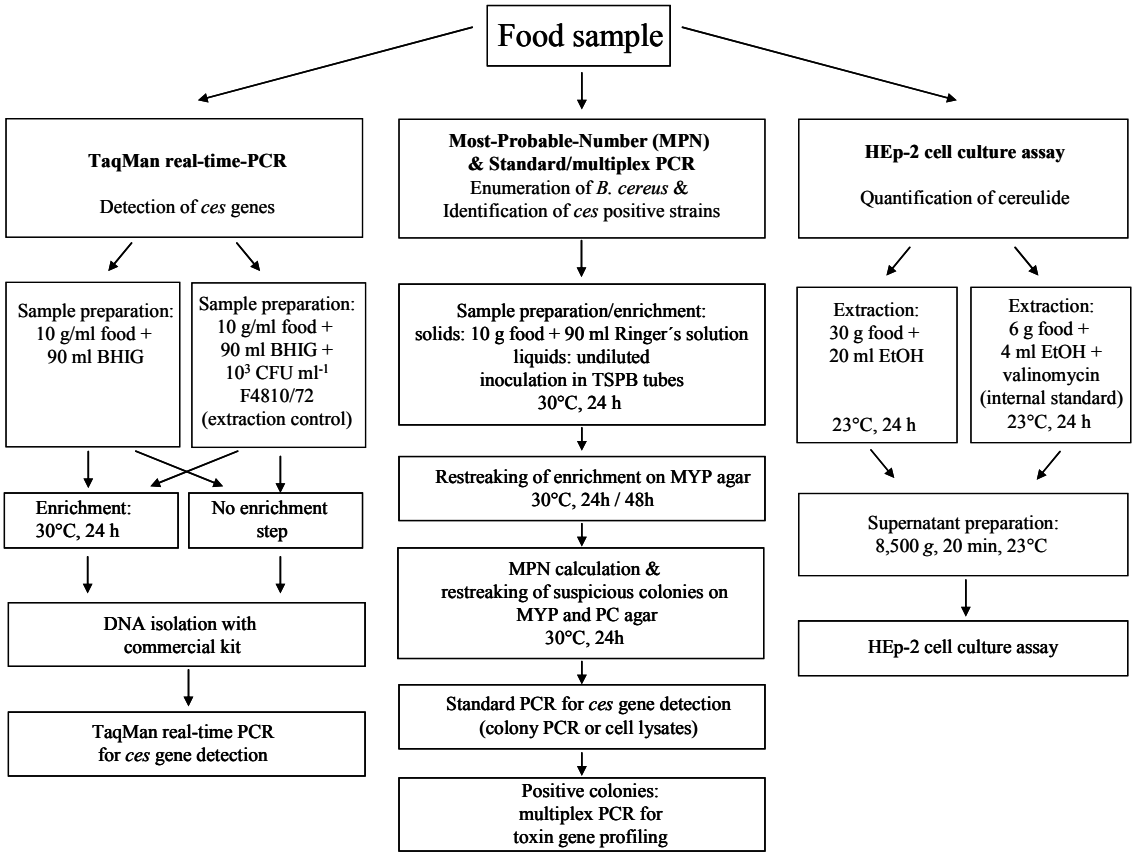

Figure A1: Workflow for the enumeration of *B. cereus* group organisms and the detection of emetic *B. cereus* and cereulide in food samples. The polyphasic approach is based on a recently developed TaqMan real-time assay for the detection of cereulide synthetase (*ces*) genes in DNA extracts of foods (Fricker *et al.* 2007), the classic MPN technique in combination with a recently developed multiplex assay for toxin gene profiling of *B. cereus* isolates (Ehling-Schulz *et al.* 2006), and the HEp-2 cytotoxicity assay for detection of cereulide in food extracts. Preparation of the ethanolic food extracts was described by (Frenzel *et al.* 2011). For further details on assays, see Materials and Methods.

Table A1: *In silico* binding prediction of *B. subtilis* transcription factors towards the entire non-coding region between *cesH* and *cesP* including the main *ces* operon promoter[a]

Trans-crip-tion factor	Short description of transcription factor-function in *B. subtilis*	Number of motifs in *ces* region	Score[b]	Start and end position of match sequence[c]
AbrB	Pleiotropic regulator of transition state	1	5.94	**965-977**
AhrC	Regulates arginine metabolism genes	4	6.95 6.26 6.07 5.93	179-191 427-439 497-509 507-519
CodY	Pleiotropic regulator of transition state and N-metabolism	1	5.84	**647-658**
ComK	Central regulator of competence of DNA uptake	2	5.62 5.62	**942-955** **972-985**
DegU	Pleiotropic two-component response regulator; active during transition state	7	4.94 5.79 5.26 5.57 5.88 5.25 5.88	168-183 202-218 **619-634** **681-696** **722-737** **819-837** **968-986**
Fur	Iron-sensing regulator of iron homeostasis and ferri-siderophore synthesis/uptake	1	6.54	551-571
GlnR	Regulates glutamine metabolism genes	1	6.61	**622-639**
GltC	Activator of glutamate synthase operon	2	6.38 6.24	243-258 583-598
GltR	Function unknown; probably involved in glutamate synthesis	1	8.15	583-598
HrcA	Repressor of class I heat-shock (chaperone) genes	1	9.21	577-604
LevR	Regulation of levan and fructose utilization	2	6.14 6.14	**652-663** **801-812**
LexA	Repressor of SOS regulon	1	7.26	**708-720**
MntR	Regulation of manganese uptake	2	6.62 8.15	60-79 **927-946**
PerR	Regulator of peroxide regulon; oxidative stress response	3	6.14 5.87 6.89	554-569 **720-735** **828-843**
PurR	Purine metabolite-dependent regulator of purine biosynthesis	1	6.51 5.88	**841-855** **627-638**
SinR	Pleiotropic regulator of transition state	1	6.60	**614-621**
TnrA	Global N-metabolism regulator	2	8.15 6.63	**622-639** **757-774**
Zur	Zinc-sensing regulator of zinc homeostasis	1	6.71	**782-796**

[a] *In silico* footprinting was performed on the DBTBS server accessible at http://dbtbs.hgc.jp/.
[b] Measure for the regulatory potential of the predicted match sequence (0=low, 10=high) based on experimentally derived position specific weight matrices.
[c] Bold numbers indicate a binding site in proximity to the -35 and -10 boxes of P_{cesP1} and P_{cesP2}.

Table A2: Differentially expressed protein spots assessed by comparative 2-D DIGE analysis of cytosolic and secreted subproteomes of *B. cereus* F4810/72 (WT), *B. cereus* F48(pCER270-) (pCER), and the *ces* operon-deficient F48ΔcesP/polar mutant (ΔcesP)

Spot number	Accession number (NCBI)	Designation	Functional annotation	Av ratio[a] pCER/WT	Av ratio Δces/WT	Av ratio Δces/pCER	Localization[b]	Signal-peptide[c]	pCER270 encoded	Regulated by PlcR[d]	Protein group[e]
2328	BCAH187_C0034	Chitin binding protein	Chitin-binding domain protein	-24.2	n.s.	31.9	S	•	•		1
2330	BCAH187_C0034	Chitin binding protein	Chitin-binding domain protein	-121.3	n.s.	157.2	S	•	•		1
2331	BCAH187_C0034	Chitin binding protein	Chitin-binding domain protein	-186.9	n.s.	206.2	S	•	•		1
1446	BCAH187_C0038	NprC38 (novel)[f]	Putative metallopeptidase, hypothetical	-13.5	n.s.	10.01	S	•	•		1
2343	BCAH187_C0038	NprC38 (novel)[f]	Putative metallopeptidase, hypothetical	-14.0	n.s.	11.9	S	•	•		1
936	BCAH187_C0096	RepX	Tubulin/FtsZ domain-containing protein	-7.1	n.s.	7.1	C		•		1
238	BCAH187_A1065	EA1	S-layer protein EA1	-11.2	n.s.	9.8	C	•			1
395	BCAH187_A1064	SAP	Crystal protein	-3.1	n.s.	2.8	S	•			1
2344	BCAH187_A1064	SAP	Crystal protein	-3.4	n.s.	2.9	S	•			1
1338	BCAH187_A1995	NheA	Enterotoxin A	1.7	n.s.	-1.7	S	•		•	1
153	BCAH187_A1996	NheB	Enterotoxin B	1.5	n.s.	-1.8	S	•		•	1
2340	BCAH187_A1996	NheB	Enterotoxin B	1.6	n.s.	-1.7	S	•		•	1
606	BCAH187_A0684	ColC	Putative microbial collagenase	1.8	n.s.	-1.7	S	•		•	1
955	BCAH187_A3327	Clo	Anthrolysin O	1.6	n.s.	-1.9	S	•		•	1
1402	BCAH187_A2787	NprP2	Metalloendopeptidase	9.6	n.s.	-14.0	S	•		•	1
1413	BCAH187_A2787	NprP2	Metalloendopeptidase	2.7	n.s.	-3.2	S	•		•	1
1806	BCAH187_A1835	FlgA	Flagellin	5.4	n.s.	-8.2	S				1
1986	BCAH187_A0804	PC-plC	Phospholipase C	1.5	n.s.	-2.0	S	•		•	1
657	BCAH187_A5285	GpmI	Phosphoglycerate mutase	n.s.	1.7	1.9	S				2
705	BCAH187_A5516	PyrG	CTP synthetase	n.s.	1.9	1.7	S				2
785	BCAH187_A1922	MalS	Malate dehydrogenase	n.s.	1.7	1.7	S				2
894	BCAH187_A0438	AhpF	Alkyl hydroperoxide reductase, F subunit	n.s.	1.6	1.9	S				2
979	BCAH187_A4088	PdhD	Dihydrolipoamide dehydrogenase; E3 component of pyruvate complex	n.s.	2.0	2.1	S				2
1013	BCAH187_A4218	Pyn2	Pyrimidine-nucleoside phosphorylase	n.s.	1.7	1.9	S				2
1019	BCAH187_A5042	Pgi	Glucose-6-phosphate isomerase	n.s.	1.7	1.6	S				2
1090	BCAH187_A5284	Eno	Phosphopyruvate hydratase	n.s.	2.2	2.0	S				2
2042	BCAH187_A4408	SodA-1	Superoxide dismutase, Mn	n.s.	1.6	1.8	S				2

Table A2-*continued*

1855	BCAH187_A3551	VanW[g]	VanW-related protein	-1.9	-1.9	n.s.	S	•	3
596	BCAH187_A4645	SdhA	Succinate dehydrogenase, flavoprotein subunit	-6.7	-8.7	n.s.	C/M		3
602	BCAH187_A4645	SdhA	Succinate dehydrogenase, flavoprotein subunit	-7.5	-8.8	n.s.	C/M		3
610	BCAH187_A4645	SdhA	Succinate dehydrogenase, flavoprotein subunit	2.3	2.3	n.s.	C/M		3
1272	BCAH187_A4358	GcvT	Glycine cleavage system, aminomethyltransferase T	1.7	1.6	n.s.	C		3
996	BCAH187_A4357	YqhJ (GcvP)	Glycine dehydrogenase, subunit 1	2.0	n.s.	n.s.	S		4
2245	BCAH187_A0439	AhpC	Peroxiredoxin	-2.0	1.9	3.9	S		4
807	BCAH187_A4906	PckA	Phosphoenolpyruvate carboxykinase	1.5	2.0	1.4	S		4
971	BCAH187_A4293	BfmbC	Dihydrolipoamide dehydrogenase; E3 component of the branched-chain alpha-keto acid dehydrogenase complex	n.s.	1.9	n.s.	S		4
637	BCAH187_A5064	ManB	Phosphoglucomutase/phosphomannomutase family protein	1.2	1.9	1.5	S		4

[a] Av. ratio denotes the average in-/decrease of spot abundance of condition 1-proteins (left hand side of slash) compared to control-group proteins (right hand side of slash). n.s., no significant differences in protein expressed based on the statistical FDR analysis.
[b] The protein was identified in the C, cytosol or S, secretome fraction.
[c] The presence of a signal peptide was predicted on the SignalIP 3.0 server (see Material and Methods).
[d] Regulation by PlcR was inferred from previous studies (e.g. Gohar *et al.* 2008; Sastalla *et al.* 2010), and deduced from the absence or presence of a PlcR consensus box in the putative promoter region.
[e] (1), proteins are specifically regulated by absence of pCER270, *ces* inactivation has no influence; (2), proteins are specifically regulated upon *ces* cluster inactivation, but curing of the pCER270-plasmid has no effect; (3), proteins are speficically regulated upon *ces* cluster inactivation; (4), regulation of protein spots can not be unequivocally assigned to regulatory scheme.
[f] Novel protein; hereafter referred to as NrpC38; 52% similarity to neutral protease B (NprB; bacillolysin) of *B. cereus* ATCC10987 and *B. anthracis* CI.
[g] 99% identity to *B. anthracis* Ames (RA3) vancomycin B-type resistance protein VanW.